MiRNAs and prostate cancer: Identification, functional characterization and their potential use in medical practice

Dissertation

zur Erlangung des akademischen Grades des

Doktors der Naturwissenschaften (Dr. rer. nat.)

eingereicht im Fachbereich Biologie, Chemie, Pharmazie

der Freien Universität Berlin

vorgelegt von

Dipl.-Ing. für Biotechnologie (FH) Annika Fendler

aus Darmstadt

Mai 2011

Die Dissertation wurde von Juni 2008 bis April 2011 in der Forschungsabteilung der Klinik für Urologie, Charité- Universitätsmedizin Berlin und dem Berliner Forschungsinstitut für Urologie, Berlin unter der Leitung von Prof. Dr. Jung durchgeführt

1. Gutachter: Prof. Dr. Michael Lein
2. Gutachter: Prof. Dr. Rupert Mutzel

Disputation am: 29.09.2011

Abstract

microRNAs (miRNAs) are small non-coding RNAs that are crucial regulators of carcinogenesis. In this thesis, the deregulation of miRNAs in prostate cancer was investigated. miRNA microarray profiling was performed in fresh frozen prostate cancer and matched normal adjacent tissues. Differentially expressed miRNAs were subsequently validated by real-time quantitative PCR (RT-qPCR). Fifteen miRNAs differentially regulated in prostate cancer in comparison with normal tissue. Expression of 5 miRNAs was correlated with the pathological stage and the Gleason score.

The diagnostic potential was calculated by receiver operating characteristic curves and logistic regression. Two miRNAs alone correctly classified 84% of malignant and non-malignant samples.

The prognostic value of the miRNAs in prostate cancer specimens after radical prostatectomy was calculated by a Kaplan-Meier analysis and a multivariate Cox regression analysis. miR-96 expression was associated with biochemical relapse, which is defined as an increased value of prostate-specific antigen after surgery and which is indicative of prostate cancer recurrence. The prognostic value of miR-96 was validated with an independent sample set. The multivariate Cox regression analysis confirmed that miR-96 expression is an independent marker of biochemical relapse.

To further identify miRNAs concurrent with a biochemical relapse, miRNA profiling was performed in formalin-fixed, paraffin-embedded tissues from biochemical relapse patients. The deregulation of miR-10b and miR-222 in patients experiencing an early biochemical relapse was validated by RT-qPCR.

Based on the profiling studies and the important role of miR-96 as a prognostic marker, miR-96 function was investigated. miR-96 overexpression increased proliferation and impaired apoptosis of LNCaP prostate cancer cells upon induction by camptothecin. In-silico target prediction identified putative apoptosis-related target genes, among them FOXO1 and ITPR1. The direct binding of miR-96 to the FOXO1 3' UTR was shown by a reporter gene assay and resulted in a downregulation of the FOXO1 transcript and protein. The binding of miR-96 to the ITPR1 3' UTR was only shown for the second predicted binding site. miR-96 expression was inversely correlated with FOXO1 protein expression in prostate cancer and matched normal adjacent tissue.

A second miRNA, miR-133b, was functionally characterized in this thesis. A collaborating group has previously identified miR-133b as a regulator of extrinsic apoptosis. In this thesis, miR-133b is shown to be downregulated in prostate cancer and an overexpression of miR-133b in PC3 prostate cancer cells is described to impair proliferation. Microarray profiling revealed that an abundance of genes was downregulated upon miR-133b transfection. The downregulation of GSTP1, FAIM, CAV1 and VEGFC was verified on

transcript and protein levels. The direct binding of miR-133b to the CAV1 3' UTR was not detected in a reporter gene assay, suggesting an indirect regulation. miR-133b and FAIM transcript expression were inversely correlated, whereas all other target genes were not correlated with miR-133b expression. Therefore the regulation of these genes by miR-133b might be superimposed by other regulatory mechanisms in prostate cancer.

This thesis provides evidence of the miRNA deregulation in prostate cancer and that differential miRNAs are useful diagnostic and prognostic indicators. Furthermore, the regulatory roles of miR-96 and miR-133b in apoptosis and proliferation in prostate cancer cells are established for the first time in this cancer entity. These roles provide new insights into prostate cancer carcinogenesis.

Zusammenfassung

miRNAs sind kurze nicht-protein-kodierende RNAs und wichtige Regulatoren der Karzinogenese. In dieser Arbeit wurde die miRNA-Expression im Prostatakarzinom untersucht. Mit einem Microarray wurde ein miRNA-Profil in gepaartem Prostata- und angrenzendem Normalgewebe erstellt und mittels RT-qPCR validiert. 15 miRNAs waren im Prostatakarzinom unterschiedlich exprimiert. Die Expression von 5 miRNAs korrelierte mit dem histologischen Differenzierungsgrad nach Gleason und dem pathologischen Tumorstadium.

Das diagnostische Potential aller miRNAs wurde mit Hilfe von „Receiver Operating Characteristics“ Kurven und logistischer Regression berechnet. Schon die Kombination zweier miRNAs konnte 84% aller malignen und nicht-malignen Proben richtig klassifizieren.

Die Expression der miR-96 war in der Kaplan-Meier-Analyse mit einem biochemischen Rezidiv, definiert als Wiederanstieg des prostataspezifischen Antigens nach radikaler Prostatektomie, assoziiert. Der prognostische Wert dieser miRNA wurde in einer unabhängigen Kohorte validiert. Multivariate Cox Regressionsanalysen bestätigten, dass die Expression der miR-96 ein unabhängiger Marker für ein biochemisches Rezidiv ist.

Um weitere miRNAs zu identifizieren, die mit einem biochemischen Rezidiv assoziiert sind, wurde ein miRNA-Profil aus formalin-fixierten, paraffin-eingebetteten Gewebeblöcken von Patienten mit einem biochemischen Rezidiv erstellt. Die Deregulation der miR-10b und miR-222 in Patienten mit einem frühen Rezidiv wurde in der RT-qPCR bestätigt.

Auf Grund der Assoziation der miR-96 mit einem biochemischen Rezidiv wurde die Funktion der miR-96 im Prostatakarzinom untersucht. Induzierte miR-96-Überexpression in LNCaP-Zellen erhöhte deren Proliferation und inhibierte die Apoptose in Camptothecin-behandelten Zellen. Durch in-silico Prädiktion wurden mögliche Apoptose-assoziierte Zielgene identifiziert, unter ihnen FOXO1 und ITPR1. Im Reportergenassay wurde eine direkte Bindung zwischen der miR-96 und der FOXO1 3’-UTR bewiesen, welche mit einer verminderten FOXO1 Transkript- und Proteinexpression einherging. Die Expression miR-96 war invers mit der FOXO1-Protein-Expression im Prostatakarzinomgewebe korreliert. Eine Bindung der miR-96 an die ITPR1 3’-UTR konnte nur für die zweite Bindungsstelle nachgewiesen werden.

Weiterhin wurde die Funktion der miR-133b im Prostatakarzinom untersucht. Eine Studie unserer Projektpartner hatte die regulatorische Funktion der miR-133b während der extrinsischen Apoptose untersucht. In dieser Arbeit wurde eine verminderte Expression der miR-133b im Prostatakarzinom nachgewiesen. Die Überexpression dieser miRNA in PC3-Zellen inhibierte die Proliferation. In einem Microarray war eine Vielzahl von Genen in miR-133b überexprimierenden PC3-Zellen vermindert exprimiert. Die verminderte Expression von GSTP1, FAIM, FASN, CAV1 und VEGFC wurde auf Transkript- und Proteinebene verifiziert.

Jedoch konnte keine direkte Bindung der miR-133b an die CAV1 3'-UTR nachgewiesen werden, was auf ein indirekte Regulation hindeutet. Die Expression der miR-133b und FAIM korrelierte invers in Prostatageweben. Andere Zielgene waren nicht invers mit der miRNA korreliert, vermutlich weil die Regulation der miR-133b durch andere Regulationsmechanism überdeckt wird.

Diese Arbeit beweist, dass das Prostatakarzinom durch ein verändertes miRNA-Expressionsmuster charakterisiert werden kann und dass miRNAs als diagnostische oder prognostische Marker geeignet sind. Zudem wurde zum ersten Mal eine funktionelle Bedeutung der miR-96 und miR-133b im Prostatakarzinom nachgewiesen. Damit vermittelt diese Arbeit neue Einblicke in die Karzinogenese des Prostatakarzinoms.

List of publications

The following articles have been published in the course of this doctoral thesis:

1. **Schaefer A**, Jung M, Mollenkopf HJ, Wagner I, Stephan C, Jentzmik F, et al. Diagnostic and prognostic implications of microRNA profiling in prostate carcinoma. Int J Cancer 2010;126:1166-76.
2. **Schaefer A**, Jung M, Miller K, Lein M, Kristiansen G, Erbersdobler A, Jung K. Suitable reference genes for relative quantification of miRNA expression in prostate cancer. Exp Mol Med 2010;42:749-58.
3. Jung M, **Schaefer A**, Steiner I, Kempkensteffen C, Stephan C, Erbersdobler A, Jung K. Robust microRNA stability in degraded RNA preparations from human tissue and cell samples. Clin Chem 2010;56:998-1006.
4. Patron JP, **Schaefer A**, Jung U, Mueller H, Arntzen MO, Stephan C, Thiede B, Mollenkopf HJ, Jung K, Kaufmann SH, Schreiber J. MiR-133b targets antiapoptotic genes and enhances death receptor-induced apoptosis. J Biol Chem 2011 [submitted for publication].
5. **Fendler A**, Jung M, Stephan C, Erbersdobler A, Jung K, Yousef GM. The antiapoptotic function of miR-96 in prostate cancer by inhibition of FOXO1. Oncogene 2011 [submitted for publication].
6. **Fendler A**, Jung M, Stephan C, Honey RJ, Stewart RJ, Pace KT, Erbersdobler A, Samaan S, Jung K, Yousef GM. MiRNAs can predict prostate cancer biochemical relapse and are involved in tumor progression. Int J Oncol 2011 [submitted for publication].
7. **Schaefer A**, Jung M, Kristiansen G, Lein M, Schrader M, Miller K, et al. Micrornas and cancer: Current state and future perspectives in urologic oncology. Urol Oncol 2010;28:4-13.
8. **Schaefer A**, Stephan C, Busch J, Yousef GM, Jung K. Diagnostic, prognostic and therapeutic implications of microRNAs in urologic tumors. Nat Rev Urol 2010;7:286-97.
9. **Fendler A**, Stephan C, Yousef GM, Jung K. MiRNAs as regulators of signal transduction in urological tumors. Clin Chem [accepted for publication]**.**
10. **Schaefer A**, Jung M, Kristiansen G, Lein M, Schrader M, Miller K, et al. [microRNA in uro-oncology : New hope for the diagnosis and treatment of tumors?]. Urologe A 2009;48:877-85.
11. **Schaefer A**, Jung K. Re: MicroRNA regulation of oncolytic herpes simplex virus-1 for selective killing of prostate cancer cells. Eur Urol 2010;57:919.

Table of contents

Tables

Figures

Abbrevations

-2LL	-2 log likelihood
3' UTR	3' untranslated region
5α-DHT	5α-dihydrotestosterone
AMO	Anti-miRNA oligonucleotide
AUC	Area under the curve
bp	Basepair
BPH	Benign prostate hyperplasia
BSA	Bovine serum albumin
CPRC	Castration resistant prostate cancer
CPT	Camptothecin
Cq	Quantification cycle
CRPC	Castration resistant prostate cancer
dNTP	Deoxynucleotide triphosphate
dsRBD	Double-stranded RNA-binding domain
FFPE	Formalin-fixed, paraffin-embedded tissue
GO	Gene ontology
H/E	Haematoxylin/ eosin
IP3	Inositol 1,4,5-triphosphate
kb	Kilobases
LHRH	Luteinizing hormone-releasing hormone
M^7G	7-methylguanosine
miRISC	MicroRNA induced silencing complex
miRNA	MicroRNA
mRNA	Messenger RNA
mtAMO	Multi-target anti-miRNA oligonucleotide
MTT	3-[4,5-dimethylthiazol-2-yl]-2,5-diphenyl tetrazolium bromid
nt	nucleotide
PCA	Principal component analysis
PIN	Prostate intraepithelial neoplasia
Pre-miRNA	Precursor microRNA
Pri-miRNA	Preliminary microRNA
$PtIns(4,5)P_2$	Phosphatidylinositol 4,5-biphosphate
$PtIns(4,5)P_3$	Phosphatidylinositol 4,5-triphosphate
R1881	Methyltrienolone
RIN	RNA integrity number
RNAi	RNA interference
ROC	Receiver operating characteristics
RT-qPCR	Real time quantitative PCR
TMA	Tissue microarray
XTT	3-[1-(phenylaminocarbonyl)- 3,4-tetrazolium]-bis (4-methoxy-6-nitro benzene sulfonic acid hydrate

1. Introduction

1.1 microRNAs

microRNAs (miRNAs) are short non-protein-coding RNAs that are approximately 22 nt in length. The best-characterized function of miRNAs is posttranscriptional regulation of gene expression via 3' UTR binding of an mRNA (Bartel, 2004). miRNAs belong to the class of small RNAs, which are non-coding RNAs with a length of less than 300 nt. Small nucleolar RNAs (snoRNAs), small nuclear RNAs (snRNAs), short interfering RNAs (siRNAs) and PIWI-interacting RNAs (piRNAs) also comprise this class. Until recently, small RNAs were regarded as evolutionary trash. Their regulatory functions in gene expression and pivotal roles in physiological as well as pathological processes revealed them to be vital components of the genome (Kutter and Svoboda, 2008).

1.1.1 History of microRNAs

In 1993 Lee *et al.* (Lee *et al.*, 1993) discovered that the gene lin-4 is transcribed into a 22 nt long RNA that inhibits lin-14 by RNA interference in the nematode *Caenorhabditis elegans*. The authors concluded that *lin-4* may belong to a class of small, regulatory non-translated RNA, albeit for years there was no evidence for other lin-4-like RNAs in *C.elegans* or other organisms. The identification of a second miRNA, let-7 in *C. elegans*, *Drosophilia* and humans was identified in 2000 (Reinhart *et al.*, 2000) along with the discovery of additional 22 nt RNAs in 2001 (Lagos-Quintana *et al.*, 2001; Lau *et al.*, 2001; Lee and Ambros, 2001), prompted their characterization as microRNAs. Computational approaches predicted the existence of approximately 1000 miRNAs in the human genome (Berezikov *et al.*, 2005). In 2006, miRBase was established to provide a database of miRNA sequences and organize nomenclature (Griffiths-Jones *et al.*, 2006). One thousand and thirty-seven human miRNA were annotated at miRBase in March 2011.

1.1.2 microRNA genomic location and biogenesis

Several miRNAs are located in distinct regions far from protein-coding genes (Lee and Ambros, 2001). These miRNA genes are expressed from their own promoters. In contrast, approximately 40% of miRNAs are located in introns of protein-coding genes, primarily in the same orientation as its host genes (Rodriguez *et al.*, 2004). Those miRNAs are frequently controlled by the same promoter region and are co-expressed with their host genes. Furthermore, while some miRNA genes are located far from other miRNA loci, others are located proximal to each other and are thought to be described in clusters (Altuvia *et al.*, 2005). miRBase defines a cluster as a group of miRNAs that are located within 10 kb of each other. Clustered miRNAs are transcribed as polycystronic RNAs by polymerase II, while other miRNAs are transcribed as monocystronic miRNAs. The transcribed sequences are a few hundred to a few thousand nt in length, termed preliminary miRNAs (pri-miRNAs) (Figure

1). Pri-miRNAs harbor a 7-methyl guanosine cap and a poly(A)-tail at their 3' end, a structure typical of RNAs transcribed by polymerase II (Lee *et al.*, 2004). The mature miRNAs are located within characteristic stem-loop structures

In the nucleus, the pri-miRNA is further processed by DROSHA (Lee *et al.*, 2003). DROSHA is an RNAse III class II enzyme. These enzymes typically harbor tandem RNAse III domains and one dsRBD. The pri-miRNA is cleaved to form the preliminary microRNA of approximately 60 to 80 nt in length. The pre-miRNA harbors a 5'-phosphate and a 2 nt 3'-overhang, which is typical after RNAse III cleavage. Additionally, DGCR8 is a crucial cofactor for successful cleavage of the pri-miRNA by DROSHA (Han *et al.*, 2004).

The pre-miRNA is translocated to the cytoplasm by XPO5, which requires RAN-GTP as cofactor (Yi *et al.*, 2003). In the cytoplasm, a second RNAse III class II enzyme, DICER, further processes the pre-miRNA (Lee *et al.*, 2002). DICER yields imperfect 22 bp miRNA duplex with 2-nt-long 3'-overhangs. This duplex is composed of the mature miRNA strand and its antisense strand and it is unwound by helicases directly after processing. The mature miRNA is then incorporated into the miRNA-induced silencing complex (miRISC) (Hutvagner and Zamore, 2002). This RNA-protein complex harbors primarily argonaute proteins (AGO1-4) and facilitates gene silencing via binding to 3' UTR sequences, which are complementary to the miRNA sequence. AGO2 is the only argonaute protein with an RNAse H-like domain, which facilitates endonucleolytic cleavage (Meister *et al.*, 2004).

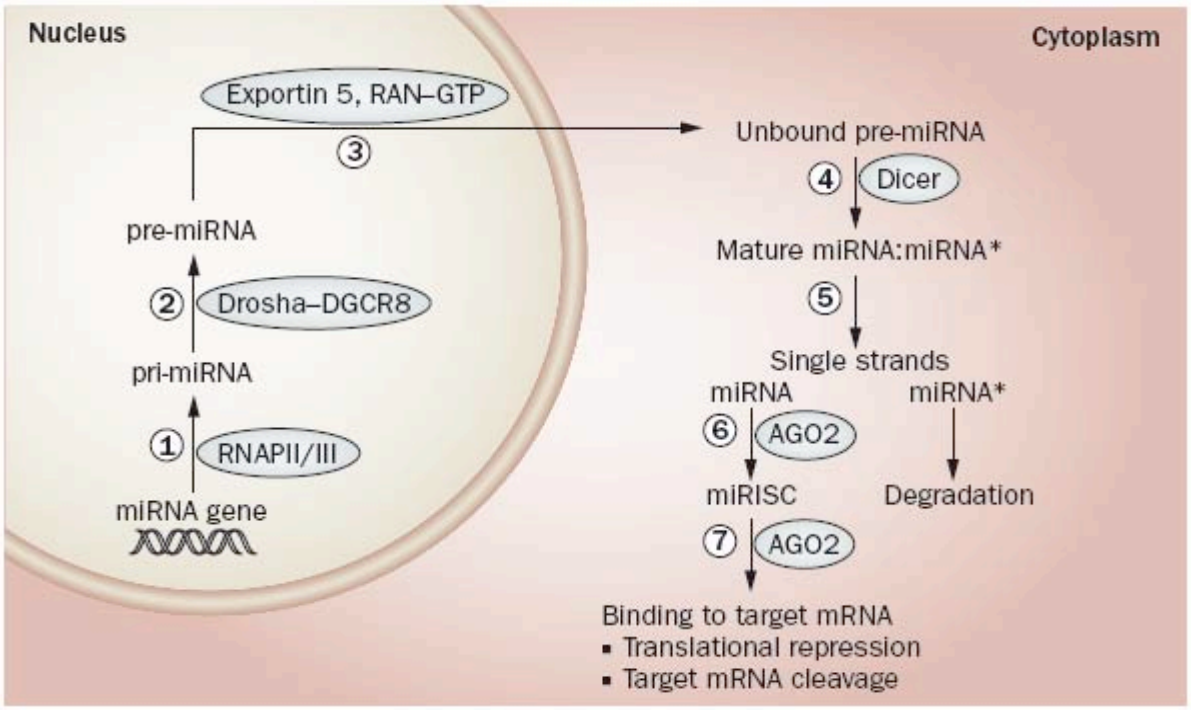

Figure 1: Schematic representation of miRNA biogenesis

A schematic representation of miRNA biogenesis. (1) miRNA genes are transcribed by RNA polymerase II as primary miRNAs (primiRNAs) of >500 up to several thousand nt. (2) The pri-miRNA is cleaved by the DROSHA–DGCR8 complex into the precursor miRNA (pre-miRNA) (3) The pre-miRNA is exported from the nucleus into the cytoplasm by XPO5 and the RAN–GTP system. (4) In the cytoplasm, the pre-miRNA is further cleaved by DICER to form the mature miRNA (5) The guiding strand of this mature miRNA duplex is incorporated into the miRISC. The passenger strand (miRNA*) is usually degraded. (6) The miRISC is a ribonucleotide complex that is primarly composed of argonaute proteins and the miRNA guiding strand as its major components. (7) The miRNA binds to regions in the 3' UTR of an mRNA, which guides the miRISC complex to its target. The figure is adopted from Schaefer *et al.* (Schaefer *et al.*, 2010b).

1.1.3 Mechanisms of miRNA mediated gene silencing

The primary function of miRNAs is posttranscriptional gene regulation, which is mediated by binding to complementary sequences in the target mRNA 3' UTR. Strikingly, perfect complementarity is the primary mechanism in plants, but infrequently occurs in vertebrates. In vertebrates, miRNAs rather exhibit complementarity to the 3' UTR in the "seed region", which is composed of nucleotides 2-8 of the 5'-end, but lack complementarity to the mRNA in the central regions (Doench and Sharp, 2004). The 3'-region of the miRNA exhibits again good complementarity to the mRNA thereby providing the necessary stability for the miRNA:mRNA interaction. The importance of complementarity at the 3'-end is dependent on the structure of the seed sequence (Brennecke *et al.*, 2005). The degree of repression is also dependent on the number of miRNA binding sites in the 3' UTR (Doench *et al.*, 2003). Because AGO2 cleavage of the mRNA, which is part of the major RNAi mechanism, requires perfect complementarity of the miRNA:mRNA duplex (Meister *et al.*, 2004), mRNA degradation is not the primary mechanism of miRNA-mediated gene silencing. AGO2 is nevertheless the primary miRISC component that facilitates miRNA-mediated

translational inhibition (Schmitter *et al.*, 2006), although AGO1, AGO3 and AGO4 at least partially impact efficiency of repression (Pillai *et al.*, 2004).

The miRISC/mRNA complex is enriched in cytoplasmic foci, termed processing bodies (p-bodies) (Liu *et al.*, 2005). P-bodies may either serve as storage compartments and/or places for eventual mRNA decay. P-bodies not only contain untranslated mRNAs but also depend on RNA for their integrity (Teixeira *et al.*, 2005). Further ribosome drop-off may be a mandatory step for localization to the p-bodies (Brengues *et al.*, 2005).

The mechanisms by which miRNAs posttranscriptionally regulate have been well discussed and several models have been proposed (Figure 2).

1. **miRNAs inhibit protein translation initiation**

   Transfection of luciferase reporters harbouring binding sites for endogenous let-7 resulted in a gradient shift of polysome profiles that strongly indicated an initiation inhibition (Pillai *et al.*, 2005). The process was dependent on the m^7G cap and the poly(A) tail, which indicates an EIF4E inhibition (Humphreys *et al.*, 2005). Initiation inhibition results in a rapid drop-off of ribosomes and subsequent storage of the miRNA:mRNA duplex to p-bodies (Pillai *et al.*, 2005).

2. **miRNAs inhibit translation enlongation or termination**

   C. elegans, lin-14 has been shown to remain assembled with polysomes despite their translational repression (Olsen and Ambros, 1999). This observation has been affirmed in mammalian cells (Petersen *et al.*, 2006). The results suggest a premature ribosome drop-off or failed processing and indicated that translational repression occurred while mRNAs were associated with polysomes.

3. **Polypeptide chain proteolysis**

   A third model has been proposed in which the miRNA interaction results in proteolysis of the nascent polypeptide chain (Olsen and Ambros, 1999). However, experiments failed to support this hypothesis (Petersen *et al.*, 2006).

4. **miRNA binding induces deadenylation and subsequent mRNA decay**

   In addition to the proposed translational inhibition of miRNAs, they have also been shown to downregulate mRNAs of predicted target genes (Lim *et al.*, 2005). The CCR4:CNOT1 deadenylase complex and TNRC6A have been identified as key mediators of miRNA-dependent RNA decay (Behm-Ansmant *et al.*, 2006). Whether this process occurs inside or outside of p-bodies remains to be elucidated.

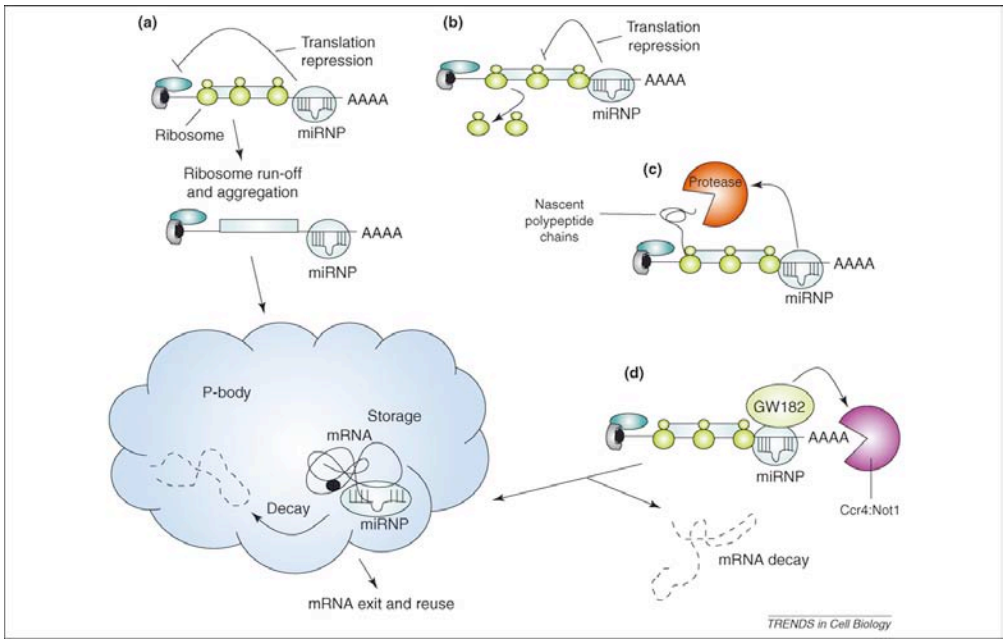

Figure 2: Overview of miRNA-mediated repression of protein translation (Pillai *et al.*, 2007).

1.2 Prostate cancer

1.2.1 Clinical definition, etiology and pathobiology

Prostate cancer is the leading malignancy in man in Germany with more than 60.000 annual incidences (26% of total cancer incidents) (2010). However, only 10% of all cancer-related deaths are due to prostate carcinoma. Prostate cancer is a disease that primarily affects elderly men at an average age of 69 years at first diagnosis. Age is the most prevalent risk factor of a prostate malignancy. Additionally, a positive family anamnesis increases the risk of prostate cancer. The presence of prostate cancer in first-grade relatives also increases risk by 2- to 3-fold (Hemminki and Czene, 2002). Several susceptible loci for familial prostate cancer, as well as polymorphisms, have been identified, but the predominantly mutated in familial carcinomas has not been identified (Nwosu *et al.*, 2001). Other risk factors in prostate cancer include diet, inflammation or sex hormone levels (Patel and Klein, 2009).

Various benign lesions of the prostate exist. Prostate benign hyperplasia (BPH) and prostatic intraepithelial neoplasia (PIN) are the predominant types of benign lesions. BPH primarily occurs in the transitional zone (Guess, 2001) and is a benign hyperplasia of epithelial as well as stromal tissue (Roehrborn, 2008). BPH is generally not regarded as a precursor lesion of prostate cancer because it arises from a different part of the prostate despite sharing common genetic signatures (Alcaraz *et al.*, 2009). PIN is the other important benign prostatic lesion (Bostwick and Brawer, 1987; McNeal, 1969; McNeal and Bostwick, 1986). PIN is characterized by anaplastic and proliferative cells that line ducts and acini of

the prostate (Bostwick and Brawer, 1987). PIN is regarded as a precursor of malignant carcinomas (Epstein, 2009).

Sixty-eight percent of prostate cancers arise from the peripheral zone of the prostate, whereas 24% arise from the transitional zone (McNeal *et al.*, 1988). Acinar prostate carcinoma is the most common histological form (Zhou, 2007), and is primarily multifocal. Other subtypes are found in 5 to 10% of prostate cancer patients and include ductal adenocarcinoma, atrophic carcinoma, pseudohyperplastic carcinoma, foamy gland carcinoma, mucinous carcinoma, signet-ring carcinoma, small cell carcinoma, sarcomatoid carcinoma, urothelial carcinoma, squamous cell carcinoma and basaloid carcinoma (Zhou, 2007).

The Gleason grading is the most common grading system for prostate cancer. Gleason grading sorts cancers on the basis of their gland architecture. While Gleason grade 1 glands are well defined and separated, gland structure is gradually lost with increasing grade, wherein epithelial cells become less differentiated, form cribriform patterns or are poorly formed. The primary and secondary Gleason grades (1 to 5), which correspond to the most common and second most common observed pattern, respectively, are combined to form the Gleason score (Epstein *et al.*, 2005). In certain tumors, a tertiary pattern can be observed. After radical prostatectomy, the primary and secondary grade form the Gleason score, and the tertiary is commented (Epstein *et al.*, 2005).

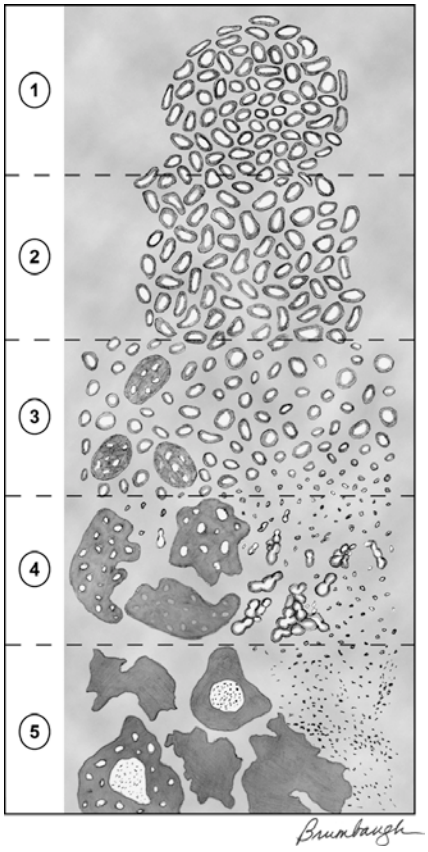

Figure 3: Gleason grading (Epstein *et al.*, 2005)

Additionally, prostate cancers are staged according to the TNM nomenclature (Sobin, 2002). T is the abbreviation for the tumor and describes the tumor size. T1 tumors are clinically non-significant, T2 tumors are still organ confined, T3 tumors penetrate the extracellular capsule and infiltrate the seminal vesicles and T4 tumors infiltrate structures other than the seminal vesicles. N and M describe the processes of metastasis, that dictate the involvement of regional lymph nodes or the occurrence of distant metastases.

1.2.2 Prostate cancer diagnosis

The most important diagnostic marker of prostate cancer is the prostate specific antigen (PSA, KLK3), which was discovered in the late 1980s (Stamey *et al.*, 1987). In the early 1990s, multicenter studies led to the introduction of PSA as a diagnostic marker (Catalona *et al.*, 1994) In Germany, the PSA test is not included in nation-wide cancer screening programs. The utility of the PSA test as a screening approach is still under discussion (Diamandis, 2010). A recent european, randomized, multicenter study revealed a relative PSA-screening-mediated reduction of mortality by 20%, which was accompanied by a high risk of over diagnosis (Schroder *et al.*, 2009), whereas a similar US study did not find significant mortality differences (Andriole *et al.*, 2009). PSA is a prostate specific marker and is elevated not only on prostate cancer but also in BPH (Guess, 2001). Reliable diagnosis is elusive, especially in patients with low PSA levels (4-10 µg/l). Therefore, needle biopsies of patients with elevated PSA levels are collected from prostate zones susceptible to cancer and are histologically characterized (Zhou, 2007). PSA diagnosis can be improved by additional markers, such as %free PSA, PSA density, proPSA, PCA3 and multivariate models as nomograms or artificial neuronal networks (Stephan *et al.*, 2009; Tosoian and Loeb, 2010). However, the models lack accuracy and may be improved by the introduction of novel molecular markers.

1.2.3 Prostate cancer prognosis

Prostate cancer is a relatively benign malignancy that exhibits a 5-year survival rates of 83-94% (2010). However, approximately 15 to 30% of patients experience a biochemical relapse after a curative treatment of radical prostatectomy or radiation therapy (Amling *et al.*, 2000; Han *et al.*, 2003; Pound *et al.*, 1999). A biochemical relapse is defined as detectable PSA levels after radical prostatectomy or a rise in PSA after a period of non-detectable PSA (Simmons *et al.*, 2007). Risk stratification models or probability tables have been established, which predict biochemical recurrence or clinical failure. For example the risk stratification model by D'Amico *et al.* (D'Amico *et al.*, 1998) uses the Gleason score, pre-operative PSA and pathological stage. The most predominant probability table is the Partin table (Partin *et al.*, 1997). Patient clustering remains a disadvantage of these models, as the broad risk groups harbour patients with extensively heterogenic disease characteristics. Therefore,

nomograms have been developed, which enhance the prediction accuracy. Nomograms allow for the use of continuous weighted variables. A commonly used nomogram by Stephenson *et al.* (Stephenson *et al.*, 2006) employs 6 covariates (clinical stage, PSA value, primary and secondary Gleason grades, number of positive and negative cores) and allows the prediction of the recurrence probability for up to 10 years. The c-indices for the internal and external calibrations were 0.76 and 0.79, respectively, indicative of sufficient but not ideal accuracy. Independent external validation studies not only confirmed accuracy but also reported a tendency to overestimate recurrence risk for predictions made 3 or more years after surgery (Isbarn *et al.*, 2009). Taken together, the clinical prediction models remain inaccurate. Therefore, identifying novel accurate prognostic markers of prostate cancer is crucial.

1.2.4 Prostate cancer therapy

Patients with localized prostate cancer face several therapy options, such as radical prostatectomy, active surveillance, watchful waiting, radio- or brachytherapy (Singh *et al.*, 2010) In Germany, treatment protocols follow the guidelines of the German Association of Urology (DGU) (2009). Radical prostatectomy is the treatment of choice for patients with localized prostate carcinomas independent of risk group. Radical prostatectomy allows for an accurate pathological staging of the tumor, which permits for a more accurate prognosis. Because of the high rate of over-treatment, active surveillance is an alternative option for patients with low grade and non-symptomatic prostate cancers and locally advanced prostate cancers. Active surveillance must be distinguished from watchful waiting. While watchful waiting employs waiting for clinical symptoms to occur, active surveillance aims to modify the therapy with changing tumor biology. Other treatment options for localized prostate cancers, such as brachytherapy and radiotherapy are less frequent and their selection is highly dependent from the tumor characteristics.

Hormone therapy is the most common second line therapy option for recurrent prostate cancer. However, biochemically relapsed patients who did not exhibit any lymph node metastases, are better candidates for radiotherapy or watchful waiting. Patients with metastases generally receive hormone therapy. Hormonal ablation can be achieved either by castration (orchiectomy, LHRH analogues, gonadotropin-releasing hormone analogues) or by antiandrogens, such as bicalutamide. Although androgen-ablation can prolong progression-free survival, it is not curative and results in the development of castration-resistant prostate cancer (CRPC). Well-defined therapies are not available for CRPC, but palliative chemotherapy with doxetacel or a change in the hormone ablation strategy are available. Moreover, numerous studies using novel drugs and drug combinations are on-going.

1.2.5 Prostate cancer biology

Prostate cancer is a heterogeneous disease that lacks causative genes associated with prostate carcinogenesis. A recent genetic study of prostate cancer integrated copy number alterations, mutations and transcriptome data to identify modified loci in prostate cancer (Taylor *et al.*, 2010). Metastatic tumors displayed the largest number of chromosomal alterations, whereas primary tumors displayed patterns from diploid genomes to frequent genomic alterations comparable to metastatic tumors. The most frequent genomic alterations in prostate cancer are 8q gains with a 20 to 40% prevalence and 8p loss with a 30 to 50% prevalence (Kim *et al.*, 2007; Lapointe *et al.*, 2007). Chromosome 8 harbours the tumor suppressor NKX3-1 on 8p21 and the oncogene MYC on 8q24.1. Other genomic alterations include the TMPRSS2-ERG gene fusion (50%) (Perner *et al.*, 2006), PTEN deletion at 10q23.31, TP53 deletion at 17p31.1 and a frequent but metastatic tumor restricted AR amplification at Xq12 (Taylor *et al.*, 2010).

The androgen receptor (AR) is one of the major intracellular regulators in prostate carcinogenesis. The AR regulates organogenesis and the initiation and progression of prostate cancer. Because of its crucial functions in prostate cancer, AR is the main therapy target in advanced cancers (1.2.4). The AR is a nuclear receptor that is activated upon 5α-dihydrotestosterone (5α-DHT) binding (Shen and Abate-Shen, 2010). 5α-DHT is produced by SRD5A2, a testosterone reductase (Wilson, 1996). Upon ligand binding, the AR regulates the transcription of a multitude of genes, which are primarily involved in cell growth and survival (Gelmann, 2002). PSA is one of the transcriptional targets of the AR (Riegman *et al.*, 1991). AR activity is dependent on a multitude of cofactors, including heatshock proteins (Marivoet *et al.*, 1992) and forkhead transcription factors (Yang *et al.*, 2005). Androgen deprivation in prostate cancer cells results in apoptosis and G1 arrest (Heisler *et al.*, 1997; Watson *et al.*, 2005). Paracrine signals have been shown as necessary for androgen-deprived cells to undergo apoptosis, highlighting the importance of the stromal microenvironment (Gao *et al.*, 2006). Unfortunately, cells under continuous androgen-ablation develop resistance mechanisms (Watson *et al.*, 2005), a progress that is inevitable in advanced prostate cancers therapy. Prostate cancer progression always involves the activation of the AR. Several AR-activating mechanisms have been proposed (Feldman and Feldman, 2001). AR mutations can lead to a chronically activated state or to AR activation by non-androgenic steroid-hormones or androgen receptor antagonists (Taplin *et al.*, 1995). Further hypersensitivity of the AR, either by amplification (Visakorpi *et al.*, 1995), increased AR sensitivity and stability (Gregory *et al.*, 2001b) or de novo androgen synthesis (Locke *et al.*, 2008) has been described. Changes in corepressor or coactivator expression have also been implicated in the development of CRPC (Gregory *et al.*, 2001a).

The PI3K/AKT signalling cascade is also frequently dysregulated in prostate cancer (Shen and Abate-Shen, 2010). PI3K is activated in cells upon growth factor receptor activation. PI3K converts PtdIns(4,5)P_2 to PtdIns(3,4,5)P_3, resulting in the phosphorylation of AKT that subsequently activates or inhibits genes that are regulators of apoptosis, such as BAD (del Peso *et al.*, 1997) and FOXO1 (Brunet *et al.*, 1999), and cell cycle transition as CDKN1B (Collado *et al.*, 2000). AKT signaling is hyperactivated in approximately 30 to 50% of prostate cancers (Morgan *et al.*, 2009). In the majority of cases, this hyperactivity is due to loss of PTEN but can also occur because of AKT or PI3K hypersensitivity (Boormans *et al.*, 2008; Lee *et al.*, 2010). AKT activation is critical for disease recurrence, wherein 90% of patients with PTEN loss and hyperactivated AKT experienced a biochemical relapse. However, 88% of patients with wildtype PTEN did not relapse (Bedolla *et al.*, 2007). Mouse models have corroborated the role of PTEN in metastasis (Ding *et al.*, 2011; Wang *et al.*, 2003).

In this thesis, the regulation of FOXO1 by miRNAs was studied. FOXO1 is a member of the forkhead box transcription factors. Members of the forkhead box transcription factor family have a conserved “forkhead” or “winged helix” DNA-binding domain (Kaufmann and Knochel, 1996). Members of the forkhead box transcription factor class O bind to the consensus motif 5'-TTGTTTAC-3' (Birkenkamp and Coffer, 2003). Other members of this class include FOXO3a and FOXO4. FOXO1 suppresses tumors via a transcriptional regulation of crucial cell cycle and apoptosis regulators, such as CDKN1B (Machida *et al.*, 2003), NOLC1 (Kops *et al.*, 2002), BAX (Kim *et al.*, 2005) and TRAIL (Modur *et al.*, 2002). Akt-mediated FOXO1 phosphorylation results in the translocalisation of phosphorylated FOXO1 to the cytoplasm (Rena *et al.*, 1999). FOXO1 activity is further regulated by AKT-independent mechanisms, such as acetylation and deacetylation (Jung-Hynes *et al.*, 2009; Motta *et al.*, 2004) and ubiquitilation (Matsuzaki *et al.*, 2003).

AR and AKT signalling are interwoven at different stages. AKT can regulate AR expression in androgen-dependent and androgen–independent cell lines (Ha *et al.*, 2011). PTEN also inhibits AR activity by AKT-independent mechanisms (Wu *et al.*, 2006b). Especially FOXO1 exemplifies a strong link between AKT and AR signalling. FOXO1 inhibits both ligand-mediated transcriptional activation of the AR (Fan *et al.*, 2007) and ligand-independent activation of AR (Liu *et al.*, 2008b). Concurrently, the ligand-bound AR can upregulate IGF1R expression thereby enhancing phosphorylation of FOXO1 (Fan *et al.*, 2007). Subsequently, FOXO1 transcriptional activity can be inhibited by androgens via interaction with the AR (Li *et al.*, 2003).

1.3 miRNA regulation in cancer

Since the discovery of miRNAs at the beginning of the decade, their regulation has been involved in a multitude of physiological and pathological processes. miRNAs were first reported to be dysregulated in cancer in 2002, when Calin *et al.* (Calin *et al.*, 2002) described a deletion at 13q14 in chronic lymphocytic leukemia. The locus harbors the miR-15/miR-16 cluster, which not only is downregulated in these tumors but also regulates BCL2 expression. Early studies suggested a predominant downregulation of miRNAs (Lu *et al.*, 2005; Michael *et al.*, 2003). This hypothesis was supported by the observation that DICER expression can be downregulated in cancer (Karube *et al.*, 2005). However, further studies revealed both up- and downregulation of miRNA in all solid tumors and leukemias. Interestingly, while some miRNAs seem to have a tissue-specific function and are only expressed in specific cancers, others are universally over- or underexpressed in cancer. For example, miR-21 has been shown to be upregulated in almost all solid tumor types, including prostate, breast, lung, pancreas, stomach, colon and glioblastoma (Chan *et al.*, 2005; Iorio *et al.*, 2005; Volinia *et al.*, 2006).

1.3.1 miRNA profiling and their utilization as molecular markers

The frequent deregulation of miRNAs in cancer makes them attractive new markers for cancer detection and monitoring. miRNAs can either serve as diagnostic, prognostic or predictive markers or can monitor therapy success. Studies have suggested that miRNAs can help to differentiate cancer from normal tissue, discriminate different tumors subtypes, characterize poorly differentiated tumors and identify tumors of unknown origin (Cowland *et al.*, 2007).

The stability of miRNAs, even in degraded material, provides an advantage in using them over other markers. Studies have shown that miRNAs can be stably expressed in degraded total RNA samples from human tissues (Jung *et al.*, 2010), and they remain detectable in archived formalin-fixed, paraffin-embedded tissue (Glud *et al.*, 2009; Hasemeier *et al.*, 2008; Hui *et al.*, 2009; Siebolts *et al.*, 2009; Szafranska *et al.*, 2008; Zhang *et al.*, 2008). miRNA measurements in body fluids, such as blood or urine, will become more crucial for diagnostic purposes. (Boeri *et al.*, 2011; Lodes *et al.*, 2009; Mitchell *et al.*, 2008; Yaman Agaoglu *et al.*, 2011). miRNAs are present in body fluids as free miRNAs in exosomes (Michael *et al.*, 2010), associated with AGO2 proteins (Arroyo *et al.*, 2011) or in circulating tumor cells (Zhou *et al.*, 2010). In prostate cancer, miR-21 and miR-141 may serve as non-invasive markers (Mitchell *et al.*, 2008; Yaman Agaoglu *et al.*, 2011; Zhang *et al.*, 2011).

The current prognostic models that rely primarily on clinical parameters remain inaccurate, as described in 1.2.3. miRNA incorporation into models based on clinical markers may improve the accuracy of the existing models. A more accurate prognosis helps to avoid

over-treatment of patients because treatment will be given to only the responsive patients, whereas the others, who gain no clinical benefit, will negate the suffering caused by severe toxic side-effects. Early studies have shown that miRNAs are associated with tumor aggressiveness (Lin *et al.*, 2008), perineural invasion (Prueitt *et al.*, 2008) and androgen-dependence (Leite *et al.*, 2009; Lin *et al.*, 2008; Porkka *et al.*, 2007).

Before this thesis was conducted several groups had performed miRNA profiling in prostate cancer. Ozen *et al.* (Ozen *et al.*, 2008) identified exclusively downregulated miRNAs, whereas 3 other studies observed both up- and downregulated patterns (Ambs *et al.*, 2008; Porkka *et al.*, 2007; Volinia *et al.*, 2006). However, the results of these studies were highly contradictory.

The Venn diagram (Figure 5) highlights the lack of concordantly up- or downregulated miRNAs identified by these studies and 17 out of 105 detected miRNAs were even described to be regulated in inverse directions. The discrepancies of these early studies may be explained by differences in tissue selection, RNA and the detection platforms used. The results highlighted the need for accurate profiling in prostate cancers.

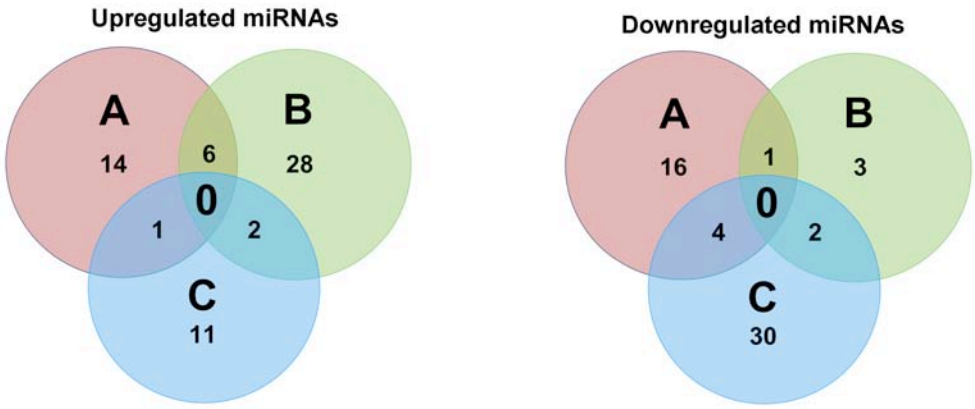

Figure 4: miRNA deregulation in prostate cancer

A Venn diagram of the upregulated and downregulated miRNAs in prostate cancer as investigated in 3 independent profiling studies. (A) Ambs *et al.* (Ambs *et al.*, 2008) investigated 329 miRNAs in total. (B) Volinia *et al.* (Volinia *et al.*, 2006) investigated 228 miRNAs in total. (C) Porkka *et al.* (Porkka *et al.*, 2007) investigated 319 miRNAs in total. The figure adopted was adopted from Schaefer *et al.* (Schaefer *et al.*, 2010a).

1.3.2 Regulation of miRNA expression

Changes in miRNA expression in cancer can be due to a plethora of intracellular changes during carcinogenesis, the most relevant of which are summarized in table 1.

miRNA genes are susceptible to mutations and are frequently located at fragile sites, minimal regions of loss of heterozygosity, and at minimal regions of amplification in cancer (Calin *et al.*, 2004). Additionally, specific single nucleotide polymorphisms have been associated with cancer risk (Gao *et al.*, 2011). As mentioned above, miRNA gene loci can be intergenic, intronic or exonic. Intronic and exonic miRNAs are coexpressed with their host genes, wherein both genes play a vital role in carcinogenesis. The combined expression of miR-106/miR-25 cluster and its host gene, MCM7, in mice induces malignant transformation (Poliseno *et al.*, 2010).

Mutations or polymorphisms in miRNA genes or target genes can result in qualitative changes in miRNA regulation because of altered miRNA target binding or de novo targeting of genes by a miRNA.

miRNA expression is not exclusively controlled by genomic variations in cancer. Epigenetic modifications play important roles in regulating miRNAs in cancer, such as the hypermethylation of promotors or histone modifications. Several miRNAs, such as miR-34a (Lodygin *et al.*, 2008), miR-101 (Varambally *et al.*, 2008), miR-126 (Saito *et al.*, 2009), miR-145 (Zaman *et al.*, 2010) and miR-193b (Rauhala *et al.*, 2010) are silenced by CpG methylation in prostate cancer. Changes in the trimethylation status of the histone 3 tail at lysines 4 or 27 correspond to expression changes of several miRNA genes (Ke *et al.*, 2009). Additionally, binding of the VDR to the MCM7 promoter induces rapid changes in histone 4 lysine 9 acetylation and in the subsequent transcription of the miR-106b/miR-25 cluster (Thorne *et al.*, 2010).

miRNA expression can also be dysregulated by aberrantly expressed transcription factors. In prostate cancer, this has been shown for miR-101, which is transcriptionally regulated by HIF1B (Cao *et al.*, 2010), and for miR-34a/c (Rokhlin *et al.*, 2008) and miR-145 (Chen *et al.*, 2010a), which are both controlled by tumor suppressor TP53. Most important, several miRNAs are regulated by the AR.

miRNAs are subjected to several post-transcriptional processing steps. In cancer, pri-miRNA levels do not correlate with mature miRNA levels, indicative of dysfunctional processing in these samples (Thomson *et al.*, 2006). DICER is downregulated in lung cancer (Karube *et al.*, 2005) but overexpressed in prostate cancer and ovarian serous carcinoma (Chiosea *et al.*, 2006; Flavin *et al.*, 2008). In breast cancer, alternative splicing and the use of an alternative promoter can alter DICER translation efficiency (Irvin-Wilson and Chaudhuri, 2005). In several mouse models, DICER functions as a haploinsufficient tumor suppressor (Kumar *et al.*, 2009). DROSHA, the second RNAse II enzyme that processes miRNA

transcripts, and XPO5 are upregulated in certain cancers (Catto *et al.*, 2009; Sand *et al.*, 2010). An inactivating mutation in XPO5 in cancer cells resulted in an accumulation of pri-miRNAs in the nucleus (Melo *et al.*, 2010). Recent studies have focused on RNA-binding proteins that may influence not only miRNA processing but also the binding of the miRISC complex to its target (Kedde *et al.*, 2007; Trabucchi *et al.*, 2009).

Table 1: Potential mechanisms for altered microRNA expression and activity in cancer (adapted according to Cowland *et al.* (Cowland *et al.*, 2007))

Mechanism of dysregulation	Effect
1. Genome alterations Deletion, amplification, translocation	Increased or decreased miRNA
2. Mutation/polymorphism of the miRNA gene	Increased or decreased miRNA Altered binding of miRNA
3. Mutation/polymorphism of the miRNA binding site in the target mRNA gene	Altered binding of miRNA
4. Mutation of a non-target mRNA gene	Possible binding of miRNA to non-target mRNA
5. Mutation in the biogenesis apparatus Upregulation of DROSHA Downregulation of DICER	Impaired processing of miRNA
6. Epigenetic mechanisms Methylation of miRNA gene promoter Histone modifications	Decreased miRNA formation

1.3.3 Function of miRNAs in carcinogenesis

miRNAs regulate all hallmarks of cancer, including apoptosis, insensitivity to anti-growth signals and self-sufficient growth signalling, tissue invasion and metastasis, sustained angiogenesis and limitless replicative potential (Hanahan and Weinberg, 2011) (Figure 5). miRNAs can act as tumor suppressors as well as oncogenes depending on their target. The miRNA regulatory machinery is highly complex, wherein one miRNA can target hundreds of mRNAs, and one mRNA can be targeted by multiple miRNAs. Currently, only a fraction of miRNA targets have been experimentally characterized. Because miRNAs take on hundreds of targets concurrently, they are attractive targets for cancer therapy. By knocking-down or re-establishing the expression of one miRNA, one might be able to target a plethora of genes. The complexity of the miRNA regulatory networks may also account for their observed tissue-specific functions, wherein different target combinations may lead to inverse functions. For example, miR-184, which is overexpressed in squamous cell carcinoma, inhibits apoptosis and increases cell proliferation (Wong *et al.*, 2009), whereas its presence neuroblastoma yields inverse effects (Tivnan *et al.*, 2010).

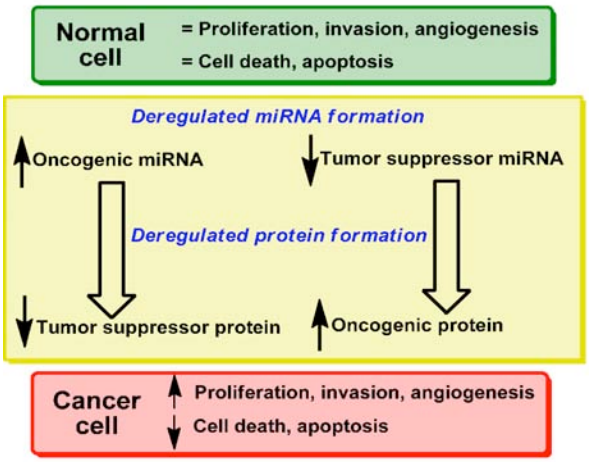

Figure 5: miRNAs regulate all hallmarks of cancer (Schaefer *et al.*, 2010a)

Even though the functional relevance of miRNA genes in prostate cancer has only been studied in recent years, they have been shown to clearly regulate all critical steps of prostate cancer carcinogenesis. A multitude of miRNAs have been described in the context of prostate carcinogenesis, the best of which are summarized in table 2.

The impact of miRNAs on androgen-independent growth in prostate cancer is well studied. Several groups have performed expression profiling on androgen-dependent and androgen-independent cell lines and have identified a subset of differentially expressed miRNAs in these cells. To identify miRNAs that play a role in androgen-signalling, miRNA profiling has been performed in androgen-dependent and androgen-independent cell lines (DeVere White *et al.*, 2009; Lin *et al.*, 2008; Sun *et al.*, 2009; Xu *et al.*, 2010). Some of the miRNAs that have been identified, have been studies more extensively in subsequent studies and have been proven to be critical regulators of androgen-independent growth. miR-125b stimulates androgen-independent growth in androgen-dependent prostate cancer cells and concordantly regulates apoptosis by inhibiting the pro-apoptotic BAK1 (DeVere White *et al.*, 2009; Shi *et al.*, 2007; Shi *et al.*, 2010b).

miR-221 and miR-222, which are strongly upregulated in androgen-independent cells induce androgen-independent growth and lower the response of the PSA-promoter to 5α−DHT treatment (Sun *et al.*, 2009). Recently, the function of the miR-221/miR-222 cluster has received a considerable attention in prostate cancer lately. The expression of this miRNA cluster not only is dependent on androgen status but also is regulated by concordant binding of C-JUN and NFKB to its promoter (Galardi *et al.*, 2011) or by thrombin (Hu *et al.*, 2009a) or genistein treatment (Chen *et al.*, 2011). Both miRNAs primarily function in cell cycle transition (Galardi *et al.*, 2007) by inhibiting CDKN1B (Galardi *et al.*, 2007; Hu *et al.*, 2009a; Mercatelli *et al.*, 2008) and promoting the tumor growth of prostate cancer xenografts in mice (Mercatelli *et al.*, 2008).

miR-21, an universal oncogene that has important regulatory functions in various tumors, has also garnered considerable attention in prostate cancer, wherein it regulates apoptosis and invasiveness by targeting PTEN and AKT, (Yang *et al.*, 2010), PDCD4 (Lu *et al.*, 2008; Shi *et al.*, 2010a), BMPRII (Qin *et al.*, 2009) and MARCKS (Li *et al.*, 2009b). miR-21 mediates resistance to the chemotherapeutic docetaxel: thus, it is a potential predictive marker for successful therapy or a target structure for a combined treatment with docetaxel (Shi *et al.*, 2010a). miR-21 expression can be regulated in prostate cancer by the not only AR (Ribas and Lupold, 2010) but also the IFN via STAT3 and NFKB (Yang *et al.*, 2010).

miR-16, the miR-34 cluster and miR-205 are the best-described tumorsuppressive miRNAs in prostate carcinogenesis. miR-16, the first-described dysregulated miRNA in cancer, inhibits growth of xenografts in mice by regulating various cell cycle genes, such as CDK1/2 and CCND1 (Bonci *et al.*, 2008; Takeshita *et al.*, 2010). Because, the miR-34 cluster sensitizes cells to docetaxel and paclitaxel, it serves as a potential predictive marker for therapy outcome or as a novel target for a combined chemo- and RNAi-therapy (Kojima *et al.*, 2010; Rokhlin *et al.*, 2008). miR-205 has been well described in the epithelial-mesenchymal transition of prostate cancer: thus it may serve as an interesting target structure for metastatic cancer therapy (Gandellini *et al.*, 2009). Additionally, it mediates the resistance to docetaxel (Bhatnagar *et al.*, 2010; Gandellini *et al.*, 2009).

The current prostate cancer studies have shown that miRNAs regulate critical steps in tumorigenesis: thus, they become attractive targets for novel therapies either alone or in combination with chemotherapeutical agents.

Table 2: The function of miRNAs in prostate cancer

miRNA	Regulation	Function	Target genes	References
miR-16		Reduces growth of bone metastases in a prostate xenograft model; malignant transformation of benign prostate cells	CCND1 WNT3A BCL2	(Bonci *et al.*, 2008; Takeshita *et al.*, 2010)
miR-21	IFN recruits Stat3 and NFKB to the miR-21 promoter, regulated by AR	Resitance to docetaxel, apoptosis, invasiveness, enhanced tumor growth in xenografts	PDCD4 PTEN AKT MARCKS BMPRII	(Li *et al.*, 2009b; Lu *et al.*, 2008; Qin *et al.*, 2009; Ribas and Lupold, 2010; Shi *et al.*, 2010a; Yang *et al.*, 2010)
miR-34a/ miR-34c	Hypermethylation of promoter, regulated by p53, downregulated upon radiation	Mediate resistance to doxorubicin and paclitaxel, inhibits cancer cell stemness	SIRT1 BCL2	(Josson *et al.*, 2008; Kojima *et al.*, 2010; Liu *et al.*, 2011; Lodygin *et al.*, 2008; Rokhlin *et al.*, 2008; Sarveswaran *et al.*, 2010)
miR-125b	Regulated by AR	Androgen-independent growth, growth of xenografts in intact and castrated nude mice	Bak1 P53 PUMA	(DeVere White *et al.*, 2009; Shi *et al.*, 2007; Shi *et al.*, 2010b; Takayama *et al.*, 2011)
miR-205	Hypermethylation of promoter	Mediates resistance to docetaxel, epithelial-mesenchymal transition	BCL2 E2F6 PKCE	(Bhatnagar *et al.*, 2010; Gandellini *et al.*, 2009)
miR-221/ miR-222	c-Jun and NFKB form transcriptional complex, thrombin and genistein treatment upregulate expression	Cell cycle transition, promote growth in xenografts	CDKN1B ARH1	(Chen *et al.*, 2011; Galardi *et al.*, 2007; Galardi *et al.*, 2011; Hu *et al.*, 2009a; Mercatelli *et al.*, 2008)

1.3.4 miRNAs as putative therapeutics

The discovery of the roles of miRNAs in carcinogenesis has propelled miRNAs to become focal targets for novel therapeutic approaches, and efforts have been made in recent years to develop miRNA-based therapeutics. Generally, the discussed approaches can be included into one of the following groups (Table 3):

1. **Inhibition of an oncogenic miRNA**

   Treating cells with the antisense strand of the miRNA, termed anti-miRNA oligonucleotides (AMOs), is the most direct approach to target the function of an oncogenic miRNA, (Esau, 2008). The feasibility of this approach has been discussed in several studies to date. To improve the effect of AMOs, multitarget AMOs (mtAMOs) that target multiple miRNAs concurrently, have been developed. This technique improves the effect on prostate cancer cells as compared with single AMOs (Wang, 2011). miRNA sponges offer a second approach to improve therapy with antisense oligonucleotides (Ebert *et al.*, 2007). miRNA sponges are expressed from transgenes and harbor multiple complementary binding sites for a single oncogenic miRNA. Binding of the miRNA to the sponge relieves the repression of its target genes. miRNA erasers, long tandem repeats of antisense miRNAs, employ a similar approach (Sayed *et al.*, 2008). Inhibition of an oncogenic miRNA can also be accomplished by small molecules. Recently, several small molecules that either inhibit miRNAs directly or inhibit components of the miRNA processing pathway have been identified (Chintharlapalli *et al.*, 2009; Watashi *et al.*, 2010).

2. **Restoration of a tumorsuppressive miRNA**

   The restoration of a tumorsuppressive miRNA results in an inhibition of a set of oncogenic mRNAs. Oligonucleotides that directly mimic a tumorsuppressive miRNA may restore miRNA function or inhibit an oncogenic mRNA. Designing artificial miRNAs to target the 3' UTR of oncogenic mRNAs on the basis of currently known target-binding algorithms has resulted in a marked inhibition of this oncogene (De Guire *et al.*, 2010). Hairpin-oligodesoxynucleotides have also been shown to bind and inhibit oncogenic mRNAs (Hofmann *et al.*, 2009).

3. **Epigenetic modulation of miRNA expression**

   Epigenetic silencing is an important mechanism by which miRNA genes are silenced during carcinogenesis. Therefore, interaction with the epigenetic machinery to re-express miRNAs is an attractive approach. Combination therapy with histone deacetylase and methyltransferase inhibitors upregulates epigenetically silenced miRNA levels (Saito *et al.*, 2009). Hydroxamic acid HDACi LAQ824 treatment upreguated 22 miRNAs and downregulated 5 miRNAs (Scott *et al.*, 2006).

4. Improvement of existing therapies

Recent therapeutic strategies not only have focused on the regulation of miRNA function but also have tried to improve existing therapies. For example, glioma cells can be sensitized to treatment with 5-fluoroacyl if it is simultaneously delivered to cells with miR-21 (Ren *et al.*, 2010). Cells can also be sensitized to doxorubicin if they are cotransfected with TP53 and a synthetic p21-targeting miRNA (Idogawa *et al.*, 2009). Moreover, miR-521 can sensitize cancer cells to radiation (Josson *et al.*, 2008). The specificity of viral-based treatments can be enhanced by introducing miRNA binding sites to the viral genome, thereby viral replication is prevented in all cells but the target cells. The introduction of miR-145 and miR-143 binding sites downstream of the herpes simplex virus ICP4 gene restricts oncolytic activity to prostate cancer cells where expression of this miRNA is lost (Lee *et al.*, 2009a). A similar approach has been administered to improve the specificity of an oncolytic virus in liver cancer (Cawood *et al.*, 2009). Four binding sites of the liver-specific miR-122 were introduced downstream of the EA1 binding cassette in a cytotoxic liver adenovirus.

Table 3: Approaches to therapeutically target miRNA function

Approach	Description	References
A) Inhibition of an oncogenic miRNA		
Anti-miRNA oligonucleotides	Targeting the function of a single miRNA with an antisense oligodesoxyribonucleotide	(Esau, 2008)
Multi-targeting anti-miRNA oligonucleotides	Targeting the function of multiple miRNAs with a single antisense oligodeoxyribonucleotide	(Wang, 2011)
Sponges	Targeting the function of a single miRNA by a transgene that carries multiple binding sites for the miRNA	(Ebert *et al.*, 2007)
Erasers	Targeting the function of a single miRNA by transfection of a double stranded oligonucleotide with long tandem repeats of the antisense sequence	(Sayed *et al.*, 2008)
Small Molecules	Targeting the function of a single miRNA or components of miRNA processing by small molecules	(Chintharlapalli *et al.*, 2009; Watashi *et al.*, 2010)
B) Inhibition of an oncogenic mRNA/ Restoration of miRNA function		
Design of artificial miRNAs	Designing novel miRNAs to target 3' UTRs of oncogenic mRNAs	(De Guire *et al.*, 2010)
Design of hairpin-loop oligodeoxynucleotides	Designing short DNA sequences to target binding sites of known miRNA inhibition	(Hofmann *et al.*, 2009)
Delivery by viral expression vectors	Reexpression of miRNAs through viral vector-mediated delivery	(Kota *et al.*, 2009; Nair, 2008; Wang *et al.*, 2011)
C) Epigenetic modulation of miRNA expression		
Combined treatment with methyltransferase and histone deacetylase inhibitors	Reexpression of epigenetically silenced miRNAs	(Saito *et al.*, 2009)
Treatment with hydroxamic acid HDACi LAQ824	Reexpression of epigenetically silenced miRNAs or inhibition of aberrantly expressed miRNAs	(Scott *et al.*, 2006)
D) Improvement of existing therapies		
Sensitizing cells to radiation	Overexpression of miR-106b or miR-521 to sensitize cells to radiation	(Josson *et al.*, 2008)
Sensitizing cells to chemotherapeuticals	miRNA overexpression can sensitize cells to treatment with chemotherapeutical (5-Fluoroacyl or doxorubicin)	(Idogawa *et al.*, 2009; Ren *et al.*, 2010)
Improving specificity of viral treatment	Introduction of miRNA binding sites downstream of viral reproduction genes can restrict their activity to cancer cells	(Cawood *et al.*, 2009; Lee *et al.*, 2009a)

Although extensive resources have been invested for the development of miRNA-based therapies, the delivery of the oligonucleotides to the target cells remains an obstacle. Efforts into developing new formulations of transfection agents have been undertaken in vitro (Akinc *et al.*, 2008; Chen *et al.*, 2010b; Liu *et al.*, 2010; Rahbek *et al.*, 2010). Furthermore, although viral-mediated delivery of miRNA genes to the tumor is investigated for cancer therapy (Kota *et al.*, 2009; Nair, 2008; Wang *et al.*, 2011), it prompts serious concern that needs to be resolved (Tenoever, 2009).

Successful in vivo studies exist for a few miRNAs in selected cancers, including the oncogenes miR-182 (Huynh *et al.*, 2010), miR-10b (Ma *et al.*, 2010) and let-7 (Trang *et al.*, 2010) and the tumorsuppressors miR-16 (Takeshita *et al.*, 2010) and miR-26a (Kota *et al.*,

2009). The studies showed that systemic treatment, primarily through tail vein injection, is a suitable approach to deliver miRNAs to primary tumors and metastases; moreover, miRNA treatment was shown to result in a tumor regression. The treatment was well tolerated by animals likely because the targeted miRNAs are inversely expressed in the surrounding normal tissues.

1.4 Thesis aims

miRNAs are highly versatile molecules that have revolutionized our understanding of gene regulation in recent years. Their deregulation in cancer allows for their potential use in a plethora of clinical applications. Studies have shown that miRNA profiling is superior to mRNA profiling in detecting tumors.

At the inception of this thesis, miRNA deregulation in prostate cancer had been inadequately described. Therefore, the first aim of this thesis was to establish a miRNA profile in fresh frozen prostate cancer specimens compared with normal adjacent tissue.

Dysregulated miRNAs were identified by microarray profiling and were validated subsequently by RT-qPCR. Identified miRNAs were statistically analyzed to investigate their potential as diagnostic and prognostic markers.

The degree of miRNA deregulation in biochemical relapse patients was determined in formalin-fixed, paraffin-embedded tissue. Those miRNAs may represent ideal biomarkers for identifying aggressive tumors either after radical prostatectomy or in fine-needle biopsies.

The second part of the thesis focuses on the functional characterization of selected miRNAs in prostate cancer. The identification of dysregulated miRNAs provided a solid basis for the subsequent functional investigation of their expression. To investigate the functional relevance of miRNAs, in silico target predictions were performed.

In subsequent steps, analysis was concentrated on the functional impact of miR-96. The oncogenic effects of miR-96 were assessed by transfection experiments in prostate cancer cell lines. The in-silico predicted targets were experimentally validated by reporter gene assays and with monitoring of the transcript and protein expression in prostate cancer cells.

miR-133b was the second miRNA to be characterized in prostate cancer. miR-133b was identified by our collaborators as a regulator of death receptor-mediated apoptosis. The observed downregulation of miR-133b in other cancer entities (Bandres *et al.*, 2006; Guo *et al.*, 2009; Ichimi *et al.*, 2009; Navon *et al.*, 2009; Wong *et al.*, 2008b) prompted us to assess miR-133b expression levels in prostate cancer and to validate its functional impact in prostate cancer cell lines, although it was not identified in the initial profiling study.

To affirm the biological significance of the identified miR-96 and miR-133b regulatory mechanisms in prostate cancer, their transcript and protein levels in human prostate cancer specimens were correlated with the expression levels of their target genes.

Taken together, this thesis elucidates the mechanisms governing the deregulation of miRNA expression in prostate cancer and demonstrates that miR-96 and miR-133b can significantly affect carcinogenesis in prostate cancer.

2. Material and methods

2.1 Material

2.1.1 Equipment

2100 Bioanalyzer	Agilent Technologies GmbH, Böblingen, Germany
2301 Macrodrive 1 Power Supply	LKB Bromma
ABI 7900	Applied Biosystems, Darmstadt, Germany
Agagel Mini	Biometra, Goettingen, Germany
Antares 48 Laminar Flow Box	Cotech Vertrieb GmbH, Berlin, Germany
CB 210 Incubator	Binder, Tuttlingen. Germany
Coolpix 990	Nikon GmbH, Düsseldorf, Germany
DM 2000 microscope	Leica Mikrosysteme Vertrieb GmbH, Wetzlar, Germany
DNA Microarray laser scanner	Agilent Technologies, Böblingen, Germany
Ecom 6122	Eppendorf AG, Hamburg, Germany
FACSCalibur	BD Biosystems, Heidelberg, Germany
FACScan	BD Biosystems, Heidelberg, Germany
Fluoro-S Multiimager	BioRad, München, Germany
Fluoroskan Ascent	Thermo Lab Systems, Langenselbold, Germany
Fluoroskan Ascent FL	Thermo Lab Systems, Langenselbold, Germany
HT III photometer	Anthos Labtech Instruments GmbH, Wals-Siezenheim, Austria
Leitz DMRBE fluorescence microscope	Leica Mikrosysteme Vertrieb GmbH, Wetzlar, Germany
Leitz Fuovert Microscope	Leica Mikrosysteme Vertrieb GmbH, Wetzlar, Germany
LightCycler 480	Roche Applied Sciences, Mannheim, Germany
Mini Power Pack P20	Biometra, Goettingen, Germany
Mitrras LB 940	Berthold Technologies, Bad Wildbad, Germany
NanoDrop ND-1000	NanoDrop, Wilmington, DE, USA
RM 2125 microtome	Leica Mikrosysteme Vertrieb GmbH, Wetzlar, Germany
TissueLyser	Qiagen, Hilden, Germany
UNO Thermoblock	Biometra, Goettingen, Germany
XCell SureLock	Invitrogen, Darmstadt, Germany

2.1.2 Consumables

24-Multiwell Insert System	BD Biosystems, Heidelberg, Germany
Biocoat Tumor Invasion System 24 Well	
Biocoat FluoroBlock	BD Biosystems, Heidelberg, Germany
Falcon cell cultureware (T25 and T75 flask, 96-, 24- and 6- well plates)	BD Biosystems, Heidelberg, Germany
Immobilon-P^{SQ} transfer membranes (0.45 µm)	Millipore Corporation, Billerica, MA, USA
Lab-Tek Chamberslides	Nunc, Roskilde, Denmark
Primaria cell culture ware (T25, T75 flask, 96-, 24-, 6-well plates)	BD Biosystems, Heidelberg, Germany
White 96-well plates, flat bottom; untreated	Nunc, Roskilde, Denmark
White 96-well RT-qPCR plates	Roche Applied Sciences, Mannheim, Germany

2.1.3 Chemicals, reagents and kits

RNA and DNA extraction

miRNAeasy Mini Kit	Qiagen, Hilden, Germany
QIAprep Spin Mini Prep Kit	Qiagen, Hilden, Germany
QiaQuick Gel Extraction Kit	Qiagen, Hilden, Germany
RecoverAll Total Nucleid Acid Isolation Kit	Ambion, Austin, TX, USA

PCR

2X TaqMan Fast Universal PCR Master Mix, No AmpErase UNG	Applied Biosystems, Darmstadt Germany
2X TaqMan Universal Mastermix II, no UNG	Applied Biosystems, Darmstadt, Germany
2X TaqMan Universal PCR Master Mix, No AmpErase UNG	Applied Biosystems, Darmstadt, Germany
AmpliTaq Gold Polymerase	Invitrogen, Darmstadt, Germany
Fast SYBR Green Master Mix	Applied Biosystems, Darmstadt, Germany
PCR Supermix High Fidelity	Invitrogen, Darmstadt, Germany
Platinum Pfx DNA Polymerase	Invitrogen, Darmstadt, Germany
TaqMan MicroRNA reverse transcription kit	Applied Biosystems, Darmstadt, Germany
Transcriptor First Strand cDNA Synthesis Kit	Roche Applied Sciences, Mannheim, Germany
Universal Probes Master	Roche Applied Sciences, Mannheim, Germany

Profiling

8-plex 15K miRNA microarrays (AMADID 016436)	Agilent Technologies, Böblingen, Germany
Megaplex Primer Pool, Human Pools Set v3.0	Applied Biosystems, Darmstadt Germany
TaqMan Array Human MicroRNA A+B Cards v3.0	Applied Biosystems, Darmstadt Germany
Whole human genome 44k microarrays (AMADID-014850)	Agilent Technologies, Böblingen, Germany

Kits for Tissue Culture

ApoTarget Annexin-V FITC apoptosis kit	Invitrogen, Darmstadt, Germany
Cell Proliferation Kit II (XTT)	Roche Applied Sciences, Mannheim, Germany Dual Light Luciferase and β-Galactosidase Reportergene Assay
	Applied Biosystems, Darmstadt, Germany

Enzymes

Calf Intestine Alkaline Phosphatase	GE Healthcare, München, Germany
DNAse	Qiagen, Hilden, Germany
NaeI	New England Biolabs, Frankfurt am Main, Germany
RNAse A	Qiagen, Hilden, Germany
SacI	New England Biolabs, Frankfurt am Main, Germany
SpeI	New England Biolabs, Frankfurt am Main, Germany
T4 DNA Ligase	New England Biolabs, Frankfurt am Main, Germany

Molecular Weight Markers

Full-Range Rainbow Molecular Weight Marker	GE Healthcare, München, Germany
HiMark Pre-stained High Molecular Weight Protein Standard	Invitrogen, Darmstadt, Germany
MagicMark XP Western Protein Standard	Invitrogen, Darmstadt, Germany
Molecular Weight Marker X	Roche Applied Sciences, Mannheim, Germany
Molecular Weight Marker XIV	Roche Applied Sciences, Mannheim, Germany

Transfection Reagents

siPort NeoFX	Ambion, Austin, TX, USA
FuGene HD	Roche Applied Sciences, Mannheim, Germany

Chemicals and others

3-[4,5-dimethylthiazol-2-yl]-2,5-diphenyl tetrazolium bromid (MTT)	Sigma Aldrich, München, Germany
4-12% Tris-Glycine gel	Invitrogen, Darmstadt, Germany
Acrylamide Bis (37.5:1) 40% solution	Serva, Heidelberg, Germany
Advanced ECL	GE Healthcare, München, Germany
Ammonium peroxydilsulfate	Merck KgH, Darmstadt, Germany
Ampicilline, ready made solution	Sigma Aldrich, München, Germany
Antibody diluent	Sigma Aldrich, München, Germany
Aquatex mounting medium	Merck KgH, Darmstadt, Germany
Bisbenzimide	Sigma Aldrich, München, Germany
Camptothecin	Sigma Aldrich, München, Germany
Chloroform	Sigma Aldrich, München, Germany
DMSO	Sigma Aldrich, München, Germany
ECL	Pierce, Bonn, Germany
Eosin solution, 1%	Waldeck GmbH und Co. Kg., Münster, Germany
Ethanol, absolute	J.T. Baker, Deventer, Holland
Ethidiumbromid	Sigma Aldrich, München, Germany
Eukitt mounting medium	Sigma Aldrich, München, Germany
Fluorescence mounting medium	Dako Deutschland GmbH, Hamburg, Germany
Formaldehyde, 4% solution	Herbeta Arzneimittel, Berlin, Germany
Kanamycine, 100x	Invitrogen, Darmstadt, Germany
Lovostatin	Biozol Diagnostika Vertrieb GmbH, Eching, Germany
LSAB system test	Dako Deutschland GmbH, Hamburg, Germany
Mayer's hemalaun solution	Hollborn und Söhne, Leipzig, Germany
Protein Assay	BioRad, München, Germany
Protein standard (Bovine serum albumin)	Sigma Aldrich, München, Germany
R1881	Perkin Elmer, Waltham, MA, USA
TEMED	Sigma Aldrich, München, Germany
Ultrapure X-Gal	Invitrogen, Darmstadt, Germany
Xylol	Sigma Aldrich, München, Germany

2.1.4 Buffers, solutions and cell culture media

PBS Buffer

TBE Buffer (Agarose gel electrophoresis)

90 mM	Tris base	Sigma Aldrich, München, Germany
90 mM	Boric acid	Pharmacia Biotech, Uppsala, Sweden
2 mM	EDTA	Sigma Aldrich, München, Germany
pH = 8		

Loading Buffer (DNA electrophoresis)

20%	Ficoll 400	Sigma Aldrich, München, Germany
0.1 M	Na_2EDTA, pH 8	Pharmacia Biotech, Uppsala, Sweden
1%	SDS	Sigma Aldrich, München, Germany
0.25%	Bromo phenolblue	Sigma Aldrich, München, Germany
0.25%	Xylene cyanol	Serva, Heidelberg, Germany

t-TBS

10 mM	Tris base	Sigma Aldrich, München, Germany
100 mM	NaCl	Merck KgH, Darmstadt, Germany
0.1%	Tween 20	Serva, Heidelberg, Germany

Laemmli Buffer

2.5 mM	Tris base	Sigma Aldrich, München, Germany
19.2 mM	Glycine	Sigma Aldrich, Germany
0.01%	SDS	Serva, Heidelberg, Germany
pH 8.3 to 8.8		

Anode Buffer I

25 mM	Tris base	Sigma Aldrich, München, Germany
20%	Methanol	J.T. Baker, Deventer, Holland

Anode Buffer II

300 mM	Tris base	Sigma Aldrich, München, Germany
20%	Methanol	J.T. Baker, Deventer, Holland

Cathode Buffer

25 mM	Tris base	Sigma Aldrich, München, Germany
40 mM	6-aminocaproic acid	Sigma Aldrich, München, Germany

Sample Buffer (2X, SDS-PAGE)

0.125 M	Tris base	Sigma Aldrich, München, Germany
20%	Glycerine	Merck KgH, Darmstadt, Germany
2%	SDS	Serva, Heidelberg, Germany
0.01%	bromo phenolblue	Sigma Aldrich, München, Germany
1%	DTT	Sigma Aldrich, München, Germany

RIPA buffer

150 mM	NaCl	Merck KgH, Darmstadt, Germany
1%	NP-40	Sigma Aldrich, München, Germany
0.5%	sodium deoxycholate	Serva, Heidelberg, Germany
0.1%	SDS	Serva, Heidelberg, Germany
50 mM	Tris base	Sigma Aldrich, München, Germany
10 mM	PMSF	Serva, Heidelberg, Germany
1 mg/ml	Aprotinin	Sigma Aldrich, München, Germany
10 mg/ml	Soybean Trypsine Inhibitor	MP biomedicals, Solo; OH, USA
0.5 M	EDTA	Sigma Aldrich, München, Germany

Stripping buffer

1 x	Laemmli Buffer	
20%	Methanol	J.T. Baker, Deventer, Holland

PI-staining solution

20 µg/ml	Propidiume iodide	Sigma Aldrich, München, Germany
200 µg/ml	RNAse A	Qiagen, Hilden, Germany
0.1%	Triton X-100	Serva, Heidelberg, Germany

Calcein staining solution

4 mg/ml	Calcein (Invitrogen, Darmstadt, Germany) in HBSS

Growth media for LNCaP, DU-145 and PC-3 cell lines:

500 ml	RPMI 1640	Invitrogen, Darmstadt, Germany
10%	FCS	PAA, Pasching, Austria
1 x	Penicillin/Streptomycin	PAA, Pasching, Austria

Growth media for BPH-1 cell line:

500 ml	RPMI 1640	Invitrogen, Darmstadt, Germanny
20%	FCS	PAA, Pasching, Austria
20 ng/ml	DHT	Sigma Aldrich, München, Germany
5 µg/ml	Transferrin	Roche Applied Sciences, Mannheim, Germany
5 ng/µl	Natriumselenit	Sigma Aldrich, München, Germany
5 ng/µl	Insulin	Sigma Aldrich, München, Germany

Synchronisation Medium

500 ml	RPMI 1640 w/o phenol red	Invitrogen, Darmstadt Germany
0.25%	charcoal FCS	PAA, Pasching, Austria
1 x	Penicillin/Streptomycin	PAA, Pasching, Austria

Medium for androgen treatment

500 ml	RPMI 1640 w/o phenolred	Invitrogen, Darmstadt, Germany
10%	charcoal FCS	PAA, Pasching, Austria
1 x	Penicillin/Streptomycin	PAA, Pasching, Austria

2.1.6 Oligonucleotides

Primers were designed using Primer3 (http://biotools.umassmed.edu/bioapps/primer3_www.cgi) or OligoPerfect Designer (http://tools.invitrogen.com/content.cfm?pageid=9716) and purchased from TIB Molbiol (Berlin, Germany). Universal probe library (UPL) probes were purchased from Roche Applied Sciences (Mannheim, Germany). Primer/probe sets were designed at the Roche Applied Sciences Homepage (http://www.roche-applied-science.com/sis/rtpcr/upl/ezhome.html).

TaqMan MicroRNA Arrays containing primers for reverse transcription, RT-qPCR primers and TaqMan probes were purchased from Applied Biosystems (Darmstadt, Germany).

For detection of FAIM, FASN, GSTP1 and GAPDH expression, commercially available mRNA-specific QuantiTect Primer Assays (Qiagen, Hilden, Germany) were used.

Table 4: Primers

Name	Application	Probe	Sequence 5' → 3'	Product size (nt)
Cav1_3UTR_BD1_f	PCR (Cloning)		GACTAGTTTCTGCCTTCTCATGATCCA	274
Cav1_3UTR_BD1_r	PCR (Cloning)		GGCCGGCGATGAAGCCCAGAAGTGAGC	
Cav1_3UTR_BD2_f	PCR (Cloning)		GACTAGTGCTCACTTCTGGGCTTCATC	306
Cav1_3UTR_BD2_r	PCR (Cloning)		GGCCGGCATTTTACAGCCCCTCCTTGG	
Cav1_3UTR_BD3_f	PCR (Cloning)		GACTAGTTCCTGGTGCCAATTTCAAGT	222
Cav1_3UTR_BD3_r	PCR (Cloning)		GGCCGGCCAGCCAATAAAGCGATGGTT	
Cav1_3UTR_f	PCR (Cloning)		GACTAGTTCCTGGTGCCAATTTCAAGT	1822
Cav1_3UTR_r	PCR (Cloning)		GGCCGGCTTGTGCAGGCTTGTAACCTT	
FOXO1_bd1_f	PCR (Cloning)		GACTAGTCTTTCGTCAGACTTGGCAGC	301
FOXO1_bd1_r	PCR (Cloning)		GGAGCTCAAGACATGAGGCCCATCACA	
FOXO1_bd2_f	PCR (Cloning)		GACTAGTATCATCCTCATTTTGGGGC	201
FOXO1_bd2_r	PCR (Cloning)		GGAGCTCTAATGAACAAATGGGGGCTC	
ITPR1_bd1_f	PCR (Cloning)		GACTAGTCTGATTCACCCACGAAGGTT	200
ITPR1_bd1_r	PCR (Cloning)		GGAGCTCTGCAAATCAGGTGCTTTCTG	
ITPR1_bd2_f	PCR (Cloning)		GACTAGTTTGTAGCTCCCGAGTGTCCT	175
ITPR1_bd2_r	PCR (Cloning)		GGAGCTCCGAGAAACAGCATCACCAGA	
FOXO1_SYBR_f	SYBR green qPCR		AAGAGCGTGCCCTACTTCAA	232
FOXO1_SYBR_r	SYBR green qPCR		GGCTTCGGCTCTTAGCAAAT	
TUBA1B_SYBR_f	SYBR green qPCR		CCAGATGCCAAGTGACAAGA	241
TUBA1B_SYBR_r	SYBR green qPCR		GATCTCCTTGCCAATGGTGT	
Cav1	UPL qPCR	UPL #26	TTCCTTCCTCAGTTCCCTTAAA	123
Cav1	UPL qPCR		GGGAACGGTGTAGAGATGTCC	
FOXO1_UPL_f	UPL qPCR	UPL #11	AAGGGTGACAGCAACAGCTC	86
FOXO1_UPL_r	UPL qPCR		TTCTGGCACACGAATGAACTTG	
ITPR1-realtime-f	UPL qPCR	UPL #2	AGTGACCGAGTGTTCCATGA	91
ITPR1-realtime-r	UPL qPCR		AGCGACAGAAAAAGGAGTGC	
TUBA1B_UPL_f	UPL qPCR	UPL #64	CCTTCGCCTCCTAATCCCTA	87
TUBA1B_UPL_r	UPL qPCR		AGCAGGCATTGCCAATCT	

Underlined sequences present introduced recognition sites for restriction enzymes.

Table 5: TaqMan miRNA Assays

miRNA	Mature miRNA Sequence
miR-10b	UACCCUGUAGAACCGAAUUUGUG
miR-16	UAGCAGCACGUAAAUAUUGGCG
miR-31	AGGCAAGAUGCUGGCAUAGCU
miR-96	UUUGGCACUAGCACAUUUUUGCU
miR-125b	UCCCUGAGACCCUAACUUGUGA
miR-130b	CAGUGCAAUGAUGAAAGGGCAU
miR-133b	UUUGGUCCCCUUCAACCAGCUA
miR-145	GUCCAGUUUUCCCAGGAAUCCCU
miR-149	UCUGGCUCCGUGUCUUCACUCCC
miR-181b	AACAUUCAUUGCUGUCGGUGGGU
miR-182	UUUGGCAAUGGUAGAACUCACACU
miR-182*	UGGUUCUAGACUUGCCAACUA
miR-183	UAUGGCACUGGUAGAAUUCACU
miR-184	UGGACGGAGAACUGAUAAGGGU
miR-205	UCCUUCAUUCCACCGGAGUCUG
miR-221	AGCUACAUUGUCUGCUGGGUUUC
miR-222	AGCUACAUCUGGCUACUGGGU
miR-375	UUUGUUCGUUCGGCUCGCGUGA
RNU6B	CGCAAGGAUGACACGCAAAUUCGUGAAGCGUUCCAUAUUUUU
Z30	UGGUAUUGCCAUUGCUUCACUGUUGGCUUUGACCAGGGUAUGAU CUCUUAAUCUUCUCUCUGAGCUG

2.1.8 Expression vectors and synthetic microRNAs

Synthetic microRNAs:

Synthetic pre-miR miRNA precursors and anti-miR miRNA inhibitors for transfecting into mammalian cells, were purchased from Applied Biosystems for the following miRNAs

Table 6: Synthetic miRNA precursors and inhibitors

miRNA	StemLoop Sequence 5' → 3'
miR-96	UGGCCGAUUUUGGCACUAGCACAUUUUUGCUUGUGUCUCUCCGCUCUGAGCAAU CAUGU GCAGUGCCAAUAUGGGAAA
miR-133b	CCUCAGAAGAAAGAUGCCCCCUGCUCUGGCUGGUCAAACGGAACCAAGUCCGUC UUCCUGAGAGGUUUGGUCCCCUUCAACCAGCUACAGCAGGGCUGGCAAUGCCCA GUCCUUGGAGA
miR-10b	CCAGAGGUUGUAACGUUGUCUAUAUAUACCCUGUAGAACCGAAUUUGUGUGGUA UCCGU
miR-21	AUAGUCACAGAUUCGAUUCUAGGGGAAUAUAUGGUCGAUGCAAAAACUUCA UGUCGGGUAGCUUAUCAGACUGAUGUUGACUGUUGAAUCUCAUGGCAACACCAG UCGAU GGGCUGUCUGACA
miR-16	GUCAGCAGUGCCUUAGCAGCACGUAAAUAUUGGCGUUAAGAUUCUAAAAUUAUCU CCAG UAUUAACUGUGCUGCUGAAGUAAGGUUGAC
miR-NC#1	N/A

Expression Vectors:

Table 7: Expression vectors

Expression vector	Description		Supplier
pMiR Report Luciferase Vector	Encodes for firefly luciferase controlled by a CMV promotor. Selection by ampicillin or puromycin resitance	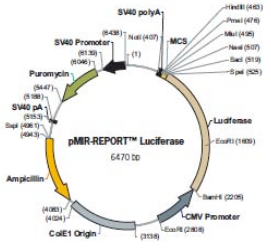	Ambion, Austin, TX, USA
pMiR Report β-gal control Plasmid	Encodes for firefly luciferase controlled by a CMV promotor. Selection by ampicillin or puromycin resitance	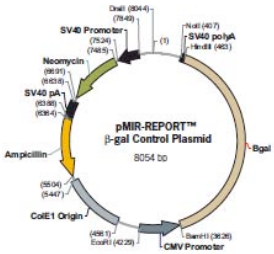	Ambion, Austin, TX, USA
pCR 2.1-TOPO	Linearized vector with single 3'-Thymidine overhangs and covalently bound topoisomerase I	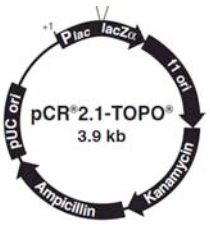	Invitrogen, Darmstadt, Germany
pCR-Blunt II-TOPO	Linearized vector with covalently bound topoisomerase I	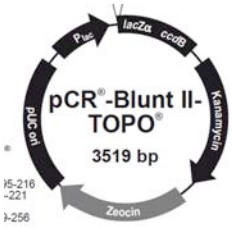	Invitrogen, Darmstadt, Germany
pCMV miR	Vector for miRNA expression controlled by CMV promotor. Selection by neomycin or kanamycin resistance. GFP reporter for monitoring of transfectione efficiency	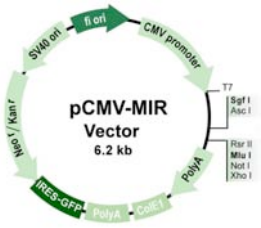	Origene, Rockville, MD, USA
Expression plasmid for human microRNA miR-133b	Encoding for pri-miR-133b under control of a CMV promotor		Origene, Rockville, MD, USA

2.1.7 Antibodies

Table 8: Antibodies and dilutions

Antibody	Host species	Clonality	Dilution Westernblot	Dilution Immunhisto-chemistry	Supplier
Anti-VEGFC	Rabbit IgG	Polyclonal	1:1000		Cell Signaling Technologies, Danvers, MA, USA
Anti-ITPR1	Rabbit IgG	Polyclonal	1:1000		Bethyl Laboratories Inc., Montgomery, TX, USA
Anti-FOXO1	Rabbit IgG	Monoclonal, clone C29H4		1:50	Cell Signaling Technologies, Danvers, MA, USA
Anti-FOXO1	Rabbit IgG	Polyclonal	1:1000		Sigma Aldrich, München, Germany
Anti-Faim-s	Rabbit IgG	Polyclonal	1:3000		AntibodyBcn, Barcelona, Spain
Anti-Akt	Rabbit IgG	Polyclonal	1:1000		Cell Signaling Technologies, Danvers, MA, USA
Anti-pAkt	Rabbit IgG	Polyclonal	1:1000		Cell Signaling Technologies, Danvers, MA, USA
Anti-GSTP1	Mouse IgG	Monoclonal, clone 3F2	1:1000		Cell Signaling Technologies, Danvers, MA, USA
Anti-ACTB	Mouse IgG	Monoclonal	1:2000		Sigma Aldrich, München, Germany
Anti-mouse, HRP-conjugated	Rabbit IgG	polyclonal	1:2500		Dako Deutschland GmbH, Hamburg, Germany
Anti-rabbit, HRP-conjugated	Goat IgG	polyclonal	1:2500		Dako Deutschland GmbH, Hamburg, Germany

2.1.5 Bacteria

DH5α (Invitrogen, Darmstadt, Germany) or TOP10 (Invitrogen, Darmstadt, Germany) chemically competent bacterial strains were used for plasmid DNA transformation and amplification. Bacterial cultures were grown in suspension cultures in LB media (Sigma Aldrich, München, Germany), supplemented with either 1x kanamycin or 1x ampicillin, or on LB-agar plates (Sigma Aldrich, München, Germany). Cryostocks were generated from transformed clones using LB with 15% glycerol and stored at -80° C.

2.1.5 Cell lines

For the in vitro studies, the following prostate cancer cell lines were used: LNCaP, PC3 and DU-145. Additionally BPH-1 was used as a benign prostate cell line. All cell lines were purchased from the American Type Culture Collection (ATCC) or the German Collection of Microorganisms and Cell Cultures (DSMZ). The cells were cultivated at 37°C and 5% CO_2 in a humidified atmosphere. Cryostocks were generated using full growth media with 10% DMSO and were stored in liquid nitrogen. Cell lines are periodically monitored for

mycoplasmic contamination by RT-qPCR according to van Kuppeveld (van Kuppeveld, 1994). Additionally, the identity of prostate cancer cells was verified by the German Prostate Cancer Consortium in 2009.

2.2 Methods

2.2.1 Tissue

All tissues were collected after radical prostatectomy between 2001 and 2008 at Charité – University Hospital, Berlin, Germany. The study was approved by the ethical board of the hospital. The following clinical and pathological information was gathered from all patients: age, pre-operative prostate specific antigene (PSA), tumor classification according to the UICC 2002 TNM system (Sobin, 2002), tumor grading according to Gleason (Epstein *et al.*, 2005), follow-up time after surgery, and the PSA concentration during follow up. A biochemical relapse was defined as the first time point after radical prostatectomy where the PSA value was above 0.1 µg/l followed by at least one subsequent rising PSA-value. Only patients with a non-detectable PSA after surgery were considered for prognostic evaluation.

2.2.1.1 Fresh frozen tissue

Fresh prostate tissue was sampled directly after gland removal. One full frontal section, which suspiciously resembled a tumor, was snap frozen in liquid nitrogen. Diagnostic Hematoxylin–Eosin (H/E) staining was performed to verify tumor content and to distinguish areas of benign and malignant tissue. Regions of interest were punch-biopsied with a 1 mm tissue microarray needle and histologically analyzed to verify a tumor content of at least 90%.

2.2.1.2 Formalin-fixed, paraffin-embedded tissue

Prostate tissue was routinely formalin-fixed promptly after surgery and subsequently paraffin-embedded. H/E staining was performed to identify malignant and benign areas. Areas of interest were punch-biopsied with a 1 mm tissue microarray needle. Tumor content was histologically reconfirmed to verify a tumor content of at least 90%.

2.2.1.3 Tissue Microarray

Formalin-fixed, paraffin-embedded tissue (FFPE) blocks as described above, were used to construct tissue microarrays. H/E staining was performed to identify malignant and benign areas. Areas of interest were punch-biopsied with a 1.5 mm tissue microarray needle and transferred to the recipient block. Each tumor was represented by one representative core. Normal tissues from the colon, pancreas, kidney and 2 prostates along with connective tissue were used as controls.

2.2.2 Molecular biology

2.2.2.1 RNA extraction

RNA extraction from fresh prostate tissue and prostate cancer cell lines

The RNA was extracted from fresh frozen tissues and prostate cancer cells with the miRNeasy Mini Kit.

Approximately 1 x 10^6 cells were harvested and lysed in 700 µl Qiazol. Tissue cores were assimilated in 700 µl Qiazol and lysed using a TissueLyser. RNA was extracted by phenol-chloroform extraction and centrifugation at 4°C for 15 min at 12,000 g. The aqueous phase was purified using a spin-column according to the manufacturer's recommendations. RNA was eluted in 40 µl H_2O.

Extraction of total RNA from formalin-fixed, paraffin-embedded tissue

Total RNA was extracted from FFPE was using the Recover All Total Nucleic Acid Extraction Kit.

FFPE tissue was minced with a scalpel and deparaffinized in Xylol for 3 min at 50°C. Tissue was washed with absolute ethanol, dissolved in digestion buffer and homogenized using a TissueLyser. Proteins were denaturated by incubation with 4 µl Protease for 15 min at 50°C and 15 min at 80°C. After protease digestions, samples were demodified in 5 M NH_4Cl for 5 min at 95°C to extract miRNA that remained integrated in protein complexes (Oberli *et al.*, 2008). RNA samples were purified using spin-columns according to the manufacturer's recommendations and were extracted using 30-50 µl H_2O.

Quantification and qualification of RNA samples

The total RNA quantity was assessed by measuring the absorbance of the solution at 260 nm with a NanoDrop ND 1000 spectrometer. A260/230 and A260/280 ratios were calculated to estimate the contamination of organic compounds and proteins. Samples with ratios below 1.8 were excluded from subsequent analysis

To further investigate the quality of the RNA, electropherogram analysis was performed using a 2100 Bioanalyzer and the RNA integrity number (RIN) was calculated for each sample as a measure of RNA degradation in the sample. Only fresh frozen samples with RIN values above 6 were included into the analysis. For FFPE tissue, RIN values below 6 were accepted because previous studies have shown that miRNAs are stable in degraded samples (Jung *et al.*, 2010) and could be reliably detected in FFPE tissue (Glud *et al.*, 2009; Hasemeier *et al.*, 2008; Hui *et al.*, 2009; Siebolts *et al.*, 2009; Szafranska *et al.*, 2008; Zhang *et al.*, 2008).

2.2.2.2 Plasmid isolation

Plasmids were isolated from overnight cultures was performed using the QIAprep Spin Miniprep Kit according to the manufacturer's recommendations. Briefly, 2 ml of bacterial overnight cultures were centrifuges for 3 min at 6,800 g and the bacterial pellet was resuspended in 250 µl buffer P1. Subsequently. 250 µl buffer P2 was added and suspension were mixed by inverting the tube. To stop lysis, 350 µl buffer N3 was added and the solution was centrifuged for 10 min at 12,000 g. The supernatant was purified using a spin-column according to the manufacturer's recommendations, and DNA was eluted in 40 µl H_2O.

2.2.2.3 miRNA Microarray analysis

miRNA microarray

All reaction steps were carried out as described in the miRNA Microarray System Protocol Version 1.0, April 2007. One hundred nanograms of total RNA was dephosphorylated with Calf Intestine Alkaline Phosphatase, denaturated with DMSO and used as an RNA acceptor in a T4 RNA ligase-mediated reaction, wherein the RNA donor 3',5'-cytidine bisphosphate had a single Cy3 label attached to the 3'-phosphate of the nucleotide (Cy3-pCp). The labeling reaction was performed at 16°C for 2 h, column purified, dessicated and resuspended in blocking and hybridization buffers. Labeled samples were prepared according to the Agilent Microarray Chamber Kit instructions. After hybridization for 20 h at 55°C, microarrays were washed, scanned, and processed according to the manufacturer's instructions. After scanning at 5 µM resolution with a DNA Microarray laser, the scanner features were extracted with an image analysis tool version A.9.5.3 using default protocols and settings (Agilent Technologies, Böblingen, Germany). Data analysis was performed using the Rosetta Resolver System Version 7.0 (Rosetta Biosoftware, Seattle, WA, USA). Intensity experiments were created with the Intensity Experiment Manager from Resolver by combining all hybridizations derived from either malignant or non-malignant samples. In silico ratio profiles and ratio experiments were generated by the Ratio Experiment Wizard after selecting either malignant or non-malignant samples patient-dereived samples or by combining malignant and non-malignant intensity experiments.

A two-sample Student t-test was used to validate intensity profiles, whereas a one-sample t test was applied to the ratio experiments composed of individual patients. Regulated reporters were identified by a three-step statistical analyses. First, a two-sample t-test was applied to all intensity profiles. Next, the intensity of prostate cancer and matched normal adjacent tissue were combined in two intensity experiments and compared according for presence or absence of data points. After in silico generation of the ratio experiments corresponding to individual sample pairs, a one-sample t-test was applied to all ratio experiments. The intersection of results that passed the intensity profiles two-sample t-test, the intensity experiments present-absent criterion "present in either", and the ratio

experiments one-sample t-test comprised 78 reporters for all 24 sample pairs. Further procedures included a Principal Component Analysis (PCA) and cluster analysis on features or reporter levels with the 2D Matrix Wizard from Resolver with an agglomerative algorithm using average link as heuristic criteria and Manhattan distance as the metric similarity measure for both intensity profiles and ratio experiments.

Whole genome mRNA array

Microarray experiments were performed as dual-color hybridizations. To compensate for dye-specific effects, a dye-reversal color-swap was applied. RNA was labeled with the Quick Amp Labeling Kit (Agilent Technologies). Briefly, mRNA was reverse transcribed and amplified using an oligo-dT-T7-promoter primer, and the resulting cDNA was labeled with dyes. One and twenty-five hundredths micrograms of each labeled cDNA was fragmented and subsequently hybridized to whole human genome 44k microarrays (AMADID-014850) according to the supplier's protocol (Agilent Technologies). Data files were further analyzed with the Rosetta Resolver Biosoftware, Build 7.2 (Rosetta Biosoftware, Seattle, WA, USA). A 1.5-fold change in the expression cut-off for ratio experiments was applied together with an anticorrelation of ratio profiles, which rendered the microarray analysis highly significant (P-value > 0.01), robust and reproducible.

2.2.2.4 TaqMan low density miRNA array

Multiplex RT-qPCR was performed using the TaqMan Array Human MicroRNA A+B Cards v3.0 according the manufacturer's instructions. A pool of 10 RNA samples was prepared for each relapse group using 400 ng RNA per sample. Five hundred and seventeen naograms of pooled RNA was reverse transcribed using the Megaplex reverse transcription primers A or B from the Megaplex Primer Pool, Human Pools Set v3.0 and the TaqMan MicroRNA reverse transcription kit according to the manufacturer's recommendations. RT-qPCR was performed on the ABI 7900 machine for 40 cycles. Expression was normalized to RNU6B, which is provided as an endogenous control on the arrays. Cq values above 32 were indicative of no expression according to the manufacturer's recommendations. miRNAs that exhibited a 1.5-fold increase or decrease between the groups were regarded as significantly dysregulated.

2.2.2.5 Real time quantitative PCR

Relative quantification of miRNA expression

TaqMan miRNA RT-qPCR was performed using miRNA-specific primer-probe mixes according to the manufacturer's recommendations.

Six and sixty-seven hundreths nanograms of total RNA were reverse transcribed using miRNA-specific stem-looped primers, 10 nmol dNTP mix, 2.6 U RNase inhibitor, 33.5

U MultiScribe RT enzyme and 1 x RT buffer. Controls were included for each run to assess precision of the RT-reaction (SD=0.24; 1.11% intra-run precision).

Table 9: Cycling protocol for reverse transcription of miRNAs.

Step	Time	T [°C]
Annealing	30 min	16
Elongation	30 min	42
Inactivation	5 min	80
	∞	4

RT-qPCR was performed on the Light Cycler 480 Instrument with Software version 1.3.0 in white 96-well PCR-plates. For relative quantification of miRNAs, 1 µl cDNA was amplified using the TaqMan Universal PCR Master Mix, No AmpErase UNG and 0.5 µl miRNA-specific primer/probe-mix in a total volume of 10 µl.

Table 10: Cycling protocol for relative quantification of miRNAs.

Step	Time	T [°C]	Cycles
Activation	10 min	95	45
Denaturation	15 sec	95	
Annealing/Elongation	60 sec	95	
Cooling	1 sec	40	

Samples were measured in triplicate and a no-template control and 2 interplate controls were included in each PCR run. To minimize the analytical variation, paired malignant and non-malignant samples were always analyzed on the same PCR plate. The analytical accuracy of the PCR measurements was characterized by the intra-run precision for all miRNAs.

Table 11: Intra-run precision of miRNA quantitative real-time RT-PCR measurements

miRNA	Mean Cq (N=5)	±SD	Analytical precision (%)	Efficiency
Hsa-miR-16	27.54	0.11	0.39	1.83
Hsa-miR-10b	29.94	0.16	0.54	1.99
Hsa-miR-31	30.41	0.09	0.30	1.83
Hsa-miR-96	24.61	0.09	0.37	1.83
Hsa-miR-125b	28.51	0.08	0.28	1.83
Hsa-miR-133b	24.39	0.11	0.45	1.94
Hsa-miR-145	25.98	0.18	0.69	1.83
Hsa-miR-149	28.97	0.07	0.24	1.83
Hsa-miR-181b	30.60	0.08	0.26	1.83
Hsa-miR-182	30.10	0.11	0.36	1.83
Hsa-miR-182*	25.72	0.16	0.62	1.83
Hsa-miR-183	25.53	0.14	0.55	1.83
Hsa-miR-184	27.56	0.11	0.40	1.83
Hsa-miR-205	28.67	0.10	0.35	1.83
Hsa-miR-221	29.51	0.21	0.71	1.83
Hsa-miR-222	28.26	0.07	0.25	1.83
Hsa-miR-375	27.00	0.09	0.33	1.83
RNU6B	32.30	0.17	0.53	1.83
RNU44	21.35	0.04	0.19	1.87

Expression data from fresh frozen tissue were normalized to miR-130b, and expression data from FFPE were normalized to the geometric mean of miR-130b and RNU44.

Relative quantification of mRNA expression

Total RNA was reverse transcribed using the Transcriptor First Strand cDNA Synthesis Kit. One microgram of total RNA was reverse transcribed using 1 U Transcriptor Reverse Transcriptase, 1 nM dNTP mix, 2.5 µM anchored oligo$(dT)_{18}$ primer and 60 µM random hexamer primer.

Table 12: Cycling protocol for reverse transcription of total RNA

Step	Time	T [°C]
Annealing	10 min	25
Elongation	30 min	55
Inactivation	5 min	85
	∞	4

mRNA expression was normalized to expression of TUBA or GAPDH.

mRNA quantification using SYBR green

For relative quantification of transcripts, 1 µl cDNA was amplified using the Fast SYBR Green Master Mix and 0.25 µM transcript-specific primers. A melting curve was included to verify the specificity of the reaction. Primers were designed using Primer3, or pre-designed Quantitect RT-qPCR assays were used.

Table 13: Cycling protocol for relative quantification of mRNAs using SYBR Green.

Step	Time	T [°C]	Cycles
Activation	10 min	95	
Denaturation	30 sec	95	40
Annealing/Elongation	30 sec	60	

mRNA quantification using UPL probes

For relative quantification of mRNA, 1 µl cDNA was amplified using a 1x Universal Probes Master, 0.1 µM UPL probe and 0.25 µM transcript-specific primers.

Table 14: Cycling protocol for relative quantification of mRNAs using UPL probes.

Step	Time	T [°C]	Cycles
Activation	10 min	95	
Denaturation	10 sec	95	
Annealing	20 sec	60	45
Elongation	1 sec	72	
Cooling	1 sec	40	

mRNA expression was normalized to TUBA expression. Data normalization was performed as described above.

Normalization of RT-qPCR data

miRNA and mRNA expression levels were normalized to the indicated reference genes. Further expression was normalized to the efficiency of the reaction as estimated by a dilution series, and interplate variance was normalized by using 2 standards, which were represented on each plate. The normalization strategy is based on the $2^{-\Delta\Delta Cq}$ method and was performed using Genex (http://multid.se/).

Following formulas were used for normalization:

Efficiency:
$$Cp_{E=100\%} = Cp_E \frac{\log(1+E)}{\log 2} \quad (1)$$

Interplate normalization:
$$Cp_{Platenorm} = Cp - \frac{1}{n}\sum_{i=1}^{n} Cp_{IC} \quad (2)$$

Normalization of the gene of interest (GOI) to reference gene:
$$Cp_{GOI,norm} = Cp_{GOI} - \frac{1}{n}\sum_{i=1}^{n} Cp_{RG} \quad (3)$$

Normalization of tumor to normal tissue:
$$RatioT/N = 2^{-CP(Tumor)+Cp(Normal)} \quad (4)$$

2.2.2.6 Amplification of 3' UTR sequences by PCR

Primers for PCR were designed using Primer3 or OligoPerfect. Restriction sites for the required endonucleases were added upstream. Additionally one guanine was added at the 5`-end to increase the probability for the Taq polymerase to produce 3'-end adenosine overhangs, which are crucial for TOPO-TA cloning. Primer specificity was assessed using Primer-BLAST (http://www.ncbi.nlm.nih.gov/tools/primer-blast/).

For amplification of partial 3' UTR sequences, 250 to 500 µg cDNA or genomic DNA from various prostate cancer cell lines were amplified using 1x AmpliTaq Gold buffer, 0.63 U AmpliTaq gold polymerase, 2 mM $MgCl_2$, 0.8 mM dNTP and 0.2 µM gene specific primers.

Table 15: Cycling protocol for relative quantification of mRNAs using SYBR Green.

Step	Time	T [°C]	Cycles
Activation	5 min	95	
Denaturation	15 sec	95	
Annealing	15 sec	57-60	35
Elongation	15-20 sec	72	
Final elongation	7	72	

For amplification of whole 3' UTR sequences above 1000 bp, a proofreading polymerase was used. Sequences at the 3' UTR were amplified from 100 µg PC3 genomic DNA using 1 U Platinum Pfx DNA polymerase, 0.3 mM dNTP, 0.3 µM sequence-specific primers and 1 mM Mg SO_4.

Table 16: Cycling protocol for relative quantification of mRNAs using SYBR Green.

Step	Time	T [°C]	Cycles
Activation	5 min	94	
Denaturation	15 sec	94	
Annealing	15 sec	55	35
Elongation	210 sec	72	

2.2.2.7 Bacterial PCR

Bacterial PCR was performed to identify positive clones. A PCR mastermix was prepared from 1x AmpliTaq Gold buffer, 0.63 U AmpliTaq Gold polymerase, 0.8 mM dNTPs and 0.2 µM sequence-specific primers.

Table 17: Cycling protocol for relative quantification of mRNAs using SYBR Green.

Step	Time	T [°C]	Cycles
Activation	5 min	95	
Denaturation	15 sec	95	
Annealing	15 sec	57-60	35
Elongation	15-20 sec	72	
Final elongation	7	72	

2.2.2.8 Agarose gel electrophoresis

DNA fragments were separated on agarose gels to confirm, the specificity and performance of the PCR reaction or to separate fragments after endonuclease digestion.

Depending on the length of the expected fragments, 1% to 2% agarose was dissolved in TBE buffer by heating and supplemented with 50 µg/ml ethidium bromide. The TBE running buffer was additionally supplemented with 50 µg/ml ethidium bromide. DNA samples were mixed with 1x loading buffer and 10 to 25 µl samples were pipetted into each well. Fragments were separated at constant voltage of 120 V for 30 to 60 min. Gels were analyzed on the Fluoro-S MultiImager using the Quantity-One software. Each gel was exposed for 20 sec.

2.2.2.9 Construction of luciferase reporter vectors

All 3' UTR sequences were first cloned into the pCR2.1-TOPO vector, using Taq-amplified sequences with A-overhangs or the pCR-Blunt II-TOPO vector, using Platinum pfx DNA polymerase amplified sequences with blunt ends. Inserts were used in 5-fold molar excess to the vector.

Cloning reaction

1-4 µl	amplified 3' UTR sequence
1 µl	salt solution
1 µl	pCR 2.1-TOPO vector or PCR-Blunt II-TOPO vector
	add water to 6 µl

The cloning reaction was incubated at RT for 10 min. Two microliters of the cloning reaction was added to the bacterial suspension. Bacteria were incubated on ice for 15 min and were heat-shocked for 30 s at 42°C. Suspensions were supplemented with 250 µl S.O.C media and were shaken gently for 1 h at 37°C. Twenty to fifty microliters of the suspensions were plated onto LB-agar. Twenty microliters of S.O.C media was added, and plates were incubated overnight at 37°C. pCR2.1-TOPO-transformed bacteria were plated onto LB-agar plates containing 40 µg/µl X-Gal for blue-white selection. pCR-Blunt II-TOPO-transformed bacteria were plated onto conventional LB-agar plates. Plates were supplemented with either ampicillin or kanamycin.

White colonies were picked and suspended in LB media containing ampicillin or kanamycin. Cultures were shaken gently at 37°C overnight. Positive clones were identified by bacterial PCR, and plasmids were isolated. The correct insert sequence was verified by sequencing (Eurofins MWG Operon, Ebersberg, Germany).

Correct inserts were excised from the pCR2.1-TOPO vector or pCR-Blunt II-TOPO vectors.

Restriction reaction:

2 µg	Plasmid-DNA/pMiR Report
2.5 µl	Buffer 4
1 µl	BSA (100x solution, 1:4 diluted)
1 µl	SpeI
1 µl	SacI or NaeI
	Water to 25 µl

Restriction digests with SpeI and SacI were performed overnight at RT. Restriction digests with SpeI and NaeI were performed for 1 h at 37°C. Enzymes were inactivated at 80°C for 20 min.

Restriction digestion reactions were resolved on a 1% agarose gel, excised from the gel and purified using the QIAquick Gel Extraction kit according to the manufacturer's recommendations. All fragments were extracted in 30 µl water.

Inserts were ligated with the pMiR Report Luciferase Expression Vector using 5-fold molar excess of the insert.

Ligation

6 µl restricted insert
2 µl restricted pMiR Report Luciferase Vector
1 µl 10x T4-DNA ligase buffer
1 µl T4-DNA ligase

The ligation was performed for 1h at RT and the enzyme was inactivated for 10 min at 37°C.

DH5α cells were thawed on ice, and 2 µl ligation products were added to the cells. The suspensions were incubated for 30 min on ice and heat-shocked for 20 s at 42°C. Nine hundred and fifty microliters of S.O.C media was added and cells were incubated at 37°C and gentle shaking for 1 hour. One hundred microliters of the suspension was plated onto LB-agar plates supplemented with ampicillin and incubated overnight at 37°C.

The clones were picked and suspended in LB media containing ampicillin or kanamycin. Positive clones were identified by bacterial PCR. The suspensions were shaken gently at 37°C overnight. The plasmids were isolated as described above.

2.2.3 Cell Biology

2.2.3.2 Transient transfection with synthetic pre-miRNAs and antisense inhibitors

Prostate cancer cells were grown to a density of 70 to 90% and seeded into appropriate tissue culture plates. The cells were transfected with 10 nM pre-miR microRNA precursors, anti-miR microRNA inhibitors or a pre-miR negative control #1 using the siPort NeoFX Transfection Agent (Table 15). siPORT was diluted in Opti-MEM and was incubated 10 min at RT. The miRNA precursors and miRNA inhibitors were diluted in Opti-MEM. The transfection agent was mixed with RNA and incubated for an additional 10 min at RT. The transfection complexes were added drop-wise to the cell cultures. The cells were allowed to rest for 24 h prior to subsequent assays.

Table 18: Amount of miRNA and transfection agent in different tissue culture plates

Tissue culture plate	miRNA (10 µM) [µl]	siPort [µl]	Final volume in Opti-MEM [µl]
96-well	0.1 or 0.3	0.5	20
6-well	2.5 or 7.5	5	200
Chamberslides	1.5	1	50

The transfection efficiency was monitored by RT-qPCR and a transfection with FAM-labeled miRNA precursors. The cells were seeded into chamberslides, transfected with 5, 10,

20 or 30 nM FAM-labeled pre-miR NC#1 as described above, and allowed to rest for 24 h. The cultures were washed in PBS and fixed for 20 min at RT in 4% formaldehyde. The nuclei were stained for 5 min in 4 µg/ml bisbenzimide. The slides were covered in fluorescence mounting medium, and positive cells were counted under a fluorescence microscope.

2.2.3.4 MTT and XTT assays for metabolic activity detection

The growth of pre-miR-96-transfected prostate cancer cells was assessed by metabolic conversion of 3-[4,5-dimethylthiazol-2-yl]-2,5-diphenyl tetrazolium bromide (MTT) or sodium 3-[1-(phenylaminocarbonyl)- 3,4-tetrazolium]-bis (4-methoxy-6-nitro benzene sulfonic acid hydrate (XTT). The cells were grown to 80% confluence, seeded into 96-well plates at a final concentration of 6 x 10^3 cells/well (LNCaP) or 2 x 10^3 cells/well (PC3) and transfected as described above. The cells were serum starved for 24 h. Cultures were incubated in 5 mg/ml MTT for 4 h and lysed in 10% SDS in 0.01 M HCl. Lysates were incubated at 37°C overnight, and formazan salt absorbance was measured at 550 nm. Alternatively, cells were cultured in XTT for 4 h at 37°C, and formazan salt absorbance was measured at 450 nm. Each reaction was performed in triplicate, and results are shown as the average of 3 independent assays.

2.2.3.5 Detection of apoptotic cells by flow cytometry

Apoptotic cells were detected using the ApoTarget Annexin-V FITC Apoptosis Kit. The cells were stained with Annexin-V FITC and propidium iodide (PI), which distinguishes the following fractions in prostate cancer cultures:

(1) Viable cells (Annexin V $FITC^-/PI^-$),

(2) Early apoptotic cells (Annexin V $FITC^+/PI^-$)

(3) Late apoptotic cells (Annexin V $FITC^+/PI^+$)

(4) Necrotic cells (Annexin V $FITC^-/PI^+$),

Prostate cancer cells were seeded into 6-well plates at a final concentration of 1.6 x 10^6 cells/well and transfected as described above. Apoptosis was induced with 10 µM camptothecin (CPT) for 24 h. The cells were harvested, diluted in an Annexin-V FITC buffer containing Annexin-V FITC and propidium iodide. The cells were incubated for 15 min at RT, and apoptotic cells were detected by flow cytometry. The cells were excited using a 488 nm Argon laser. The Annexin V-FITC channel (bandpass: 530/30 nm) and PI channels (bandpass: 585/42 nm) were plotted against each other, allowing for the separation of the above-mentioned cell fractions. The plots were separated into 4 quadrants and the percent of cells per quadrant was calculated. Each reaction was performed in triplicate, and the results are shown as the average of 3 independent assays.

2.2.3.6 Detection of cell cycle progression by flow cytometry

The fraction of cells in each cell cycle stage was analyzed by staining DNA content with PI. The cells were seeded into 6-well plates at a final concentration of 1.6 x 10^5 cells/well and transfected as described above. The cells were serum-starved for 48 hrs and fixed in 70% ice-cold ethanol. Fixed cells were stored at 4°C for at least 16 h. The cells were stained in PI-staining solution for 30 min at RT and were analyzed by flow cytometry. The cells were excited using a 488 nm Argon laser. A histogram of the PI channel (bandpass: 585/42 nm) was drawn, and the area of each peak was calculated, corresponding to cells in G1, S and G2/M. The number of cells in each peak was represented as the percentage of total cell number. Each reaction was performed in triplicate, and the results are shown as the average of 3 independent assays.

2.2.3.7 Wound-healing Assay

To determine the rate of cell motility in miRNA-transfected prostate cancer cells, cells were seeded into 6-well plates and transfected as described above. The cells were grown to confluence and scratched with a 1000-µl pipette tip. Remigration into the wound was observed by life cell imaging for 24 h (1 picture every 10 min). The percentage of open area was determined with the TScratch software (Geback *et al.*, 2009) at 0, 5, 10, 15 and 20 hrs. All values were normalized to the percentage of open area at 0 h. In each culture, 2 randomly chosen points of the scratch were measured. The data are represented as average of 3 independent assays.

2.2.3.8 Luciferase reporter gene assay

LNCaP cells were grown to 80% confluency and seeded into 6-well plates at a final density of 2 x 10^5 cells per well. The cultures were cotransfected with 10 nM pre-miRNAs, miRNA inhibitors or pre-miR NC#1, 500 ng pMiR Report vector and a β-Galactosidase control vector. After 48 h hours, cells were detached with a scraper, and total protein was extracted in 80 µl lysis buffer. The extracts were centrifuged at the maximum force for 2 min. Supernatant was transferred to a new tubes, and processed immediately or stored at -80°C.

Firefly luciferase and β-galactosidase activities in the extracts were detected using the Dual-Light Combined Reporter Gene Assay System according to the manufacturer's recommendations. A Galacton-Plus substrate was diluted 1:1000 in Buffer B. Assays were performed in white microtiter plates. Two to ten microliters of protein and 25 µl Buffer A was added to each well. 100 µl Galacton-Plus substrate was injected automatically per well and luciferase signal was measured with one sec delay for one sec. The plates were incubated at RT for 1 h. One hundred microliters of Accelerator II was automatically injected, and the **β**-galactosidase signal was measured for one sec with a one sec delay. The luciferase activity

in each well was normalized to β-galactosidase activity. Each reaction was performed in duplicate, and the results are shown as the average of 3 independent assays.

2.2.3.9 R1881 treatment of androgen-dependent prostate cancer cells

LNCaP cells were grown to 70 to 90% confluency and were passaged 1:3 into T75 tissue flask in synchronization media and incubated for 5 days. On the fifth day, cells were passaged 1:2 into T75 flasks and cultivated for 24 hrs in media supplemented with 10% charcoal-filtered FCS. On the sixth day, the cells were treated with 10 and 0.1 nM methytrienolone (R1881) or vehicle control for 72 hrs. The cells were harvested for RNA extraction, and miRNA expression levels were analyzed by RT-qPCR. The data are represented as the average of 3 independent assays.

2.2.4 Biochemistry

2.2.4.1 Protein extraction

Cells were seeded into 6-well plates at a final concentration of 2 x 10^3 cells per well and were transfected with pre-miRNAs as described above. Protein was extracted 72 hrs post transfection. The cells were trypsinized, washed twice in PBS and centrifuged at 300g for 3 min. The pellets were resuspended in 150 µl RIPA buffer per 5 x 10^6 cells. The cells were lysed for 1 hr on ice and centrifuged for 20 min at 4°C and 15000 g. The supernatants were collected and stored at -80°C.

2.2.4.2 Measurement of total protein after Bradford

Total protein was measured using the Bradford assay (Bradford, 1976). Proteins were diluted 1:5 to 1:10 in NaCl and mixed with Coomassie Blue in 500 µl microcuvettes. The reaction was performed for 5 min at RT and the extinction was measured at 595 nm. Two BSA dilutions (0.4 and 0.8 µg/µl) were included in each assay to calculate total protein concentration.

2.2.4.3 SDS-PAGE

SDS-PAGE was performed according to Laemmli (Laemmli, 1970). Protein solutions were resolved on 10% or 12.5% SDS-polyacrylamide gels or 4-12.5% gradient gels. The proteins were diluted in 1x loading puffer and denaturated for 5 min at 95°C. Twenty to twenty-five micrograms of protein were injected in each well. The gels were run in Laemmli buffer at 15 mA constant current until they passed the stacking gel and subsequently at 30 mA constant current. The gradient gels were run at 120 V constant voltage.

2.2.4.4 Western blotting and immunostaining

The proteins were transferred from SDS-polyacrylamide gels to polyvinyldifluoride membranes, with a 0.45 µm pore size, by semi-dry western blotting to. The membranes were

equilibrated for 1 min in methanol, 2 x 10 min in H_2O and for 10 min in anode buffer I. Polyacrylamid gels were equilibrated 10 min in cathode buffer. Polyacrylamide gel and membrane were positioned between filter papers in a Hoefer chamber, and the proteins were transferred for 1 h at 45 mA constant voltage.

To inhibit non-specific antibody binding, the membran was blocked for 1 h at RT, or over night at 4°C, in 2% non-fat milk in t-TBS. The membrane was probed with a primary antibody at appropriate concentrations (Table 4). The membrane was washed 3 times in t-TBS and probed with a secondary antibody at appropriate concentrations (Table 4). The membranes were washed 3 times for 10 min in t-TBS. Antibody staining was developed visualized using an ECL solution. The membrane were incubated for 5 min at RT in ECL and developed for up to 5 min using a Fluoro-S MultiImager, shooting one picture per min. To determine the relative concentration of stained protein, staining intensity was measured using ImageJ 1.43r (http://rsb.info.nih.gov/ij). The background staining was substracted. Each band was marked and intensity peaks were determined. The area under the peak was calculated. Each peak area was normalized to the area of ACTB staining of the corresponding sample.

The membrane was stripped after detection and subsequently probed with an anti-ACTB antibody. Therefore, they were preincubated for 30 min in t-TBS and incubated for 30 min at RT in stripping buffer. The membrane was washed 3 times for 10 min in t-TBS and blocked and immunostained as described above.

2.2.4.5 Immunhistochemistry

Immunohistochemistry was performed on a tissue microarray. Two micrometer slides were cut from the paraffin block using a microtome and were bedded onto microscopic glass slides.

The tissue was deparaffinized 3 times for 10 min in Xylol and then washed 3 times in 100% EtOH, 1 time in 96%, 1 time in 80%, 1 time in 70% and one time in H_2O. The slides were stored in TBS until necessary.

The proteins were demasked in citrate buffer in a pressure cooker for 5 min and washed 10 min in TBS. The slides were incubated for 10 min in a protein-blocking solution and probed for 1 h at RT with a primary antibody at appropriate concentrations (Table 4). The slides were washed in H_2O and t-TBS and probed with biotinylated linker antibodies for 20 min at RT, washed in TBS and probed with streptavidin-conjugated secondary antibody for 20 min. The slides were stained with Fast Red for 5 to 20 min. The staining was monitored under a microscope until the desired staining intensities were attained. For nuclear counterstaining, the, slides were incubated for 1 min and 15 sec in hemalaun and incubated in H_2O for 4 min. The slides were developed under running warm water until the desired intensity was reached. The slides were covered using the Aquatex mounting medium.

2.2.4.6 Haematoxylin/Eosin staining

Tissue Microarray slides were cut and deparaffinized as described above. Slides were incubated for 5-10 min in hemalaun, and staining was developed in running warm water. The slides were washed in dH_2O and stained for 2 to 5 min with eosin. The slides were washed with tap water and H_2O. The slides were dipped in 70, 80, 96 and 100% alcohol in secession and twice in Xylol. Finally, they were incubated in Xylol for 5 min. Afterwards, the slides were covered in eucit mounting medium.

2.2.5 Statistical Analysis

Statistical analysis of RT-qPCR data were performed with SPSS version 17.0 (SPSS Inc., Chicago, IL), GraphPad Prism version 5.01 (GraphPad Software Inc., La Jolla, CA), and MedCalc version 10.3.2 (MedCalc Software, Mariakerke, Belgium) software. Kolmogorov-Smirnof normality test, Wilcoxon test with combined Monte-Carlo analysis of 10000 random samples, Mann-Whitney *U* test, and Spearman rank correlation coefficients were used. All tests were performed two-tailed, and *p*-values <0.05 were considered statistically significant.

Receiver operating characteristics (ROC) curves with combined bootstrap analysis of 10,000 random samples were calculated to determine the potential of genes of interest to discriminate between malignant and non-malignant samples. Binary logistic regression with subsequent cross validation was performed to identify the best discriminating combinations of miRNAs and to calculate overall correct classifications.

For disease progression analyses, the Kaplan-Meier approach (log-rank test) and Cox proportional hazard regression analysis were used.

Sample size determinations were performed using GraphPad Statmate version 2.0 and MedCalc software on the basis of a two-sided alpha error of 5% and a power of 80%. Considering a proportional difference of approximately 0.40 in Kaplan-Meier curves as observed in patients after radical prostatectomy depending on the main risk factors, Gleason score and tumour stage, about 25 subjects in each group have to be investigated. We decided to study at least 70 patients in the follow-up study to obtain a power of at least 80%, because the sample size between the groups of tumor recurrence or no recurrence could not be predicted.

3. Results

3.1 miRNA profiling in prostate cancer

miRNAs are commonly dysregulated in human malignancies. Investigations of the suitability of miRNAs as molecular markers for cancer detection have shown that miRNA profiling might outperform mRNA profiling as a molecular marker for cancer diagnosis and prognosis (Lu *et al.*, 2005). Based on these encouraging results regarding the use of miRNAs as tumor markers, global changes in miRNA expression were studied in prostate cancer to identify dysregulated miRNAs in prostate cancer and to explore their potential use as diagnostic and prognostic markers.

3.1.1 Patients and tumor characteristics

miRNA profiling was performed in a set of 76 matched fresh-frozen prostate cancer and normal adjacent tissues. Expression of one miRNA (miR-96) was subsequently validated in an independent sample set of 79 patients. Tumor characteristics and clinical data did not differ between both clinical subsets (Table 19).

Table 19: Patients and tumour characteristics

Characteristic		**Patient set 1 (N = 76) N (%)**	**Patient set 2 (N = 79) N (%)**	***p-value***
Age, years	Median	63	62	0.55
	Range	49 - 74	43 - 70	
Pre-operative PSA, µg/l	Median	6.7	8.0	
	Range	0.92 - 41.90	0.58 - 34.90	0.16
T stage	pT2a	2 (3)	8 (10)	
	pT2b	11 (15)	11 (14)	0.36
	pT2c	32 (42)	35 (44)	
	pT3a	24 (32)	19 (24)	
	pT3b	7 (9)	6 (8)	
N stage	pN0/Nx	74 (97)	79 (100)	
	pN1	2 (3)	0	0.46
M stage	M0/Mx	76 (100)	79 (100)	
	M1	0	0	0.75
Surgical margins	R0	46 (60)	54 (56)	
	R1	27 (36)	34 (44)	0.51
	Rx	3 (3)	0	
Gleason score	5	1 (1)	7 (9)	
	6	31 (41)	20 (25)	0.10
	7	30 (40)	34 (43)	
	8	9 (12)	11 (14)	
	9	5 (7)	7 (9)	
Follow-up, months	Median	50[2]	50	
	Range	1 - 93	1-99	0.37
Biochemical recurrence		12 (16)	14 (18)	0.91

3.1.2 miRNA microarray expression analysis

To identify dysregulated miRNAs, miRNA microarray expression analysis for 470 human miRNAs and 64 viral miRNAs from Sanger Base v9.1 was performed in a subset of 24 matched tumor and normal adjacent tissue samples. Seventy-eight candidate reporters were dysregulated in this sample set and were evaluated with principal component analysis and hierarchical 2D clustering using the similarity measure Pearson correlation and the heuristic criteria average link.

Principal component analysis revealed that the samples clustered according to their malignancy, but groups we not clearly separated from each other, wherein 4 malignant samples were assigned to the normal group and 1 malignant sample was assigned to the malignant group (Figure 6A). Hierarchical cluster analysis confirmed this observation as the hierarchical tree of intensity profiles shows misalignment of the same 5 samples (Figure 6B).

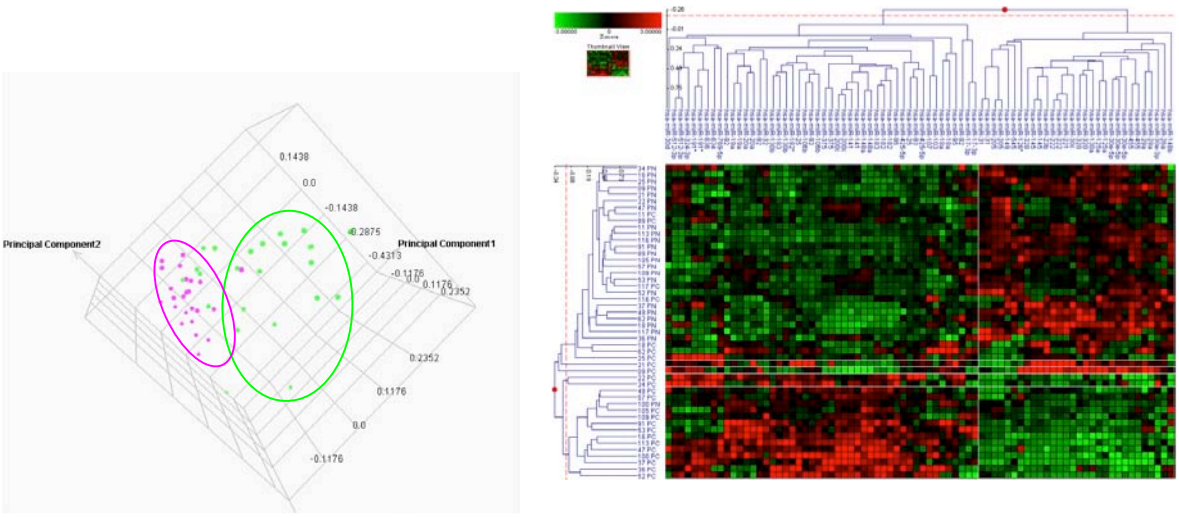

Figure 6: Unsupervised analysis of miRNA regulation in prostate cancer specimens
miRNA microarray analysis of 470 miRNAs was performed in 24 matched malignant and normal adjacent tissues. A) 78 dysregulated reporters were used for principal component analysis of malignant (pink) and normal samples (green). B) Unsupervised hierarchical cluster analysis. Hierarchical trees of intensity profiles (left) and reporters (top) and heatmap are displayed. Z-score was cropped to -3 to 3. Green squares encode for a downregulation, red squares for an upregulation.

In a second analysis step, all reporters that detected the same miRNAs were combined into a single value. A 1.5-fold difference between malignant and normal adjacent tissue was set as the cut-off for the inclusion, and expression was required to be detectable in both tumor and matched normal tissue. Ten miRNAs were identified with greater than 1.5-fold difference, of which 4 were downregulated and 6 were upregulated (Table 20). Furthermore, 5 candidates that satisfied the inclusion criteria in at least 12 of the 24 sample pairs were identified.

Table 20: miRNAs differentially expressed in malignant to matched non-malignant tissue samples of prostate cancer

	microRNA	Fold Change	p-value
Overexpressed			
1	hsa-miR-375[1]	1.52	0.01
2	hsa-miR-130b[1]	1.54	<0.001
3	hsa-miR-182[1]	1.74	<0.001
4	hsa-miR-96[1]	1.75	<0.001
5	hsa-miR-634[2]	2.01	0.18
6	hsa-miR-183[1]	2.24	0.01
7	hsa-miR-182*[1]	2.69	<0.01
8	hsa-miR-524*[2]	3.45	0.13
Underexpressed			
1	hsa-miR-31[1]	-1.85	0.05
2	hsa-miR-149[2]	-1.73	<0.01
3	hsa-miR-181b[2]	-1.72	<0.001
4	hsa-miR-368[2]	-1.62	<0.01
5	hsa-miR-221[1]	-1.59	<0.01
6	hsa-miR-222[1]	-1.59	<0.01
7	hsa-miR-205[1]	-2.58	<0.01

[1] passed inclusion criteria in 24/24 pairs, [2] passed inclusion criteria in > 12/24 pairs.

3.1.3. Identification of suitable endogenous control genes for miRNA expression analysis

The importance of miRNA regulation in human cancers has only been established during the last decade. Due to the infancy of miRNA expression analysis, some analytical pitfalls have not been properly addressed so far. In real-time PCR, the most common approach to studying gene expression is the relative quantification of the target gene, where expression of the gene of interest is normalized to an endogenous control gene (Bustin *et al.*, 2009). The use of suitable reference genes for RT-qPCR can have a major effect on the reliability of profiling results. It is therefore important to validate the expression stability for each tissue and application prior to use (Dheda *et al.*, 2005).

Recent studies have established several criteria that should be fulfilled by a reference gene (Bustin and Nolan, 2004; Peltier and Latham, 2008; Radonic *et al.*, 2004; Vandesompele *et al.*, 2002):

A) The gene has to be stably expressed among disease groups
B) The range of expression should be similar to those of the target gene in order to measure both genes in a single dilution
C) The reference gene should be of similar length as the target gene to guarantee similar efficiencies during isolation and reverse transcription

For miRNA expression analysis in prostate, cancer no general accepted reference genes exist, as is highlighted by a literature research in PubMed. In 16 articles that included the performance of miRNA expression analysis in prostate cancer specimen through September 2009, the most commonly used reference gene was RNU6B (Ambs *et al.*, 2008;

Jiang *et al.*, 2005; Noonan *et al.*, 2009; Prueitt *et al.*, 2008). Other studies have used RNU43 (Leite *et al.*, 2009), the combination of RNU6B/RNU43 (Ozen *et al.*, 2008; Spahn *et al.*, 2010), the combination of RNU6B/miR-16 (Josson *et al.*, 2008), RNU6B/RPP30 (Gandellini *et al.*, 2009), or let-7/miR-16 (Mattie *et al.*, 2006). Even larger transcripts, such as GAPDH (Place *et al.*, 2008; Rokhlin *et al.*, 2008) and TBP (Porkka *et al.*, 2007), were used; however, the use of mRNAs as reference genes for miRNA expression studies has several disadvantages as described above. Three studies provide some information justifying the selection of the reference gene, but none were statistically sound (Jiang *et al.*, 2005; Josson *et al.*, 2008; Mattie *et al.*, 2006).

Based on our miRNA microarray profiling data and the literature, we choose to analyze the stability of 4 putative reference genes, namely miR-16, miR-130b, Z30 and RNU6B. To obtain an overview of their expression levels and variability in prostate cancer and normal adjacent tissue, we prepared 2 pools that represented prostate cancer and normal adjacent tissue. For each pool, we used total RNA from 12 patients at the same concentration and volume to obtain a final concentration of 250 ng/µl. The expression of each gene was measured in these pools using RT-qPCR.

All genes were well detectable with RT-qPCR (Figure 7). miR-16 had the highest expression with Cq values below 22, while the other 3 putative reference genes had a distinctly lower expressions, though the Cq values were still below 30. One major criterion for a suitable reference gene is stable expression between the study groups. Therefore, a threshold of 1.5-fold difference was set as an inclusion criterion. This relatively high threshold was chosen to minimize the risk of type II errors. As Z30 did not meet this criterion, it was excluded from further analysis. Although RNU6B barely passed the selection criterion with a fold change of 1.48, it was included in more detailed analyses.

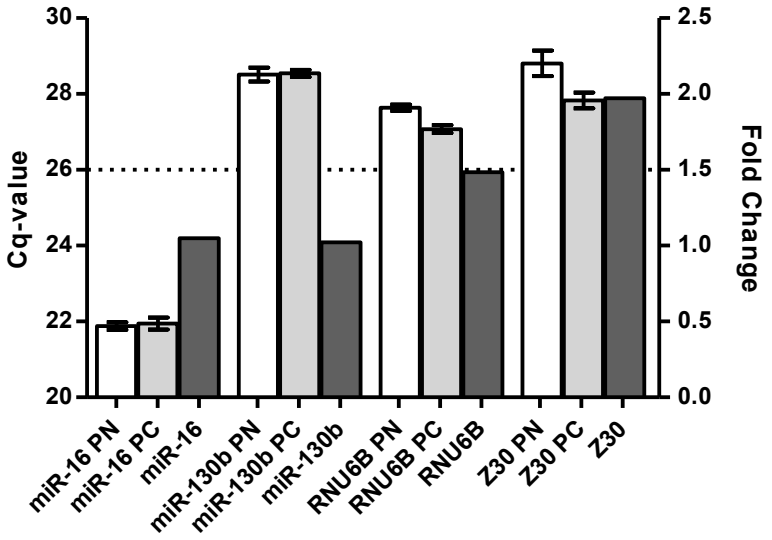

Figure 7: Expression of putative reference genes in pooled RNA samples corresponding to malignant and normal adjacent tissue.

Expression of reference gene candidates measured in RNA pools obtained from matched non-malignant (PN) and malignant (PC) prostate cancer tissue specimens. The first 2 columns of every gene represent the expression value as the mean Cq-values ± SD (n=3; blank, non-malignant tissue; light grey, malignant tissue) relative to the left y-axis scale. The third column (medium grey) represents the median fold change between pools from non-malignant and malignant tissue related to the right y-axis scale. The line at 1.5 represents the arbitrary threshold of the allowed differential expression between groups.

Expression of the remaining 3 putative reference genes was measured in all 76 matched prostate cancer and normal adjacent tissues. Cq values for each gene were normalized to the RT-qPCR efficiency and interplate calibrators for subsequent analysis. Expression of the 3 candidate genes did not correlate with pathological stage or Gleason score, indicating a stable expression in the tumor tissue (Table 21).

Table 21: Correlation of the expression of putative reference genes with tumor stage and Gleason score.

	pT stage		Gleason score	
Gene name	**r_s**	**p-value**	**r_s**	**p-value**
Hsa-miR-16	-0.01	0.95	-0.18	0.11
Hsa-miR-130b	-0.05	0.67	-0.15	0.19
RNU6B	-0.05	0.67	0.07	0.51
Geometric mean (hsa-miR-130b/RNU6B)	-0.07	0.57	-0.02	0.86

The expression of miR-130b and RNU6b was not significantly different between malignant and normal adjacent tissue, while miR-16 had a significantly lower expression in tumor tissue in comparison to matched normal tissue (Wilcoxon signed rank test; $p<0.001$; Figure 8). miR-16 was therefore excluded from further statistical evaluation of expression

stability. Due to the large number of samples as well as the high significance, both type I and type II errors could be excluded with great certainty.

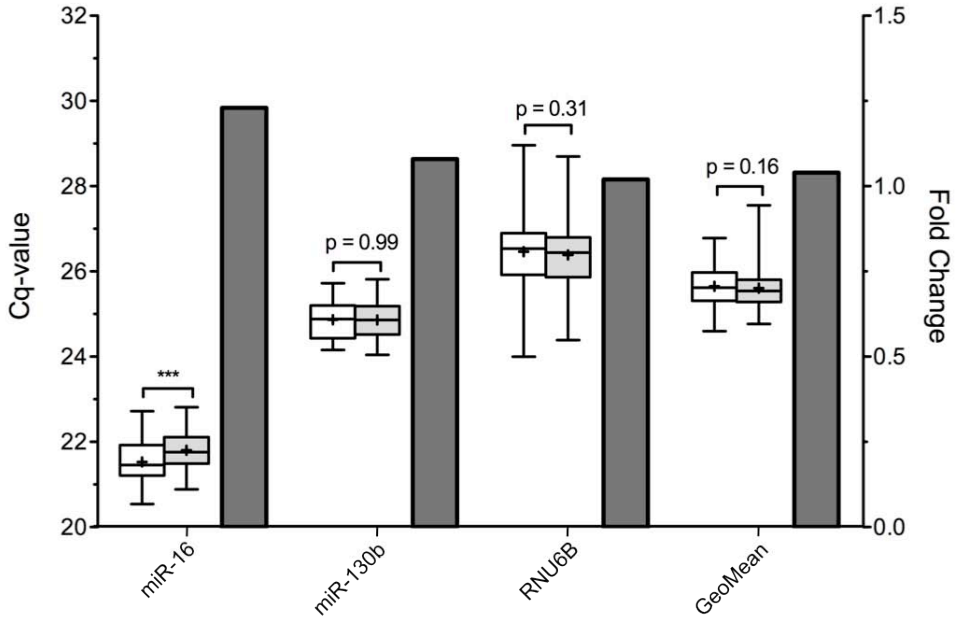

Figure 8: Expression of candidate reference genes in matched malignant and normal adjacent prostate tissue.

Expression of reference gene candidates in matched non-malignant and malignant sample pairs from 76 prostate cancer tissue specimens. Left y-axis: Expression values are given as Cq values, which were corrected for assay efficiency and 2 interplate controls. Boxes (blank: non-malignant tissue; grey: malignant tissue) represent lower and upper quartiles with the median represented as a horizontal line and the mean as a cross. The whiskers represent the range of expression. Right y-axis: The columns (dark grey) represent the median fold change between the malignant and non-malignant tissue samples. *** $p < 0.001$; Wilcoxon signed rank test.

Although miR-130b and RNU6B expression was not statistically different between prostate tissue and normal adjacent tissue, this finding does not prove that both genes are equally expressed among the groups. Therefore, an equivalence test according to Haller *et al.* (Haller *et al.*, 2004) was performed for miR-130b, RNU6B and the geometric mean of both. The maximal allowed difference was set at 0.26, which represents a 1.2-fold change. While miR-130b and the geometric mean were equal between malignant and matched normal tissue, RNU6B was not.

Not only equivalence between groups, but also overall stability of expression across all samples is a major criterion for a suitable reference gene. The variability of expression is a measurement of stability. Therefore, variance of miR-130b and RNU6B expression and the geometric mean was compared. Variance of RNU6B expression was significantly higher than the variance of miR-130b (Levene's test; $p < 0.001$), while variance of miR-130b expression and the geometric mean did not differ significantly (Levene's test; $p=0.52$).

We further calculated stability measurements using either the GeNorm or the Normfinder algorithm (Andersen *et al.*, 2004; Vandesompele *et al.*, 2002). GeNorm calculates the stability value (M-value) and repeatedly excludes the candidate with the highest stability value until the 2 most stably expressed genes remain. Stability values below 1.5 were defined as a critical limit. GeNorm identified miR-130b and the geometric mean as the most stable reference genes with an M-value of 0.47 (Figure 9).

Normfinder calculates a stability value, termed variability, for each gene. It estimates the single most stable gene and the best combination of 2 genes. In contrast to GeNorm this program can account for group differences. Normfinder identified miR-130b as the single most stable reference gene, with a variability of 0.08. The geometric mean of hsa-miR-130b and RNU6B had an even lower stability of 0.03, accounting for an increased stability by using the geometric mean.

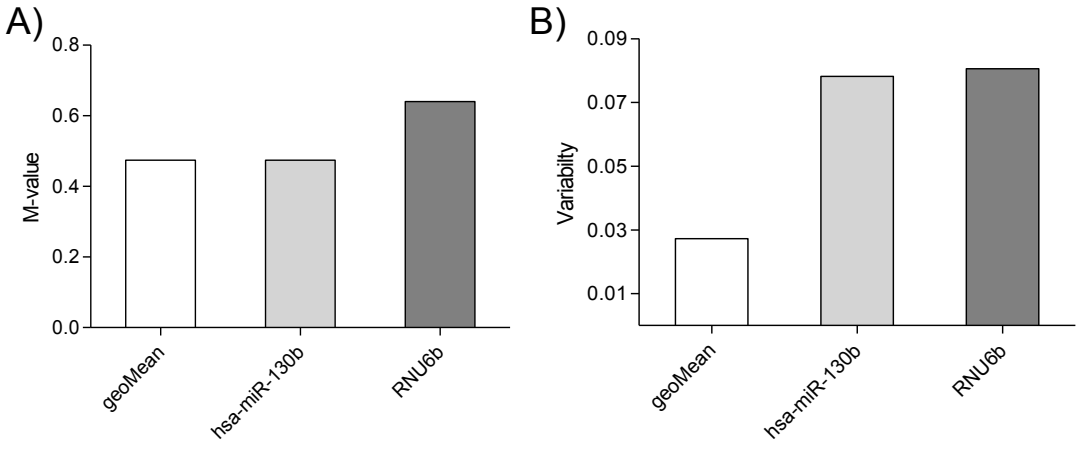

Figure 9: Stability of candidate reference genes
Stability analyses of selected candidate reference genes. A) Stability value M of candidate reference genes calculated using GeNorm. B) Variability of candidate reference genes calculated using Normfinder. Highly stable expression of genes is indicated by a low M value in GeNorm and a low variability value in Normfinder.

Based on the statistical analysis of miR-130b and the geometric mean of miR-130b and RNU6B, expression was equivalent and stable in prostate cancer and normal tissue. RNU6B expression displayed a large intragroup variability and was therefore less suited as a reference gene. Based on these observations miR-130b was chosen as reference gene for all subsequent expression studies.

3.1.4 Validation of differentially expressed miRNAs using RT-qPCR

The expression of the dysregulated miRNAs, which were identified based on microarray analysis, and 4 additional miRNAs (hsa-miR-125b, hsa-miR-145, hsa-miR-184, hsa-miR-373), which were identified by literature research (Huang *et al.*, 2008; Lin *et al.*, 2008; Molnar *et al.*, 2008; Ozen *et al.*, 2008; Porkka *et al.*, 2007; Yang *et al.*, 2009), was validated by RT-qPCR in 76 matched prostate cancer tissues and normal adjacent tissues,

including the 24 pairs that were used for microarray profiling. To determine if the TaqMan RT-qPCR assay provided the necessary sensitivity to detect the miRNA transcripts, expression of each miRNA was measured in 2 pools representing malignant and normal adjacent tissue. Four miRNAs were excluded as the Cq-values were >35 in both pooled samples (hsa-miR-368, miR-373, hsa-miR-634, and hsa-miR-524). Expression of the remaining miRNAs was measured in each of the 76 tissue pairs.

Expression analysis of 76 matched prostate cancer tissues and normal adjacent tissue identified 15 significantly dysregulated miRNAs in prostate cancer (Figure 10), of whom 10 miRNAs were downregulated and 5 miRNAs were upregulated. Each miRNA showed only a moderate expression change, ranging from -3.69- to 1.50-fold.

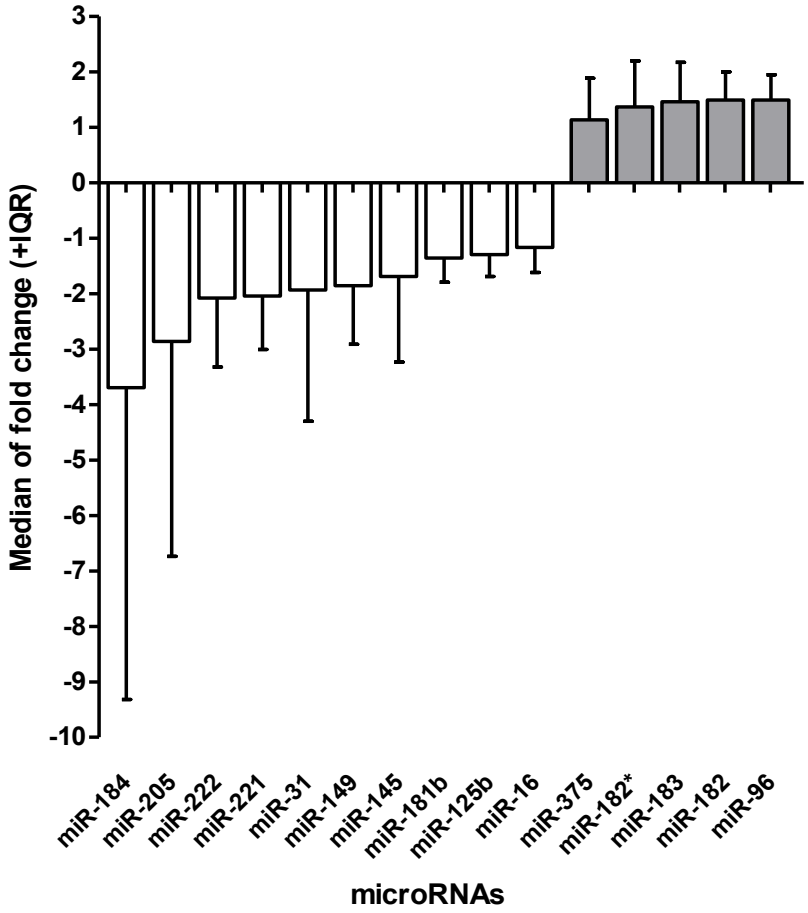

Figure 10: Differentially regulated miRNAs in prostate cancer.
The expression of 15 miRNAs was measured in 76 matched prostate cancer and normal adjacent tissues by RT-qPCR. miRNA expression was normalized to the expression of miR-130b, interplate controls and efficiency. Fold change was calculated for each tissue pair. Data are shown as the median fold change (+interquartile range).

We correlated the expression of each miRNA with each other and identified a strong correlation between miR-96, miR-182, miR-182*, miR-183 and miR-375 (Figure 11). miR-96, miR-182 and miR-183 are located on chromosome 7 and are transcribed as a single polycistronic cluster. MiR-375 is an intergenic monocystronic miRNA located on chromosome 2. miR-221 and miR-222 were also highly correlated with each other. Both genes are located in close proximity on chromosome X and are also transcribed as polycistronic pri-miRNA.

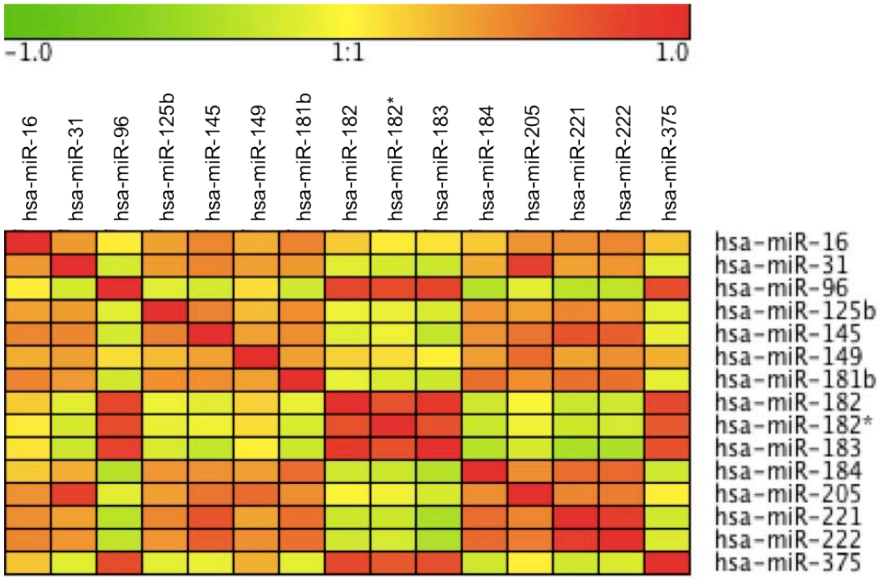

Figure 11: Correlation heatmap of miRNA expression in prostate cancer
Correlation of miRNAs was calculated by Spearman correlation.

3.1.5 Clinical relevance of miRNA expression

3.1.5.1 Association of miRNAs with clinico-pathological data

To determine whether miRNAs are further dysregulated during prostate cancer progression, miRNA expression was correlated with the Gleason score, and pathological stage. The expression of miR-31, miR-96 and miR-205 moderately correlated with Gleason score, while miR-125b, miR-205 and miR-222 expression correlated with pathological stage (Table 22).

Table 22: Spearman rank correlation coefficients between the differentially expressed miRNAs in prostate cancer tissue samples and the Gleason score and pathological tumor stage

hsa-miR	Gleason score		Pathological stage	
	r_s	p-value	r_s	p-value
hsa-miR-16	-0.03	0.82	-0.02	0.87
hsa-miR-31	**-0.28**	**0.02**	-0.16	0.17
hsa-miR-96	**0.27**	**0.02**	0.02	0.85
hsa-miR-125b	0.03	0.82	**-0.27**	**0.02**
hsa-miR-145	-0.12	0.30	-0.01	0.39
hsa-miR-149	0.02	0.88	-0.06	0.63
hsa-miR-181b	-0.04	0.75	-0.01	0.94
hsa-miR-182	0.17	0.14	0.18	0.11
hsa-miR-182*	0.19	0.11	0.02	0.85
hsa-miR-183	**0.21**	**0.07**	0.19	0.09
hsa-miR-183	-0.06	0.62	-0.13	0.27
hsa-miR-205	-0.24	0.03	**-0.27**	**0.02**
hsa-miR-221	-0.11	0.35	-0.17	0.15
hsa-miR-222	-0.19	0.09	**-0.23**	**0.04**
hsa-miR-375	0.12	0.28	0.13	0.28

3.1.5.2 miRNAs as diagnostic markers for prostate cancer detection

In order to elucidate the putative diagnostic properties of miRNA expression, receiver operating characteristic (ROC) curves were calculated for single miRNAs and the combination of all miRNAs. To improve the robustness of the statistical analysis, ROC analysis was combined with bootstrapping of 10,000 random repeats as an internal validation. Logistic regression was internally validated by cross-validation.

Using the majority of miRNAs, the analysis was able to discriminate tumor from normal adjacent tissue, with 11 miRNAs having AUC's greater 0.7. miR-205 was identified as the most suitable miRNA for discrimination of tumor tissue from normal adjacent tissue, with an overall correct classification of 72% of the samples. To further improve discriminative potential, miRNA expression was analyzed by logistic regression, and the prediction for each patient was forwarded to ROC analysis. We either included all miRNAs into the predictor or identified the minimal number of miRNAs necessary by forward likelihood elimination (entry: $p = 0.1$; elimination: $p = 0.05$).

Combining each of the miRNAs into a single predictor enhanced the AUC to 0.86, with an overall correct classification of 82%, yet this did not provide a significant advantage over discrimination by miR-205 alone ($p = 0.29$). Forward likelihood elimination identified a 6-miRNA predictor, which had an AUC of 0.88 and an overall correct classification of 80%. Additionally, we combined the best discriminating upregulated miRNA, miR-205, with the best discriminating downregulated miRNA, miR-183, into a single predictor. This predictor showed a trend for improved discrimination in comparison to miR-205 alone ($p = 0.06$).

Table 23: Performance of miRNAs to discriminate between malignant and non-malignant tissue samples from prostate cancer

miRNA	AUC	95% CI of AUC	Overall correct classification (%)
hsa-miR-375	0.59*	0.51-0.69	53
hsa-miR-16	0.64*	0.55-0.73	59
hsa-miR-182*	0.66*	0.57-0.74	58
hsa-miR-125b	0.67***	0.58-0.75	59
hsa-miR-182	0.70***	0.62-0.79	61
hsa-miR-184	0.72***	0.64-0.8	61
hsa-miR-96	0.72***	0.64-0.8	67
hsa-miR-181b	0.73***	0.65-0.81	65
hsa-miR-149	0.74***	0.66-0.82	65
hsa-miR-221	0.75***	0.66-0.82	66
hsa-miR-31	0.76***	0.68-0.83	63
hsa-miR-183	0.77***	0.69-0.84	68
hsa-miR-145	0.78***	0.7-0.85	71
hsa-miR-222	0.78***	0.7-0.85	68
hsa-miR-205	0.82***	0.76-0.89	72
Combinations			
All miRNAs	0.86***	0.79-0.91	82
hsa-miR-96, -149, -181b, -182, 205, -375	0.88***	0.82-0.93	80
hsa-miR-205 + hsa-miR-183	0.88***	0.81-0.92	84

*p < 0.05, **p < 0.01, *** p < 0.001

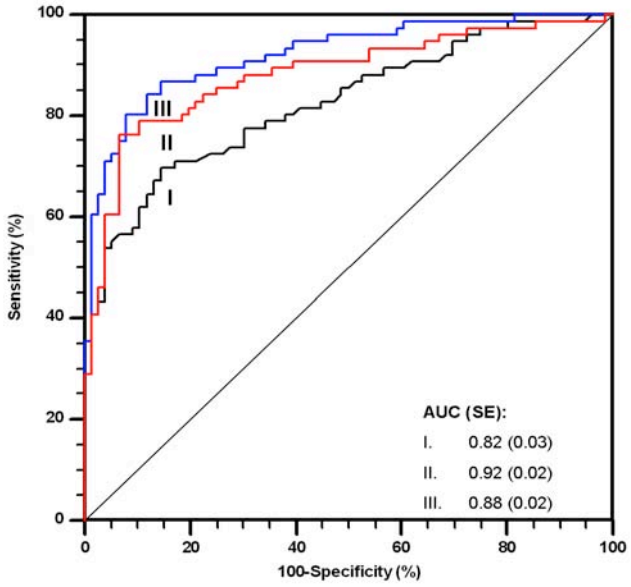

Figure 12: Performance of selected miRNAs and miRNA combinations to discriminate tumor and normal prostate tissue.

ROC analysis was performed from the expression of I) miR-205 or combinations of either II) all miRNAs or only III) miR-205 and miR-183 as obtained by logistic regression. To render the analysis more robust to statistical errors, we performed bootstrapping with 10,000 random repeats.

3.1.5.3 miRNAs as prognostic markers for prostate cancer biochemical recurrence

Accurate prognosis of prostate cancer recurrence after radical prostatectomy is still a major challenge. To date, prostate cancer is categorized into risk groups by using clinical and pathological parameters, such as the TNM stage, Gleason score, pre-operative PSA value and surgical margins. Additionally, patients are monitored periodically for increases in PSA. The introduction of molecular markers might improve prognosis so as to provide patients with more aggressive cancers with timely follow-up and more intensive treatment. Therefore, miRNA expression was analyzed for predictive significance in prostate cancer.

Follow-up data of the PSA concentration was available for 75 out of the 76 clinically characterized prostate cancer patients (Table 19). These patients were included to analysis of disease recurrence. Median follow-up was 50 months (1-93). The time of recurrence was defined as described in the material and methods section.

Performance of miRNAs as prognostic markers was analyzed by univariate Kaplan-Meier analysis as well as univariate Cox regression of dichotomized variables. Each miRNA was dichotomized according to their median expression in tumor tissue.

Recurrence-free survival was significantly reduced in patients with a high Gleason score or advanced pathological stage (Table 24, Figure 8A+B), while there was no reduction of recurrence-free survival in patients with high pre-operative PSA values, increased age or positive surgical margins (Table 24). Only miR-96 showed a significant association with biochemical relapse (Table 24, Figure 13).

Table 24: Univariate Cox proportional hazard analysis of clinico-pathologic parameters and differentially expressed miRNAs in prostate cancer patients with regard to the recurrence-free interval after radical prostatectomy

Variable	HR (95% CI)	p-value
Age	1.79 (0.56-5.74)	0.31
PSA prior surgery	0.7 (0.22-2.20)	0.54
Tumour stage	6.53 (1.41-30.3)	0.01
Gleason score	3.61 (1.54-8.47)	0.01
Surgical margins	1.88 (0.57-6.22)	0.29
hsa-miR-16	1.42 (0.43-4.73)	0.56
hsa-miR-31	0.37 (0.1-1.38)	0.12
hsa-miR-96	3.7 (0.99-13.9)	0.04
hsa-miR-125b	0.9 (0.28-2.88)	0.85
hsa-miR-145	0.74 (0.23-2.34)	0.61
hsa-miR-149	0.68 (0.22-2.15)	0.51
hsa-miR-181b	1.51 (0.47-4.83)	0.48
hsa-miR-182	2.47 (0.73-8.35)	0.13
hsa-miR-182*	1.6 (0.5-5.11)	0.42
hsa-miR-183	2.98 (0.8-11.0)	0.09
hsa-miR-184	0.61 (0.19-1.94)	0.40
hsa-miR-205	0.37 (0.1-1.4)	0.13
hsa-miR-221	0.93 (0.3-2.89)	0.90
hsa-miR-222	0.69 (0.22-2.17)	0.52
hsa-miR-375	0.74 (0.23-2.33)	0.60

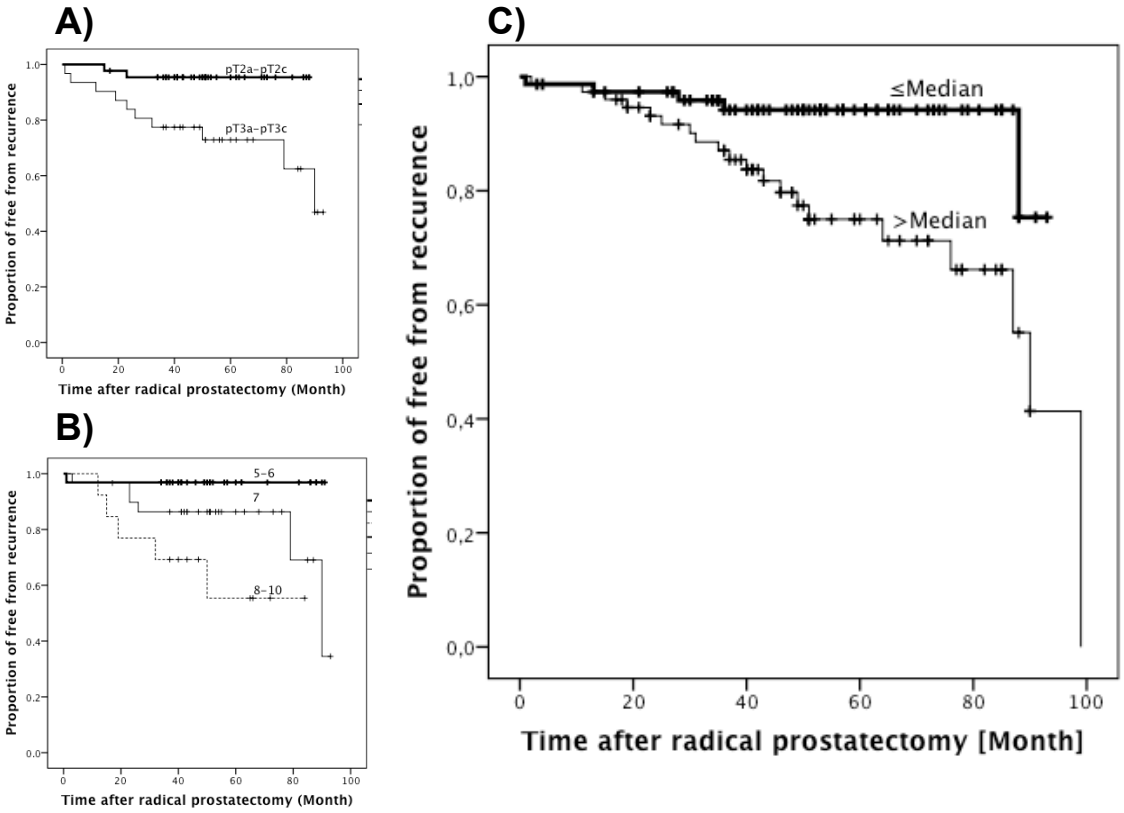

Figure 13: Kaplan-Meier analysis of recurrence free survival

Recurrence-free survival in relation to A) pathological stage, B) Gleason score, and C) miR-96 expression. The time of recurrence was defined as the first post-operative PSA value >0.1 µg/l PSA as confirmed by at least one subsequent rising value after the patients had reached an undetectable PSA level (detection limit <0.04 µg/l after surgery).

To validate whether the association of miR-96 with biochemical relapse is robust, expression was measured in a second independent set of 79 prostate cancer tissue specimens. In the validation cohort, significant association of miR-96 expression with biochemical relapse was confirmed. For all subsequent statistical analyses, we combined both patient subsets.

Clinico-pathological parameters (Gleason score, pathological stage, surgical margins and pre-operative PSA) as well as dichotomized miR-96 expression of all 155 prostate cancer specimens were forwarded to multivariate COX regression analysis.

In the full model, Gleason score, pathological stage and miR-96 were independent variables (Table 25). Interestingly, miR-96 had the highest hazard ratio of each of the parameters. Using forward and backward elimination approaches (entry: p = 0.1; elimination: p = 0.05), a reduced model was identified. The reduced model contained the variables for Gleason score and miR-96, which both were highly independent from each other.

Table 25: Cox regression model

Model	Covariate	β	HR	95% CI	p-value
Full model	miR-96	1.28	3.58	1.19-10.78	0.02
	Gleason score	0.99	2.69	1.45-4.98	<0.001
	Pathological stage	1.23	3.41	1.10-10.57	0.03
	Surgical margins	0.40	1.48	0.57-3.86	0.42
	Pre-operative PSA	0.09	1.10	0.48-2.49	0.83
Reduced model	miR-96	1.48	4.38	1.57-12.22	0.01
	Gleason score	1.27	3.55	1.98-6.36	<0.0001

To evaluate the goodness of the estimated prediction models, Chi^2 test of the -2 log likelihood (-2LL) was performed.

As shown in table 26, -2LL was significantly improved by addition of each parameter to the full model. The reduced prediction model was significantly improved by adding both variables to the model; however, interestingly, adding the Gleason score or miR-96 to the model or adding miR-96 to a model that already contains Gleason score significantly improved the -2LL.

Table 26: Goodness of prediction models

Model	Covariate	-2LL	Chi^2	p-value
Full model	none	214.97		
	+ miR-96, Gleason score, pathological stage, surgical margins, pre-operative PSA value	174.40	44.39	<0.0001
Reduced model	none	220.14		
	+Gleason score	196.53	22.70	<0.0001
	+miR-96	190.32	6.22	0.013
	+Gleason score, miR-96	190.32	29.45	<0.0001

To further verify the predictive power of our model, we compared the predicted survival curves with the observed survival curves. The survival curves were not significantly different from each other, confirming the good performance of this model (Figure 14).

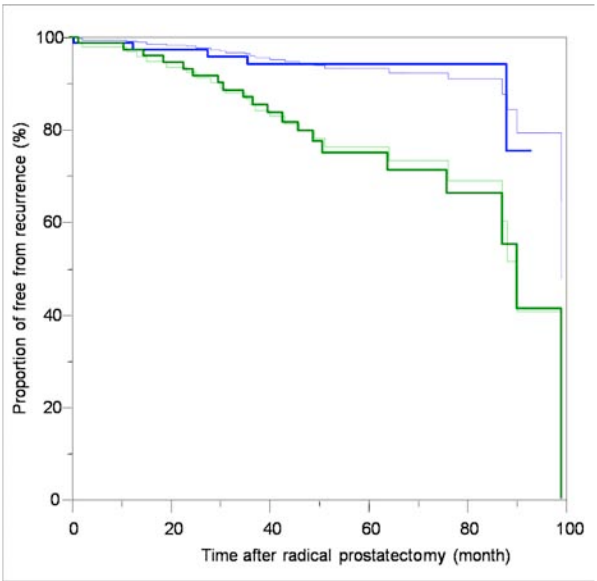

Figure 14: Comparison of the observed and expected biochemical recurrence
The observed biochemical recurrence of patients with high/low miR-96 expression was displayed as a Kaplan-Meier Plot (blue and green line). Additionally, the expected biochemical recurrence was predicted by miR-96 and plotted (light blue and green line).

As a final verification step, the c-index was calculated. The c-index determines the probability that the prediction model predicts the survival time for each patient in the correct order, The c-index was 0.85, confirming the high accuracy of this model.

3.1.5.4 miRNAs in formalin-fixed, paraffin-embedded prostate cancer tissue for risk stratification after radical prostatectomy

The exploration of miRNA expression in fresh-frozen prostate cancer tissue established that miRNAs may be suitable markers for both diagnostic as well as prognostic monitoring. Based on these observations, the hypothesis was established that miRNA expression may also differentiate patients experiencing an early biochemical relapse after radical prostatectomy from those patients with a long relapse-free interval or no biochemical relapse. Measurement of those patients was performed using FFPE tissue, which is routinely archived for each patient. miRNAs are remarkably stable in highly degraded tissue (Jung *et al.*, 2010) and studies in FFPE tissue pinpoint to the stable expression of miRNAs in these tissues (Glud *et al.*, 2009; Hasemeier *et al.*, 2008; Hui *et al.*, 2009; Siebolts *et al.*, 2009; Szafranska *et al.*, 2008; Zhang *et al.*, 2008).

We profiled miRNA expression in patients with biochemical relapse using a multiplex miRNA RT-qPCR Arrays in a 384-well format. This approach provides higher sensitivity and accuracy for miRNA analysis in comparison to microarray profiling (Mees *et al.*, 2009). Prostate cancer patients were divided into 3 groups (Table 27):

A) Patients with an early biochemical relapse (<1 year after radical prostatectomy)
B) Patients with a late biochemical relapse (1-5 years after radical prostatectomy)
C) Patients with no biochemical relapse

Table 27: Patient and tumor characteristics for prostate cancer relapse patients

	Relapse < 1 year N = 24		**Relapse > 1 - 4 years N = 23**		**No Relapse within 3 years N =12**	
	Median (range)	**N (%)**	**Median (range)**	**N (%)**	**Median (range)**	**N (%)**
Age (yrs)	61 (51-71)		62 (49-73)		65.5 (55-72)	
Pre-operative PSA (ng/ml)	8.9 (0.8-25.0)		8.0 (0.4-41.9)		6.5 (3.7-25.8)	
Pathological tumor stage						
pT2a				1 (4%)		
pT2b		3 (13%)		4 (17%)		1 (8%)
pT2c		5 (21%)		5 (22%)		4 (33%)
pT3a		12		11 (48%)		5 (42%)

pT3b		(50%) 4 (17%)	2 (9%)	2 (17%)
Gleason Score 6 7 8 9 10		3 (13%) 13 (54%) 7 (29%) 1 (4%)	1 (4%) 12 (52%) 4 (17%) 4 (26%)	3 (25%) 5 (42%) 3 (25%) 1 (8%)
Surgigal margins R0 R1		15 (63%) 9 (38%)	12 (52%) 11 (48%)	7 (58%) 5 (42%)
PSA-free survival (month)	4.57 (1-12)	25.5 (14-50)		51.9 (37-65)

For the initial screening step, 3 RNA pools were prepared corresponding to the groups of early, late and no relapse patients. Each pool was prepared from 10 RNA samples using the same quantity of total-RNA from each patient sample. Multiplex miRNA RT-qPCR was performed in a 384-well format using 2 different card versions. The combination of these cards allowed the quantification of 762 miRNAs per sample.

One hundred ninety-eight of the seven hundred sixty-two miRNAs showed a detectable signal (< 32 Cq) in at least one pool. Differential expression was assumed, if the fold-change in comparison to the no relapse pool was ≥1.5 in at least one pool. According to this definition, 63 miRNAs were differentially expressed, of which 35 miRNAs were upregulated and 28 miRNAs were downregulated. The most highly dysregulated miRNAs are summarized in table 28.

Table 28: Top dysregulated miRNA in relapsing prostate cancer

miRNA	No Relapse	Late relapse	Early relapse
hsa-miR-23a	NE	(89.44)	(646.34)
hsa-miR-449a	NE	(22.25)	(247.59)
hsa-miR-449b	NE	(68.46)	(207.79)
hsa-miR-200a	1.00	1.12	2.53
hsa-miR-1233	1.00	2.23	2.36
hsa-miR-10b	1.00	2.53	1.90
hsa-miR-1825	1.00	1.11	1.84
hsa-miR-186	1.00	0.64	0.67
hsa-miR-1275	1.00	1.08	0.65
hsa-miR-532-5p	1.00	0.99	0.64
hsa-miR-193b	1.00	1.10	0.64
hsa-miR-886-3p	1.00	1.13	0.60
hsa-miR-664	1.00	1.29	0.58
hsa-miR-196b	1.00	0.45	0.58
hsa-miR-1274B	1.00	1.19	0.57
hsa-miR-720	1.00	1.19	0.51
hsa-miR-146b-5p	1.00	0.83	0.49
hsa-miR-222	1.00	0.85	0.44
hsa-miR-31	1.00	0.91	0.43
hsa-miR-127-5p	1.00	0.27	NE

NE = not expressed

The 63 dysregulated miRNAs are located at 67 chromosomal locations, with 4 miRNAs having 2 genomic loci. Twenty-eight of the sixty-three miRNAs are located in an intron of a protein-coding gene, 2 miRNAs are located in an intron and exon of a protein-coding gene and one miRNA has an exonic location. The 32 remaining miRNA loci are intergenic. The group of dysregulated miRNAs was also analyzed for clustered miRNAs. A cluster is defined by a group of miRNAs that are located less than 10 kB from each other. We identified members of 6 different miRNA clusters, of whom 4 clusters had a concordant expression (miR-200a/miR-429; miR-518b/miR-519-3p; miR-449a/miR-449b; miR-221/miR-222).

The initial screen showed that multiplex RT-qPCR is a valid approach for identifying dysregulated miRNAs from FFPE tissue. To further verify the specificity and sensitivity of the assay, 2 miRNAs (miR-10b and miR-222) were chosen for validation in 46 samples. For the validation patients were divided into patients a biochemical relapse within less than 1 year and patients with a biochemical relapse after at least 2 years or no biochemical relapse. miR-10b and miR-222 were chosen because they were highly expressed in the patients, were more than 2-fold different in expression in at least one pool and have been shown to be associated with biochemical relapse in other cancers (Greither *et al.*, 2010; Li *et al.*, 2010c; Ma *et al.*, 2007; Sasayama *et al.*, 2009; Veerla *et al.*, 2009).

miR-10b was 1.67-fold higher expressed in patients with early biochemical relapse in comparison to patients with late or no biochemical relapse (Mann-Whitney; $p < 0.05$, Figure

15A). miR-222 expression was not significantly different between the groups; however, there was a trend for reduced expression in early relapse patients with an 1.21-fold lower expression (Figure 15B).

To enhance the discriminative power between the groups, the expression ratio of miR-222/miR-10b was calculated (Figure 15C). The ratio was 1.69-fold lower in patients with early biochemical relapse in comparison to patients with late or no biochemical relapse.

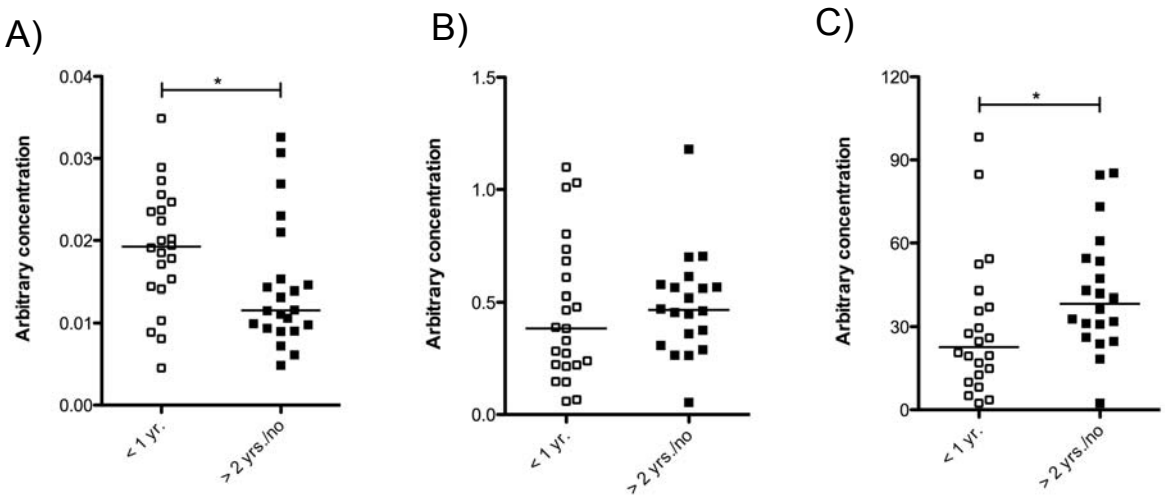

Figure 15: miRNA expression in prostate cancer patients with biochemical relapse.
Scatter dotplot of A) miR-10b and B) miR-222 expression and C) the expression ratio of miR-222/miR-10b. miRNA expression was measured by TaqMan RT-qPCR. Expression was normalized to the geometric mean of miR-130b and RNU44, interplate controls and RT-qPCR efficiency. Lines represent the median expression. * $p < 0.05$, Mann-Whitney test.

miR-10b did not correlate with clinico-pathological parameters, but miR-222 was significantly correlated with histological grade (Gleason score) (Table 29).

Table 29: Spearman correlation of predictive miRNA markers with clinico-pathological data

	miR-10b		**miR-222**	
	r_S	p-value	r_S	p-value
Gleason score	0.24	0.11	-0.31	0.04
Pathological stage	0.17	0.28	-0.22	0.16
Surgical margins	-0.02	0.92	0.17	0.27
Preoperative PSA	0.14	0.37	-0.08	0.91

* $p < 0.05$

To analyze the power of each miRNA to discriminate patients with an early biochemical relapse, ROC analysis and logistic regression was performed. miR-10b expression and the expression ratio of both miRNAs were good discriminators of early relapsing patients, with an AUC of 0.72 and 0.70, respectively (Figure 16). In contrast, miR-222 was a worse discriminator (AUC: 0.56; p = 0.15). However, comparison of the ROC curves revealed no significant improvement of discrimination for miR-222/miR-10b over miR-222. Only comparison of the ROC curves of miR-222 and the ratio showed a borderline significance (p = 0.07).

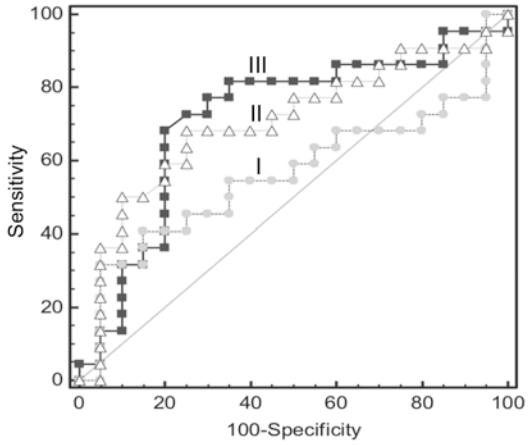

Figure 16: Ability of selected miRNAs and miRNA combinations to discriminate early relapse patients from no-relapse or late relapsing patients
ROC analysis was performed on the miRNA expression of I) miR-222 or II) Ratio or III) miR-10b.

We then performed Kaplan-Meier analysis and multivariate Cox regression to determine, which miRNAs were significantly associated with biochemical relapse. miR-10b, miR-222, miR-222/miR-10b ratio and the preoperative PSA were dichotomized according to the median. The Gleason score was trichotomized into a group of 6, 7, and above 7. Pathological stage was dichotomized so that all samples with pT2 were grouped as well as all samples with pT3.

Kaplan-Meier analysis revealed a significant association of miR-10b expression with biochemical relapse (log rank test, p = 0.023; Figure 17A), while miR-222 was not significantly associated with biochemical relapse (Figure 17B). Surprisingly, none of the clinico-pathological variables were significantly associated with biochemical relapse (data not shown). In a multivariate Cox regression model, only miR-10b was an independent variable and remained the only variable in the model using forward and backward elimination methods (Table 30).

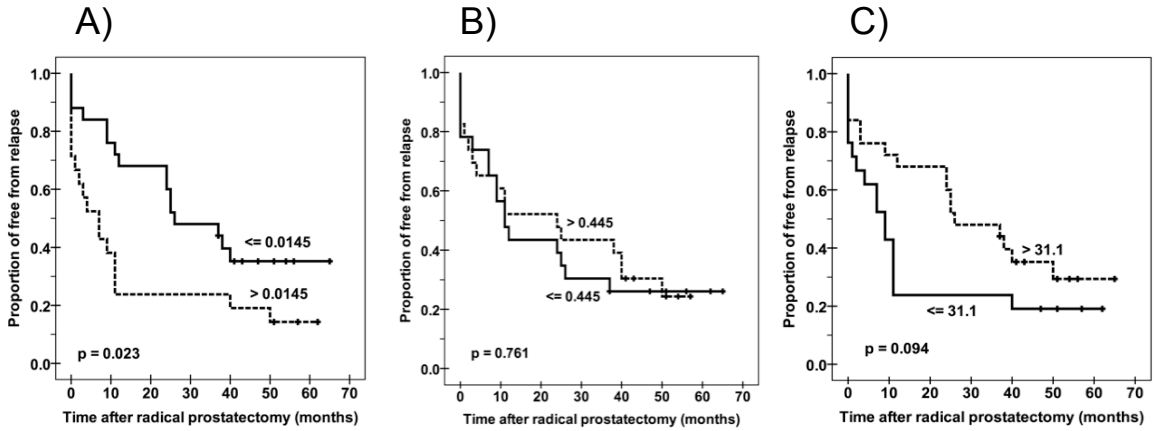

Figure 17: Kaplan-Meier analysis of recurrence-free survival

Recurrence-free survival in relation to dichotomized A) miR-10b expression, B) miR-222 expression, and C) miR-222/miR-10b in tumor tissue relative to expression in normal adjacent tissue. The time of recurrence was defined as the first post-operative PSA value >0.1 µg/l PSA confirmed by at least one subsequent rising value after the patients had reached an undetectable PSA level (detection limit <0.04 µg/l) after surgery.

Table 30: Cox regression of dysregulated miRNAs and clinic-pathological variables

Method	Variable	β	HR	95% CI	p-value
Inclusion	miR-10b	0.76	2.14	1.02-4.51	0.04
	Gleason score	-0.22	0.80	0.37-1-72	0.57
	Pathological stage	-0.11	0.90	0.40-1.99	0.79
	Surgical margins	0.07	1.07	0.50-2-28	0.86
	Pre-operative PSA	0.25	1.28	0.64-2-58	0.0.48
Forward LR	miR-10b	0.74	2.10	1.06-4.17	0.03
Backward LR	miR-10b	0.74	2.10	1.06-4.17	0.03

3.2 Functional relevance of miRNAs in prostate cancer

3.2.1 In silico target prediction for prostate cancer-related miRNAs

miRNAs posttranscriptionally inhibit gene expression by binding to complementary binding sites in the 3' UTR of protein-coding transcripts, resulting either in translational inhibition or degradation of the mRNA. While one miRNA can bind to hundreds of mRNAs, one mRNA can be targeted by a multitude of miRNAs. In silico target prediction is therefore a mandatory tool to identify putative binding sites. To date, various algorithms exist to predict miRNA binding sites. Each of them use different criteria to predict binding sites and therefore have different advantages and disadvantages. Most algorithms account for perfect complementarily of the seed sequence, evolutionary conservation and free energy of the miRNA:mRNA duplex. Proximity of different binding sites of the same miRNA can also be a criterion for identification of biologically significant binding sites. The most commonly used miRNA target prediction algorithms are TargetScan, picTar and miRanda. Each has a more

stringent algorithm in comparison to other prediction algorithms. In this thesis, targets for each of the differentially regulated miRNAs were predicted using miRecords (http://mirecords.umn.edu/miRecords). miRecords combines the target prediction of 11 algorithms. To further narrow the results, we applied the following criteria for a putative target gene:

A) A target gene had to be concordantly identified by miRanda, picTar and TargetScan
B) A target gene had to be predicted by at least 2 other prediction algorithms

In-silico target prediction was performed for each miRNA that was differentially regulated in prostate cancer in comparison to normal adjacent tissue (Figure 18). The median number of predicted target genes was 84 (0-337) per miRNA. In silico target prediction was also performed for miRNAs dysregulated in the biochemical relapse patients. Targets were identified for 36 of the 68 miRNAs and ranged from 3 to 347 targets per gene.

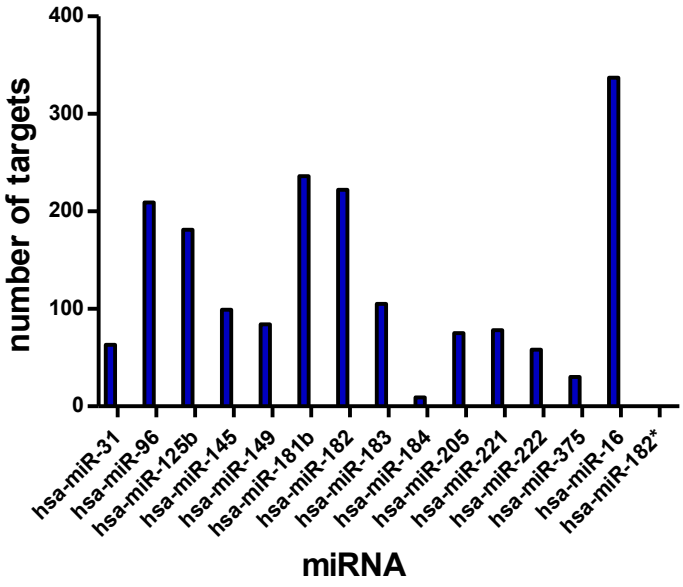

Figure 18: Overview of predicted target genes for miRNAs differentially expressed in prostate cancer

miRNA targets were predicted using miRecords. A prediction was accepted as valid if it was identified simultaneously by TargetScan, miRanda and picTar and at least 2 other algorithms.

The results from the in silico target prediction were used for further in silico approaches to explore miRNA function and as decision criteria for experimental target predictions for 2 selected miRNAs (see 3.2.4 and 3.2.5).

3.2.2 miRNAs in cancer progression

miR-10b and miR-222 were identified to discriminate patients with early relapsing tumors. The expression of these miRNAs in more aggressive tumors in comparison to non-aggressive tumors raises the possibility that these miRNAs play a functional role in tumor progression.

To explore the potential functional role of miR-10b and miR-222 in prostate cancer, in silico analysis was performed on the basis of the predicted targets. The predicted miR-10b and miR-222 targets analyzed by Gene Ontology term clustering by DAVID (http://david.abcc.ncifcrf.gov/home.jsp) and pathway analysis was performed using reactome skypainter (http://www.reactome.org/cgi-bin/skypainter2).

Reactome skypainter analysis of the 58 potential miR-222 target genes revealed an over-representation of regulators of protein stability and TRKA signalling (CDKN1B and RALA). The over-representation of TRKA signalling is in accordance with previous reports of miR-222 function in prostate cancer, because the regulation of CDKN1B by miR-222 is well established.

Pathway analysis for the 55 predicted target genes of miR-10b revealed an overrepresentation of genes involved in transcriptional regulation (TBX5, NFAT5, HOXA1, KLF13 and others). Gene ontology analysis and subsequent clustering by DAVID confirmed transcription to be the most relevant biological term in the set of target gene predictions.

Previous studies suggest a role for miR-10b in metastasis (Chai *et al.*, 2010; Ma *et al.*, 2007; Ma *et al.*, 2010; Tian *et al.*, 2010). Therefore, the impact of miR-10b overexpression on cell motility and proliferation was studied in LNCaP and DU-145 cells.

Overexpression of miR-10b in DU-145 prostate cancer cells increased cell migration in the wound-healing assay in comparison to the control cells ($p<0.05$; Two-way ANOVA; Figure 19A). Cotransfection with anti-miR-10b abolished the activating effect of miR-10b, while transfection of the antisense strand alone had no effect on cell migration. However, ectopic overexpression of miR-10b did not effect cell proliferation in serum-starved LNCaP cells over 3 days (Figure 19B). The results suggest that miR-10b mainly participates in tumor progression and metastasis, in accordance with the overexpression observed in prostate cancer patients with aggressive early relapsing tumors. Re-analyzing the target gene list revealed several putative target genes that may mediate miR-10b-dependent cell motility (TBX5, EPHA4, NFACS, ACTG1, NRP2, HOXA1, ELAL3).

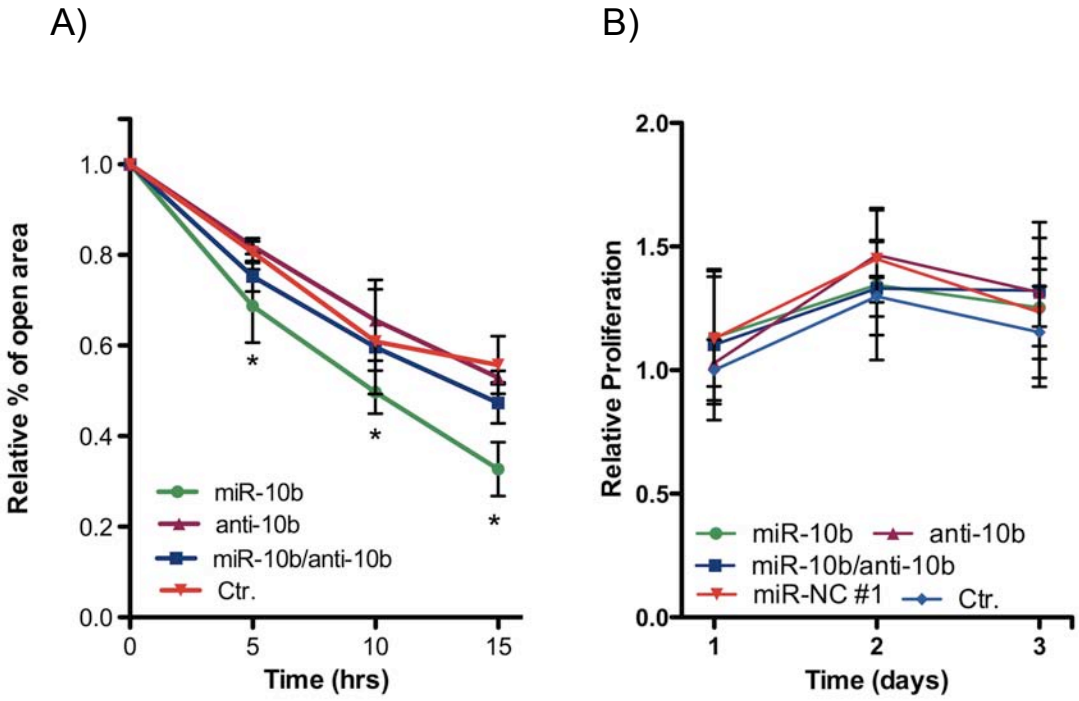

Figure 19: miR-10b induces cell motility in DU-145 prostate cancer cells

Cells were transfected with 10 nM pre-miR-10b, anti-miR-10b, pre-miR-NC #1 or a combination of pre-miR-10b and anti-miR-10b. A) DU-145 cells were transfected and grown to 100% density. The monolayer was scratched with a pipette tip and remigration to the wound was analyzed for 15 hrs by live cell imaging. Pictures were captured every 10 min. The percentage of open area was determined every 5 hrs using TScratch software. B) The effect on cell proliferation of LNCaP cells was measured by MTT assay over 3 days. Data are presented as the mean values from 3 independent assays (±SD). *$p < 0.05$, Two-way ANOVA.

3.2.3 Androgen-dependent regulation of miRNA expression

Androgen-dependence is one of the major characteristics of prostate cancer cell growth. Androgen depletion is the prevalent therapy option for recurrent prostate cancers. Yet, patients inevitably develop CRPC, which is not curable so far. Due to the major importance of androgens in prostate cancer, the expression of 17 prostate cancer-associated miRNAs was analyzed in the androgen-dependent LNCaP cell line after treatment with the synthetic androgen R1881. Prostate cancer cells were synchronized in RPMI w/o phenolred and 0.25% charcoal-FCS and were subsequently treated with 0.1 or 10 nM R1881 for 72 hrs.

Expression of the majority of miRNAs was not regulated by R1881. Only 4 miRNAs (miR-10b, miR-149, miR-221 and miR-222) were significantly downregulated by androgen treatment (Figure 20). miR-221 expression was most prominently dysregulated, having a 1.49-fold and 3-fold downregulation after treatment with 0.1 nM and 10 nM R1881, respectively. These results suggest a role of this miRNA in prostate cell proliferation.

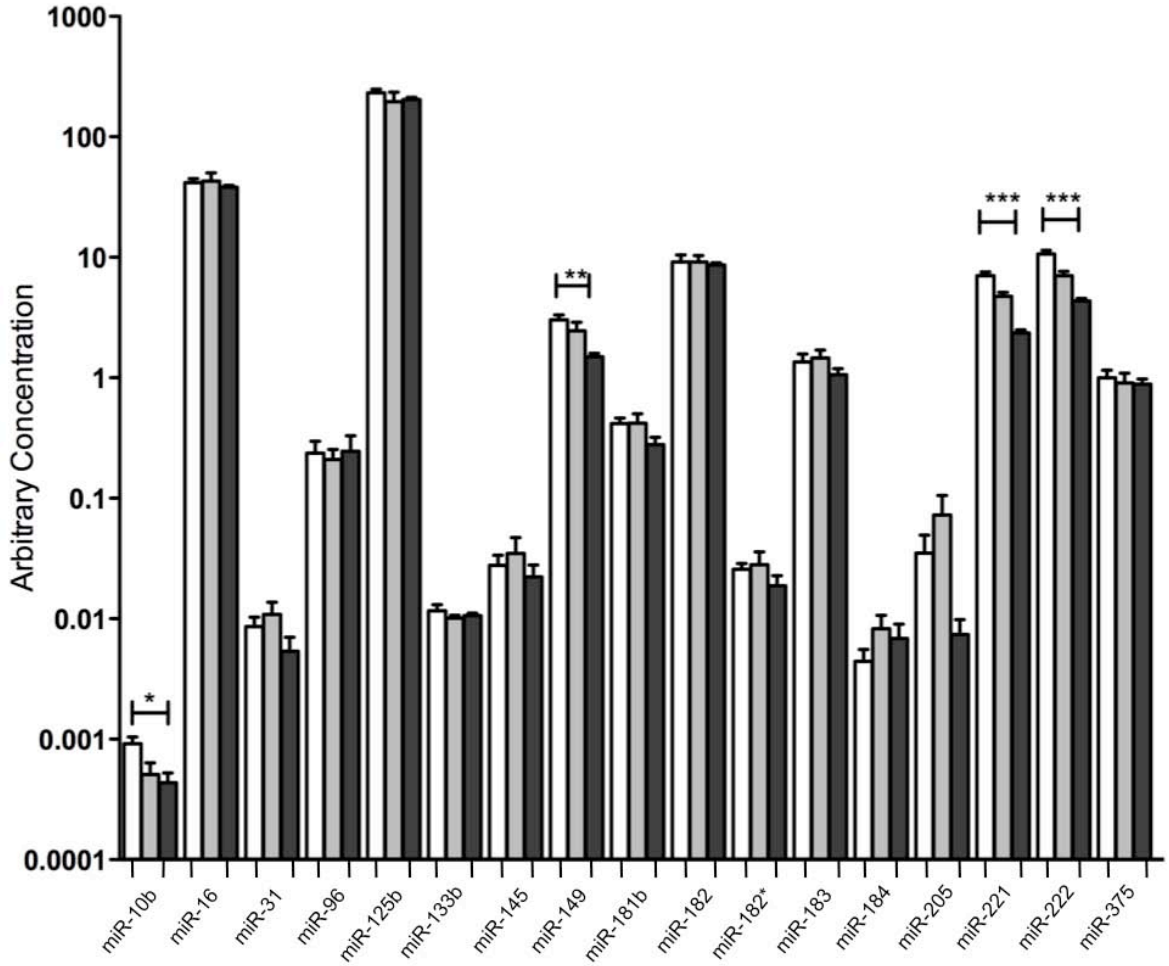

Figure 20: Androgen-dependent expression of miRNAs in LNCaP cells

LNCaP cells were synchronized in RPMI media w/o phenolred and 0.25% charcoal FCS) for 5 days. Cultures were then treated with 0.1 nM or 10 nM R1881 for 3 days in RPMI w/o phenolred and 10% charcoal-FCS. miRNA expression was measured by RT-qPCR. Expression was normalized to efficiency, interplate controls and miR-130b. Data are represented as the mean (+SD) of 3 independent assays. *p < 0.05, **p < 0.01, ***p < 0.001, One-Way ANOVA.

3.2.4 miR-96: an oncogenic miRNA in prostate cancer

miR-96 expression was upregulated in prostate cancer tissue in comparison to normal adjacent tissue, and high expression of this miRNA is associated with biochemical relapse (see 3.1). The upregulation of miR-96 in prostate cancer tissue raises the question as to whether this miRNA may have oncogenic properties in prostate cancer. To address the functional relevance of miR-96, the LNCaP prostate cancer cell line was transfected with synthetic miRNA precursors or antisense inhibitor oligonucleotides to either transiently amplify or inhibit miR-96 expression. This cell line was chosen because of its low endogenous miR-96 expression and low aggressiveness (Figure 21).

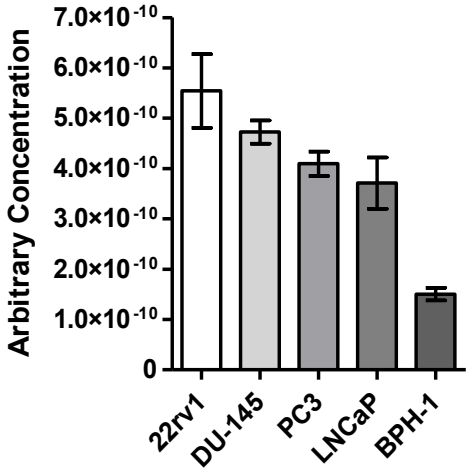

Figure 21: Expression of miR-96 in prostate cancer cell lines
miR-96 expression was measured by TaqMan RT-qPCR. Data are shown as mean arbitrary expression units (±SD).

3.3.4.1 Regulation of apoptosis by miR-96

Cancer cells are characterized by self-sufficiency in growth signalling and resistance to anti-growth signals (Hanahan and Weinberg, 2011). Therefore, the influence of miR-96 on prostate cancer cell growth was studied by the metabolic conversion of XTT as indicator of an increased growth rate.

Serum starved LNCaP cells, which were transfected with 10 nM synthetic pre-miR-96 showed enhanced proliferative activity in comparison to non-transfected cell lines or cells transfected with a scrambled control (Figure 22). The growth promoting effect could be partially inhibited by cotransfecting the cells with the pre-miR-96 and the antisense inhibitor. Transfection with only the antisense inhibitor did not affect cell growth.

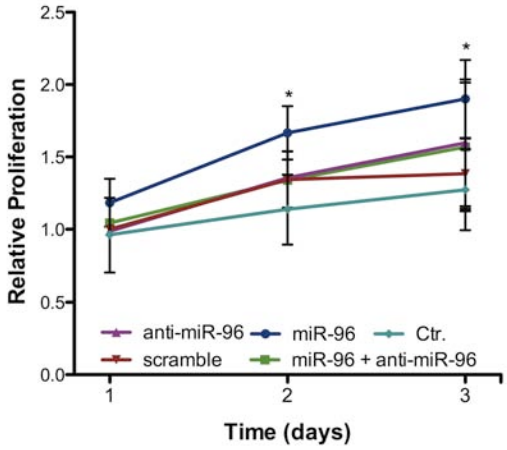

Figure 22: Metabolic conversion of XTT in miR-96 overexpressing LNCaP cells
LNCaP cells were transfected with 10 nM pre-miR-96, anti-miR-96, pre-miR-NC #1 or a combination of pre-miR-96 and anti-miR-96. The effect on cell proliferation during serum starvation was measured by the XTT assay over 3 days. The data are shown as the mean (±SD) of 3 independent assays. *p < 0.05, Two-way ANOVA.

To analyze whether the elevated metabolic activity of LNCaP cells was due to faster cell cycle transition upon transfection with pre-miR-96, we analyzed the DNA content of LNCaP cells by flow cytometry.

Cell cycle analysis showed that the majority of LNCaP cells were in the G1 phase upon serum starvation (71.00% to 76.65% of total) and only a small fraction of cells were synthesizing DNA (4.79% to 5.32%) or were in G2/M phase (18.56% to 23.69%, Figure 23). However, the cell cycle transition in cells transfected with pre-miR-96 was not significantly different than in non-transfected cells. These results indicate that the enhanced metabolic activity of the LNCaP cells was not due to an increase of mitotic cells after transfection with pre-miR-96.

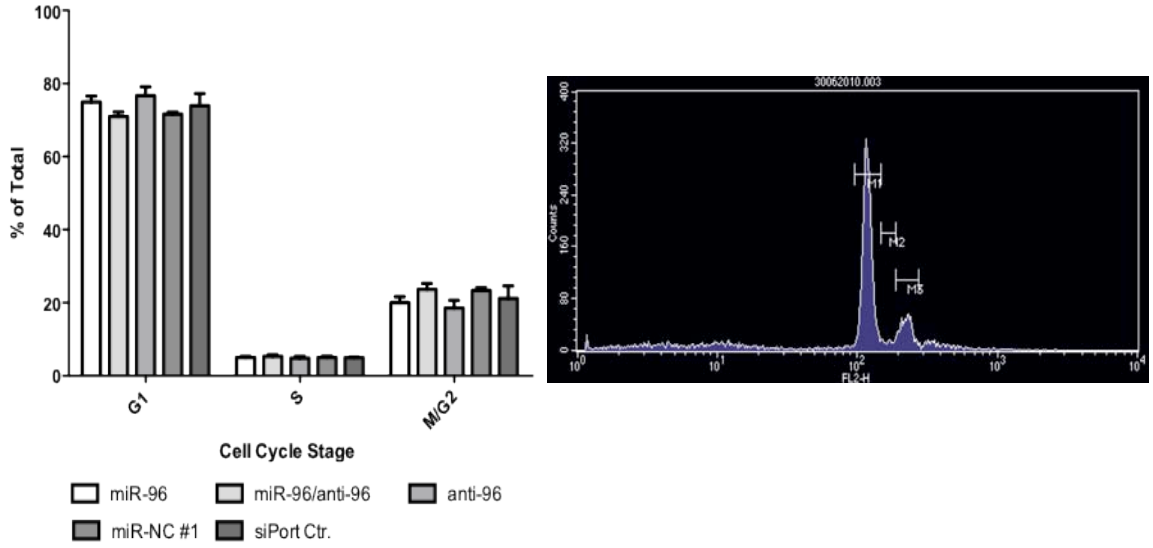

Figure 23: Cell cycle analysis of LNCaP cells transfected with miR-96
LNCaP cells were transfected with 10 nM pre-miR-96, anti-miR-96, pre-miR-NC #1 or a combination of pre-miR-96 and anti-miR-96. 24 hrs after transfection, cells were serum starved for an additonal 24 hrs. Cells were fixed in 70% ethanol and stained in PI-staining solution. DNA content was measured by flow cytometry. Data are shown as the mean (+SD) of 3 independent assays.

Because the enhanced metabolic activity could not be explained by a faster cell cycle transition, the effect of miR-96 expression on apoptosis was measured. Apoptosis was induced by treatment with 10 µM CPT subsequent to transfection with the synthetic oligonucleotides. CPT induces DNA damage, resulting in activation of intrinsic apoptotic pathways (Glynn *et al.*, 1992). Cells were stained with Annexin-V FITC and PI. Annexin-V FITC binds to phosphatidylserine residues that are transported to the cell surface during early apoptosis. PI is a marker for membrane integrity, as it cannot cross the membrane of intact cells to bind DNA.

Flow cytometric analysis of Annexin-V FITC/PI stained cells showed, that 10 µM CPT successfully induced apoptosis in LNCaP cells, with 13.17% early apoptotic cells and 5.55% late apoptotic cells in the control culture (Figure 24). Transient transfection with pre-miR-96 reduced the fraction of early apoptotic cells by 46% and the fraction of late apoptotic cells by 15%. To determine whether inhibition of apoptosis was miR-96-specific, 2 miRNAs were included as control. miR-21 is a known oncogene in prostate cancer and has been shown to inhibit apoptosis in prostate cancer cells (Li *et al.*, 2009b; Shi *et al.*, 2010a; Yang *et al.*, 2010). LNCaP cells transiently expressing pre-miR-21 showed a similar apoptotic phenotype to the pre-miR-96 transfected cells. As a negative control, we used miR-16, for which no anti-apoptotic function has been described in prostate cancer. Transfection with pre-miR-16 did not affect the fraction of apoptotic cells.

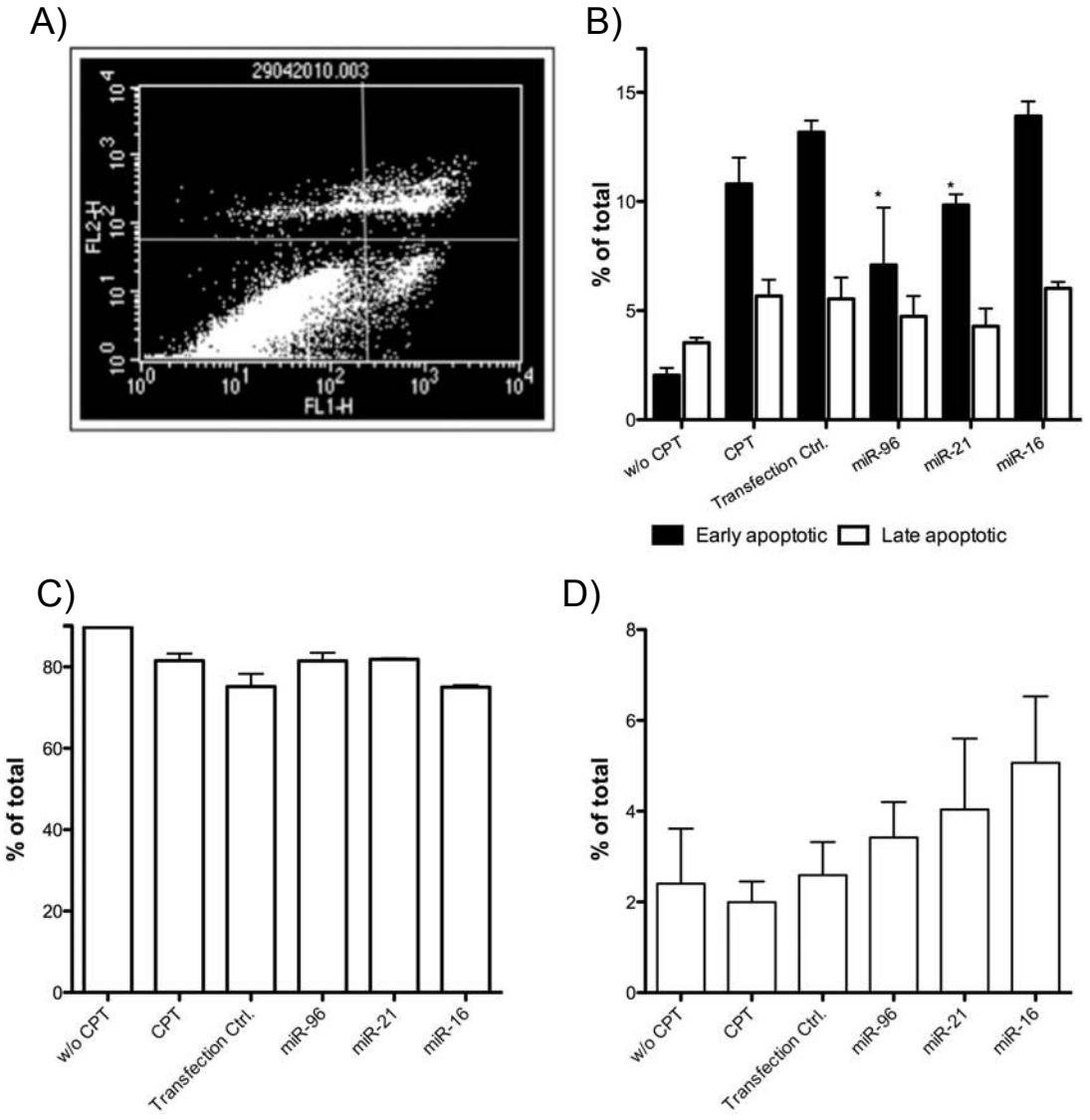

Figure 24: Analysis of apoptosis in miR-96 overexpressing cells LNCaP cells by Annexin-V FITC staining

LNCaP cells were transfected with 10 nM pre-miR-96, anti-miR-96, pre-miR-NC #1 or a combination of pre-miR-96 and anti-miR-96. 24 hrs after transfection cells were treated with 10 µM CPT for 24 hrs. Cells were stained with Annexin V-FITC and PI. A) Example of density blot, B) Early and late apoptotic cells, C) Vital cells, and D) Necrotic cells. Fluorescence intensity was measured by flow cytometry. The data are shown as the mean (+SD) of 3 independent assays. *p < 0.05, Two-way ANOVA with Bonferroni posttest.

These experiments established a role for miR-96 in apoptotic signalling in prostate cancer. To determine whether miR-96 may yet induce other carcinogenic pathways in prostate cancer, a wound-healing assay was performed in DU-145 cells. LNCaP cells could not be used for this assay due to their very low migrative properties.

DU-145 cells have a migrative phenotype and were able to remigrate up to 60% of the initial wound in 20 hrs (Figure 25). Transfection with pre-miR-96 did not affect in DU-145 cells had no effect on cell migration in comparison to transfection with a scrambled control.

Likewise, transfection with the antisense inhibitor did not alter the migrative phenotype in these cells.

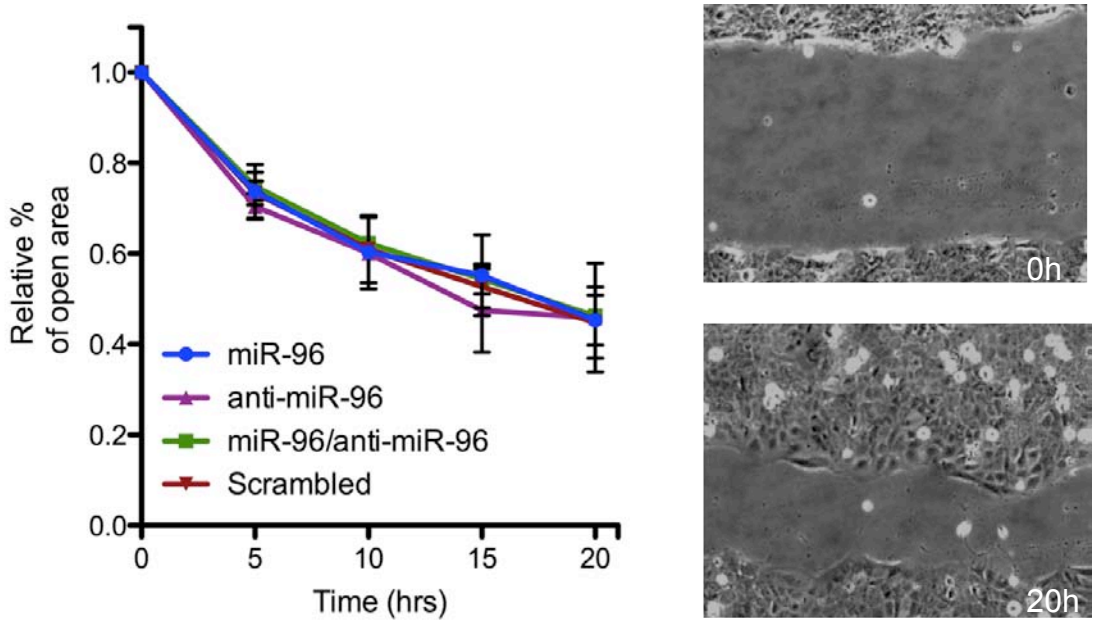

Figure 25: Migration of miR-96 overexpressing DU-145 cells
Du-145 cells were transfected with 10 nM pre-miR-96, anti-miR-96, pre-miR-NC #1 or a combination of pre-miR-96 and anti-miR-96 and grown to 100% density. The monolayer was scratched with a pipette tip, and remigration to the wound was analyzed for 20 hrs by live cell imaging. Images were captured every 10 min. Percentage of open area was determined every 5 hours using TScratch software.

3.2.4.2 miR-96 as an effector of apoptosis-related genes

Identification of predicted target genes that regulate apoptosis

Studies of miR-96 function in prostate cancer cells have established an exclusive role of this miRNA in apoptosis. However, the genes targeted by miR-96 that mediate the anti-apoptotic function of this miRNA are unknown. In silico target-prediction was performed for miR-96, as described in 3.3.1. The set of predicted targets was analyzed with regard to their GO terms in order to identify apoptosis-related genes.

Twenty-one of the two hundred and nine predicted miR-96 targets had an apoptosis-related GO term (Table 31). Having identified 21 putative apoptosis-related miR-96 target genes, we performed literature search to determine the role of this genes in prostate cancer. We further analyzed the number of miR-96 binding sites in the 3' UTR of target genes and determined evolutionary conservation of the binding sites across species: these are 2 important criteria to determine miRNA-mediated gene regulation. FOXO1 was identified as an interesting target for miR-96-mediated regulation. FOXO1 is a transcription factor that regulates the expression of apoptosis-promoting genes, such as BCL2L11 (Stahl *et al.*,

2002), BAX (Kim *et al.*, 2005) and TRAIL (Modur *et al.*, 2002). FOXO1 activity is regulated by PI3K/AKT signalling. Upon activation by a growth signal, AKT phosphorylates FOXO1, resulting in relocation of this transcription factor to the cytoplasm (Rena *et al.*, 1999). In prostate cancer, FOXO1 has also been shown to interact with the androgen-receptor and to inhibit its function in a ligand-dependent and-independent fashion (Fan *et al.*, 2007; Liu *et al.*, 2008b). In addition, the androgen-receptor can inhibit the function of FOXO1 (Li *et al.*, 2003). In retinoblastoma cells, FOXO1 expression and transcriptional activity have been linked to CPT-mediated apoptosis (Han and Wei, 2011).

Table 31: Predicted miR-96 target genes with a known function in apoptosis

Accession No.	Gene Symbol	Count	GO Term
NM_004985	KRAS	6	Negative regulation of neuron apoptosis
NM_005400	PRKCE	6	Induction of apoptosis
NM_002015	FOXO1	6	Anti-apoptosis
NM_002959	SORT1	6	Induction of apoptosis by extracellular signals, negative regulation of apoptosis
NM_000945	PPP3R1	6	Activation of pro-apoptotic gene products
NM_002222	ITPR1	6	Cell death
NM_020796	SEMA6A	5	Apoptosis
NM_033285	TP53INP1	5	Induction of apoptosis
NM_052876	BTBD14B	5	Induction of apoptosis
NM_080872	UNC5D	5	Apoptosis
NM_144704	AIFM3	5	Activation of caspase activity by cytochrome C, apoptosis, induction of apoptosis
NM_145735	ARHGEF7	5	Apoptosis, induction of apoptosis by extracellular signals, positive regulation of apoptosis
NM_000248	MITF	5	Negative regulation of apoptosis
NM_002576	PAK1	5	Apoptosis
NM_002752	MAPK9	5	Induction of apoptosis in response to chemical stimulus
NM_004379	CREB1	5	Regulation of apoptosis
NM_005802	TOPORS	5	Apoptosis
NM_006908	RAC1	5	Induction of apoptosis by extracellular signals
NM_014762	DHCR24	5	Anti-apoptosis, apoptosis, negative regulation of caspase activity
NM_015313	ARHGEF12	5	Apoptosis, induction of apoptosis by extracellular signals
NM_173475	DCUN1D3	5	Positive regulation of apoptosis

Inhibition of FOXO1 expression by miR-96

The link of FOXO1 to prostate cancer makes this gene an interesting target for miR-96 regulation. To identify putative binding sites in the 3' UTR, we used TargetScan5.1. TargetScan5.1 uses a stringent algorithm, which is mainly based on complementarity of the seed sequence, conservation of the seed sequence and conserved complementary sides at the 3' end (Lewis *et al.*, 2005). The FOXO1 3' UTR harbors two 8-mer miR-96 binding sites at position 264-270 and position 2139-2145. While the first binding site is highly conserved, the second miRNA binding site is not. To experimentally verify that miR-96 is able to bind to the predicted binding site, we constructed a luciferase reporter plasmid. A 200 bp sequence flanking the predicted miR-96 binding site 1 and a 300 bp sequence flanking the miR-96

binding site 2 were cloned into the pMiR Report vector downstream of the firefly luciferase gene. LNCaP cells were transfected with those reporter genes plus synthetic oligonucleotides for miR-96.

Cotransfection of the pMiR report construct containing miR-96 binding site 1 with pre-miR-96 led to a 40% reduction in luciferase activity as compared to the control transfected cells, while cotransfection of the plasmid with either the antisense inhibitor or a scrambled control did not result in a significant change in luciferase activity (Figure 26). Although the second predicted miR-96 binding site in the FOXO1 3' UTR is only partially conserved, cotransfection of the luciferase report vector and pre-miR-96 also reduced luciferase activity by 42%, while the scrambled control and the antisense inhibitor did not affect luciferase activity. In both cases, cotransfection of pre-miR-96 and the antisense inhibitor only slightly relieved the inhibition of luciferase activity.

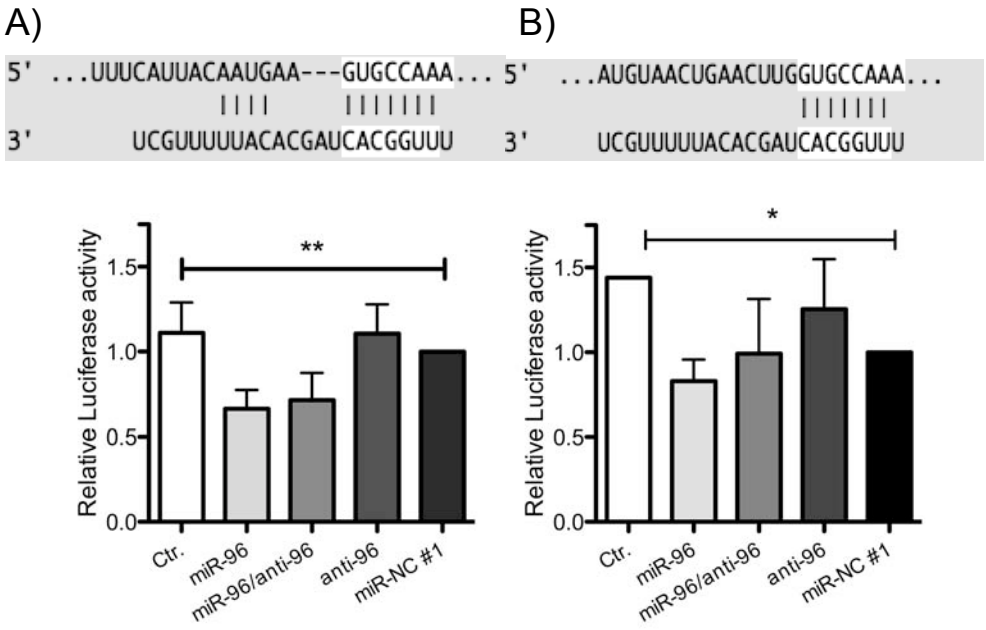

Figure 26: miR-96 binds to the predicted miR-96 binding sites in the FOXO 3' UTR

LNCaP cells were transfected with 10 nM pre-miR-96, anti-miR-96, pre-miR-NC #1 or a combination of pre-miR-96 and anti-miR-96 as well as 500 ng β-galactosidase reporter control plasmid and 500 ng pMiR reporter plasmid containing FOXO1 3' UTR binding site 1 or 2. Protein was extracted after 48 hrs. Luciferase activity was normalized to β-Galactosidase activity. * $p < 0.05$, **$p < 0.01$, One-way ANOVA.

Inhibition of luciferase activity by miR-96 is a proof for a mechanistical binding of the miR-96 to the predicted sites with the FOXO1 3' UTR sequences. To further explore, whether this binding results in a significant downregulation of FOXO1 in prostate cancer, LNCaP and BPH-1 cell lines were transfected with pre-miR-96, anti-miR-96 or scrambled control and FOXO1 mRNA or protein expression was analyzed.

Transient transfection of LNCaP cells with pre-miR-96 resulted in a 440% higher expression of the mature miR-96 transcript after 24 hrs (Figure 27A). Concordantly, the cells ectopically overexpressing miR-96 had a 2-fold reduction of FOXO1 mRNA expression in comparison to the control cells (Figure 27B). Overexpression of either the antisense inhibitor or the scrambled control did not affect on FOXO1 mRNA expression. Cotransfection of the miR-96 precursor and the inhibitor did not diminish mature miR-96 expression and did not affect miR-96-mediated FOXO1 inhibition. In addition, a 1.4-fold reduction of FOXO1 protein expression in BPH-1 cells upon transfection with the miR-96 precursor was observed (Figure 27C).

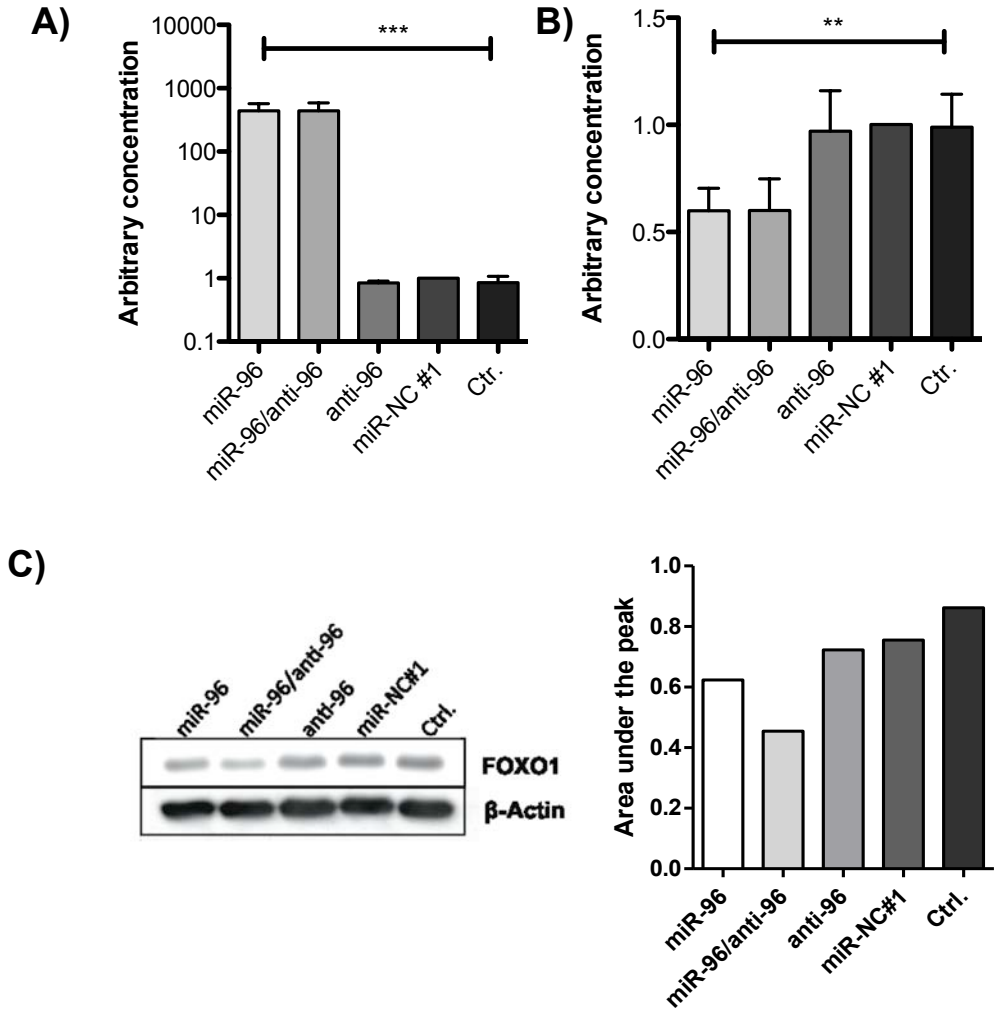

Figure 27: Overexpression of miR-96 significantly reduces FOXO1 transcript and protein
LNCaP cells were transfected with 10 nM pre-miR-96, anti-miR-96, pre-miR-NC #1 or combination of pre-miR-96 and anti-miR-96. RNA was harvested 72 hrs after transfection. A) miR-96 and B) FOXO1 expression was measured by RT-qPCR. Data are shown as mean (+SD) of 3 independent assays. Protein was extracted 72 hrs after transfection. C) FOXO1 protein expression was visualized by western blotting and relative protein quantity was determined by densitometry. ** $p < 0.01$, *** $p < 0.001$, One-way ANOVA.

FOXO1 is a member of the PI3K/AKT signalling pathway and is phosphorylated by growth factor-induced AKT activation. To determine if miR-96 expression may also target AKT signalling further upstream, we measured the expression of activated and total AKT kinase in miR-96 overexpressing cells.

When miR-96 was ectopically overexpressed in BPH-1 cells, total AKT expression and pAkt expression was not different in comparison to control cells (Figure 28A+B). Only transfection with the scrambled control seemed to non-specifically upregulate pAKT levels.

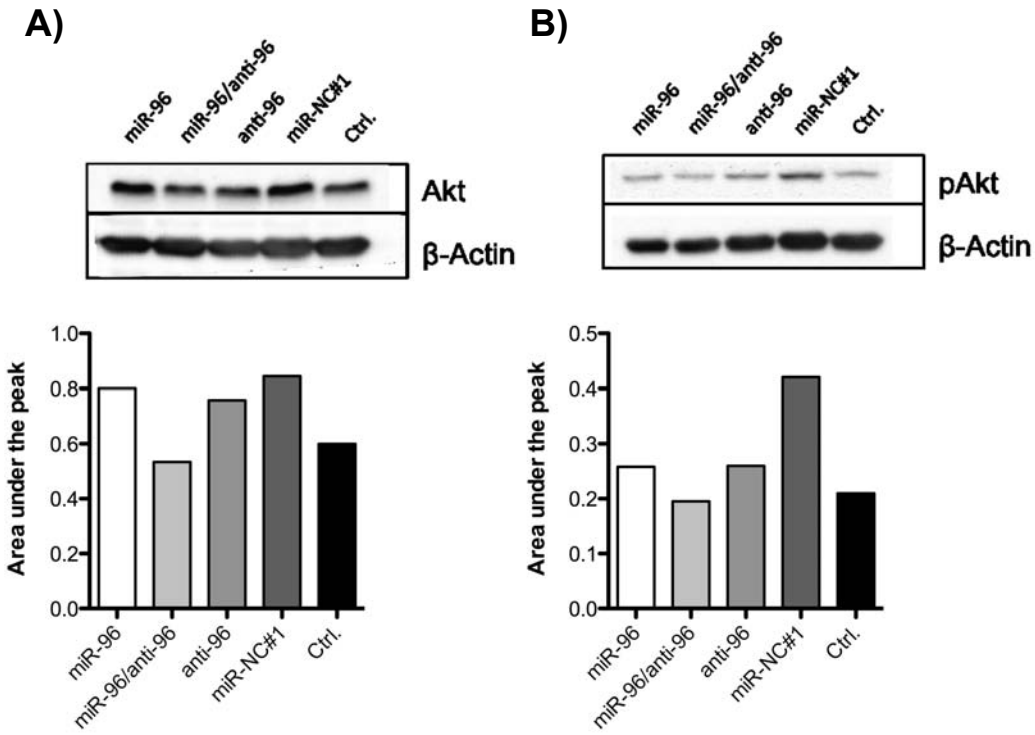

Figure 28: AKT expression in miR-96 overexpressing cells

BPH-1 cells were transfected with 10 nM pre-miR-96, anti-miR-96, pre-miR-NC #1 or a combination of pre-miR-96 and anti-miR-96. Protein was harvested 72 hrs after transfection. A) AKT or B) pAKT protein expression was determined by western blotting and the relative protein quantity was determined by densitometry.

Inhibition of ITPR by miR-96

ITPR1 is another potential miR-96 target gene. ITPR1 is a receptor for inositol 1,4,5-triphosphate (IP3) and is located on the endoplasmatic reticulum. Upon an extrinsic apoptotic signal, IP3 binds to its receptor and triggers a release of calcium into the cytoplasm. The massive increase in calcium concentration mediates release of cytochrome c from mitochondria (Mendes *et al.*, 2005; Szalai *et al.*, 1999). Cytochrome c, in turn, blocks the negative feedback of calcium on the receptor, resulting in sustained calcium release and subsequent activation of downstream apoptotic signalling (Boehning *et al.*, 2003). ITPR1 is also phosphorylated and inactivated by AKT (Khan *et al.*, 2006).

The ITPR1 3' UTR contains 2 predicted miR-96 binding sites at positions 209-215 (8-mer) and 481-487 (7mer-1A). Only the first binding site shows a high level of conservation.

Sequences of 200 to 300 bp containing the predicted binding sites were cloned into the pMiR reporter vector. LNCaP cells were cotransfected with the luciferase reporters and the miR-96 precursor.

Cotransfection of miR-96 with the ITPR1 predicted that the binding site 1 luciferase reporter did not alter activity of the luciferase activity compared to the control cells (Figure 29A). In addition, transfection with the antisense inhibitor and the scrambled control did not alter luciferase activity. Although the second predicted binding site is only partially conserved among species, cotransfection of the pre-miR-96 and the ITPR1 predicted binding site reporter resulted in a moderate inhibition of luciferase activity by 19% (One-way ANOVA, $p < 0.05$; Figure 29B). However, the significance of this miR-96-dependent effect on only one of the 2 predicted binding sites to ITPR1 expression in vivo is doubtful.

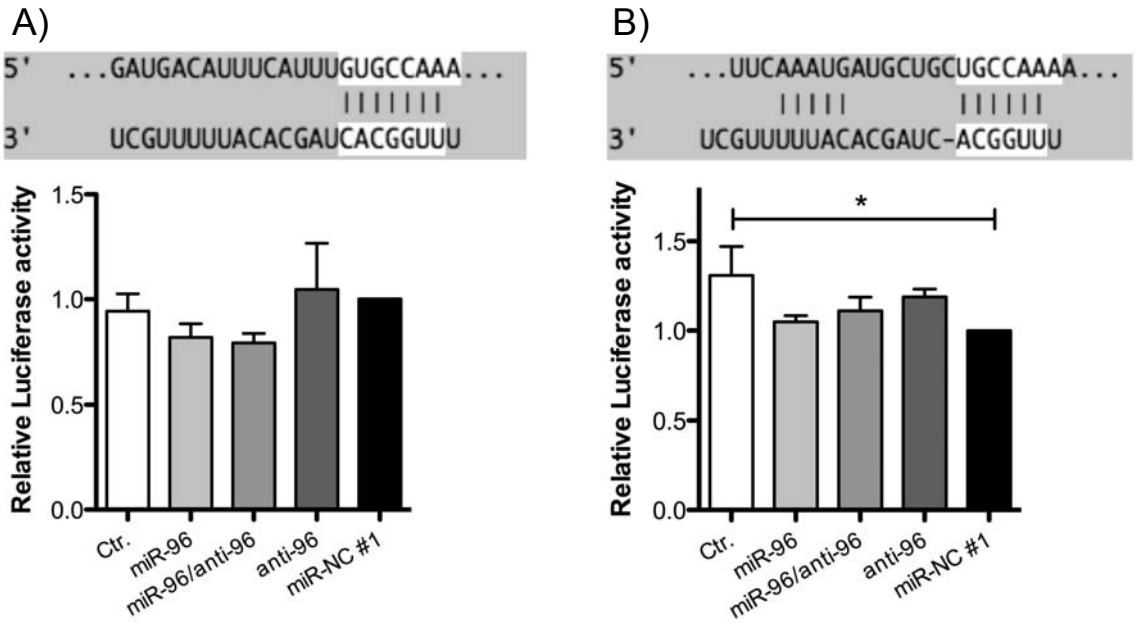

Figure 29: Binding of miR-96 to predicted binding sites in the ITPR1 3' UTR
LNCaP cells were transfected with 10 nM pre-miR-96, anti-miR-96, pre-miR-NC #1 or a combination of pre-miR-96 and anti-miR-96 with 500 ng β-galactosidase control plasmid and 500 ng pMiR Report plasmid for ITPR1 3' UTR A) binding site 1 or B) binding site 2. Protein was extracted after 48 hrs. Luciferase activity was normalized to β-Galactosidase activity. * $p < 0.05$, One-way ANOVA.

LNCaP cells were transfected with the miR-96 precursor, the antisense inhibitor or the scrambled control, and ITPR1 mRNA and protein expression was measured 72 hrs post transfection.

Overexpression of miR-96 in prostate cancer cells did not show significantly altered ITPR1 mRNA expression (Figure 30A). However, ITPR1 protein expression was 1.5-fold

reduced (Figure 30B). In conclusion, ITPR1 seems to be only moderately influenced by miR-96

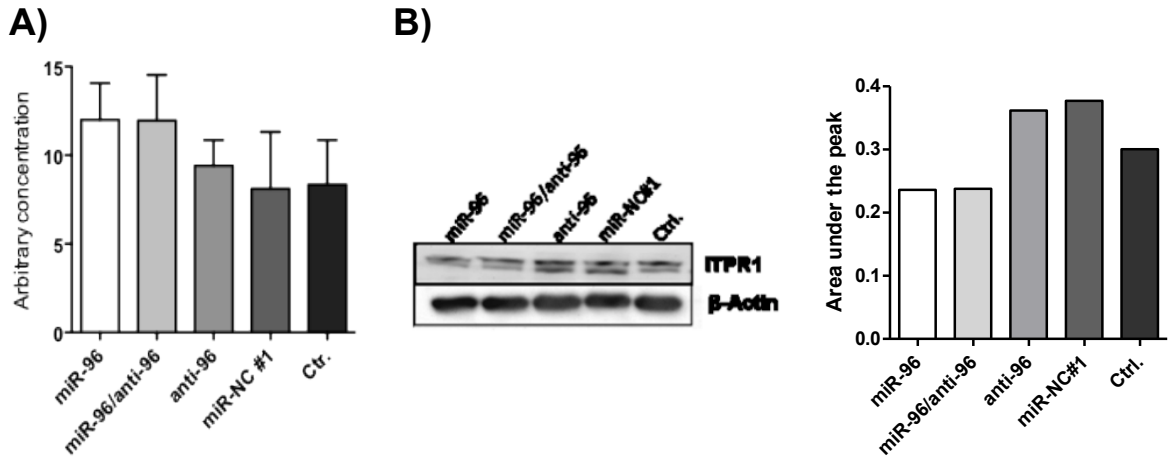

Figure 30: Effects of miR-96 overexpression in LNCaP cells on ITPR1 mRNA and protein levels
LNCaP cells were transfected with 10 nM pre-miR-96, anti-miR-96, pre-miR-NC #1 or a combination of pre-miR-96 and anti-miR-96. A) RNA was harvested 72 hrs after transfection. ITPR1 expression was measured by RT-qPCR and normalized to effiency and TUBA expression. B) ITPR1 protein expression was visualized by western blotting and relative protein quantity was determined by densitometry.

Correlation of FOXO1 and miR-96 expressiom in prostate cancer tissue

The in vitro results suggest a role of miR-96 in anti-apoptotic signalling through regulation of FOXO1 expression. To investigate whether the herein proposed regulation of FOXO1 by miR-96 plays a significant role in vivo, FOXO1 mRNA and protein expression was determined in 69 prostate cancer and normal adjacent tissues and was correlated with miR-96 expression.

FOXO1 mRNA had a median downregulation of 1.2-fold in prostate cancer tissue in comparison to normal adjacent tissue (Wilcoxon signed rank test; $p < 0.001$), with 71% of all patients having lower expression in the tumor tissue (Figure 31A). The miR-96 T/N ratio with the FOXO1 T/N ratio was not significantly correlated (r_s=0.02; p=0.89; Figure 31B).

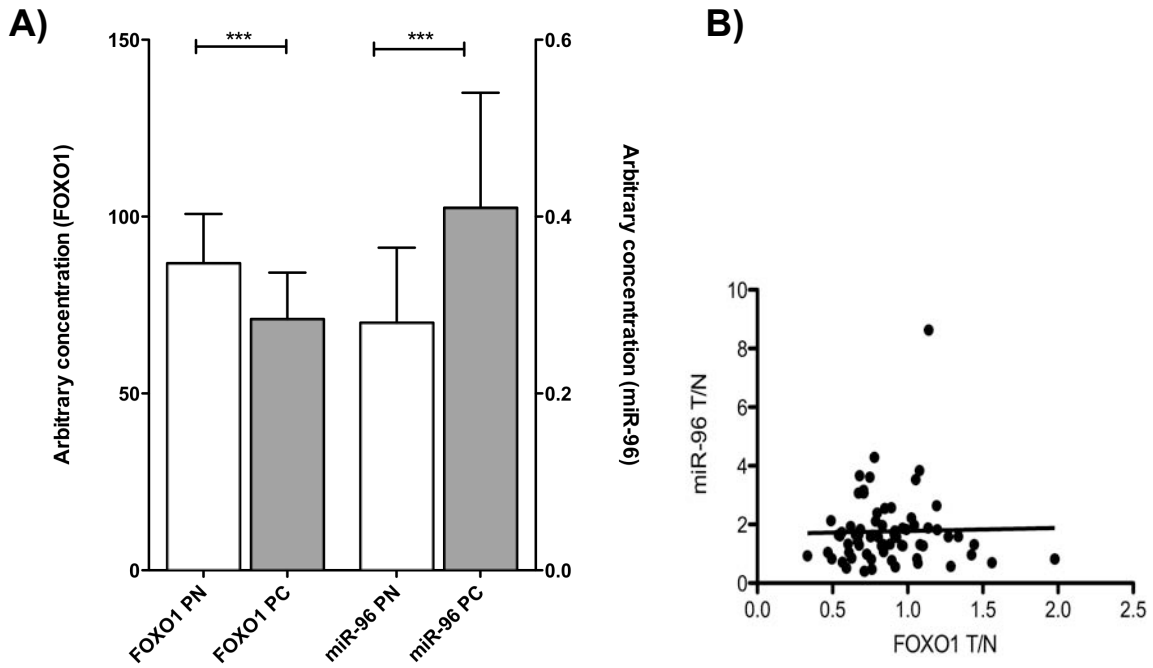

Figure 31: FOXO1 mRNA expression in prostate cancer

A) miR-96 expression and FOXO1 mRNA expression were measured by RT-qPCR in 69 matched prostate cancer and normal adjacent tissue. All data were normalized to efficiency and interplate controls. FOXO1 expression was normalized to TUBA expression and miR-96 expression was normalized to miR-130b expression. Data are represented by the median expression (+interquartile range). FOXO1 expression is displayed on the left y-axis, miR-96 expression on the right y-axis. B) Linear regression of the tumor to normal expression ratio of FOXO1 mRNA and miR-96. ***p < 0.001; Wilcoxon signed rank test.

FOXO1 expression was not significantly correlation with the clinico-pathological data (Table 32).

Table 32: Correlation of FOXO1 expression with clinico-pathological factors in prostate cancer

	r_s	p-value
Gleason score	0.002	0.99
Pathological stage	-0.14	0.27
Pre-operative PSA	0.17	0.17
Surgical margins	0.09	0.44
Age	-0.01	0.94

To demonstrate the relationship of FOXO1 mRNA expression in tumor tissue to the biochemical relapse, FOXO1 was dichotomized according to the median expression, and Kaplan-Meier analysis was performed.

Low FOXO1 expression was associated with biochemical relapse in prostate cancer (p = 0.04, log rank test; Figure 32). Yet, in a multivariate survival model containing the variables miR-96, Gleason score and FOXO1, FOXO1 expression was not significantly independent from the remaining variables (Table 33).

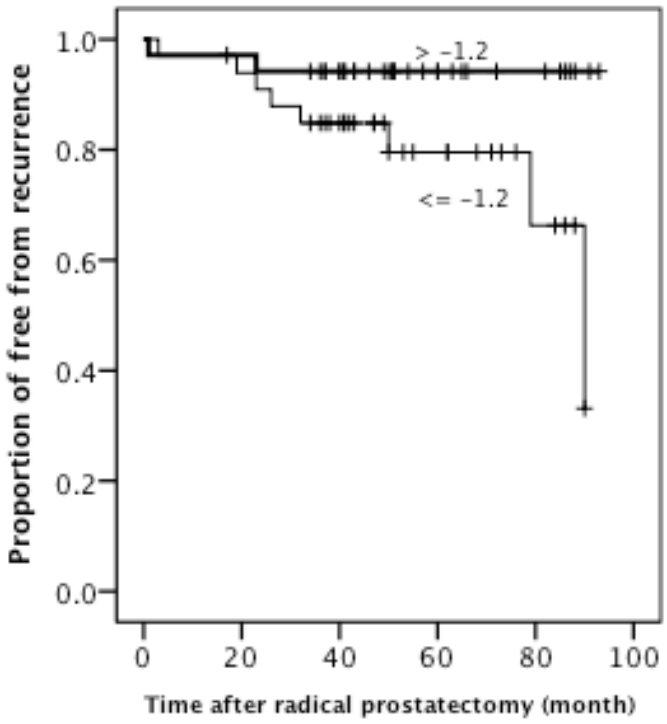

Figure 32: Kaplan-Meier analysis of recurrence-free survival

Recurrence-free survival in relation to dichotomized FOXO1 expression in tumor tissue relative to expression in normal adjacent tissue (thin line: low low fold change; thick line: high fold change). The time of recurrence was defined as the first post-operative PSA value >0.1 µg/l PSA confirmed by at least one subsequent rising value after the patients had reached an undetectable PSA level (detection limit <0.04 µg/l) after surgery.

Table 33: Multivariate Cox regression

Covariate	β	HR	95% CI	p-value
FOXO1	-1.38	0.25	0.05-1.21	0.08
miR-96	1.87	6.48	1.09-38.59	0.04
Gleason score	1.14	3.11	1.16-8.34	0.02

To measure FOXO1 protein expression, we constructed a tissue microarray (TMA) containing tissue cores from 69 prostate cancer patients. Each core had a diameter of 1.5 mm. FOXO1 expression was determined with immunochemistry in the normal and tumor ducts of each patient.

FOXO1 expression was strictly restricted to epithelial cells with a predominant localization in the nucleus of normal tissue and a shift to cytoplasmatic localization in the tumor cells (Figure 33B+C). FOXO1 was expressed in 60% of the normal prostate epithelial cells, but only in 30% of the malignant cells, and expression was significantly reduced in tumor tissue in comparison to normal adjacent tissue (McNemar test; $p<0.01$, Figure 33D). In 36 of the patients on the TMA, FOXO1 expression as well as miR-96 expression was available. miR-96 expression was dichotomized according to the median. There was a

significant inverse relation of miR-96 expression and FOXO1 protein expression (McNemar test; p = 0.02, Figure 33E).

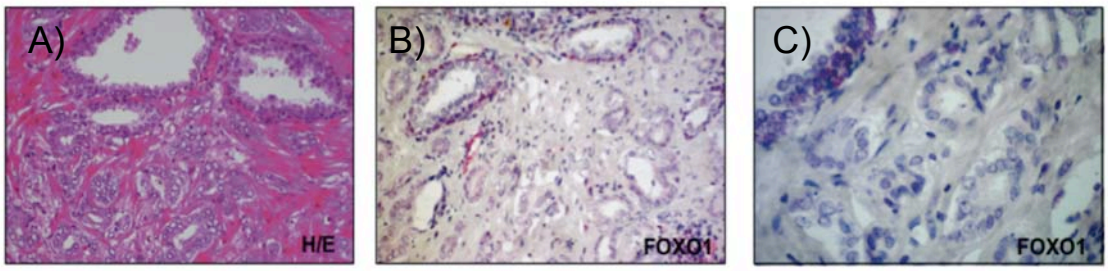

D)

		FOXO1 PN		P < 0.01
FOXO1 PC		0	1	
	0	12	9	21 (70%)
	1	0	9	9 (30%)
		12 (40%)	18 (60%)	*30*

E)

		FOXO1		P = 0.02
miR-96		0	1	
	0	11	5	21 (44%)
	1	17	3	9 (56%)
		28 (78%)	8 (22%)	*36*

Figure 33: FOXO1 protein expression in prostate cancer

A) Haematoxilin-eosin (H/E) staining was performed to identify tumor ducts B)-C) FOXO1 expression was detected by immunohistochemistry on a tissue microarray containing tissue cores from 69 prostate cancer patients. Each core had a diameter of 1.5 mm. D) FOXO1 expression was defined as present (1) or absent (2). E) FOXO1 expression in tumor tissue was correlated with miR-96 expression. miR-96 expression was dichotomized according to the median expression. Significant associations were determined by the McNemar test of categorical data.

3.2.5 miR-133b is a negative regulator of prostate cancer carcinogenesis

3.2.5.1 Expression of miR-133b in prostate cancer

miR-133b initially was thought to be exclusively expressed in skeletal muscle; however, recent studies suggest broader expression in various tissues. miR-133b is downregulated in various cancer types, including head and neck, oral, bladder, non-small cell lung and esophageal cancer (Bandres *et al.*, 2006; Guo *et al.*, 2009; Hu *et al.*, 2010a; Ichimi *et al.*, 2009; Navon *et al.*, 2009; Tran *et al.*, 2007; Wong *et al.*, 2008a; Wong *et al.*, 2008b). Functional studies of lung cancer and esophageal squamous cell carcinoma suggest that miR-133b regulates mitochondrial membrane integrity through BCL2L2 and FSCN1 (Crawford *et al.*, 2009; Kano *et al.*, 2010). Investigation of miR-133b expression in prostate cancer was an interdisciplinary project. Our collaborators have recently identified miR-133b to regulate DR-mediated apoptosis in HeLa cells and have validated several apoptosis-related genes to be regulated by miRNAs (Patron Arcila, 2010). The apoptosis-related function of miR-133b as well as the downregulation of miR-133b expression in bladder cancer led us to study this miRNA in prostate cancer carcinogenesis. Re-analysis of the miRNA microarray data of the prostate cancer specimen (4.1) identified a previously

unnoticed downregulation of miR-133b in the 24 matched prostate cancer samples (FCH: -2.6). The downregulation was not detected by our previous analysis because the miRNA expression data did not pass t-test on intensity profile level. We validated the downregulation in a set of 69 prostate cancer and matched normal adjacent tissues (for clinico-pathological and tumor characteristics refer to table 19).

The mean expression of miR-133b was reduced 1.70-fold in prostate cancer tissue in comparison to normal adjacent tissue (Wilcoxon signed rank test; $p < 0.01$). 75% of the patients had a lower expression in the tumor tissue. Expression of miR-133b was not significantly correlated with the Gleason score (r_s=-0.20; $p = 0.10$) and pathological stage (r_s=-0.16;p=0.18).

To analyze the discriminative power of the miRNA in prostate cancer, ROC analysis and univariate logistic regression was performed. miR-133b expression was a good discriminator of tumor and normal adjacent tissue with an AUC of 0.73 ($p < 0.001$) and an overall correct classification of 68% (HR=0.94: 95% CI = 0.91-0.98; $p < 0.01$).

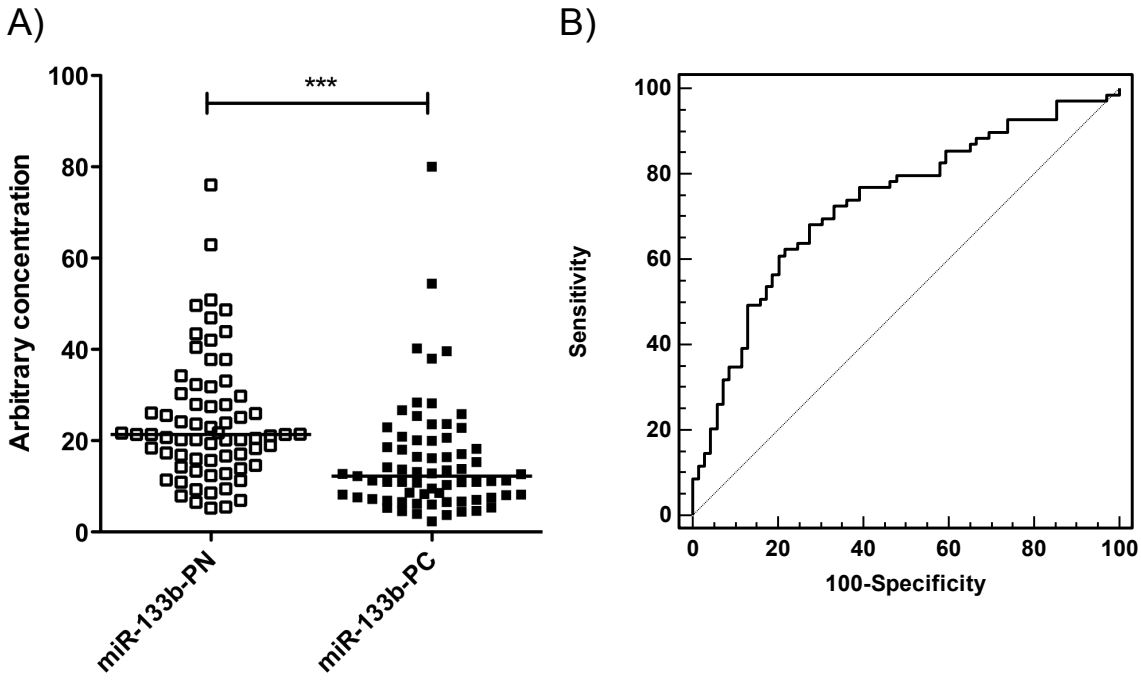

Figure 34: Expression of miR-133b in prostate cancer and normal adjacent tissue
A) miR-133b expression was measured by RT-qPCR in 69 matched prostate cancer and normal adjacent tissues. All data were normalized to efficiency, interplate control and miR-130b expression. Data are represented as a scatter dot plot. Lines indicate mean expression. ***p < 0.001, Wilcoxon signed rank test. B) ROC analysis of miR-133b. Dotted line indicates an AUC of 0.5.

To predict whether the downregulation of miR-133b predicts biochemical relapse in prostate cancer, miR-133b T/N expression ratio was dichotomized by the median expression and forwarded to Kaplan-Meier analysis.

Patients with a low T/N expression ratio had a significantly higher risk of biochemical relapse (log rank test; $p < 0.05$; Figure 35).

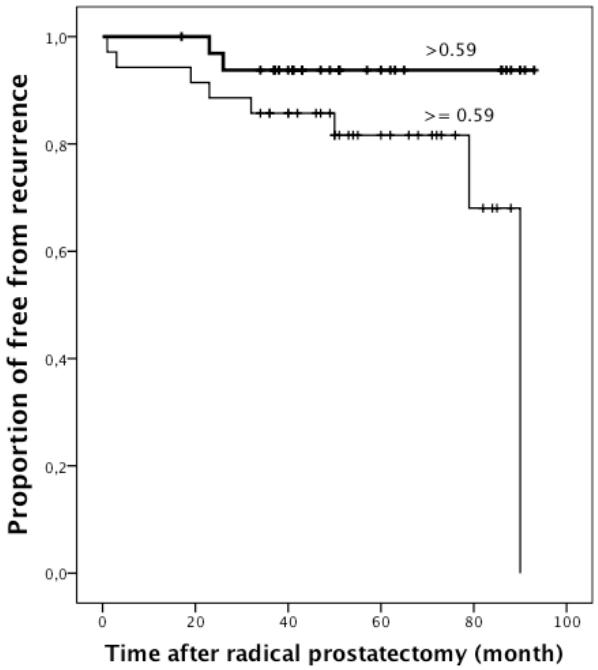

Figure 35: Kaplan-Meier analysis of recurrence-free survival

Recurrence free survival in relation to the miR-133b T/N expression ratio. The time of recurrence was defined as the first post-operative PSA value >0.1 µg/l PSA confirmed by at least one subsequent increase after the patients had reached an undetectable PSA level (detection limit <0.04 µg/l) after surgery.

3.2.5.2 Functional relevance of miR-133b in prostate cancer

Our collaborators have determined that miR-133b regulates DR-mediated apoptosis in HeLa cells. To investigate whether miR-133b also induces phenotypical changes in prostate cancer cell lines, we determined the metabolic activity of PC3 prostate cancer cells under serum starvation after transient transfection with the miR-133b precursor and inhibitors.

miR-133b significantly reduced metabolic activity in serum-starved PC3 cells over 3 days in comparison to non-transfected control, while the antisense inhibitor did not affect PC3 cell proliferation (Figure 36).

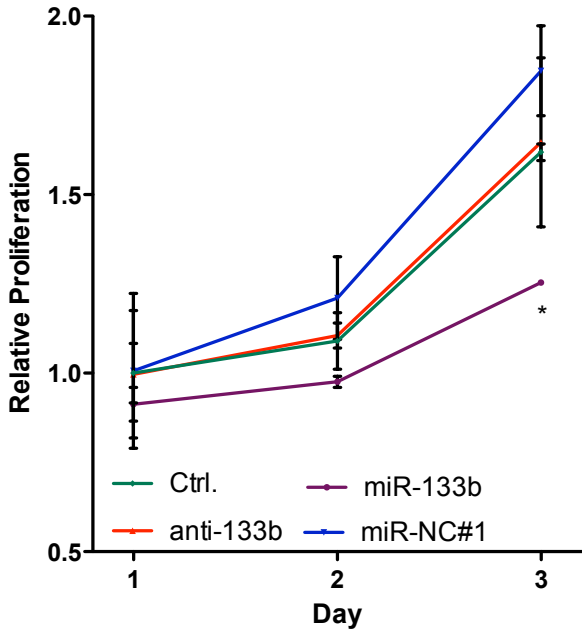

Figure 36: Metabolic conversion of XTT in miR-133b overexpressing PC3 cells
PC3 cells were transfected with 10 nM pre-miR-133b, anti-miR-133b, pre-miR-NC #1 or a combination of pre-miR-133b and anti-miR-133b. The effect on cell proliferation under serum starvation was measured by XTT assay over 3 days. All data are shown as mean (+SD) of 3 independent assays. *p < 0.05, Two-way ANOVA.

3.2.5.3 Regulation of gene expression by miR-133b

The in vitro results suggest that miR-133b can induce phenotypical changes in prostate cancer and can regulate tumorigenesis in the prostate. Our collaborators have previously identified FAIM and GSTP1 as direct targets of miR-133b in HeLa cells (Patron Arcila, 2010). To investigate whether these genes may also be regulated in prostate cancer, we analyzed mRNA and protein expression in miR-133b overexpressing PC3 cells.

Ectopic overexpression of pre-miR-133b resulted in a strong reduction of FAIM and GSTP1 mRNA in comparison to the scrambled control (Figure 37). The protein expression of both targets was also significantly reduced in comparison to cells transfected with the scrambled control. The inhibitory effects of miR-133b were abolished by cotransfection with the antisense inhibitor.

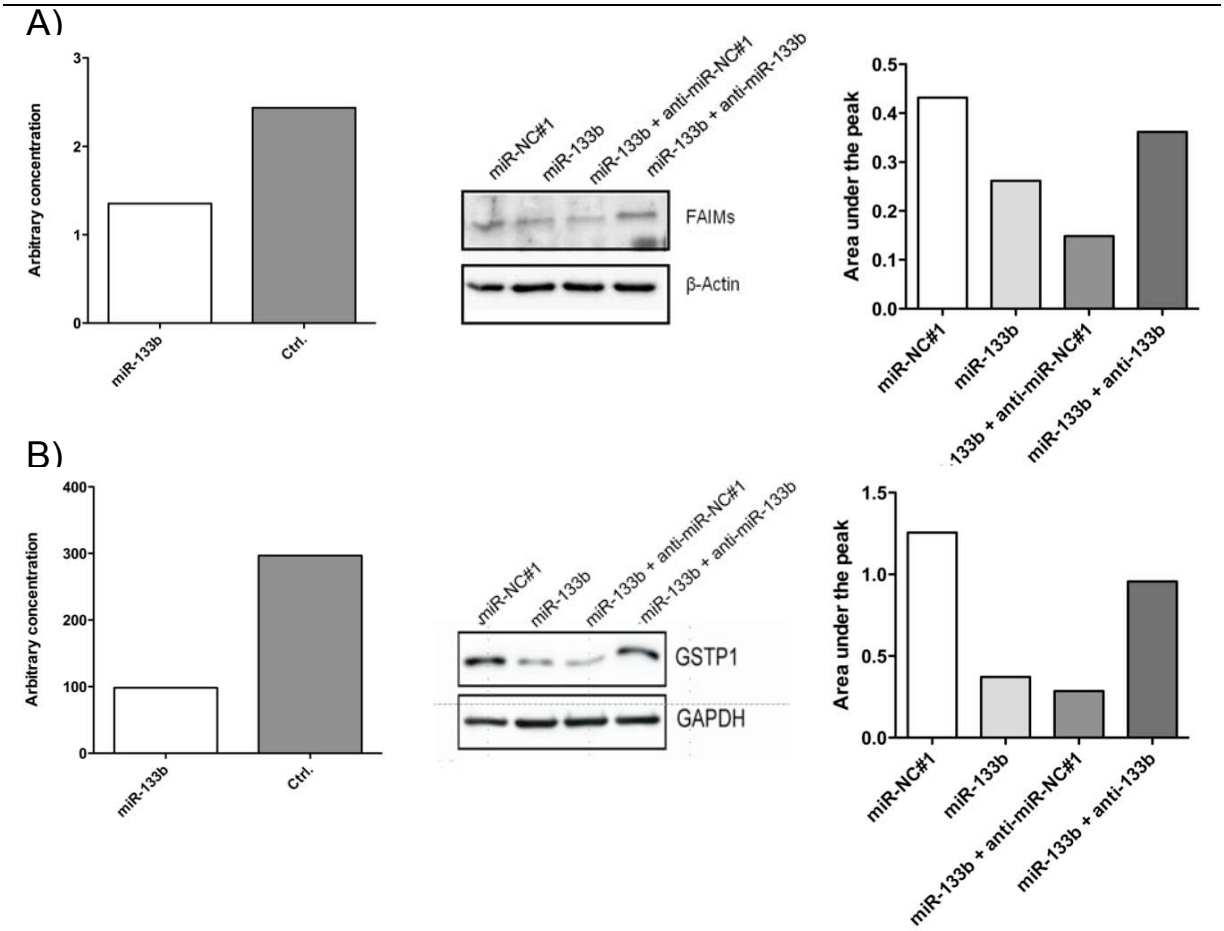

Figure 37: The effect of miR-133b overexpression on GSTP1 and Faims in PC3 prostate cancer cells

PC3 cells were transfected with 10 nM pre-miR-133b, pre-miR-NC #1, anti-miR-NC#1 or anti-miR-133b. RNA and protein were harvested 24 hrs after transfection. A) FAIM mRNA expression was measured by RT-qPCR. Expression was normalized to GAPDH expression. FAIM protein expression was detected by westernblotting and quantified by densitometry relative to β-Actin expression. B) GSTP1 mRNA expression was measured b RT-qPCR. Expression was normalized to GAPDH. GSTP1 protein expression was detected by westernblotting and quantified by densitometry relative to β-Actin expression.

GSTP1 and FAIM are directly targeted in prostate cancer, yet miR-133b may target a different set of genes in prostate cancer as miRNA-mediated regulation has been shown to be tissue specific. Therefore, global changes in gene expression in miR-133b overexpressing PC3 cells were monitored using a whole genome array in order to identify all prostate cancer-related target genes. PC3 miRNA microarrays were performed in the lab of our collaborators. In total, 754 genes displayed reduced expression in miR-133b overexpressing PC3 cells, highlighting the variety of changes that can be induced by one miRNA either by direct binding or secondary off-target effects. Although a plethora of mRNA was regulated by miR-133b, the fold changes were moderate with the greatest downregulation being approximately 4-fold and a median fold change of 1.92 across all significantly reduced genes. Two hundred and two of the seven hundred fifty-four genes were predicted targets of miR-133b. Therefore a direct interaction may be assumed. GSTP1 and FAIM were both

downregulated. To investigate whether the downregulated genes are participating in specific carcinogenic pathways, we performed Gene ontology analysis and clustering of GO terms by DAVID (http://david.abcc.ncifcrf.gov/home.jsp) and pathway analysis by reactome skypainter (http://www.reactome.org/cgi-bin/skypainter2). The clusters most highly enriched in the DAVID analysis suggested a role of miR-133b target genes in cytoskeletal organization, cell motility and cell cycle. Reactome skypainter identified, VEGF signalling as well as mitosis to be most overrepresented biological pathways in our set of genes.

The in silico analysis suggested that VEGF signalling is the central pathway regulated by miR-133b. The microarray data demonstrated downregulation of VEGFC in miR-133b overexpressing cells (FCH: -2.41), and it was predicted as a direct target for miR-133b by 3 independent algorithms. VEGF protein expression was 2.2-fold reduced in prostate cancer cells overexpressing miR-133b in comparison to control cells (Figure 38).

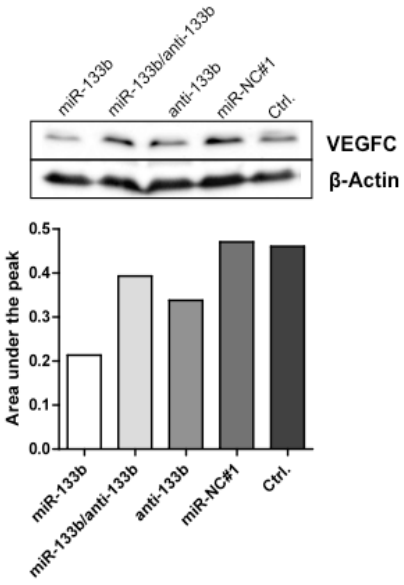

Figure 38: VEGFC expression is reduced in miR-133b overexpressing PC3 prostate cancer cella

PC3 cells were transfected with 10 nM pre-miR-133b, anti-miR-133b, pre-miR-NC #1 or a combination of pre-miR-133b and anti-miR-133b. Protein was harvested 72 hrs after transfection. VEGFC protein expression was determined by western blotting and the relative protein quantity was determined by densitometry relative to β-Actin expression.

Analysis of the microarray results identified other members of the VEGFC signalling pathway in the list of miR-133b-regulated genes. Of these genes, CAV1 was strongly reduced and was therefore more closely investigated. A regulatory positive feedback loop between VEGF and CAV1 has been shown in prostate cancer (Li *et al.*, 2009a; Tahir *et al.*, 2009). To confirm the downregulation of CAV1 by miR-133b, mRNA and protein expression was measured in pre-miR-133b-transfected PC3 cells.

CAV1 mRNA expression was 2.02-fold reduced in PC3 cells transfected with pre-miR-133b (Figure 39A). Concordantly, CAV1 protein was 2.48-fold downregulated in the miR-133b overexpressing cells (Figure 39B). These results indicate that miR-133b may be a direct target of miR-133b regulated inhibition.

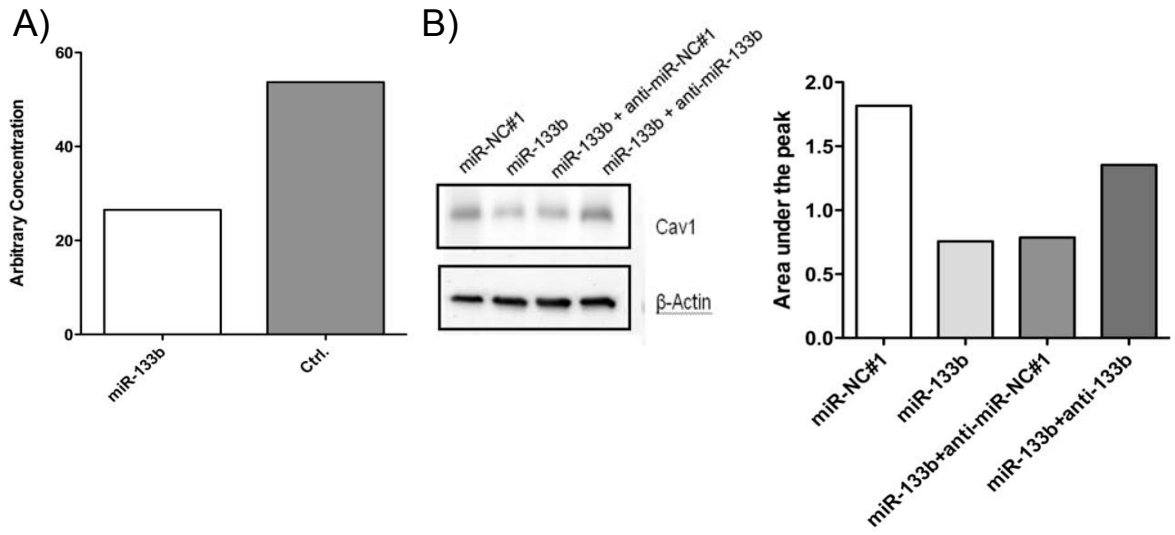

Figure 39: CAV1 expression is downregulated in miR-133b overexpressing PC3 cells
PC3 cells were transfected with 10 nM pre-miR-133b, pre-miR-NC #1, anti-miR-NC#1 or anti-miR-133b. RNA and protein were harvested 24 hrs after transfection. A) CAV1 mRNA expression was measured b RT-qPCR. Expression was normalized to GAPDH expression. B) CAV1 protein expression was detected by westernblotting and quantified by densitometry relative to β-Actin expression.

In silico target analysis predicted CAV1 as a miR-133b target (predicted by TargetScan, miRanda and PITA). TargetScan identified 2 poorly conserved binding sites at positions 735-741 (7mer-m8) and 888-894 (7mer-1A) in the CAV1 3' UTR. Additionally, Pita identified another binding site at position 54 in the 3' UTR. Luciferase reporter genes were constructed containing each of the 3 predicted binding sites and the complete CAV1 3' UTR.

Although CAV1 expression was markedly downregulated in prostate cancer cells upon miR-96 transfection, the luciferase reporter gene assays were not able to establish a direct interaction of the miRNA with the predicted binding sites in the CAV1 3' UTR (Figure 40). These results suggest that the regulation of CAV1 by miR-133b is indirect and is not directly mediated by binding of the miRNA to the CAV1 3' UTR

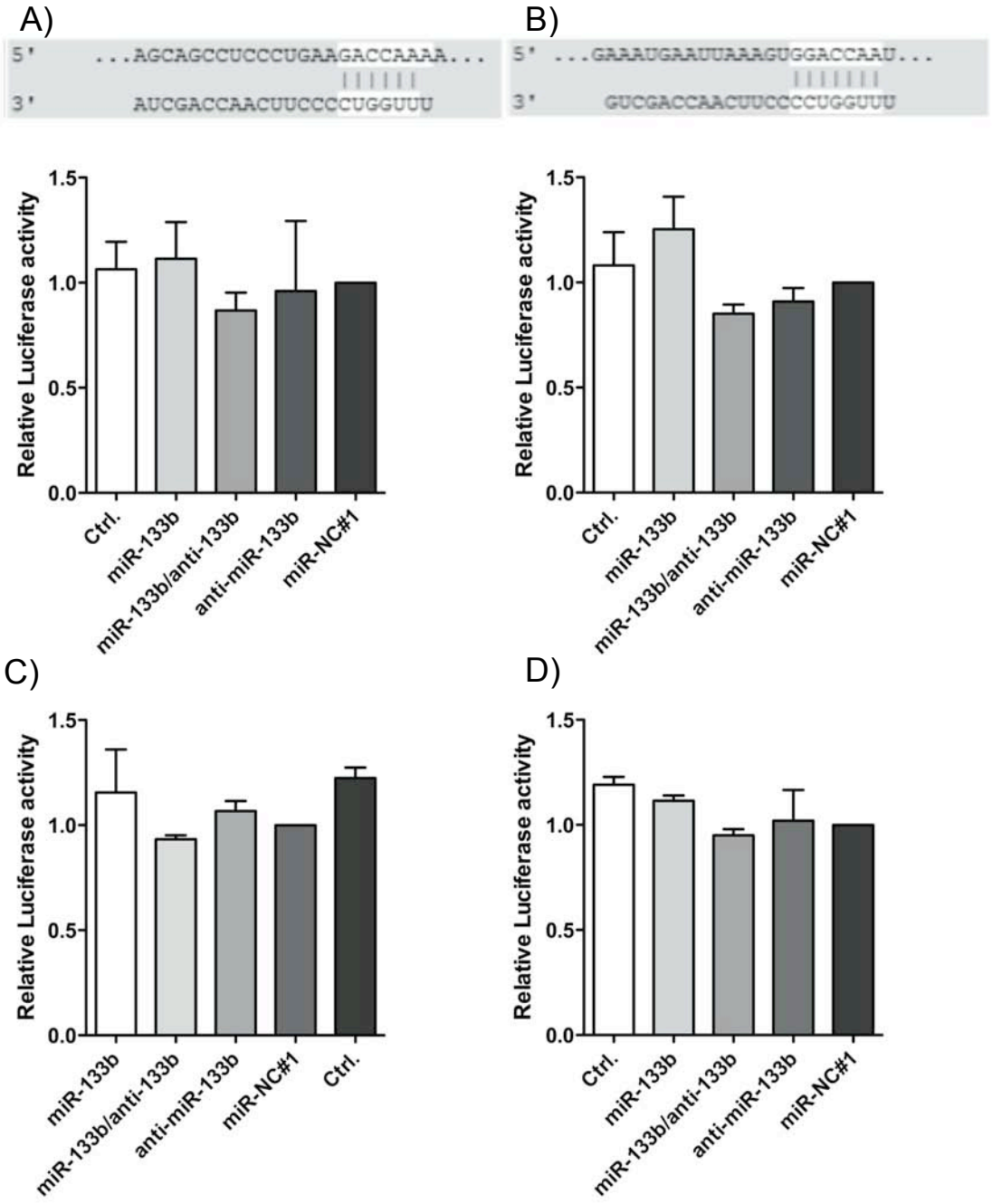

Figure 40: Binding of miR-133b to predicted binding sites in the CAV1 3' UTR

PC3 cells were transfected with 10 nM pre-miR-133b, anti-miR-133b, pre-miR-NC #1 or a combination of pre-miR-133b and anti-miR-133b with 500 ng β-galactosidase control plasmid and 500 ng pMiR Report plasmid containing CAV1 3' UTR A) binding site 1, B) binding site 2, C) binding site 3, and D) complete 3' UTR. Protein was extracted after 48 hrs. Luciferase activity was normalized to β-galactosidase activity. Data are shown as the mean (+SD) of 3 independent assays.

3.2.5.4 Correlation of the expression of miR-133b and target genes in prostate cancer tissue

The results described above have shown that miR-133b regulates a plethora of genes upon overexpression in PC3 cells. Yet, the question remains, whether these interactions have biological significance in human prostate carcinogenesis. Therefore GSTP1 and FAIM mRNA expression was measured in 69 prostate cancer and normal adjacent tissues and was correlated with miR-133b expression. In addition, we measured the expression of FASN. FASN was strongly downregulated in the microarray of miR-133b overexpressing HeLa cells (Patron Arcila, 2010). However, no binding sites for miR-133b were identified, suggesting that FASN is indirectly mediated by miR-133b. Studies in prostate cancer suggest that the downregulation of FASN by miR-133b may be regulated via CAV1 (Di Vizio *et al.*, 2007; Di Vizio *et al.*, 2008).

Although the in vitro results also suggested an upregulation of the 3 genes in prostate cancer tissue, where miR-133 expression is markedly reduced, these genes showed variable expression patterns in prostate cancer (Figure 41). Expression of GSTP1 was significantly downregulated in prostate cancer tissue in comparison to normal adjacent tissue (Wilcoxon signed rank test; $p < 0.001$). In contrast, FASN expression was strongly increased in the prostate cancer tissues in comparison to the matched normal tissue (Wilcoxon signed rank test; $p < 0.001$). Although FAIM appeared to be slightly higher expressed in prostate cancer in comparison to normal adjacent tissue, this was not statistically significant.

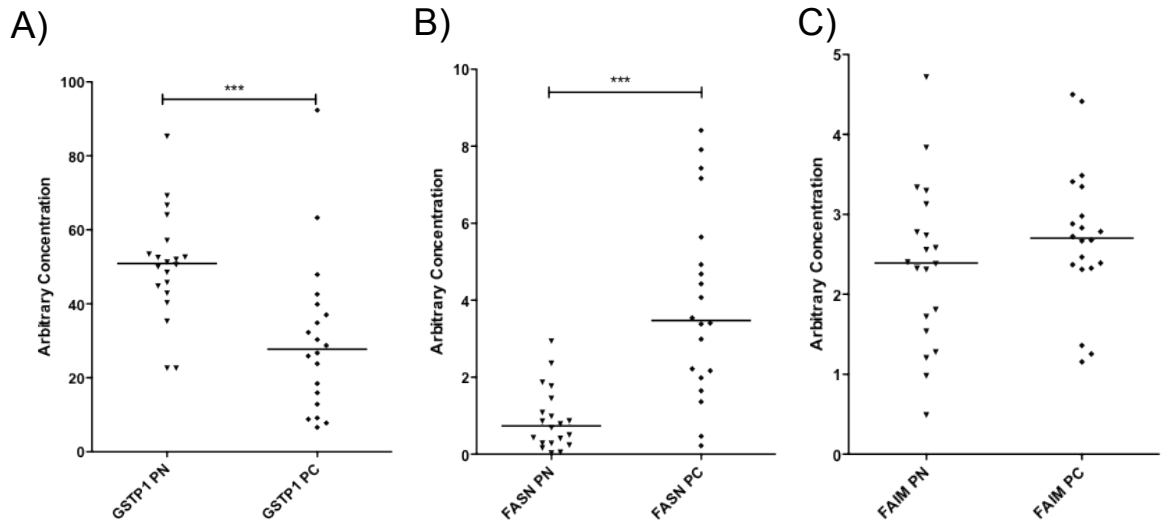

Figure 41: Expression of putative miR-133b regulated genes in prostate cancer specimen
Expression of A) FASN, B) GSTP1, and C) FAIM was measured by RT-qPCR in matched prostate cancer and normal adjacent tissue. Gene expression was measured in 20 samples. Expression was normalized to interplate controls, efficiency and TUBA expression. Lines represent median expression. *** $p < 0.001$, Wilcoxon signed rank test.

To assess whether miR-133b regulates these genes, which have been established as targets, in vivo, miR-133b and mRNA expression levels were correlated with each other.

Although FAIM expression was not significantly upregulated in prostate cancer tissue, its expression was inversely correlated with miR-133b. FASN expression was also inversely correlated with miR-133b expression. GSTP1 expression was not significantly correlated with miR-133b expression in prostate cancer cells. CAV1 expression was studied previously in our lab (Steiner *et al.*, unpublished data). Interestingly, although CAV1 expression was not overexpressed in the prostate cancer tissue, thereby not suggesting a regulation by miR-133b in vivo, miR-133b and CAV1 showed a strong unexpected positive correlation.

Table 34: Correlation of mRNA expression with miR-133b expression in prostate cancer

Gen Symbol	R_s	p-value
FAIM	-0.38	0.05
CAV1	0.80	<0.001
FASN	-0.37	0.002
GSTP1	0.35	0.14

Taken together, the in vitro and in vivo results suggest an important regulatory function of miR-133b in prostate cancer. However, discrepancies between the in vitro and in vivo results demonstrate the importance of validating the biological significance of in vitro data.

4. Discussion

miRNAs were discovered approximately 10 years ago and since have received a great deal of attention as novel, highly versatile regulators of physiological and pathological cellular processes .In cancer, miRNAs control major breakpoints in carcinogenesis. Therefore, in recent years, miRNAs have been moved to the center of attention in cancer research. miRNA may be useful in a broad range of clinical applications, such as cancer diagnosis and prognosis as well as cancer therapy. This thesis focussed on the dysregulation of miRNAs in prostate cancer. miRNA profiling is a relatively new techniques and some experimental pitfalls still exist. To render the analysis more robust, suitable reference genes were identified prior to the profiling experiment. Using microarray analysis and RT-qPCR analysis, a set of miRNAs was identified to be regulated in prostate cancer tissue in comparison to normal adjacent tissue. These miRNAs were statistically analyzed in order to identify novel diagnostic markers. Furthermore, the profiling study provided a solid basis for subsequent functional characterization. Functional studies mainly focused on miR-96 and miR-133b, which were identified as important regulators of carcinogenesis in prostate cancer.

4.1 miRNA profiling

4.1.1 Identification of suitable reference genes

Expression profiling with RT-qPCR has become the method of choice for the identification of miRNA dysregulation in physiological and pathological processes. Yet, the reliability of these results is highly dependent on utilization of suitable reference genes, as it has been shown that the use of improper reference genes can significantly bias results (Dheda *et al.*, 2005; Ohl *et al.*, 2005). When this thesis was started, no reference genes were experimentally proven to be suitable for normalization of miRNA expression in prostate cancer. Therefore, in order to avoid erroneous expression results due to an incorrect normalization approach, the suitability of 4 candidate reference genes was studied. In the majority of miRNA profiling studies in prostate cancer, small RNAs have been used for normalization. These were regarded to be suitable, due to their comparable length. Studies have also used longer mRNAs, such as GAPDH, TBP and RPP30, as reference genes (Gandellini *et al.*, 2009; Place *et al.*, 2008; Porkka *et al.*, 2007; Rokhlin *et al.*, 2008). However, whether these RNAs can be used as reference genes for miRNA profiling studies is doubtful, as mRNAs have different extraction efficiencies, are degraded more easily and have to be reverse transcribed by other techniques, thereby increasing technical errors (Peltier and Latham, 2008). GAPDH is also a non-suitable reference gene in prostate cancer mRNA profiling (Ohl *et al.*, 2005) and even is even differentially regulated in advanced prostate cancer (Rondinelli *et al.*, 1997).

The expression stability of Z30, miR-16, RNU6B and miR-130b was studied. Z30 was excluded, as it was dysregulated in pooled tissue samples. The remaining 3 genes were measured in 76 matched prostate cancer and normal adjacent tissues.

miR-16 expression was significantly downregulated in tumor tissues in comparison to the matched controls and was therefore excluded from subsequent statistics. Although miR-16 has been used as a reference gene in previous studies (Josson *et al.*, 2008; Mattie *et al.*, 2006) and expression was reported to be stable between LNCaP and PC3 cells, our observation that miR-16 is regulated in prostate cancer is supported by other studies (Bonci *et al.*, 2008; Hao *et al.*, 2011; Porkka *et al.*, 2007). If miR-16 were used as a reference gene, reduced miRNA expression would be underestimated, while increased miRNA expression would be overestimated Thus, from the data presented here, it has to be concluded that miR-16 is an inappropriate reference gene.

The remaining genes miR-130b and RNU6B were both not significantly dysregulated in prostate cancer. Nevertheless, assuming an allowed fold-change of 1.2, RNU6B expression was not equivalent in tumor and normal tissue. RNU6B is the most commonly used reference gene in prostate cancer studies. RNU6B is reported to be stably expressed in prostate cancer cell lines and across treatment groups (Jiang *et al.*, 2005; Josson *et al.*, 2008). Although both studies show that RNU6B is expressed in comparable levels, they do not provide statistical proof of its stability. Furthermore, to date, there is no evidence that RNU6B is indeed stably expressed in tissue. miR-130b, in contrast, was equivalently expressed in prostate cancer tissue and normal adjacent tissue when assuming an allowed fold change of 1.2. The variance of RNU6B expression was also significantly higher than that of miR-130b, and RNU6B was the least stable gene tested by GeNorm and Normfinder, whereas miR-130b was the most stable single gene. Therefore, we concluded that normalization to miR-130b is more reliable than normalization to RNU6B, especially when differences between cancer and normal adjacent tissue are small.

Previous studies regarding reference genes suggest that normalization to at least 2 reference genes is superior to normalization to one (Vandesompele *et al.*, 2002). Therefore, we calculated the geometric mean of RNU6B and miR-130b. The variance of the geometric mean was also significantly lower than that of RNU6B, and it was identified by GeNorm and Normfinder to be most stable.

GeNorm and Normfinder are the most commonly used algorithms to determine the stability of genes for normalization. However, the results obtained by these 2 algorithms in this study are limited. Both algorithms acquire input of at least 3 independent, non-regulated genes, albeit 5 to 10 are recommended (Andersen *et al.*, 2004). In this study, only 2 genes were unregulated. The geometric mean was added to the study group, yet the geometric mean was not independent of miR-130b and RNU6B and may therefore bias the results

(Vandesompele *et al.*, 2002). In spite of these limitations, the GeNorm and Normfinder results support our hypothesis that miR-130b and the geometric mean are suitable reference genes. The small number of investigated genes is clearly a limitation, but was due to limitation available material. In contrast, the sample number was comparably high (N=76), thereby providing strong statistical evidence that miR-130b is indeed stably expressed in prostate cancer. A high arbitrary threshold was used in the first part of the study (measurement in pooled tissue), which minimizes the risk of type I and type II errors as far as possible.

These results are only applicable to RT-qPCR expression profiling as the data are solely based on measurements using this platform. Using miRNA microarray profiling performed, an overexpression of miR-130b was observed, which could not be detected by RT-qPCR. This discrepancy may be due to different detection platforms and technical as well as experimental errors as well as the use of only a small subset of samples for the microarray.

Although reference genes are the most common approach for normalization of RT-qPCR data, other methods have been suggested that do not rely on previously defined reference genes. Based on the assumption that a set of miRNAs is unregulated across all study groups, these miRNAs, called invariants, are defined for each experiment separately (Pradervand *et al.*, 2009). Other normalization strategies, such as quantile normalization and variance stabilizing normalization exist (Meyer *et al.*, 2010), which were adapted from mRNA profiling experiments (Bolstad *et al.*, 2003). There is no consensus as to which method is superior (Pradervand *et al.*, 2009).

In conclusion, this work demonstrates that miR-130b and RNU6B are suitable reference genes for miRNA RT-qPCR analysis of fresh frozen prostate cancer tissue.

4.1.2 Identification of dysregulated miRNAs in prostate cancer

In this thesis, miRNA deregulation in prostate cancer was studied, and the dysregulated miRNAs were analyzed to determine their diagnostic and prognostic potential.

Dysregulation of miRNA expression in human prostate cancer has been inadequately described when this thesis was started. Conflicting results obtained from 4 forgoing studies (Ambs *et al.*, 2008; Ozen *et al.*, 2008; Porkka *et al.*, 2007; Volinia *et al.*, 2006) clearly indicate that reliable profiling in prostate cancer is mandatory. We therefore performed miRNA microarray profiling of 470 human miRNAs in 24 matched prostate cancer and normal adjacent tissues and validated the results in 76 matched tissue pairs by RT-qPCR. Concordance between both platforms was generally good, except for one miRNA, miR-130b, which appeared to be downregulated by microarray profiling, but was subsequently identified to be highly stable expressed and to be a suitable reference gene for RT-qPCR data.

To date, 6 other miRNA profiling studies in prostate cancer have been performed using more than 10 samples per study beside this study (Ambs *et al.*, 2008; Ozen *et al.*, 2008; Porkka *et al.*, 2007; Spahn *et al.*, 2010; Tong *et al.*, 2009; Volinia *et al.*, 2006). Although a discrepancy in the identification of miRNAs differentially regulated exists in these studies, a subset of commonly identified miRNAs was determined. The majority of these miRNAs, were also shown to be dysregulated in this thesis. The expression of miR-145 was shown to be downregulated in 6 studies (Ambs *et al.*, 2008; Ozen *et al.*, 2008; Porkka *et al.*, 2007; Szczyrba *et al.*, 2010; Tong *et al.*, 2009), miR-221 in 5 studies (Ambs *et al.*, 2008; Porkka *et al.*, 2007; Spahn *et al.*, 2010; Tong *et al.*, 2009), miR-125b in 4 studies (Ozen *et al.*, 2008; Porkka *et al.*, 2007; Spahn *et al.*, 2010), miR-16 (Porkka *et al.*, 2007; Spahn *et al.*, 2010) and miR-222 (Porkka *et al.*, 2007; Tong *et al.*, 2009) in 3 studies. The concordance of identified upregulated miRNAs was less pronounced. We have identified the miR-96 cluster as upregulated in prostate carcinoma. miR-182 was concordantly identified by Ambs *et al.* (Ambs *et al.*, 2008), and the upregulation of miR-375 was also identified by 2 other studies (Szczyrba *et al.*, 2010; Wach *et al.*, 2011).

Despite the good concordance to other studies, some of the miRNAs that were identified to be dysregulated in this thesis were inversely expressed in other studies (miR-16, miR-31, miR-181b and miR-184) (Ambs *et al.*, 2008; Volinia *et al.*, 2006). However, there are some important differences in study design, which might account for these discrepancies. First of all, none of these miRNAs were validated with RT-qPCR and the results rely only on high-throughput data. The study by Volinia *et al.* (Volinia *et al.*, 2006) was conducted using a microarray that partially detected miRNA precursors that may have biased the results. Differences in study design were also found in the sample preparation. While matched samples of tumor and normal tissue from the same prostate were used in this study, the 2 other studies used normal tissue from healthy donors as a control. Given the small changes in miRNA expression in the prostate, the intraindividual variability may significantly bias the results.

The expression of the members of 2 miRNA clusters, miR-96/miR-182/miR-183 and miR-221/miR-222, was highly correlated with each other. The good correlation of both clusters supports the validity of this study. Nevertheless, we failed to identify both members of the miR-143/miR-145 cluster. miR-143 and miR-145 are located in close proximity on chromosome 5. Whereas miR-145 was clearly downregulated, miR-143 was not studied by RT-qPCR. However, reanalysis of the microarray data revealed a moderate downregulation of miR-143. Because it did not pass the t-test on intensity level and ratio profile level, it was excluded from further analysis.

The deregulation of the herein identified miRNAs has also been observed in other cancer entities. For example, miR-145, miR-205, miR-221 and miR-222, were also found to

be downregulated in triple-negative breast cancers (Radojicic *et al.*, 2011). However, studies of other cancers have not always supported the results presented in this thesis, particularly for miR-375, which is downregulated in the sputum of lung cancer patients, gastric cancer and head and neck squamous cell carcinomas (Ding *et al.*, 2010; Hui *et al.*, 2010; Tsukamoto *et al.*, 2010; Yu *et al.*, 2010a). Although miR-375 is upregulated in breast cancer by ESR1 in a positive feedback loop and its inhibition impairs proliferation (de Souza Rocha Simonini *et al.*, 2010), the same miRNA inhibits proliferation via JAK2 regulation in gastric cancer (Ding *et al.*, 2010). These observations point to the tissue-specific expression and function of miRNAs in different tissues and cancer entities, making it necessary to investigate the miRNA expression each cancer type. Reasons for these discrepancies might be found in the highly complex regulatory networks that are controlled by miRNAs, as mentioned before. Thus in each tissue, one miRNA may target a different set of genes, resulting in a tissue-specific phenotype.

Our analysis demonstrates that miRNAs are useful diagnostic discriminators of prostate cancer tissues. Even a single miRNA (miR-205) was able to correctly classify 72% of all patients and the combination of miR-205 and miR-183 improved the overall correct classification to 84%. These results are supported by the findings that miRNA profiling is superior to mRNA profiling in the identification of poorly differentiated tumors (Lu *et al.*, 2005) and highlight the potential of miRNAs as diagnostic markers. Therefore, the miRNAs that well discriminate prostate tumor from the normal adjacent tissue might be useful markers for the detection of tumors of unknown origin. Because the measurement of miRNAs in tissue for diagnostic purposes is limited, non-invasive measurement of molecular markers will be of critical importance in the future. Accordingly, miRNA expression has recently been studied in the plasma and sera of prostate cancer patients (Brase *et al.*, 2011; Lodes *et al.*, 2009; Mitchell *et al.*, 2008; Moltzahn *et al.*, 2011; Yaman Agaoglu *et al.*, 2011; Zhang *et al.*, 2011). Specifically, miR-141 has been concordantly identified to be of diagnostic value, although this miRNA is not relevantly dyregulated in prostate cancer tissue. Of the dysregulated in prostate tissue that were identified in this thesis, only miR-221 was detected in plasma (Yaman Agaoglu *et al.*, 2011), suggesting that the other miRNAs might not be released from prostate tumor cells, at least not in detectable levels. The mechanism of how miRNAs are released from cancer cells has not been investigated thoroughly, but it has been shown that miRNAs are associated with exosomes (Duijvesz *et al.*, 2010; Michael *et al.*, 2010) and argonaute (Arroyo *et al.*, 2011) proteins in the blood of cancer patients.

This thesis has shown the upregulation of miR-96, miR-183 and miR-182* for the first time. Together with miR-182, these miRNAs are transcribed as a single polycistronic pri-miRNA on chromosome 7. The upregulation of these miRNAs in prostate cancer and their correlation with tumor aggressiveness have been confirmed by microarray and ISH analysis

(Navon *et al.*, 2009; Yin *et al.*, 2010). In addition, miR-96 expression is upregulated in several other cancers, including colon cancer, hepatocellular carcinoma, WNT-associated medulloblastomas, breast cancer, lymphomas, land cancers found in the liver, ovary, testes and lung (Gokhale *et al.*, 2010; Lin *et al.*, 2010; Navon *et al.*, 2009; Sarver *et al.*, 2009; Sato *et al.*, 2011). Only in mantle cell lymphoma and pancreatic cancer, miR-96 has been described to be downregulated (Pal *et al.*, 2007; Yu *et al.*, 2010b). miR-96 and miR-183 expression was also correlated with the Gleason score. miR-96 seems to be of special interest as molecular marker in prostate cancer, because uni- and multivariate survival analyses have established the association of miR-96 expression and biochemical recurrence. We have validated this association in a second, independent samples set. Using Cox regression, we identified a survival model comprising the Gleason score and miR-96 that significantly improves the recurrence-free prediction of prostate cancer patients after radical prostatectomy. The Kleinbaum approach of graphically comparing observed and expected survival and the c-index approach underscores the validity of this model. Typically, models with c-indices greater than 0.8 are regarded as useful prognostic clinical tools (Harrell, 2001). The diagnostic and prognostic role of miR-96 in cancer has also been studied by several other groups. In urothelial carcinoma patients, miR-96 is highly elevated in urine, and the combination of cytology and miR-96 expression improves the overall correct classification to 79% (Yamada *et al.*, 2011). In colon cancer, miR-96 is elevated in stage IV tumors as compared with to stage II tumors (Sarver *et al.*, 2009) and miR-96 is associated with recurrence in hepatocellular carcinoma (Sato *et al.*, 2011).

In this thesis, miRNA profiling was performed according to the “Reporting Recommendations for Tumor Marker Prognostic Studies” (McShane *et al.*, 2005). Nevertheless, some study limitations need to be discussed. The number of patients with biochemical recurrence is relatively small, although the proportion corresponds to the failure rates generally observed (Guillonneau *et al.*, 2003; Lein *et al.*, 2006). The prognostic value of Gleason score and pathological stage were reproduced, indicating the representativeness of this study cohort. Furthermore, the prognostic impact of elevated miR-96 expression was verified in a second independent sample set. Therefore, the risk of type II errors can be neglected with good certainty. Due to the high significance of dysregulated miRNAs in prostate tumor tissue, risk I errors can also be excluded. This study was also clearly limited by its retrospective nature; however, all measurements were performed in a blinded manner.

4.1.3 Identification of dysregulated miRNA in prostate cancer relapse

In this thesis, the dysregulation of 15 miRNAs was established by miRNA profiling in fresh frozen prostate cancer and normal adjacent tissue and miR-96 was identified as a suitable prognostic marker. In a second step, we performed a proof-of-principle study to identify dysregulated miRNAs in patients with biochemical relapse in FFPE tissue.

FFPE tissue is routinely archived from all prostatectomized patients and is therefore the ideal sample for the detection of prognostic markers. mRNA expression profiling fails to be reliable in FFPE tissues due to their high level of degradation in these tissue samples (Bresters *et al.*, 1994; Macabeo-Ong *et al.*, 2002). In contrast, miRNAs are considerably more stable, which is likely due to their small size and their incorporation into large ribonucleoprotein complexes (Glud *et al.*, 2009; Hasemeier *et al.*, 2008; Hui *et al.*, 2009; Siebolts *et al.*, 2009; Szafranska *et al.*, 2008; Zhang *et al.*, 2008); therefore, they represent promising detection markers in FFPE tissue.

Using pooled RNA from patients with (i) early biochemical relapse (< 1 year), (ii) late biochemical relapse (1 to 5 years) and (iii) no biochemical relapse (> 5 years), we were able to show that a set of miRNAs is differentially expressed between the study groups.

In prostate cancer relapse patients, 68 miRNAs were identified to be dysregulated between the groups. Of these a subset of 13 miRNAs (miR-10b, miR-30d, miR-31, miR-133b, miR-135a, miR-143, miR-151-3p, miR-200a, miR-221, miR-222, miR-375, miR-429, and miR-516-3p) have been previously described to be dysregulated in tumor progression or metastasis. (Avissar *et al.*, 2009; Bandres *et al.*, 2006; Clape *et al.*, 2009; Corbetta *et al.*, 2010; Dyrskjot *et al.*, 2009; Foekens *et al.*, 2008; Gramantieri *et al.*, 2008; Hu *et al.*, 2009b; Hu *et al.*, 2010b; Hu *et al.*, 2011; Hu *et al.*, 2010c; Li *et al.*, 2010a; Ma *et al.*, 2007; Ma *et al.*, 2010; Mathe *et al.*, 2009; Nam *et al.*, 2008; Navarro *et al.*, 2009; Pons *et al.*, 2009; Sasayama *et al.*, 2009; Slaby *et al.*, 2007; Spahn *et al.*, 2010; Valastyan *et al.*, 2009a; Valastyan *et al.*, 2009b; Veerla *et al.*, 2009; Visone *et al.*, 2009; Wang *et al.*, 2009; Yao *et al.*, 2010; Yu *et al.*, 2010a). Additionally, a subset of 6 miRNAs have been previously described to be dysregulated in prostate cancer as compared with normal tissue (miR-31, miR-133b, miR-143, miR-221, miR-222 and miR-375) (Ambs *et al.*, 2008; Porkka *et al.*, 2007; Spahn *et al.*, 2010; Szczyrba *et al.*, 2010; Tong *et al.*, 2009; Wach *et al.*, 2011). Therefore, the dysregulation of these miRNAs may be highly interesting in terms of biochemical relapse and thus requires further investigation.

Because these results are based only on the measurement of 3 pools from 10 samples each, the risk of type I and II errors is high. Therefore, the expression of 2 miRNAs was validated in 59 samples. The measurement in these samples confirmed the upregulation of miR-10b and revealed a slightly lower expression of miR-222 in patients with early relapse. These results support the hypothesis that miRNAs can predict biochemical relapse. Statistical analyses were performed to assess whether both miRNAs can separate patients with early biochemical relapse from those with no relapse. As expected, miR-222 did not well differentiate the patients. However, miR-10b and the miR-222/miR-10b expression ratio were good discriminators with an overall correct classification up to 68%. In addition, the miR-

222/miR-10b ratio was inversely correlated with the Gleason score, further highlighting the association of this miRNAs with tumor aggressiveness.

This is the first study to describe miR-10b dysregulation in prostate cancer relapse. miR-10b has been previously described in relation to tumor progression and metastases in several different tumors. This miRNA has been reported to be overexpressed in metastatic breast cancer (Ma *et al.*, 2007; Ma *et al.*, 2010), is further associated with high-grade gliomas (Sasayama *et al.*, 2009) and is highly expressed in hepatocellular carcinoma (Ladeiro *et al.*, 2008). miR-10b is also part of a 7 miRNA signature that predicts gastric cancer survival (Li *et al.*, 2010c). A comparison of primary and metastatic tumors from the breast, bladder, lung and colon revealed miR-10b to be overexpressed in bladder transitional cell carcinomas (Baffa *et al.*, 2009).

The expression ratio of miR-221/222 was reported to be negatively associated with poor survival in ovarian cancer (Wurz *et al.*, 2010), and high miR-222 expression was reported to be associated with poor survival in pancreatic cancer (Greither *et al.*, 2010) and invasive tumors in urothelial carcinomas (Veerla *et al.*, 2009). Because the results are based solely on miRNA expression from 3 pools that contain the RNA from 10 patients each, this study has to be seen as a proof-of-principle. Nevertheless, the validation of 2 miRNAs, miR-10b and miR-222, confirms that miRNA dysregulation occurs in patients with highly aggressive cancers and that miRNAs can correctly classify samples according to the time of recurrence. To provide a thorough overview of miRNA dysregulation in biochemical relapse patients, it is necessary to repeat the profiling in a larger sample set and subsequently validate the results by RT-qPCR.

4.2 Functional relevance of miRNAs in prostate cancer

4.2.1 In-silico target prediction

The identification of dysregulated prostate cancer miRNAs is important for more than just the identification of novel diagnostic and prognostic markers; these miRNAs may also control essential checkpoints involved in prostate carcinogenesis. Therefore, they may help to elucidate the mechanisms of tumor initiation and progression, which may eventually provide a basis for novel therapeutic strategies.

miRNAs exert their effects mainly via regulation of mRNA decay and protein translation by binding to complementary sequences in the target mRNA 3' UTR. Because one miRNA can target hundreds of mRNAs, bioinformatic in silico analysis has emerged as an important miRNA binding sites identification tool. We have performed in silico target analysis for all identified miRNAs using miRecords. miRecords combines 11 algorithms including Diana, Microinspector, MiRanda, Mirtarget2, Mitarget, Nbmirtar, picTar, Pita, RNA22, RNAHybrid and TargetScan. To further confine the list of putative targets, we only

regarded a prediction as valid if MiRanda, picTar and TargetScan and any 2 other algorithms concordantly identified the gene. miRanda, picTar and TargetScan were choosen because they are the most commonly used target prediction algorithms and are more stringent in their selection criteria in comparison with others. The TargetScan algorithm combines thermodynamic-based modelling of RNA interactions with the identification of conserved binding sites (Lewis *et al.*, 2003). PicTar also searches for Watson-Crick base pairing of the seed sequence, calculates the free energy of the miRNA:mRNA duplex and takes conservation into consideration. Additionally, picTar accounts for the synergistic effects of multiple binding sites for the same miRNA or several miRNAs in the 3' UTR (Krek *et al.*, 2005). miRanda also identifies perfect seed-complementarity, calculates the free energy of miRNA:mRNA duplex and accounts for evolutionary conservation (Enright *et al.*, 2003). We identified a mean of 84 targets per gene. This high number of putative targets per miRNA pinpoints a dynamic and versatile process.

Other groups have already described a subset of the herein identified miRNAs to be functionally relevant in prostate cancer. Specifically, the functional relevance of miR-16, miR-125b, miR-205 and miR-221/-222 as discussed in the introduction (1.3.3), in addition to other miRNAs has been functionally characterized in prostate cancer.

miR-145 expression is related to tumor recurrence (Leite *et al.*, 2011) and miR-145 downregulation occurs due to the hypermethylation of the promotor region as well as transcriptional regulation of TP53 (Suh *et al.*, 2011; Zaman *et al.*, 2011). Functionally, miR-145 has been related to the regulation of apoptosis and cell cycle via regulation of TNFSF10 (Zaman *et al.*, 2011), as well as invasion via FCSN1 (Fuse *et al.*, 2011) and SWAP70 (Chiyomaru *et al.*, 2011).

miR-31 overexpression in PC3 prostate cancer cell lines inhibited proliferation, an effect that was only observed in TP53 negative cells (Creighton *et al.*, 2010) and promoted apoptosis induced by docetaxel and cisplatin via inhibition of BCL2L2 and E2F6 (Bhatnagar *et al.*, 2010).

4.2.2 miRNA regulation by androgens

Androgen-regulation is an important mechanism of prostate cancer cell growth. Therefore, the androgen-dependence of all dysregulated miRNAs found in this thesis was investigated in cell culture experiments. We have identified 4 miRNAs that were downregulated with elevated concentrations of the synthetic androgen R1881.

Androgen regulation of miR-149 was shown for the first time in prostate cancer. To date, this miRNA has not been functionally characterized in prostate cancer or in other cancer, but its dysregulation by androgens clearly suggests a functional relevance in prostate cancer.

miR-10b was also, for the first time, described in the context of androgen-dependence. This thesis is the first to describe a deregulation and functional role of this miRNA in prostate cancer. We discuss the functionality of this miRNA in more detail below.

Furthermore, miR-221/-222 were identified to be downregulated in androgen-dependent cell lines upon androgen-treatment in comparison to cells under androgen-ablation, an observation that has been supported by another study that investigated the role of these miRNAs in androgen-independent prostate cancer growth (Sun *et al.*, 2009). Although miR-221 and miR-222 has been frequently described to be downregulated, experimental evidence suggested an oncogenic role of this cluster in prostate cancer. Therefore, the biological relevance of this miRNA cluster in prostate cancer remains questionable.

4.2.3 Combination of computational and experimental methods to confirm the function of miR-10b in prostate cancer recurrence

In-silico target analysis was performed for all dysregulated miRNAs from prostate cancer relapse patients, and we identified targets of 36 miRNAs. Analysis was further narrowed to the characterization of miR-10b, which is upregulated in biochemical relapse. The function of miR-10b has been mainly studied in breast cancer. In vitro, it has been shown to promote migration and invasion in breast, esophageal and peripheral nerve sheath cancer cell lines (Chai *et al.*, 2010; Ma *et al.*, 2007; Tian *et al.*, 2010). In addition, in vivo studies have highlighted the importance of miR-10b in metastasis. While mice treated systemically with antagomiR-10b developed less metastasis than their non-treated counterparts (Ma *et al.*, 2010), miR-10b overexpression, in otherwise non-metastatic breast cancer bearing mice, initiated tumor cell invasion and metastasis (Li *et al.*, 2010a). Several 10b targets have been identified, which further indicate a central role of miR-10b in migration and invasion. miR-10b directly targets HOXD10 (Debernardi *et al.*, 2007; Ma *et al.*, 2007; Ma *et al.*, 2010; Sasayama *et al.*, 2009). Deregulation of this transcription factor results in the subsequent regulation of important prometastatic genes, including RHOA, RHOC and PLAUR (Bourguignon *et al.*, 2010). Additionally, miR-10b targets KLF4 (Tian *et al.*, 2010) and activates Ras-signalling (Chai *et al.*, 2010). The regulation of miR-10b expression has also been studied. One important miR-10b regulator is the TWIST1 transcription factor (Bourguignon *et al.*, 2010). Furthermore, it has been suggested that and BRMS1 containing SIN3:HDAC complex regulated the miR-10b promoter (Edmonds *et al.*, 2009). To determine the function of miR-10b, pathway and Gene ontology term analysis were performed using the list of putative targets. Transcriptional regulation was identified as an overrepresented process in the set of target genes, which supports the previous experimental results. The results in this thesis have proven that miR-10b promotes prostate cancer cell migration and

suggest a role for this miRNAs in invasion and metastasis, which is in concordance with the previous results in breast cancer.

4.2.4 The regulation of apoptosis by miR-96 and FOXO1 in prostate cancer

Prostate cancer miRNA profiling revealed an upregulation of the miR-96 cluster. Interestingly, miR-96 not only correlated with the Gleason score but also associated with biochemical relapse. Based on these profiling results, the functional role of miR-96 in prostate carcinogenesis was investigated.

miR-96 expression has been first described exclusively in the retina where it controls the circadian rhythm via ADCY6 (Loscher *et al.*, 2007; Xu *et al.*, 2007b). However, recent studies report a broader expression pattern. The miR-96 cluster appears to be an important regulator of inner ear development, and the loss of this cluster or mutations of its seed region inhibits the differentiation of hair cells and the cochlea, resulting in progressive hearing loss (Kuhn *et al.*, 2011; Lewis *et al.*, 2009; Li *et al.*, 2010b; Mencia *et al.*, 2009; Sacheli *et al.*, 2009; Weston *et al.*, 2011). miR-96 cluster overexpression has also been associated with cancer (Gokhale *et al.*, 2010; Lin *et al.*, 2010; Navon *et al.*, 2009; Sarver *et al.*, 2009; Sato *et al.*, 2011).

The results in this thesis show that the overexpression of miR-96 in LNCaP prostate cancer cells results in increased proliferation under serum starvation. Furthermore, we provided evidence to demonstrate that the increased proliferation could be explained by impaired chemosensitivity to CPT-mediated intrinsic apoptosis, but not by enhanced cell cycle transition.

Thus far, a few studies have also investigated the miR-96 cancer function and these reports mainly confirm an oncogenic role for this miRNA. In breast cancer, miR-96 regulates proliferation and anchorage-independent growth and modulates the transition of cells from the G1 to the S-phase (Lin *et al.*, 2010). In endometrial carcinoma, the cell cycle effect has been confirmed, and its impairment of apoptosis has been described (Myatt *et al.*, 2010). An effect of miR-96 on cell cycle and cell motility has not been observed, suggesting tissue-specific functions for this miRNA. In pancreatic cancer, miR-96 has been described to have tumorsuppressive properties by downregulating KRAS, thereby impairing cancer cell invasion, migration and tumor growth in vivo (Yu *et al.*, 2010b), further supporting the hypothesis that miRNA function can differ in different tissues.

Having revealed that miR-96 inhibits apoptosis in prostate cancer, putative miR-96 targets mediating this effect were identified. In silico target prediction revealed 209 putative miR-96 targets of which 21 were associated with apoptosis. The first putative target, which was experimentally validated here, is FOXO1.

FOXO1 is known to be a downstream mediator of CPT-triggered apoptosis (Han and Wei, 2011; Huang *et al.*, 2006; Zeng *et al.*, 2009), which makes it an ideal candidate because

of the observation that miR-96 inhibits CPT-triggered apoptosis. FOXO1 is a transcription factor whose activity is regulated by the AKT kinase signalling pathway. Upon phosphorylation by AKT, FOXO1 is translocated to the cytoplasm (Rena *et al.*, 1999). FOXO1 activity is regulated by posttranslational mechanisms such as CDK1 phosphorylation (Liu *et al.*, 2008a), acetylation/deacetylation (Motta *et al.*, 2004) and ubiquitination (Matsuzaki *et al.*, 2003). In a nonphosphorylated state, FOXO1 transcriptionally regulates the expression of genes involved in cell cycle, including CDKN1B (Machida *et al.*, 2003) and RBL2 (Kops *et al.*, 2002), and proapoptotic genes such as BAX (Kim *et al.*, 2005) and TRAIL (Modur *et al.*, 2002). In prostate cancer, FOXO1 has been shown to promote apoptosis (Huang *et al.*, 2004; Liu *et al.*, 2008a; Modur *et al.*, 2002; Zhang *et al.*, 2010) and to inhibit the androgenic and androgen-independent AR activation. FOXO1 interacts with the N- and C-terminus of the AR and impairs ligand-induced subcellular compartmentalization (Fan *et al.*, 2007; Ma *et al.*, 2009; Yanase and Fan, 2009). For AR inhibition by FOXO1, the forkhead domain and the C-terminal activation domain are required (Ma *et al.*, 2009). Furthermore, the activity of cofactors, such as HDAC3 (Liu *et al.*, 2008b) and MYBBP1A, is necessary (Ma *et al.*, 2009). The interaction of AR with FOXO1 also inhibits FOXO1 transcriptional activity and results in impaired apoptosis and cell cycle arrest (Li *et al.*, 2003). Androgens can also regulate FOXO1 transcriptional activation, and hence its apoptotic function, by the induction of FOXO1 cleavage (Huang *et al.*, 2004).

FOXO1 is silenced in prostate cancer by several mechanisms. As previously mentioned, FOXO1 activity is inhibited due to hyperactive AKT signalling, which occurs in up to 50% of prostate cancers and is mostly a result of PTEN deletion (Morgan *et al.*, 2009). Furthermore, the FOXO1 locus at 13q14 can also be deleted in prostate cancer patients (Dong *et al.*, 2006). This study confirms that miR-96 can also downregulate FOXO1 at the transcript and protein levels by binding to 2 sites in its 3' UTR, thereby presenting an alternative mechanism for FOXO1 prostate cancer inactivation. The regulation of FOXO1 by miR-96 has been confirmed in breast cancer and in endometrial carcinomas (Guttilla and White, 2009; Myatt *et al.*, 2010).

FOXO3A, another member of the forkhead box O family of transcription factors, is also regulated by miR-96 in breast cancer, which results in the subsequent downregulation of CDKN1A and CDKN1B (Lin *et al.*, 2010). In conclusion, these data support the hypothesis that miR-96-mediated regulation of apoptosis is dependent on its regulation of forkhead transcription factors.

To confirm that the FOXO1 inhibition by miR-96 is relevant in prostate cancer in vivo, miR-96 expression was correlated with FOXO1 transcript and protein expression levels in matched primary prostate cancer and normal adjacent tissues. While no correlation was observed with FOXO1 mRNA expression, FOXO1 protein and miR-96 expression were

inversely correlated with each other. These data suggest a mainly translational inhibition, although mRNA degradation was observed in vitro. The observed degradation might occur due to the high overexpression of miR-96 in vitro, which is much higher than the moderate upregulation observed in prostate cancer tissue.

FOXO1 protein expression in the tissue microarray was only detected in epithelial tissue, and localization of FOXO1 was predominantly in the nucleus in normal tissue, while in the majority of cancer ducts it was located in the cytoplasm. This observation confirms the results from a previous study (Li *et al.*, 2007). In addition, an association of a low FOXO1 T/N ratio with biochemical relapse in prostate cancer was observed. Yet, in a multivariate model including the Gleason score and miR-96, FOXO1 was not an independent marker of biochemical relapse. Cytoplasmic, phosphorylated FOXO1 has been previously associated with biochemical relapse (Li *et al.*, 2007).

In this thesis, a second putative miR-96 target, which may be involved in miR-96 regulated apoptosis, was investigated. The inositol 1,4,5 triphosphate receptor 1 (ITPR1) is a receptor located on the endoplasmatic reticulum (Taylor and Tovey, 2010). The inositol 1,4,5 triphosphate receptor family consists of 3 members (ITPR1, ITPR2 and ITPR2), which all seem to have at least partially different functions (Diaz and Bourguignon, 2000; Leite *et al.*, 2003; Mendes *et al.*, 2005). Upon IP3 activation, ITPR1 releases Ca^{2+} to the cytoplasm. This increased cytoplasmic Ca^{2+} concentration induces the opening of mitochondrial permeability transition pores and results in cytochrome c release (Szalai *et al.*, 1999). Cytochrome c binds to ITPR1, resulting in sustained calcium release (Boehning *et al.*, 2003). ITPR is cleaved during apoptosis by CASP3, which results in a permanent cytoplasmic calcium increase (Diaz and Bourguignon, 2000; Hirota *et al.*, 1999; Nakayama *et al.*, 2004). Other factors can also mediate ITPR1 activity. PKA, PP1 and PP2A are components of an ITPR1 signalling complex, and PKA phosphorylation of ITPR1 increases channel activity (DeSouza *et al.*, 2002). The anti-apoptotic regulator BCL2 competes with ITPR1 for PP1 binding, thus reducing IP3 mediated calcium signalling (Xu *et al.*, 2007a). BCL2L2 also interacts with the C-terminus of ITPR1, and this binding is antagonized by BAX and BID (White *et al.*, 2005). In addition, AKT and the CDK1/CCNB1 complex can phosphorylate ITPR1, thereby either inhibiting or activating its function (Khan *et al.*, 2006; Malathi *et al.*, 2005). Six independent algorithms have predicted miR-96 to bind to the ITPR1 3' UTR. Two miR-96 binding sites were identified in the 3' UTR and subsequently cloned into a luciferase vector. In a luciferase assay, only a moderate inhibition of the nonconserved binding site was observed, which was accompanied by a small reduction in protein levels with no degradation of messenger RNA. Therefore, the significance of the binding remains questionable.

The characterization of miR-96 identified a novel inhibitor of apoptosis in prostate cancer. The anti-apoptotic function of miR-96 is in part explained by its inhibition of FOXO1.

However, miR-96 also targets an abundance of other mRNAs. To identify these targets, high-throughput profiling, especially of proteins with altered expression, may be a useful technique.

4.2.5 Characterization of miR-133b in prostate cancer

The investigation of miR-133b function in prostate cancer was collaborative project. Our collaborators investigated the role of this miRNA in DR-mediated apoptosis (Patron Arcila, 2010) and have shown that miR-133b significantly enhances extrinsic apoptosis triggered by TNFα or FASL.

Thus far, miR-133b has been almost exclusively described in the context of miR signatures from tumor samples or cancer cell lines where it is generally downregulated and its potential as predictive and diagnostic marker has been investigated (Bandres *et al.*, 2006; Guo *et al.*, 2009; Hu *et al.*, 2010a; Ichimi *et al.*, 2009; Navon *et al.*, 2009; Tran *et al.*, 2007; Wong *et al.*, 2008a; Wong *et al.*, 2008b). Based on the observation that miR-133b regulates extrinsic apoptosis and is downregulated in several other cancers its expression and function was studied in prostate cancer.

miR-133b expression is reduced in the majority of prostate cancers as compared with normal adjacent tissue. Importantly, patients with a low amount of miR-133b tend to experience biochemical relapse more frequently. Transfection of the PC3 prostate cancer cell line with a synthetic miR-133b mimic resulted in the sequence-specific impairment of proliferative capacity, suggesting a functional relevance of the reduced miR-133b expression in cancerous prostate cells.

The apoptotic response upon transfection of miR-133b was the consequence of global changes in transcript and protein expression in HeLa cells (Patron Arcila, 2010). In this model, several genes have been identified as direct miRNA targets, including FAIM and GSTP1 (Patron Arcila, 2010).

In this thesis, FAIM and GSTP1 downregulation was confirmed in prostate cancer cell lines. FAIM was first identified as an antagonist of FAS-mediated apoptosis in B-cells (Schneider *et al.*, 1999). Because it does not share sequence homology with other FAS apoptosis modulators, its mechanism of action remains largely unelucidated. Two isoforms of FAIM exist: the long form, which is predominantly expressed in neuron, and the short isoform, which has a much broader expression spectrum (Segura *et al.*, 2007). Previously, a role for FAIM in TNFα- and FASL-mediated apoptosis upstream of CASP3 and CASP8 as well as neurite outgrowth by NFKB activation have been revealed (Segura *et al.*, 2007; Sole *et al.*, 2004). Furthermore, FAIM-negative thymocytes are more sensitive to FAS-mediated apoptosis and display an increased CASP8 and CASP9 activation, and FAIM regulates AKT activation and NUR77 ubiquitination (Huo *et al.*, 2010). Another mechanism by which FAIM can mediate apoptosis is by CFLAR regulation (Huo *et al.*, 2009). FAIM expression displayed

a trend towards a slightly lower expression in human prostate cancer tissue in this study. Moreover, a strong inverse correlation was observed between miR-133b and FAIM transcript expression, thus supporting our view that miR-133b can inhibit FAIM in prostate cancer.

GSTP1 is a phase II detoxifying enzyme (Townsend and Tew, 2003). The pi class glutathione-s-transferase enzymes have been shown to directly participate in MAP kinase signalling via interaction with JNK1 and ASK1 and to regulate TNFα via TRAF2 signalling inhibition (Wu *et al.*, 2006a). To investigate the importance of miR-133b regulated GSTP1 expression in prostate cancer, we correlated the expression of GSTP1 mRNA and miR-133b expression in prostate cancer specimens. miR-133b downregulation did not result in a measurable enrichment of GSTP1 in prostate cancer. In contrast, prostate tumors displayed lower levels of GSTP1 than normal adjacent tissue, with no significant correlation to miR-133b expression. Although GSTP1 has frequently been observed as an oncogene in other cancers, the observed downregulation of GSTP1 in the prostate is in accordance with previous reports (Lee *et al.*, 1994). Silencing of the GSTP1 promoter by hypermethylation seems to be a concurrent epigenetic prostate cancer alteration (Lee *et al.*, 1994; Santourlidis *et al.*, 1999). Moreover, GSTP1 promoter methylation is an early event in prostate cancer carcinogenesis that even occurs in high grade PIN with high frequency (Brooks *et al.*, 1998). Thus far, the functionality of GSTP1 hypermethylation has not been extensively studied. GSTP1 reexpression in LNCaP cells did not affect growth in vitro or in vivo (Lin *et al.*, 2001); however, with regards to its role in detoxification and its oxidative stress response response, it is hypothesized that GSTP1 silencing might lower the protection of the cells from cancer-inducing agents (Meiers *et al.*, 2007). This well-established epigenetic process most likely superimposes the effect of GSTP1 inhibition by miR-133b at least in prostate cancer; however, the role of miR-133b regulation cancers overexpressing GSTP1 cancers requires further investigation.

To investigate prostate cancer-specific miR-133b gene regulation, mRNA profiling in PC3 prostate cancer cells that ectopically overexpress miR-133b and subsequent pathway analysis was performed. The profiling and subsequent in silico analysis revealed that components of the VEGF signalling pathway were overrepresented in the list of dysregulated genes. VEGFs are cytokines that control blood and lymphatic vessel formation. There are 7 family members, including VEGFA, VEGFB, VEGFC, VEGFD, VEGFE, VEGFF and PGF (Yamazaki and Morita, 2006). VEGFs bind to their cognate cell surface receptors (VEGFR-1 and VEGFR-2) and activate downstream signalling transducers such as AKT and MAP kinases, thereby controlling growth, motility and angiogenesis (Epstein, 2007). VEGFC is upregulated in prostate cancer patients and associates with lymph node metastasis (Jennbacken *et al.*, 2005) and controls lymphangiogenesis (Wong *et al.*, 2005). Orthotopic and subcutaneous PC3 tumors that overexpress VEGFC are larger than control tumors,

metastasize to lymph nodes, show a highly angiogenic morphology and have a higher blood capillaries density (Tuomela *et al.*, 2009). In this study, VEGFC was identified to be downregulated by miR-133b in PC3 prostate cancer cells at the transcript and protein level.

One of the miR-133b regulated genes that were associated with VEGF signalling is CAV1. VEGF and CAV1 are upregulated by each other in a positive autoregulatory feedback loop (Li *et al.*, 2009a), and CAV1 is required for basal and VEGF-triggered VEGFR2 phosphorylation (Tahir *et al.*, 2009). Secreted CAV1 is taken up by endothelial cells via caveolae and induces angiogenic activity (Tahir *et al.*, 2008). Concordantly, CAV1 positive tumors have higher microvessel densities (Yang *et al.*, 2007). In nude mice, CAV1 secreted from CAV1-positive LNCaP tumors can increase the growth of CAV1 negative tumors in the contralateral flank (Bartz *et al.*, 2008). CAV1 knockout in TRAMP mice does not influence the primary tumor size but significantly impairs the metastatic potential (Li *et al.*, 2001; Williams *et al.*, 2005). In a conditional mouse model, CAV1 overexpression increases hyperplasia and renders cells insensitive to castration-induced prostatic regression (Watanabe *et al.*, 2009). The influence of CAV1 expression on androgen-sensitivity has been confirmed by several studies (Lu *et al.*, 2001; Nasu *et al.*, 1998; Tahir *et al.*, 2001). Additionally, an anti-apoptotic CAV1 function has been described in prostate cancer, thus providing a possible link to miR-133b function (Li *et al.*, 2001). CAV1 inhibits apoptosis by inhibiting PP1 and PP2A, which results in elevated AKT activity and phosphorylation of antiapoptotic genes, such as FOXO1, GSK3 and MDM2 (Li *et al.*, 2003). In neural invasion, TGFB1 mediates CAV1 secretion to the tumor microenvironment in a paracrine anti-apoptotic loop that results in impaired tumor cell apoptosis (Ayala *et al.*, 2006). CAV1 was one of the most prominently downregulated genes in miR-133b overexpressing PC3 prostate cancer cells, and its downregulation was confirmed at the protein level in this study. Three putative binding sites were identified by in silico target analysis. However, in a luciferase assay, miR-133b binding to these binding sites or to the complete 3' UTR was not observed. Therefore, miR-133b does not seem to directly mediate CAV1 expression. Hence, CAV1 may be indirectly regulated by miR-133b via VEGFC. In future studies, investigation of the direct binding of miR-133b to the VEGFC 3' UTR will be essential.

CAV1 is located on chromosome 7 in a region that is frequently deleted in castration-resistant prostate cancer (Nupponen *et al.*, 1998). CAV1 overexpression mainly occurs in high grade and metastatic prostate cancer and is associated with recurrence (Di Vizio *et al.*, 2008; Gould *et al.*, 2010; Karam *et al.*, 2007; Satoh *et al.*, 2003; Tahir *et al.*, 2001; Yang *et al.*, 1999). High serum CAV1 levels also serve as a prognostic marker for recurrence (Langeberg *et al.*, 2010; Tahir *et al.*, 2006). The assumed CAV1 upregulation has been challenged by other studies, which reported a downregulation of CAV1 that most likely occurred by promotor hypermethylation (Bachmann *et al.*, 2008; Cui *et al.*, 2001; Engelman

et al., 1998) and described its tumorsuppressive function (Chen *et al.*, 2009). In our lab, CAV1 mRNA downregulation of has also been observed, which clearly questions the oncogenic function of CAV1 in prostate cancer (Steiner *et al.*, unpublished data). Surprisingly, miR-133b and CAV1 were highly correlated with each other, which contradict the in vitro results that show CAV1 downregulation in miR-133b overexpressing cells. Thus, the mechanisms by which miR-133b and CAV1 are functionally connected in prostate cancer remains to be elucidated so far.

Another putative miR-133b target gene, which caught our attention due to its downregulation at the mRNA and protein level in TNFa-induced and miR-133b transfected HeLa cells, is FASN but no direct interaction with miR-133b could be shown (Patron Arcila, 2010). FASN catalyses the synthesis of palmitate from acetyl-CoA, and is not expressed in human tissues except for in liver and adipose tissues but is increased in a variety of cancers including prostate cancer (Prowatke *et al.*, 2007; Shah *et al.*, 2006). FASN overexpression protects LNCaP and iPrE cells from intrinsic apoptosis but not extrinsic apoptosis, mediates growth and colony formation of iPrE cells (Migita *et al.*, 2009), and has been shown to regulate c-Met, thereby leading to enhanced apoptosis in diffuse large B-cell lymphoma (Uddin *et al.*, 2010). FASN colocalizes with CAV1 in prostate cancer in a process that is controlled by SRC, AKT and EGFR signaling (Di Vizio *et al.*, 2008). CAV1 expression is mandatory for FASN overexpression in the tumor and CAV1-negative tumors are smaller in size and do not metastasize (Di Vizio *et al.*, 2007). In this thesis, we have proven that FASN and miR-133b expression is inversely correlated in cancer, which suggests that FASN expression is under the control of miR-133b. However, no miR-133b binding site was identified in the FASN 3' UTR. To date we cannot present conclusive evidence of whether correlation of FASN and miR-133b expression is due to miR-133b binding to a previously unidentified site or whether a secondary mechanism is responsible. It is possible that mir-133b regulates upstream FASN modulators, thereby also enhancing FASN expression. FASN prostate cancer expression is androgen-regulated via the SREBP transcription factor (Lee *et al.*, 2009b). This transcriptional activation is under the control of ERBB2 and EGFR, and their signals are mediated by the PI3K-Akt and MAPK signalling pathways, respectively (Kumar-Sinha *et al.*, 2003; Menendez and Lupu, 2007).

In conclusion, the results presented here show that miR-133b is downregulated in prostate cancer and also serves as a tumorsuppressor by targeting a variety of genes either directly or indirectly. However, some of the observed in vitro regulations do not reflect what is found in human prostate cancer tissue, because they are most likely superimposed by other upstream regulatory mechanisms.

5. Conclusion and outlook

Recently, miRNAs have gained attention in translational cancer research, and they are promising new cancer markers and may be useful for the identification of the origin of poorly differentiated tumors, for diagnosis and prognosis or for the prediction of disease and therapy outcome. This thesis investigated the deregulation of miRNAs in prostate cancer. The description of miRNA regulation in previous studies has been insufficient and the results have been conflicting. The reasons for these discrepancies can be explained mainly by the differences in study design and the analytical problems of the early studies. To render our analysis more robust, we first investigated the expression of putative target genes. All of the preceding studies used reference genes without prior analysis of their stability. Here, miR-130b was identified as a highly stable reference gene for miRNA expression studies by RT-qPCR.

Altogether, 15 miRNAs were found to be dysregulated in prostate cancer. The differently expressed miRNAs were analyzed according to their diagnostic and prognostic value. The combination of only 2 miRNAs was able to correctly classify up to 84% of samples correctly. With regards to miRNA diagnostic markers, their measurement in blood and urine will become more important, and the herein identified miRNAs may help to identify tumors of unknown origin.

This thesis is the first to investigate the role of miR-96 in prostate cancer, which has been associated with biochemical relapse. A Cox regression model was established, which included the variables miR-96 and Gleason Score. The c-index of the model was 0.85, which underscores its good prognostic properties. miR-96 may therefore be an interesting new molecule, which may improve the sensitivity of the existing clinical prognosis models .

miRNA manipulation in prostate cancer may help to control prostate cancer in its early and advanced stages. In particular, the development of novel therapies is a crucial task for castration-resistant prostate cancer. However, miRNA-regulated pathways in prostate carcinogenesis are now only partially understood. Functional analysis revealed that miR-96 impairs apoptosis via FOXO1 regulation. The thesis is the first study that demonstrated that miR-96 presents as a novel oncogenic molecule in prostate cancer. In silico analysis has predicted a set of other potential miR-96 targets. To investigate, which other proapoptotic genes are involved in miR-96 regulated apoptosis, high-throughput methods such as mRNA profiling and especially protein expression analysis (e.g. the pSilac method) should be used.

miR-133b, which is downregulated in prostate cancer, was also investigated for the first time in prostate cancer. In an earlier study of our collaborators, miR-133b was investigated as a proapoptotic molecule in HeLa cells. In this thesis, its tumorsuppressive function was shown in prostate cancer and several oncogenic targets were identified.

The results presented in this thesis identify both miR-96 and miR-133b as attractive new targets for prostate cancer therapy. The overexpression or knockout of these miRNAs may impair tumor growth and sensitize tumors to chemo- or radiotherapy. However, the usefulness of miR-96 or miR-133b targeting therapies needs to be further investigated in in vivo models. The development of miRNA-based therapies is still in its infancy, but some mouse models have demonstrated that systemic treatment with antagomiRs or miRNA mimics can result in tumor regression, which is generally well tolerated by the animals.

In conclusion, this thesis is one of the first to provide solid evidence of the deregulation of miRNAs in prostate cancer, and it is the first to describe the functional role of miR-96 and miR-133b in this cancer type. Therefore, this thesis is a basis for the future development of miRNA-based diagnostic and prognostic markers and novel therapies.

References

Akinc A, Zumbuehl A, Goldberg M, Leshchiner ES, Busini V, Hossain N *et al* (2008). A combinatorial library of lipid-like materials for delivery of RNAi therapeutics. *Nat Biotechnol* **26:** 561-569.

Alcaraz A, Hammerer P, Tubaro A, Schroder FH, Castro R (2009). Is there evidence of a relationship between benign prostatic hyperplasia and prostate cancer? Findings of a literature review. *Eur Urol* **55:** 864-873.

Altuvia Y, Landgraf P, Lithwick G, Elefant N, Pfeffer S, Aravin A *et al* (2005). Clustering and conservation patterns of human microRNAs. *Nucleic Acids Res* **33:** 2697-2706.

Ambs S, Prueitt RL, Yi M, Hudson RS, Howe TM, Petrocca F *et al* (2008). Genomic profiling of microRNA and messenger RNA reveals deregulated microRNA expression in prostate cancer. *Cancer Res* **68:** 6162-6170.

Amling CL, Blute ML, Bergstralh EJ, Seay TM, Slezak J, Zincke H (2000). Long-term hazard of progression after radical prostatectomy for clinically localized prostate cancer: continued risk of biochemical failure after 5 years. *J Urol* **164:** 101-105.

Andersen CL, Jensen JL, Orntoft TF (2004). Normalization of real-time quantitative reverse transcription-PCR data: a model-based variance estimation approach to identify genes suited for normalization, applied to bladder and colon cancer data sets. *Cancer Res* **64:** 5245-5250.

Andriole GL, Crawford ED, Grubb RL, III, Buys SS, Chia D, Church TR *et al* (2009). Mortality results from a randomized prostate-cancer screening trial. *NEnglJMed* **360:** 1310-1319.

Arroyo JD, Chevillet JR, Kroh EM, Ruf IK, Pritchard CC, Gibson DF *et al* (2011). Argonaute2 complexes carry a population of circulating microRNAs independent of vesicles in human plasma. *Proc Natl Acad Sci U S A*.

Avissar M, Christensen BC, Kelsey KT, Marsit CJ (2009). MicroRNA expression ratio is predictive of head and neck squamous cell carcinoma. *Clin Cancer Res* **15:** 2850-2855.

Ayala GE, Dai H, Tahir SA, Li R, Timme T, Ittmann M *et al* (2006). Stromal antiapoptotic paracrine loop in perineural invasion of prostatic carcinoma. *Cancer Res* **66:** 5159-5164.

Bachmann N, Haeusler J, Luedeke M, Kuefer R, Perner S, Assum G *et al* (2008). Expression changes of CAV1 and EZH2, located on 7q31 approximately q36, are rarely related to genomic alterations in primary prostate carcinoma. *Cancer Genet Cytogenet* **182:** 103-110.

Baffa R, Fassan M, Volinia S, O'Hara B, Liu CG, Palazzo JP *et al* (2009). MicroRNA expression profiling of human metastatic cancers identifies cancer gene targets. *J Pathol* **219:** 214-221.

Bandres E, Cubedo E, Agirre X, Malumbres R, Zarate R, Ramirez N *et al* (2006). Identification by Real-time PCR of 13 mature microRNAs differentially expressed in colorectal cancer and non-tumoral tissues. *Mol Cancer* **5:** 29.

Bartel DP (2004). MicroRNAs: genomics, biogenesis, mechanism, and function. *Cell* **116:** 281-297.

Bartz R, Zhou J, Hsieh JT, Ying Y, Li W, Liu P (2008). Caveolin-1 secreting LNCaP cells induce tumor growth of caveolin-1 negative LNCaP cells in vivo. *Int J Cancer* **122:** 520-525.

Bedolla R, Prihoda TJ, Kreisberg JI, Malik SN, Krishnegowda NK, Troyer DA *et al* (2007). Determining risk of biochemical recurrence in prostate cancer by immunohistochemical detection of PTEN expression and Akt activation. *Clin Cancer Res* **13:** 3860-3867.

Behm-Ansmant I, Rehwinkel J, Doerks T, Stark A, Bork P, Izaurralde E (2006). mRNA degradation by miRNAs and GW182 requires both CCR4:NOT deadenylase and DCP1:DCP2 decapping complexes. *Genes Dev* **20:** 1885-1898.

Berezikov E, Guryev V, van de Belt J, Wienholds E, Plasterk RH, Cuppen E (2005). Phylogenetic shadowing and computational identification of human microRNA genes. *Cell* **120:** 21-24.

Bhatnagar N, Li X, Padi SK, Zhang Q, Tang MS, Guo B (2010). Downregulation of miR-205 and miR-31 confers resistance to chemotherapy-induced apoptosis in prostate cancer cells. *Cell Death Dis* **1:** e105.

Birkenkamp KU, Coffer PJ (2003). FOXO transcription factors as regulators of immune homeostasis: molecules to die for? *J Immunol* **171:** 1623-1629.

Boehning D, Patterson RL, Sedaghat L, Glebova NO, Kurosaki T, Snyder SH (2003). Cytochrome c binds to inositol (1,4,5) trisphosphate receptors, amplifying calcium-dependent apoptosis. *Nat Cell Biol* **5:** 1051-1061.

Boeri M, Verri C, Conte D, Roz L, Modena P, Facchinetti F *et al* (2011). MicroRNA signatures in tissues and plasma predict development and prognosis of computed tomography detected lung cancer. *Proc Natl Acad Sci U S A* **108:** 3713-3718.

Bolstad BM, Irizarry RA, Astrand M, Speed TP (2003). A comparison of normalization methods for high density oligonucleotide array data based on variance and bias. *Bioinformatics* **19:** 185-193.

Bonci D, Coppola V, Musumeci M, Addario A, Giuffrida R, Memeo L *et al* (2008). The miR-15a-miR-16-1 cluster controls prostate cancer by targeting multiple oncogenic activities. *Nat Med* **14:** 1271-1277.

Boormans JL, Hermans KG, van Leenders GJ, Trapman J, Verhagen PC (2008). An activating mutation in AKT1 in human prostate cancer. *Int J Cancer* **123:** 2725-2726.

Bostwick DG, Brawer MK (1987). Prostatic intra-epithelial neoplasia and early invasion in prostate cancer. *Cancer* **59:** 788-794.

Bourguignon LY, Wong G, Earle C, Krueger K, Spevak CC (2010). Hyaluronan-CD44 interaction promotes c-Src-mediated twist signaling, microRNA-10b expression, and RhoA/RhoC up-regulation, leading to Rho-kinase-associated cytoskeleton activation and breast tumor cell invasion. *J Biol Chem* **285:** 36721-36735.

Bradford MM (1976). A rapid and sensitive method for the quantitation of microgram quantities of protein utilizing the principle of protein-dye binding. *Anal Biochem* **72:** 248-254.

Brase JC, Johannes M, Schlomm T, Falth M, Haese A, Steuber T *et al* (2011). Circulating miRNAs are correlated with tumor progression in prostate cancer. *Int J Cancer* **128:** 608-616.

Brengues M, Teixeira D, Parker R (2005). Movement of eukaryotic mRNAs between polysomes and cytoplasmic processing bodies. *Science* **310:** 486-489.

Brennecke J, Stark A, Russell RB, Cohen SM (2005). Principles of microRNA-target recognition. *PLoS Biol* **3:** e85.

Bresters D, Schipper ME, Reesink HW, Boeser-Nunnink BD, Cuypers HT (1994). The duration of fixation influences the yield of HCV cDNA-PCR products from formalin-fixed, paraffin-embedded liver tissue. *J Virol Methods* **48:** 267-272.

Brooks JD, Weinstein M, Lin X, Sun Y, Pin SS, Bova GS *et al* (1998). CG island methylation changes near the GSTP1 gene in prostatic intraepithelial neoplasia. *Cancer Epidemiol Biomarkers Prev* **7:** 531-536.

Brunet A, Bonni A, Zigmond MJ, Lin MZ, Juo P, Hu LS *et al* (1999). Akt promotes cell survival by phosphorylating and inhibiting a Forkhead transcription factor. *Cell* **96:** 857-868.

Bustin SA, Nolan T (2004). Pitfalls of quantitative real-time reverse-transcription polymerase chain reaction. *J Biomol Tech* **15:** 155-166.

Bustin SA, Benes V, Garson JA, Hellemans J, Huggett J, Kubista M *et al* (2009). The MIQE guidelines: minimum information for publication of quantitative real-time PCR experiments. *Clin Chem* **55:** 611-622.

Calin GA, Dumitru CD, Shimizu M, Bichi R, Zupo S, Noch E *et al* (2002). Frequent deletions and down-regulation of micro- RNA genes miR15 and miR16 at 13q14 in chronic lymphocytic leukemia. *Proc Natl Acad Sci U S A* **99:** 15524-15529.

Calin GA, Sevignani C, Dumitru CD, Hyslop T, Noch E, Yendamuri S *et al* (2004). Human microRNA genes are frequently located at fragile sites and genomic regions involved in cancers. *Proc Natl Acad Sci U S A* **101:** 2999-3004.

Cao P, Deng Z, Wan M, Huang W, Cramer SD, Xu J *et al* (2010). MicroRNA-101 negatively regulates Ezh2 and its expression is modulated by androgen receptor and HIF-1alpha/HIF-1beta. *Mol Cancer* **9:** 108.

Catalona WJ, Richie JP, Ahmann FR, Hudson MA, Scardino PT, Flanigan RC *et al* (1994). Comparison of digital rectal examination and serum prostate specific antigen in the early detection of prostate cancer: results of a multicenter clinical trial of 6,630 men. *J Urol* **151:** 1283-1290.

Catto JW, Miah S, Owen HC, Bryant H, Myers K, Dudziec E *et al* (2009). Distinct microRNA alterations characterize high- and low-grade bladder cancer. *Cancer Res* **69:** 8472-8481.

Cawood R, Chen HH, Carroll F, Bazan-Peregrino M, van Rooijen N, Seymour LW (2009). Use of tissue-specific microRNA to control pathology of wild-type adenovirus without attenuation of its ability to kill cancer cells. *PLoS Pathog* **5:** e1000440.

Chai G, Liu N, Ma J, Li H, Oblinger JL, Prahalad AK *et al* (2010). MicroRNA-10b regulates tumorigenesis in neurofibromatosis type 1. *Cancer Sci* **101:** 1997-2004.

Chan JA, Krichevsky AM, Kosik KS (2005). MicroRNA-21 is an antiapoptotic factor in human glioblastoma cells. *Cancer Res* **65:** 6029-6033.

Chen RS, Song YM, Zhou ZY, Tong T, Li Y, Fu M *et al* (2009). Disruption of xCT inhibits cancer cell metastasis via the caveolin-1/beta-catenin pathway. *Oncogene* **28:** 599-609.

Chen X, Gong J, Zeng H, Chen N, Huang R, Huang Y *et al* (2010a). MicroRNA145 targets BNIP3 and suppresses prostate cancer progression. *Cancer Res* **70:** 2728-2738.

Chen Y, Zhu X, Zhang X, Liu B, Huang L (2010b). Nanoparticles modified with tumor-targeting scFv deliver siRNA and miRNA for cancer therapy. *Mol Ther* **18:** 1650-1656.

Chen Y, Zaman MS, Deng G, Majid S, Saini S, Liu J *et al* (2011). MicroRNAs 221/222 and genistein-mediated regulation of ARHI tumor suppressor gene in prostate cancer. *Cancer Prev Res (Phila)* **4:** 76-86.

Chintharlapalli S, Papineni S, Abdelrahim M, Abudayyeh A, Jutooru I, Chadalapaka G *et al* (2009). Oncogenic microRNA-27a is a target for anticancer agent methyl 2-cyano-3,11-dioxo-18beta-olean-1,12-dien-30-oate in colon cancer cells. *Int J Cancer* **125:** 1965-1974.

Chiosea S, Jelezcova E, Chandran U, Acquafondata M, McHale T, Sobol RW *et al* (2006). Up-regulation of dicer, a component of the MicroRNA machinery, in prostate adenocarcinoma. *Am J Pathol* **169:** 1812-1820.

Chiyomaru T, Tatarano S, Kawakami K, Enokida H, Yoshino H, Nohata N *et al* (2011). SWAP70, actin-binding protein, function as an oncogene targeting tumor-suppressive miR-145 in prostate cancer. *Prostate*.

Clape C, Fritz V, Henriquet C, Apparailly F, Fernandez PL, Iborra F *et al* (2009). miR-143 interferes with ERK5 signaling, and abrogates prostate cancer progression in mice. *PLoS One* **4:** e7542.

Collado M, Medema RH, Garcia-Cao I, Dubuisson ML, Barradas M, Glassford J *et al* (2000). Inhibition of the phosphoinositide 3-kinase pathway induces a senescence-like arrest mediated by p27Kip1. *J Biol Chem* **275:** 21960-21968.

Corbetta S, Vaira V, Guarnieri V, Scillitani A, Eller-Vainicher C, Ferrero S *et al* (2010). Differential expression of microRNAs in human parathyroid carcinomas compared with normal parathyroid tissue. *Endocr Relat Cancer* **17:** 135-146.

Cowland JB, Hother C, Gronbaek K (2007). MicroRNAs and cancer. *APMIS* **115:** 1090-1106.

Crawford M, Batte K, Yu L, Wu X, Nuovo GJ, Marsh CB *et al* (2009). MicroRNA 133B targets pro-survival molecules MCL-1 and BCL2L2 in lung cancer. *Biochem Biophys Res Commun* **388:** 483-489.

Creighton CJ, Fountain MD, Yu Z, Nagaraja AK, Zhu H, Khan M *et al* (2010). Molecular profiling uncovers a p53-associated role for microRNA-31 in inhibiting the proliferation of serous ovarian carcinomas and other cancers. *Cancer Res* **70:** 1906-1915.

Cui J, Rohr LR, Swanson G, Speights VO, Maxwell T, Brothman AR (2001). Hypermethylation of the caveolin-1 gene promoter in prostate cancer. *Prostate* **46:** 249-256.

D'Amico AV, Whittington R, Malkowicz SB, Fondurulia J, Chen MH, Tomaszewski JE *et al* (1998). The combination of preoperative prostate specific antigen and postoperative pathological findings to predict prostate specific antigen outcome in clinically localized prostate cancer. *JUrol* **160:** 2096-2101.

De Guire V, Caron M, Scott N, Menard C, Gaumont-Leclerc MF, Chartrand P *et al* (2010). Designing small multiple-target artificial RNAs. *Nucleic Acids Res* **38:** e140.

de Souza Rocha Simonini P, Breiling A, Gupta N, Malekpour M, Youns M, Omranipour R *et al* (2010). Epigenetically deregulated microRNA-375 is involved in a positive feedback loop with estrogen receptor alpha in breast cancer cells. *Cancer Res* **70:** 9175-9184.

Debernardi S, Skoulakis S, Molloy G, Chaplin T, Dixon-McIver A, Young BD (2007). MicroRNA miR-181a correlates with morphological sub-class of acute myeloid leukaemia and the expression of its target genes in global genome-wide analysis. *Leukemia* **21:** 912-916.

del Peso L, Gonzalez-Garcia M, Page C, Herrera R, Nunez G (1997). Interleukin-3-induced phosphorylation of BAD through the protein kinase Akt. *Science* **278:** 687-689.

DeSouza N, Reiken S, Ondrias K, Yang YM, Matkovich S, Marks AR (2002). Protein kinase A and two phosphatases are components of the inositol 1,4,5-trisphosphate receptor macromolecular signaling complex. *J Biol Chem* **277:** 39397-39400.

DeVere White RW, Vinall RL, Tepper CG, Shi XB (2009). MicroRNAs and their potential for translation in prostate cancer. *Urol Oncol* **27:** 307-311.

DGU (2009). Interdisziplinäre Leitlinie der Qualität S3 zur Früherkennung, Diagnose und Therapie der verschiedenen Stadien des Prostatakarzinoms. Hrsg.: Deutsche Gesellschaft für Urologie (DGU), 1 edn.

Dheda K, Huggett JF, Chang JS, Kim LU, Bustin SA, Johnson MA *et al* (2005). The implications of using an inappropriate reference gene for real-time reverse transcription PCR data normalization. *Anal Biochem* **344:** 141-143.

Di Vizio D, Sotgia F, Williams TM, Hassan GS, Capozza F, Frank PG *et al* (2007). Caveolin-1 is required for the upregulation of fatty acid synthase (FASN), a tumor promoter, during prostate cancer progression. *Cancer Biol Ther* **6:** 1263-1268.

Di Vizio D, Adam RM, Kim J, Kim R, Sotgia F, Williams T *et al* (2008). Caveolin-1 interacts with a lipid raft-associated population of fatty acid synthase. *Cell Cycle* **7:** 2257-2267.

Diamandis EP (2010). Prostate cancer screening with prostate-specific antigen testing: more answers or more confusion? *Clin Chem* **56:** 345-351.

Diaz F, Bourguignon LY (2000). Selective down-regulation of IP(3)receptor subtypes by caspases and calpain during TNF alpha -induced apoptosis of human T-lymphoma cells. *Cell Calcium* **27:** 315-328.

Ding L, Xu Y, Zhang W, Deng Y, Si M, Du Y *et al* (2010). MiR-375 frequently downregulated in gastric cancer inhibits cell proliferation by targeting JAK2. *Cell Res* **20:** 784-793.

Ding Z, Wu CJ, Chu GC, Xiao Y, Ho D, Zhang J *et al* (2011). SMAD4-dependent barrier constrains prostate cancer growth and metastatic progression. *Nature* **470:** 269-273.

Doench JG, Petersen CP, Sharp PA (2003). siRNAs can function as miRNAs. *Genes Dev* **17:** 438-442.

Doench JG, Sharp PA (2004). Specificity of microRNA target selection in translational repression. *Genes Dev* **18:** 504-511.

Dong XY, Chen C, Sun X, Guo P, Vessella RL, Wang RX *et al* (2006). FOXO1A is a candidate for the 13q14 tumor suppressor gene inhibiting androgen receptor signaling in prostate cancer. *Cancer Res* **66:** 6998-7006.

Duijvesz D, Luider T, Bangma CH, Jenster G (2010). Exosomes as Biomarker Treasure Chests for Prostate Cancer. *Eur Urol*.

Dyrskjot L, Ostenfeld MS, Bramsen JB, Silahtaroglu AN, Lamy P, Ramanathan R *et al* (2009). Genomic profiling of microRNAs in bladder cancer: miR-129 is associated with poor outcome and promotes cell death in vitro. *Cancer Res* **69:** 4851-4860.

Ebert MS, Neilson JR, Sharp PA (2007). MicroRNA sponges: competitive inhibitors of small RNAs in mammalian cells. *Nat Methods* **4:** 721-726.

Edmonds MD, Hurst DR, Vaidya KS, Stafford LJ, Chen D, Welch DR (2009). Breast cancer metastasis suppressor 1 coordinately regulates metastasis-associated microRNA expression. *Int J Cancer* **125:** 1778-1785.

Engelman JA, Zhang XL, Lisanti MP (1998). Genes encoding human caveolin-1 and -2 are co-localized to the D7S522 locus (7q31.1), a known fragile site (FRA7G) that is frequently deleted in human cancers. *FEBS Lett* **436:** 403-410.

Enright AJ, John B, Gaul U, Tuschl T, Sander C, Marks DS (2003). MicroRNA targets in Drosophila. *Genome Biol* **5:** R1.

Epstein JI, Allsbrook WC, Jr., Amin MB, Egevad LL (2005). The 2005 International Society of Urological Pathology (ISUP) Consensus Conference on Gleason Grading of Prostatic Carcinoma. *Am J Surg Pathol* **29:** 1228-1242.

Epstein JI (2009). Precursor lesions to prostatic adenocarcinoma. *Virchows Arch* **454:** 1-16.

Epstein RJ (2007). VEGF signaling inhibitors: more pro-apoptotic than anti-angiogenic. *Cancer Metastasis Rev* **26:** 443-452.

Esau CC (2008). Inhibition of microRNA with antisense oligonucleotides. *Methods* **44:** 55-60.

Fan W, Yanase T, Morinaga H, Okabe T, Nomura M, Daitoku H *et al* (2007). Insulin-like growth factor 1/insulin signaling activates androgen signaling through direct interactions of Foxo1 with androgen receptor. *J Biol Chem* **282:** 7329-7338.

Feldman BJ, Feldman D (2001). The development of androgen-independent prostate cancer. *Nat Rev Cancer* **1:** 34-45.

Flavin RJ, Smyth PC, Finn SP, Laios A, O'Toole SA, Barrett C *et al* (2008). Altered eIF6 and Dicer expression is associated with clinicopathological features in ovarian serous carcinoma patients. *Mod Pathol* **21:** 676-684.

Foekens JA, Sieuwerts AM, Smid M, Look MP, de Weerd V, Boersma AW *et al* (2008). Four miRNAs associated with aggressiveness of lymph node-negative, estrogen receptor-positive human breast cancer. *Proc Natl Acad Sci U S A* **105:** 13021-13026.

Fuse M, Nohata N, Kojima S, Sakamoto S, Chiyomaru T, Kawakami K *et al* (2011). Restoration of miR-145 expression suppresses cell proliferation, migration and invasion in prostate cancer by targeting FSCN1. *Int J Oncol* **38:** 1093-1101.

Galardi S, Mercatelli N, Giorda E, Massalini S, Frajese GV, Ciafre SA *et al* (2007). miR-221 and miR-222 expression affects the proliferation potential of human prostate carcinoma cell lines by targeting p27Kip1. *J Biol Chem* **282:** 23716-23724.

Galardi S, Mercatelli N, Farace MG, Ciafre SA (2011). NF-kB and c-Jun induce the expression of the oncogenic miR-221 and miR-222 in prostate carcinoma and glioblastoma cells. *Nucleic Acids Res*.

Gandellini P, Folini M, Longoni N, Pennati M, Binda M, Colecchia M *et al* (2009). miR-205 Exerts tumor-suppressive functions in human prostate through down-regulation of protein kinase Cepsilon. *Cancer Res* **69:** 2287-2295.

Gao H, Ouyang X, Banach-Petrosky WA, Gerald WL, Shen MM, Abate-Shen C (2006). Combinatorial activities of Akt and B-Raf/Erk signaling in a mouse model of androgen-independent prostate cancer. *Proc Natl Acad Sci U S A* **103:** 14477-14482.

Gao LB, Bai P, Pan XM, Jia J, Li LJ, Liang WB *et al* (2011). The association between two polymorphisms in pre-miRNAs and breast cancer risk: a meta-analysis. *Breast Cancer Res Treat* **125:** 571-574.

Geback T, Schulz MM, Koumoutsakos P, Detmar M (2009). TScratch: a novel and simple software tool for automated analysis of monolayer wound healing assays. *Biotechniques* **46:** 265-274.

Gelmann EP (2002). Molecular biology of the androgen receptor. *J Clin Oncol* **20:** 3001-3015.

Glud M, Klausen M, Gniadecki R, Rossing M, Hastrup N, Nielsen FC *et al* (2009). MicroRNA expression in melanocytic nevi: the usefulness of formalin-fixed, paraffin-embedded material for miRNA microarray profiling. *J Invest Dermatol* **129:** 1219-1224.

Glynn JM, Cotter TG, Green DR (1992). Apoptosis induced by Actinomycin D, Camptothecin or Aphidicolin can occur in all phases of the cell cycle. *Biochem Soc Trans* **20:** 84S.

Gokhale A, Kunder R, Goel A, Sarin R, Moiyadi A, Shenoy A *et al* (2010). Distinctive microRNA signature of medulloblastomas associated with the WNT signaling pathway. *J Cancer Res Ther* **6:** 521-529.

Gould ML, Williams G, Nicholson HD (2010). Changes in caveolae, caveolin, and polymerase 1 and transcript release factor (PTRF) expression in prostate cancer progression. *Prostate* **70:** 1609-1621.

Gramantieri L, Fornari F, Callegari E, Sabbioni S, Lanza G, Croce CM *et al* (2008). MicroRNA involvement in hepatocellular carcinoma. *J Cell Mol Med* **12:** 2189-2204.

Gregory CW, He B, Johnson RT, Ford OH, Mohler JL, French FS *et al* (2001a). A mechanism for androgen receptor-mediated prostate cancer recurrence after androgen deprivation therapy. *Cancer Res* **61:** 4315-4319.

Gregory CW, Johnson RT, Jr., Mohler JL, French FS, Wilson EM (2001b). Androgen receptor stabilization in recurrent prostate cancer is associated with hypersensitivity to low androgen. *Cancer Res* **61:** 2892-2898.

Greither T, Grochola LF, Udelnow A, Lautenschlager C, Wurl P, Taubert H (2010). Elevated expression of microRNAs 155, 203, 210 and 222 in pancreatic tumors is associated with poorer survival. *Int J Cancer* **126:** 73-80.

Griffiths-Jones S, Grocock RJ, van Dongen S, Bateman A, Enright AJ (2006). miRBase: microRNA sequences, targets and gene nomenclature. *Nucleic Acids Res* **34:** D140-144.

Guess HA (2001). Benign prostatic hyperplasia and prostate cancer. *Epidemiol Rev* **23:** 152-158.

Guillonneau B, el-Fettouh H, Baumert H, Cathelineau X, Doublet JD, Fromont G *et al* (2003). Laparoscopic radical prostatectomy: oncological evaluation after 1,000 cases a Montsouris Institute. *J Urol* **169:** 1261-1266.

Guo J, Miao Y, Xiao B, Huan R, Jiang Z, Meng D *et al* (2009). Differential expression of microRNA species in human gastric cancer versus non-tumorous tissues. *J Gastroenterol Hepatol* **24:** 652-657.

Guttilla IK, White BA (2009). Coordinate regulation of FOXO1 by miR-27a, miR-96, and miR-182 in breast cancer cells. *J Biol Chem* **284:** 23204-23216.

Ha S, Ruoff R, Kahoud N, Franke TF, Logan SK (2011). Androgen receptor levels are upregulated by Akt in prostate cancer. *Endocr Relat Cancer*.

Haller F, Kulle B, Schwager S, Gunawan B, von Heydebreck A, Sultmann H *et al* (2004). Equivalence test in quantitative reverse transcription polymerase chain reaction: confirmation of reference genes suitable for normalization. *Anal Biochem* **335:** 1-9.

Han J, Lee Y, Yeom KH, Kim YK, Jin H, Kim VN (2004). The Drosha-DGCR8 complex in primary microRNA processing. *Genes Dev* **18:** 3016-3027.

Han M, Partin AW, Zahurak M, Piantadosi S, Epstein JI, Walsh PC (2003). Biochemical (prostate specific antigen) recurrence probability following radical prostatectomy for clinically localized prostate cancer. *J Urol* **169:** 517-523.

Han S, Wei W (2011). Camptothecin induces apoptosis of human retinoblastoma cells via activation of FOXO1. *Curr Eye Res* **36:** 71-77.

Hanahan D, Weinberg RA (2011). Hallmarks of cancer: the next generation. *Cell* **144:** 646-674.

Hao Y, Zhao Y, Zhao X, He C, Pang X, Wu TC *et al* (2011). Improvement of Prostate Cancer Detection by Integrating the PSA Test With miRNA Expression Profiling. *Cancer Invest*.

Harrell FE, Jr. (2001). *Regression modeling strategies: with applications to linear models, logistic regression, and survival analysis*. Springer-Verlag: New York.

Hasemeier B, Christgen M, Kreipe H, Lehmann U (2008). Reliable microRNA profiling in routinely processed formalin-fixed paraffin-embedded breast cancer specimens using fluorescence labelled bead technology. *BMC Biotechnol* **8:** 90.

Heisler LE, Evangelou A, Lew AM, Trachtenberg J, Elsholtz HP, Brown TJ (1997). Androgen-dependent cell cycle arrest and apoptotic death in PC-3 prostatic cell cultures expressing a full-length human androgen receptor. *Mol Cell Endocrinol* **126:** 59-73.

Hemminki K, Czene K (2002). Age specific and attributable risks of familial prostate carcinoma from the family-cancer database. *Cancer* **95:** 1346-1353.

Hirota J, Furuichi T, Mikoshiba K (1999). Inositol 1,4,5-trisphosphate receptor type 1 is a substrate for caspase-3 and is cleaved during apoptosis in a caspase-3-dependent manner. *J Biol Chem* **274:** 34433-34437.

Hofmann MH, Heinrich J, Radziwill G, Moelling K (2009). A short hairpin DNA analogous to miR-125b inhibits C-Raf expression, proliferation, and survival of breast cancer cells. *Mol Cancer Res* **7:** 1635-1644.

Hu G, Chen D, Li X, Yang K, Wang H, Wu W (2010a). miR-133b regulates the MET proto-oncogene and inhibits the growth of colorectal cancer cells in vitro and in vivo. *Cancer Biol Ther* **10:** 190-197.

Hu L, Ibrahim S, Liu C, Skaar J, Pagano M, Karpatkin S (2009a). Thrombin induces tumor cell cycle activation and spontaneous growth by down-regulation of p27Kip1, in association with the up-regulation of Skp2 and MiR-222. *Cancer Res* **69:** 3374-3381.

Hu X, Macdonald DM, Huettner PC, Feng Z, El Naqa IM, Schwarz JK *et al* (2009b). A miR-200 microRNA cluster as prognostic marker in advanced ovarian cancer. *Gynecol Oncol* **114:** 457-464.

Hu X, Schwarz JK, Lewis JS, Jr., Huettner PC, Rader JS, Deasy JO *et al* (2010b). A microRNA expression signature for cervical cancer prognosis. *Cancer Res* **70:** 1441-1448.

Hu Y, Correa AM, Hoque A, Guan B, Ye F, Huang J *et al* (2011). Prognostic significance of differentially expressed miRNAs in esophageal cancer. *Int J Cancer* **128:** 132-143.

Hu Z, Chen X, Zhao Y, Tian T, Jin G, Shu Y *et al* (2010c). Serum microRNA signatures identified in a genome-wide serum microRNA expression profiling predict survival of non-small-cell lung cancer. *J Clin Oncol* **28:** 1721-1726.

Huang H, Muddiman DC, Tindall DJ (2004). Androgens negatively regulate forkhead transcription factor FKHR (FOXO1) through a proteolytic mechanism in prostate cancer cells. *J Biol Chem* **279:** 13866-13877.

Huang H, Regan KM, Lou Z, Chen J, Tindall DJ (2006). CDK2-dependent phosphorylation of FOXO1 as an apoptotic response to DNA damage. *Science* **314:** 294-297.

Huang Q, Gumireddy K, Schrier M, le Sage C, Nagel R, Nair S *et al* (2008). The microRNAs miR-373 and miR-520c promote tumour invasion and metastasis. *Nat Cell Biol* **10:** 202-210.

Hui AB, Shi W, Boutros PC, Miller N, Pintilie M, Fyles T *et al* (2009). Robust global micro-RNA profiling with formalin-fixed paraffin-embedded breast cancer tissues. *Lab Invest* **89:** 597-606.

Hui AB, Lenarduzzi M, Krushel T, Waldron L, Pintilie M, Shi W *et al* (2010). Comprehensive MicroRNA profiling for head and neck squamous cell carcinomas. *Clin Cancer Res* **16:** 1129-1139.

Humphreys DT, Westman BJ, Martin DI, Preiss T (2005). MicroRNAs control translation initiation by inhibiting eukaryotic initiation factor 4E/cap and poly(A) tail function. *Proc Natl Acad Sci U S A* **102:** 16961-16966.

Huo J, Xu S, Guo K, Zeng Q, Lam KP (2009). Genetic deletion of faim reveals its role in modulating c-FLIP expression during CD95-mediated apoptosis of lymphocytes and hepatocytes. *Cell Death Differ* **16:** 1062-1070.

Huo J, Xu S, Lam KP (2010). Fas apoptosis inhibitory molecule regulates T cell receptor-mediated apoptosis of thymocytes by modulating Akt activation and Nur77 expression. *J Biol Chem* **285:** 11827-11835.

Hutvagner G, Zamore PD (2002). A microRNA in a multiple-turnover RNAi enzyme complex. *Science* **297:** 2056-2060.

Huynh C, Segura MF, Gaziel-Sovran A, Menendez S, Darvishian F, Chiriboga L *et al* (2010). Efficient in vivo microRNA targeting of liver metastasis. *Oncogene*.

Ichimi T, Enokida H, Okuno Y, Kunimoto R, Chiyomaru T, Kawamoto K *et al* (2009). Identification of novel microRNA targets based on microRNA signatures in bladder cancer. *Int J Cancer* **125:** 345-352.

Idogawa M, Sasaki Y, Suzuki H, Mita H, Imai K, Shinomura Y *et al* (2009). A single recombinant adenovirus expressing p53 and p21-targeting artificial microRNAs efficiently induces apoptosis in human cancer cells. *Clin Cancer Res* **15:** 3725-3732.

Iorio MV, Ferracin M, Liu CG, Veronese A, Spizzo R, Sabbioni S *et al* (2005). MicroRNA gene expression deregulation in human breast cancer. *Cancer Res* **65:** 7065-7070.

Irvin-Wilson CV, Chaudhuri G (2005). Alternative initiation and splicing in dicer gene expression in human breast cells. *Breast Cancer Res* **7:** R563-569.

Isbarn H, Karakiewicz PI, Walz J, Ahyai SA, Steuber T, Haese A *et al* (2009). External Validation of a Preoperative Nomogram for Prediction of the Risk of Recurrence After Radical Prostatectomy. *IntJRadiatOncolBiolPhys*.

Jennbacken K, Vallbo C, Wang W, Damber JE (2005). Expression of vascular endothelial growth factor C (VEGF-C) and VEGF receptor-3 in human prostate cancer is associated with regional lymph node metastasis. *Prostate* **65:** 110-116.

Jiang J, Lee EJ, Gusev Y, Schmittgen TD (2005). Real-time expression profiling of microRNA precursors in human cancer cell lines. *Nucleic Acids Res* **33:** 5394-5403.

Josson S, Sung SY, Lao K, Chung LW, Johnstone PA (2008). Radiation modulation of microRNA in prostate cancer cell lines. *Prostate* **68:** 1599-1606.

Jung M, Schaefer A, Steiner I, Kempkensteffen C, Stephan C, Erbersdobler A *et al* (2010). Robust microRNA stability in degraded RNA preparations from human tissue and cell samples. *Clin Chem* **56:** 998-1006.

Jung-Hynes B, Nihal M, Zhong W, Ahmad N (2009). Role of sirtuin histone deacetylase SIRT1 in prostate cancer. A target for prostate cancer management via its inhibition? *J Biol Chem* **284:** 3823-3832.

Kano M, Seki N, Kikkawa N, Fujimura L, Hoshino I, Akutsu Y *et al* (2010). miR-145, miR-133a and miR-133b: Tumor suppressive miRNAs target FSCN1 in esophageal squamous cell carcinoma. *Int J Cancer*.

Karam JA, Lotan Y, Roehrborn CG, Ashfaq R, Karakiewicz PI, Shariat SF (2007). Caveolin-1 overexpression is associated with aggressive prostate cancer recurrence. *Prostate* **67:** 614-622.

Karube Y, Tanaka H, Osada H, Tomida S, Tatematsu Y, Yanagisawa K *et al* (2005). Reduced expression of Dicer associated with poor prognosis in lung cancer patients. *Cancer Sci* **96:** 111-115.

Kaufmann E, Knochel W (1996). Five years on the wings of fork head. *Mech Dev* **57:** 3-20.

Ke XS, Qu Y, Rostad K, Li WC, Lin B, Halvorsen OJ *et al* (2009). Genome-wide profiling of histone h3 lysine 4 and lysine 27 trimethylation reveals an epigenetic signature in prostate carcinogenesis. *PLoS One* **4:** e4687.

Kedde M, Strasser MJ, Boldajipour B, Oude Vrielink JA, Slanchev K, le Sage C *et al* (2007). RNA-binding protein Dnd1 inhibits microRNA access to target mRNA. *Cell* **131:** 1273-1286.

Khan MT, Wagner L, 2nd, Yule DI, Bhanumathy C, Joseph SK (2006). Akt kinase phosphorylation of inositol 1,4,5-trisphosphate receptors. *J Biol Chem* **281:** 3731-3737.

Kim JH, Dhanasekaran SM, Mehra R, Tomlins SA, Gu W, Yu J *et al* (2007). Integrative analysis of genomic aberrations associated with prostate cancer progression. *Cancer Res* **67:** 8229-8239.

Kim SJ, Winter K, Nian C, Tsuneoka M, Koda Y, McIntosh CH (2005). Glucose-dependent insulinotropic polypeptide (GIP) stimulation of pancreatic beta-cell survival is dependent upon phosphatidylinositol 3-kinase (PI3K)/protein kinase B (PKB) signaling, inactivation of the forkhead transcription factor Foxo1, and down-regulation of bax expression. *J Biol Chem* **280:** 22297-22307.

Kojima K, Fujita Y, Nozawa Y, Deguchi T, Ito M (2010). MiR-34a attenuates paclitaxel-resistance of hormone-refractory prostate cancer PC3 cells through direct and indirect mechanisms. *Prostate* **70:** 1501-1512.

Kops GJ, Medema RH, Glassford J, Essers MA, Dijkers PF, Coffer PJ *et al* (2002). Control of cell cycle exit and entry by protein kinase B-regulated forkhead transcription factors. *Mol Cell Biol* **22:** 2025-2036.

Kota J, Chivukula RR, O'Donnell KA, Wentzel EA, Montgomery CL, Hwang HW *et al* (2009). Therapeutic microRNA delivery suppresses tumorigenesis in a murine liver cancer model. *Cell* **137:** 1005-1017.

Krek A, Grun D, Poy MN, Wolf R, Rosenberg L, Epstein EJ *et al* (2005). Combinatorial microRNA target predictions. *Nat Genet* **37:** 495-500.

Kuhn S, Johnson SL, Furness DN, Chen J, Ingham N, Hilton JM *et al* (2011). miR-96 regulates the progression of differentiation in mammalian cochlear inner and outer hair cells. *Proc Natl Acad Sci U S A* **108:** 2355-2360.

Kumar MS, Pester RE, Chen CY, Lane K, Chin C, Lu J *et al* (2009). Dicer1 functions as a haploinsufficient tumor suppressor. *Genes Dev* **23:** 2700-2704.

Kumar-Sinha C, Ignatoski KW, Lippman ME, Ethier SP, Chinnaiyan AM (2003). Transcriptome analysis of HER2 reveals a molecular connection to fatty acid synthesis. *Cancer Res* **63:** 132-139.

Kutter C, Svoboda P (2008). miRNA, siRNA, piRNA: Knowns of the unknown. *RNA Biol* **5:** 181-188.

Ladeiro Y, Couchy G, Balabaud C, Bioulac-Sage P, Pelletier L, Rebouissou S *et al* (2008). MicroRNA profiling in hepatocellular tumors is associated with clinical features and oncogene/tumor suppressor gene mutations. *Hepatology* **47:** 1955-1963.

Laemmli UK (1970). Cleavage of structural proteins during the assembly of the head of bacteriophage T4. *Nature* **227:** 680-685.

Lagos-Quintana M, Rauhut R, Lendeckel W, Tuschl T (2001). Identification of novel genes coding for small expressed RNAs. *Science* **294:** 853-858.

Langeberg WJ, Tahir SA, Feng Z, Kwon EM, Ostrander EA, Thompson TC *et al* (2010). Association of caveolin-1 and -2 genetic variants and post-treatment serum caveolin-1 with prostate cancer risk and outcomes. *Prostate* **70:** 1020-1035.

Lapointe J, Li C, Giacomini CP, Salari K, Huang S, Wang P *et al* (2007). Genomic profiling reveals alternative genetic pathways of prostate tumorigenesis. *Cancer Res* **67:** 8504-8510.

Lau NC, Lim LP, Weinstein EG, Bartel DP (2001). An abundant class of tiny RNAs with probable regulatory roles in Caenorhabditis elegans. *Science* **294:** 858-862.

Lee CY, Rennie PS, Jia WW (2009a). MicroRNA regulation of oncolytic herpes simplex virus-1 for selective killing of prostate cancer cells. *Clin Cancer Res* **15:** 5126-5135.

Lee MY, Moon JS, Park SW, Koh YK, Ahn YH, Kim KS (2009b). KLF5 enhances SREBP-1 action in androgen-dependent induction of fatty acid synthase in prostate cancer cells. *Biochem J* **417:** 313-322.

Lee RC, Feinbaum RL, Ambros V (1993). The C. elegans heterochronic gene lin-4 encodes small RNAs with antisense complementarity to lin-14. *Cell* **75:** 843-854.

Lee RC, Ambros V (2001). An extensive class of small RNAs in Caenorhabditis elegans. *Science* **294:** 862-864.

Lee SH, Poulogiannis G, Pyne S, Jia S, Zou L, Signoretti S *et al* (2010). A constitutively activated form of the p110beta isoform of PI3-kinase induces prostatic intraepithelial neoplasia in mice. *Proc Natl Acad Sci U S A* **107:** 11002-11007.

Lee WH, Morton RA, Epstein JI, Brooks JD, Campbell PA, Bova GS *et al* (1994). Cytidine methylation of regulatory sequences near the pi-class glutathione S-transferase gene accompanies human prostatic carcinogenesis. *Proc Natl Acad Sci U S A* **91:** 11733-11737.

Lee Y, Jeon K, Lee JT, Kim S, Kim VN (2002). MicroRNA maturation: stepwise processing and subcellular localization. *EMBO J* **21:** 4663-4670.

Lee Y, Ahn C, Han J, Choi H, Kim J, Yim J *et al* (2003). The nuclear RNase III Drosha initiates microRNA processing. *Nature* **425:** 415-419.

Lee Y, Kim M, Han J, Yeom KH, Lee S, Baek SH *et al* (2004). MicroRNA genes are transcribed by RNA polymerase II. *EMBO J* **23:** 4051-4060.

Lein M, Stibane I, Mansour R, Hege C, Roigas J, Wille A *et al* (2006). Complications, urinary continence, and oncologic outcome of 1000 laparoscopic transperitoneal radical prostatectomies-experience at the Charite Hospital Berlin, Campus Mitte. *Eur Urol* **50:** 1278-1282; discussion 1283-1274.

Leite KR, Sousa-Canavez JM, Reis ST, Tomiyama AH, Camara-Lopes LH, Sanudo A *et al* (2009). Change in expression of miR-let7c, miR-100, and miR-218 from high grade localized prostate cancer to metastasis. *Urol Oncol*.

Leite KR, Tomiyama A, Reis ST, Sousa-Canavez JM, Sanudo A, Dall'oglio MF *et al* (2011). MicroRNA-100 Expression is Independently Related to Biochemical Recurrence of Prostate Cancer. *J Urol* **185:** 1118-1122.

Leite MF, Thrower EC, Echevarria W, Koulen P, Hirata K, Bennett AM *et al* (2003). Nuclear and cytosolic calcium are regulated independently. *Proc Natl Acad Sci U S A* **100:** 2975-2980.

Lewis BP, Shih IH, Jones-Rhoades MW, Bartel DP, Burge CB (2003). Prediction of mammalian microRNA targets. *Cell* **115:** 787-798.

Lewis BP, Burge CB, Bartel DP (2005). Conserved seed pairing, often flanked by adenosines, indicates that thousands of human genes are microRNA targets. *Cell* **120:** 15-20.

Lewis MA, Quint E, Glazier AM, Fuchs H, De Angelis MH, Langford C *et al* (2009). An ENU-induced mutation of miR-96 associated with progressive hearing loss in mice. *Nat Genet* **41:** 614-618.

Li G, Wu Z, Peng Y, Liu X, Lu J, Wang L *et al* (2010a). MicroRNA-10b induced by Epstein-Barr virus-encoded latent membrane protein-1 promotes the metastasis of human nasopharyngeal carcinoma cells. *Cancer Lett* **299:** 29-36.

Li H, Kloosterman W, Fekete DM (2010b). MicroRNA-183 family members regulate sensorineural fates in the inner ear. *J Neurosci* **30:** 3254-3263.

Li L, Yang G, Ebara S, Satoh T, Nasu Y, Timme TL *et al* (2001). Caveolin-1 mediates testosterone-stimulated survival/clonal growth and promotes metastatic activities in prostate cancer cells. *Cancer Res* **61:** 4386-4392.

Li L, Ren C, Yang G, Goltsov AA, Tabata K, Thompson TC (2009a). Caveolin-1 promotes autoregulatory, Akt-mediated induction of cancer-promoting growth factors in prostate cancer cells. *Mol Cancer Res* **7:** 1781-1791.

Li P, Lee H, Guo S, Unterman TG, Jenster G, Bai W (2003). AKT-independent protection of prostate cancer cells from apoptosis mediated through complex formation between the androgen receptor and FKHR. *Mol Cell Biol* **23:** 104-118.

Li R, Erdamar S, Dai H, Wheeler TM, Frolov A, Scardino PT *et al* (2007). Forkhead protein FKHR and its phosphorylated form p-FKHR in human prostate cancer. *Hum Pathol* **38:** 1501-1507.

Li T, Li D, Sha J, Sun P, Huang Y (2009b). MicroRNA-21 directly targets MARCKS and promotes apoptosis resistance and invasion in prostate cancer cells. *Biochem Biophys Res Commun* **383:** 280-285.

Li X, Zhang Y, Ding J, Wu K, Fan D (2010c). Survival prediction of gastric cancer by a seven-microRNA signature. *Gut* **59:** 579-585.

Lim LP, Lau NC, Garrett-Engele P, Grimson A, Schelter JM, Castle J *et al* (2005). Microarray analysis shows that some microRNAs downregulate large numbers of target mRNAs. *Nature* **433:** 769-773.

Lin H, Dai T, Xiong H, Zhao X, Chen X, Yu C *et al* (2010). Unregulated miR-96 induces cell proliferation in human breast cancer by downregulating transcriptional factor FOXO3a. *PLoS One* **5:** e15797.

Lin SL, Chiang A, Chang D, Ying SY (2008). Loss of mir-146a function in hormone-refractory prostate cancer. *RNA* **14:** 417-424.

Lin X, Tascilar M, Lee WH, Vles WJ, Lee BH, Veeraswamy R *et al* (2001). GSTP1 CpG island hypermethylation is responsible for the absence of GSTP1 expression in human prostate cancer cells. *Am J Pathol* **159:** 1815-1826.

Liu C, Kelnar K, Liu B, Chen X, Calhoun-Davis T, Li H *et al* (2011). The microRNA miR-34a inhibits prostate cancer stem cells and metastasis by directly repressing CD44. *Nat Med* **17:** 211-215.

Liu J, Valencia-Sanchez MA, Hannon GJ, Parker R (2005). MicroRNA-dependent localization of targeted mRNAs to mammalian P-bodies. *Nat Cell Biol* **7:** 719-723.

Liu P, Kao TP, Huang H (2008a). CDK1 promotes cell proliferation and survival via phosphorylation and inhibition of FOXO1 transcription factor. *Oncogene* **27:** 4733-4744.

Liu P, Li S, Gan L, Kao TP, Huang H (2008b). A transcription-independent function of FOXO1 in inhibition of androgen-independent activation of the androgen receptor in prostate cancer cells. *Cancer Res* **68:** 10290-10299.

Liu XQ, Song WJ, Sun TM, Zhang PZ, Wang J (2010). Targeted Delivery of Antisense Inhibitor of miRNA for Antiangiogenesis Therapy Using cRGD-Functionalized Nanoparticles. *Mol Pharm*.

Locke JA, Guns ES, Lubik AA, Adomat HH, Hendy SC, Wood CA *et al* (2008). Androgen levels increase by intratumoral de novo steroidogenesis during progression of castration-resistant prostate cancer. *Cancer Res* **68:** 6407-6415.

Lodes MJ, Caraballo M, Suciu D, Munro S, Kumar A, Anderson B (2009). Detection of cancer with serum miRNAs on an oligonucleotide microarray. *PLoS One* **4:** e6229.

Lodygin D, Tarasov V, Epanchintsev A, Berking C, Knyazeva T, Korner H *et al* (2008). Inactivation of miR-34a by aberrant CpG methylation in multiple types of cancer. *Cell Cycle* **7:** 2591-2600.

Loscher CJ, Hokamp K, Kenna PF, Ivens AC, Humphries P, Palfi A *et al* (2007). Altered retinal microRNA expression profile in a mouse model of retinitis pigmentosa. *Genome Biol* **8:** R248.

Lu J, Getz G, Miska EA, Alvarez-Saavedra E, Lamb J, Peck D *et al* (2005). MicroRNA expression profiles classify human cancers. *Nature* **435:** 834-838.

Lu ML, Schneider MC, Zheng Y, Zhang X, Richie JP (2001). Caveolin-1 interacts with androgen receptor. A positive modulator of androgen receptor mediated transactivation. *J Biol Chem* **276:** 13442-13451.

Lu Z, Liu M, Stribinskis V, Klinge CM, Ramos KS, Colburn NH *et al* (2008). MicroRNA-21 promotes cell transformation by targeting the programmed cell death 4 gene. *Oncogene* **27:** 4373-4379.

Ma L, Teruya-Feldstein J, Weinberg RA (2007). Tumour invasion and metastasis initiated by microRNA-10b in breast cancer. *Nature* **449:** 682-688.

Ma L, Reinhardt F, Pan E, Soutschek J, Bhat B, Marcusson EG *et al* (2010). Therapeutic silencing of miR-10b inhibits metastasis in a mouse mammary tumor model. *Nat Biotechnol* **28:** 341-347.

Ma Q, Fu W, Li P, Nicosia SV, Jenster G, Zhang X *et al* (2009). FoxO1 mediates PTEN suppression of androgen receptor N- and C-terminal interactions and coactivator recruitment. *Mol Endocrinol* **23:** 213-225.

Macabeo-Ong M, Ginzinger DG, Dekker N, McMillan A, Regezi JA, Wong DT *et al* (2002). Effect of duration of fixation on quantitative reverse transcription polymerase chain reaction analyses. *Mod Pathol* **15:** 979-987.

Machida S, Spangenburg EE, Booth FW (2003). Forkhead transcription factor FoxO1 transduces insulin-like growth factor's signal to p27Kip1 in primary skeletal muscle satellite cells. *J Cell Physiol* **196:** 523-531.

Malathi K, Li X, Krizanova O, Ondrias K, Sperber K, Ablamunits V *et al* (2005). Cdc2/cyclin B1 interacts with and modulates inositol 1,4,5-trisphosphate receptor (type 1) functions. *J Immunol* **175:** 6205-6210.

Marivoet S, Van Dijck P, Verhoeven G, Heyns W (1992). Interaction of the 90-kDa heat shock protein with native and in vitro translated androgen receptor and receptor fragments. *Mol Cell Endocrinol* **88:** 165-174.

Mathe EA, Nguyen GH, Bowman ED, Zhao Y, Budhu A, Schetter AJ *et al* (2009). MicroRNA expression in squamous cell carcinoma and adenocarcinoma of the esophagus: associations with survival. *Clin Cancer Res* **15:** 6192-6200.

Matsuzaki H, Daitoku H, Hatta M, Tanaka K, Fukamizu A (2003). Insulin-induced phosphorylation of FKHR (Foxo1) targets to proteasomal degradation. *Proc Natl Acad Sci U S A* **100:** 11285-11290.

Mattie MD, Benz CC, Bowers J, Sensinger K, Wong L, Scott GK *et al* (2006). Optimized high-throughput microRNA expression profiling provides novel biomarker assessment of clinical prostate and breast cancer biopsies. *Mol Cancer* **5:** 24.

McNeal JE (1969). Origin and development of carcinoma in the prostate. *Cancer* **23:** 24-34.

McNeal JE, Bostwick DG (1986). Intraductal dysplasia: a premalignant lesion of the prostate. *Hum Pathol* **17:** 64-71.

McNeal JE, Redwine EA, Freiha FS, Stamey TA (1988). Zonal distribution of prostatic adenocarcinoma. Correlation with histologic pattern and direction of spread. *Am J Surg Pathol* **12:** 897-906.

McShane LM, Altman DG, Sauerbrei W, Taube SE, Gion M, Clark GM (2005). REporting recommendations for tumor MARKer prognostic studies (REMARK). *Nat Clin Pract Urol* **2:** 416-422.

Mees ST, Schleicher C, Mardin WA, Senninger N, Colombo-Benkmann M, Haier J (2009). Analyzing miRNAs in Ductal Adenocarcinomas of the Pancreas. *J Surg Res*.

Meiers I, Shanks JH, Bostwick DG (2007). Glutathione S-transferase pi (GSTP1) hypermethylation in prostate cancer: review 2007. *Pathology* **39:** 299-304.

Meister G, Landthaler M, Patkaniowska A, Dorsett Y, Teng G, Tuschl T (2004). Human Argonaute2 mediates RNA cleavage targeted by miRNAs and siRNAs. *Mol Cell* **15:** 185-197.

Melo SA, Moutinho C, Ropero S, Calin GA, Rossi S, Spizzo R *et al* (2010). A genetic defect in exportin-5 traps precursor microRNAs in the nucleus of cancer cells. *Cancer Cell* **18:** 303-315.

Mencia A, Modamio-Hoybjor S, Redshaw N, Morin M, Mayo-Merino F, Olavarrieta L *et al* (2009). Mutations in the seed region of human miR-96 are responsible for nonsyndromic progressive hearing loss. *Nat Genet* **41:** 609-613.

Mendes CC, Gomes DA, Thompson M, Souto NC, Goes TS, Goes AM *et al* (2005). The type III inositol 1,4,5-trisphosphate receptor preferentially transmits apoptotic Ca2+ signals into mitochondria. *J Biol Chem* **280:** 40892-40900.

Menendez JA, Lupu R (2007). Fatty acid synthase and the lipogenic phenotype in cancer pathogenesis. *Nat Rev Cancer* **7:** 763-777.

Mercatelli N, Coppola V, Bonci D, Miele F, Costantini A, Guadagnoli M *et al* (2008). The inhibition of the highly expressed miR-221 and miR-222 impairs the growth of prostate carcinoma xenografts in mice. *PLoS One* **3:** e4029.

Meyer SU, Pfaffl MW, Ulbrich SE (2010). Normalization strategies for microRNA profiling experiments: a 'normal' way to a hidden layer of complexity? *Biotechnol Lett* **32:** 1777-1788.

Michael A, Bajracharya SD, Yuen PS, Zhou H, Star RA, Illei GG *et al* (2010). Exosomes from human saliva as a source of microRNA biomarkers. *Oral Dis* **16:** 34-38.

Michael MZ, SM OC, van Holst Pellekaan NG, Young GP, James RJ (2003). Reduced accumulation of specific microRNAs in colorectal neoplasia. *Mol Cancer Res* **1:** 882-891.

Migita T, Ruiz S, Fornari A, Fiorentino M, Priolo C, Zadra G *et al* (2009). Fatty acid synthase: a metabolic enzyme and candidate oncogene in prostate cancer. *J Natl Cancer Inst* **101:** 519-532.

Mitchell PS, Parkin RK, Kroh EM, Fritz BR, Wyman SK, Pogosova-Agadjanyan EL *et al* (2008). Circulating microRNAs as stable blood-based markers for cancer detection. *Proc Natl Acad Sci U S A* **105:** 10513-10518.

Modur V, Nagarajan R, Evers BM, Milbrandt J (2002). FOXO proteins regulate tumor necrosis factor-related apoptosis inducing ligand expression. Implications for PTEN mutation in prostate cancer. *J Biol Chem* **277:** 47928-47937.

Molnar V, Tamasi V, Bakos B, Wiener Z, Falus A (2008). Changes in miRNA expression in solid tumors: an miRNA profiling in melanomas. *Semin Cancer Biol* **18:** 111-122.

Moltzahn F, Olshen AB, Baehner L, Peek A, Fong L, Stoppler H *et al* (2011). Microfluidic-based multiplex qRT-PCR identifies diagnostic and prognostic microRNA signatures in the sera of prostate cancer patients. *Cancer Res* **71:** 550-560.

Morgan TM, Koreckij TD, Corey E (2009). Targeted therapy for advanced prostate cancer: inhibition of the PI3K/Akt/mTOR pathway. *Curr Cancer Drug Targets* **9:** 237-249.

Motta MC, Divecha N, Lemieux M, Kamel C, Chen D, Gu W *et al* (2004). Mammalian SIRT1 represses forkhead transcription factors. *Cell* **116:** 551-563.

Myatt SS, Wang J, Monteiro LJ, Christian M, Ho KK, Fusi L *et al* (2010). Definition of microRNAs that repress expression of the tumor suppressor gene FOXO1 in endometrial cancer. *Cancer Res* **70:** 367-377.

Nair V (2008). Retrovirus-induced oncogenesis and safety of retroviral vectors. *Curr Opin Mol Ther* **10:** 431-438.

Nakayama T, Hattori M, Uchida K, Nakamura T, Tateishi Y, Bannai H *et al* (2004). The regulatory domain of the inositol 1,4,5-trisphosphate receptor is necessary to keep the channel domain closed: possible physiological significance of specific cleavage by caspase 3. *Biochem J* **377:** 299-307.

Nam EJ, Yoon H, Kim SW, Kim H, Kim YT, Kim JH *et al* (2008). MicroRNA expression profiles in serous ovarian carcinoma. *Clin Cancer Res* **14:** 2690-2695.

Nasu Y, Timme TL, Yang G, Bangma CH, Li L, Ren C *et al* (1998). Suppression of caveolin expression induces androgen sensitivity in metastatic androgen-insensitive mouse prostate cancer cells. *Nat Med* **4:** 1062-1064.

Navarro A, Diaz T, Martinez A, Gaya A, Pons A, Gel B *et al* (2009). Regulation of JAK2 by miR-135a: prognostic impact in classic Hodgkin lymphoma. *Blood* **114:** 2945-2951.

Navon R, Wang H, Steinfeld I, Tsalenko A, Ben-Dor A, Yakhini Z (2009). Novel rank-based statistical methods reveal microRNAs with differential expression in multiple cancer types. *PLoS One* **4:** e8003.

Noonan EJ, Place RF, Pookot D, Basak S, Whitson JM, Hirata H *et al* (2009). miR-449a targets HDAC-1 and induces growth arrest in prostate cancer. *Oncogene* **28:** 1714-1724.

Nupponen NN, Kakkola L, Koivisto P, Visakorpi T (1998). Genetic alterations in hormone-refractory recurrent prostate carcinomas. *Am J Pathol* **153:** 141-148.

Nwosu V, Carpten J, Trent JM, Sheridan R (2001). Heterogeneity of genetic alterations in prostate cancer: evidence of the complex nature of the disease. *Hum Mol Genet* **10:** 2313-2318.

Oberli A, Popovici V, Delorenzi M, Baltzer A, Antonov J, Matthey S *et al* (2008). Expression profiling with RNA from formalin-fixed, paraffin-embedded material. *BMC Med Genomics* **1:** 9.

Ohl F, Jung M, Xu C, Stephan C, Rabien A, Burkhardt M *et al* (2005). Gene expression studies in prostate cancer tissue: which reference gene should be selected for normalization? *J Mol Med* **83:** 1014-1024.

Olsen PH, Ambros V (1999). The lin-4 regulatory RNA controls developmental timing in Caenorhabditis elegans by blocking LIN-14 protein synthesis after the initiation of translation. *Dev Biol* **216:** 671-680.

Ozen M, Creighton CJ, Ozdemir M, Ittmann M (2008). Widespread deregulation of microRNA expression in human prostate cancer. *Oncogene* **27:** 1788-1793.

Pal S, Baiocchi RA, Byrd JC, Grever MR, Jacob ST, Sif S (2007). Low levels of miR-92b/96 induce PRMT5 translation and H3R8/H4R3 methylation in mantle cell lymphoma. *EMBO J* **26:** 3558-3569.

Partin AW, Kattan MW, Subong EN, Walsh PC, Wojno KJ, Oesterling JE *et al* (1997). Combination of prostate-specific antigen, clinical stage, and Gleason score to predict pathological stage of localized prostate cancer. A multi-institutional update. *JAMA* **277:** 1445-1451.

Patel AR, Klein EA (2009). Risk factors for prostate cancer. *Nat Clin Pract Urol* **6:** 87-95.

Patron Arcila JP (2010). Indentification and characterization of miR-133b as a novel regulator of death receptor mediated apoptosis. PhD thesis, Humboldt Universität zu Berlin, Berlin.

Peltier HJ, Latham GJ (2008). Normalization of microRNA expression levels in quantitative RT-PCR assays: identification of suitable reference RNA targets in normal and cancerous human solid tissues. *RNA* **14:** 844-852.

Perner S, Demichelis F, Beroukhim R, Schmidt FH, Mosquera JM, Setlur S *et al* (2006). TMPRSS2:ERG fusion-associated deletions provide insight into the heterogeneity of prostate cancer. *Cancer Res* **66:** 8337-8341.

Petersen CP, Bordeleau ME, Pelletier J, Sharp PA (2006). Short RNAs repress translation after initiation in mammalian cells. *Mol Cell* **21:** 533-542.

Pillai RS, Artus CG, Filipowicz W (2004). Tethering of human Ago proteins to mRNA mimics the miRNA-mediated repression of protein synthesis. *RNA* **10:** 1518-1525.

Pillai RS, Bhattacharyya SN, Artus CG, Zoller T, Cougot N, Basyuk E *et al* (2005). Inhibition of translational initiation by Let-7 MicroRNA in human cells. *Science* **309:** 1573-1576.

Pillai RS, Bhattacharyya SN, Filipowicz W (2007). Repression of protein synthesis by miRNAs: how many mechanisms? *Trends Cell Biol* **17:** 118-126.

Place RF, Li LC, Pookot D, Noonan EJ, Dahiya R (2008). MicroRNA-373 induces expression of genes with complementary promoter sequences. *Proc Natl Acad Sci U S A* **105:** 1608-1613.

Poliseno L, Salmena L, Riccardi L, Fornari A, Song MS, Hobbs RM *et al* (2010). Identification of the miR-106b~25 microRNA cluster as a proto-oncogenic PTEN-targeting intron that cooperates with its host gene MCM7 in transformation. *Sci Signal* **3:** ra29.

Pons A, Nomdedeu B, Navarro A, Gaya A, Gel B, Diaz T *et al* (2009). Hematopoiesis-related microRNA expression in myelodysplastic syndromes. *Leuk Lymphoma* **50:** 1854-1859.

Porkka KP, Pfeiffer MJ, Waltering KK, Vessella RL, Tammela TL, Visakorpi T (2007). MicroRNA expression profiling in prostate cancer. *Cancer Res* **67:** 6130-6135.

Pound CR, Partin AW, Eisenberger MA, Chan DW, Pearson JD, Walsh PC (1999). Natural history of progression after PSA elevation following radical prostatectomy. *JAMA* **281:** 1591-1597.

Pradervand S, Weber J, Thomas J, Bueno M, Wirapati P, Lefort K *et al* (2009). Impact of normalization on miRNA microarray expression profiling. *RNA* **15:** 493-501.

Prowatke I, Devens F, Benner A, Grone EF, Mertens D, Grone HJ *et al* (2007). Expression analysis of imbalanced genes in prostate carcinoma using tissue microarrays. *Br J Cancer* **96:** 82-88.

Prueitt RL, Yi M, Hudson RS, Wallace TA, Howe TM, Yfantis HG *et al* (2008). Expression of microRNAs and protein-coding genes associated with perineural invasion in prostate cancer. *Prostate* **68:** 1152-1164.

Qin W, Zhao B, Shi Y, Yao C, Jin L, Jin Y (2009). BMPRII is a direct target of miR-21. *Acta Biochim Biophys Sin (Shanghai)* **41:** 618-623.

Radojicic J, Zaravinos A, Vrekoussis T, Kafousi M, Spandidos DA, Stathopoulos EN (2011). MicroRNA expression analysis in triple-negative (ER, PR and Her2/neu) breast cancer. *Cell Cycle* **10:** 507-517.

Radonic A, Thulke S, Mackay IM, Landt O, Siegert W, Nitsche A (2004). Guideline to reference gene selection for quantitative real-time PCR. *Biochem Biophys Res Commun* **313:** 856-862.

Rahbek UL, Nielsen AF, Dong M, You Y, Chauchereau A, Oupicky D *et al* (2010). Bioresponsive hyperbranched polymers for siRNA and miRNA delivery. *J Drug Target* **18:** 812-820.

Rauhala HE, Jalava SE, Isotalo J, Bracken H, Lehmusvaara S, Tammela TL *et al* (2010). miR-193b is an epigenetically regulated putative tumor suppressor in prostate cancer. *Int J Cancer* **127:** 1363-1372.

Reinhart BJ, Slack FJ, Basson M, Pasquinelli AE, Bettinger JC, Rougvie AE *et al* (2000). The 21-nucleotide let-7 RNA regulates developmental timing in Caenorhabditis elegans. *Nature* **403:** 901-906.

Ren Y, Kang CS, Yuan XB, Zhou X, Xu P, Han L *et al* (2010). Co-delivery of as-miR-21 and 5-FU by poly(amidoamine) dendrimer attenuates human glioma cell growth in vitro. *J Biomater Sci Polym Ed* **21:** 303-314.

Rena G, Guo S, Cichy SC, Unterman TG, Cohen P (1999). Phosphorylation of the transcription factor forkhead family member FKHR by protein kinase B. *J Biol Chem* **274:** 17179-17183.

Ribas J, Lupold SE (2010). The transcriptional regulation of miR-21, its multiple transcripts, and their implication in prostate cancer. *Cell Cycle* **9:** 923-929.

Riegman PH, Vlietstra RJ, van der Korput JA, Brinkmann AO, Trapman J (1991). The promoter of the prostate-specific antigen gene contains a functional androgen responsive element. *Mol Endocrinol* **5:** 1921-1930.

RKI (2010). Krebs in Deutschland 2005/2006. Häufigkeiten und Trends. Hrsg.: Robert-Koch-Institut (RKI) und Gesellschaft der epidemiologischen Krebsregister in Deutschland e.V., 7 edn: Berlin.

Rodriguez A, Griffiths-Jones S, Ashurst JL, Bradley A (2004). Identification of mammalian microRNA host genes and transcription units. *Genome Res* **14:** 1902-1910.

Roehrborn CG (2008). Pathology of benign prostatic hyperplasia. *Int J Impot Res* **20 Suppl 3:** S11-18.

Rokhlin OW, Scheinker VS, Taghiyev AF, Bumcrot D, Glover RA, Cohen MB (2008). MicroRNA-34 mediates AR-dependent p53-induced apoptosis in prostate cancer. *Cancer Biol Ther* **7:** 1288-1296.

Rondinelli RH, Epner DE, Tricoli JV (1997). Increased glyceraldehyde-3-phosphate dehydrogenase gene expression in late pathological stage human prostate cancer. *Prostate Cancer Prostatic Dis* **1:** 66-72.

Sacheli R, Nguyen L, Borgs L, Vandenbosch R, Bodson M, Lefebvre P *et al* (2009). Expression patterns of miR-96, miR-182 and miR-183 in the development inner ear. *Gene Expr Patterns* **9:** 364-370.

Saito Y, Friedman JM, Chihara Y, Egger G, Chuang JC, Liang G (2009). Epigenetic therapy upregulates the tumor suppressor microRNA-126 and its host gene EGFL7 in human cancer cells. *Biochem Biophys Res Commun* **379:** 726-731.

Sand M, Gambichler T, Skrygan M, Sand D, Scola N, Altmeyer P *et al* (2010). Expression levels of the microRNA processing enzymes Drosha and dicer in epithelial skin cancer. *Cancer Invest* **28:** 649-653.

Santourlidis S, Florl A, Ackermann R, Wirtz HC, Schulz WA (1999). High frequency of alterations in DNA methylation in adenocarcinoma of the prostate. *Prostate* **39:** 166-174.

Sarver AL, French AJ, Borralho PM, Thayanithy V, Oberg AL, Silverstein KA *et al* (2009). Human colon cancer profiles show differential microRNA expression depending on mismatch repair status and are characteristic of undifferentiated proliferative states. *BMC Cancer* **9:** 401.

Sarveswaran S, Liroff J, Zhou Z, Nikitin AY, Ghosh J (2010). Selenite triggers rapid transcriptional activation of p53, and p53-mediated apoptosis in prostate cancer cells: Implication for the treatment of early-stage prostate cancer. *Int J Oncol* **36:** 1419-1428.

Sasayama T, Nishihara M, Kondoh T, Hosoda K, Kohmura E (2009). MicroRNA-10b is overexpressed in malignant glioma and associated with tumor invasive factors, uPAR and RhoC. *Int J Cancer* **125:** 1407-1413.

Sato F, Hatano E, Kitamura K, Myomoto A, Fujiwara T, Takizawa S *et al* (2011). MicroRNA profile predicts recurrence after resection in patients with hepatocellular carcinoma within the Milan Criteria. *PLoS One* **6:** e16435.

Satoh T, Yang G, Egawa S, Addai J, Frolov A, Kuwao S *et al* (2003). Caveolin-1 expression is a predictor of recurrence-free survival in pT2N0 prostate carcinoma diagnosed in Japanese patients. *Cancer* **97:** 1225-1233.

Sayed D, Rane S, Lypowy J, He M, Chen IY, Vashistha H *et al* (2008). MicroRNA-21 targets Sprouty2 and promotes cellular outgrowths. *Mol Biol Cell* **19:** 3272-3282.

Schaefer A, Jung M, Kristiansen G, Lein M, Schrader M, Miller K *et al* (2010a). MicroRNAs and cancer: current state and future perspectives in urologic oncology. *Urol Oncol* **28:** 4-13.

Schaefer A, Stephan C, Busch J, Yousef GM, Jung K (2010b). Diagnostic, prognostic and therapeutic implications of microRNAs in urologic tumors. *Nat Rev Urol* **7:** 286-297.

Schmitter D, Filkowski J, Sewer A, Pillai RS, Oakeley EJ, Zavolan M *et al* (2006). Effects of Dicer and Argonaute down-regulation on mRNA levels in human HEK293 cells. *Nucleic Acids Res* **34:** 4801-4815.

Schneider TJ, Fischer GM, Donohoe TJ, Colarusso TP, Rothstein TL (1999). A novel gene coding for a Fas apoptosis inhibitory molecule (FAIM) isolated from inducibly Fas-resistant B lymphocytes. *J Exp Med* **189:** 949-956.

Schroder FH, Hugosson J, Roobol MJ, Tammela TL, Ciatto S, Nelen V *et al* (2009). Screening and prostate-cancer mortality in a randomized European study. *NEnglJMed* **360:** 1320-1328.

Scott GK, Mattie MD, Berger CE, Benz SC, Benz CC (2006). Rapid alteration of microRNA levels by histone deacetylase inhibition. *Cancer Res* **66:** 1277-1281.

Segura MF, Sole C, Pascual M, Moubarak RS, Perez-Garcia MJ, Gozzelino R *et al* (2007). The long form of Fas apoptotic inhibitory molecule is expressed specifically in neurons and protects them against death receptor-triggered apoptosis. *J Neurosci* **27:** 11228-11241.

Shah US, Dhir R, Gollin SM, Chandran UR, Lewis D, Acquafondata M *et al* (2006). Fatty acid synthase gene overexpression and copy number gain in prostate adenocarcinoma. *Hum Pathol* **37:** 401-409.

Shen MM, Abate-Shen C (2010). Molecular genetics of prostate cancer: new prospects for old challenges. *Genes Dev* **24:** 1967-2000.

Shi GH, Ye DW, Yao XD, Zhang SL, Dai B, Zhang HL *et al* (2010a). Involvement of microRNA-21 in mediating chemo-resistance to docetaxel in androgen-independent prostate cancer PC3 cells. *Acta Pharmacol Sin* **31:** 867-873.

Shi XB, Xue L, Yang J, Ma AH, Zhao J, Xu M *et al* (2007). An androgen-regulated miRNA suppresses Bak1 expression and induces androgen-independent growth of prostate cancer cells. *Proc Natl Acad Sci U S A* **104:** 19983-19988.

Shi XB, Xue L, Ma AH, Tepper CG, Kung HJ, White RW (2010b). miR-125b promotes growth of prostate cancer xenograft tumor through targeting pro-apoptotic genes. *Prostate*.

Siebolts U, Varnholt H, Drebber U, Dienes HP, Wickenhauser C, Odenthal M (2009). Tissues from routine pathology archives are suitable for microRNA analyses by quantitative PCR. *J Clin Pathol* **62:** 84-88.

Simmons MN, Stephenson AJ, Klein EA (2007). Natural history of biochemical recurrence after radical prostatectomy: risk assessment for secondary therapy. *Eur Urol* **51:** 1175-1184.

Singh J, Trabulsi EJ, Gomella LG (2010). Is there an optimal management for localized prostate cancer? *Clin Interv Aging* **5:** 187-197.

Slaby O, Svoboda M, Fabian P, Smerdova T, Knoflickova D, Bednarikova M *et al* (2007). Altered expression of miR-21, miR-31, miR-143 and miR-145 is related to clinicopathologic features of colorectal cancer. *Oncology* **72:** 397-402.

Sobin LHW, C. (2002). *TNM classification of malignant tumours*, 6 edn. Wiley-Liss: New York.

Sole C, Dolcet X, Segura MF, Gutierrez H, Diaz-Meco MT, Gozzelino R *et al* (2004). The death receptor antagonist FAIM promotes neurite outgrowth by a mechanism that depends on ERK and NF-kapp B signaling. *J Cell Biol* **167:** 479-492.

Spahn M, Kneitz S, Scholz CJ, Stenger N, Rudiger T, Strobel P *et al* (2010). Expression of microRNA-221 is progressively reduced in aggressive prostate cancer and metastasis and predicts clinical recurrence. *Int J Cancer* **127:** 394-403.

Stahl M, Dijkers PF, Kops GJ, Lens SM, Coffer PJ, Burgering BM *et al* (2002). The forkhead transcription factor FoxO regulates transcription of p27Kip1 and Bim in response to IL-2. *J Immunol* **168:** 5024-5031.

Stamey TA, Yang N, Hay AR, McNeal JE, Freiha FS, Redwine E (1987). Prostate-specific antigen as a serum marker for adenocarcinoma of the prostate. *N Engl J Med* **317:** 909-916.

Stephan C, Rittenhouse H, Cammann H, Lein M, Schrader M, Deger S *et al* (2009). New markers and multivariate models for prostate cancer detection. *Anticancer Res* **29:** 2589-2600.

Stephenson AJ, Scardino PT, Eastham JA, Bianco FJ, Jr., Dotan ZA, Fearn PA *et al* (2006). Preoperative nomogram predicting the 10-year probability of prostate cancer recurrence after radical prostatectomy. *JNatlCancer Inst* **98:** 715-717.

Suh SO, Chen Y, Zaman MS, Hirata H, Yamamura S, Shahryari V *et al* (2011). MicroRNA-145 is regulated by DNA methylation and p53 gene mutation in prostate cancer. *Carcinogenesis*.

Sun T, Wang Q, Balk S, Brown M, Lee GS, Kantoff P (2009). The role of microRNA-221 and microRNA-222 in androgen-independent prostate cancer cell lines. *Cancer Res* **69:** 3356-3363.

Szafranska AE, Davison TS, Shingara J, Doleshal M, Riggenbach JA, Morrison CD *et al* (2008). Accurate molecular characterization of formalin-fixed, paraffin-embedded tissues by microRNA expression profiling. *J Mol Diagn* **10:** 415-423.

Szalai G, Krishnamurthy R, Hajnoczky G (1999). Apoptosis driven by IP(3)-linked mitochondrial calcium signals. *EMBO J* **18:** 6349-6361.

Szczyrba J, Loprich E, Wach S, Jung V, Unteregger G, Barth S *et al* (2010). The microRNA profile of prostate carcinoma obtained by deep sequencing. *Mol Cancer Res* **8:** 529-538.

Tahir SA, Yang G, Ebara S, Timme TL, Satoh T, Li L *et al* (2001). Secreted caveolin-1 stimulates cell survival/clonal growth and contributes to metastasis in androgen-insensitive prostate cancer. *Cancer Res* **61:** 3882-3885.

Tahir SA, Frolov A, Hayes TG, Mims MP, Miles BJ, Lerner SP *et al* (2006). Preoperative serum caveolin-1 as a prognostic marker for recurrence in a radical prostatectomy cohort. *Clin Cancer Res* **12:** 4872-4875.

Tahir SA, Yang G, Goltsov AA, Watanabe M, Tabata K, Addai J *et al* (2008). Tumor cell-secreted caveolin-1 has proangiogenic activities in prostate cancer. *Cancer Res* **68:** 731-739.

Tahir SA, Park S, Thompson TC (2009). Caveolin-1 regulates VEGF-stimulated angiogenic activities in prostate cancer and endothelial cells. *Cancer Biol Ther* **8:** 2286-2296.

Takayama K, Tsutsumi S, Katayama S, Okayama T, Horie-Inoue K, Ikeda K *et al* (2011). Integration of cap analysis of gene expression and chromatin immunoprecipitation analysis on array reveals genome-wide androgen receptor signaling in prostate cancer cells. *Oncogene* **30:** 619-630.

Takeshita F, Patrawala L, Osaki M, Takahashi RU, Yamamoto Y, Kosaka N *et al* (2010). Systemic delivery of synthetic microRNA-16 inhibits the growth of metastatic prostate tumors via downregulation of multiple cell-cycle genes. *Mol Ther* **18:** 181-187.

Taplin ME, Bubley GJ, Shuster TD, Frantz ME, Spooner AE, Ogata GK *et al* (1995). Mutation of the androgen-receptor gene in metastatic androgen-independent prostate cancer. *N Engl J Med* **332:** 1393-1398.

Taylor BS, Schultz N, Hieronymus H, Gopalan A, Xiao Y, Carver BS *et al* (2010). Integrative genomic profiling of human prostate cancer. *Cancer Cell* **18:** 11-22.

Taylor CW, Tovey SC (2010). IP(3) receptors: toward understanding their activation. *Cold Spring Harb Perspect Biol* **2:** a004010.

Teixeira D, Sheth U, Valencia-Sanchez MA, Brengues M, Parker R (2005). Processing bodies require RNA for assembly and contain nontranslating mRNAs. *RNA* **11:** 371-382.

Tenoever B (2009). MicroManipulating viral-based therapeutics. *Discov Med* **8:** 51-54.

Thomson JM, Newman M, Parker JS, Morin-Kensicki EM, Wright T, Hammond SM (2006). Extensive post-transcriptional regulation of microRNAs and its implications for cancer. *Genes Dev* **20:** 2202-2207.

Thorne JL, Maguire O, Doig CL, Battaglia S, Fehr L, Sucheston LE *et al* (2010). Epigenetic control of a VDR-governed feed-forward loop that regulates p21(waf1/cip1) expression and function in non-malignant prostate cells. *Nucleic Acids Res*.

Tian Y, Luo A, Cai Y, Su Q, Ding F, Chen H *et al* (2010). MicroRNA-10b promotes migration and invasion through KLF4 in human esophageal cancer cell lines. *J Biol Chem* **285:** 7986-7994.

Tivnan A, Foley NH, Tracey L, Davidoff AM, Stallings RL (2010). MicroRNA-184-mediated inhibition of tumour growth in an orthotopic murine model of neuroblastoma. *Anticancer Res* **30:** 4391-4395.

Tong AW, Fulgham P, Jay C, Chen P, Khalil I, Liu S *et al* (2009). MicroRNA profile analysis of human prostate cancers. *Cancer Gene Ther* **16:** 206-216.

Tosoian J, Loeb S (2010). PSA and beyond: the past, present, and future of investigative biomarkers for prostate cancer. *ScientificWorldJournal* **10:** 1919-1931.

Townsend DM, Tew KD (2003). The role of glutathione-S-transferase in anti-cancer drug resistance. *Oncogene* **22:** 7369-7375.

Trabucchi M, Briata P, Garcia-Mayoral M, Haase AD, Filipowicz W, Ramos A *et al* (2009). The RNA-binding protein KSRP promotes the biogenesis of a subset of microRNAs. *Nature* **459:** 1010-1014.

Tran N, McLean T, Zhang X, Zhao CJ, Thomson JM, O'Brien C *et al* (2007). MicroRNA expression profiles in head and neck cancer cell lines. *Biochem Biophys Res Commun* **358:** 12-17.

Trang P, Medina PP, Wiggins JF, Ruffino L, Kelnar K, Omotola M *et al* (2010). Regression of murine lung tumors by the let-7 microRNA. *Oncogene* **29:** 1580-1587.

Tsukamoto Y, Nakada C, Noguchi T, Tanigawa M, Nguyen LT, Uchida T *et al* (2010). MicroRNA-375 is downregulated in gastric carcinomas and regulates cell survival by targeting PDK1 and 14-3-3zeta. *Cancer Res* **70:** 2339-2349.

Tuomela J, Valta M, Seppanen J, Tarkkonen K, Vaananen HK, Harkonen P (2009). Overexpression of vascular endothelial growth factor C increases growth and alters the metastatic pattern of orthotopic PC-3 prostate tumors. *BMC Cancer* **9:** 362.

Uddin S, Hussain AR, Ahmed M, Bu R, Ahmed SO, Ajarim D *et al* (2010). Inhibition of fatty acid synthase suppresses c-Met receptor kinase and induces apoptosis in diffuse large B-cell lymphoma. *Mol Cancer Ther* **9:** 1244-1255.

Valastyan S, Benaich N, Chang A, Reinhardt F, Weinberg RA (2009a). Concomitant suppression of three target genes can explain the impact of a microRNA on metastasis. *Genes Dev* **23:** 2592-2597.

Valastyan S, Reinhardt F, Benaich N, Calogrias D, Szasz AM, Wang ZC *et al* (2009b). A pleiotropically acting microRNA, miR-31, inhibits breast cancer metastasis. *Cell* **137:** 1032-1046.

van Kuppeveld FJJ, K.E. Galama, J.M. Kissing, J. Boelske, G. van der Logt, J.T. Melchers, W.J. (1994). Detection of mycoplasma contamination in cell cultures by a mycoplasma group-specific PCR. *Appl Environ Microbiol* **60:** 149-153.

Vandesompele J, De Preter K, Pattyn F, Poppe B, Van Roy N, De Paepe A *et al* (2002). Accurate normalization of real-time quantitative RT-PCR data by geometric averaging of multiple internal control genes. *Genome Biol* **3:** RESEARCH0034.

Varambally S, Cao Q, Mani RS, Shankar S, Wang X, Ateeq B *et al* (2008). Genomic loss of microRNA-101 leads to overexpression of histone methyltransferase EZH2 in cancer. *Science* **322:** 1695-1699.

Veerla S, Lindgren D, Kvist A, Frigyesi A, Staaf J, Persson H *et al* (2009). MiRNA expression in urothelial carcinomas: important roles of miR-10a, miR-222, miR-125b, miR-7 and miR-452 for tumor stage and metastasis, and frequent homozygous losses of miR-31. *Int J Cancer* **124:** 2236-2242.

Visakorpi T, Hyytinen E, Koivisto P, Tanner M, Keinanen R, Palmberg C *et al* (1995). In vivo amplification of the androgen receptor gene and progression of human prostate cancer. *Nat Genet* **9:** 401-406.

Visone R, Rassenti LZ, Veronese A, Taccioli C, Costinean S, Aguda BD *et al* (2009). Karyotype-specific microRNA signature in chronic lymphocytic leukemia. *Blood* **114:** 3872-3879.

Volinia S, Calin GA, Liu CG, Ambs S, Cimmino A, Petrocca F *et al* (2006). A microRNA expression signature of human solid tumors defines cancer gene targets. *Proc Natl Acad Sci U S A* **103:** 2257-2261.

Wach S, Nolte E, Szczyrba J, Stohr R, Hartmann A, Orntoft T *et al* (2011). MiRNA profiles of prostate carcinoma detected by multi-platform miRNA screening. *Int J Cancer*.

Wang CJ, Zhou ZG, Wang L, Yang L, Zhou B, Gu J *et al* (2009). Clinicopathological significance of microRNA-31, -143 and -145 expression in colorectal cancer. *Dis Markers* **26:** 27-34.

Wang S, Gao J, Lei Q, Rozengurt N, Pritchard C, Jiao J *et al* (2003). Prostate-specific deletion of the murine Pten tumor suppressor gene leads to metastatic prostate cancer. *Cancer Cell* **4:** 209-221.

Wang X, Han L, Zhang A, Wang G, Jia Z, Yang Y *et al* (2011). Adenovirus-mediated shRNAs for co-repression of miR-221 and miR-222 expression and function in glioblastoma cells. *Oncol Rep* **25:** 97-105.

Wang Z (2011). The concept of multiple-target anti-miRNA antisense oligonucleotide technology. *Methods Mol Biol* **676:** 51-57.

Watanabe M, Yang G, Cao G, Tahir SA, Naruishi K, Tabata K *et al* (2009). Functional analysis of secreted caveolin-1 in mouse models of prostate cancer progression. *Mol Cancer Res* **7:** 1446-1455.

Watashi K, Yeung ML, Starost MF, Hosmane RS, Jeang KT (2010). Identification of small molecules that suppress microRNA function and reverse tumorigenesis. *J Biol Chem* **285:** 24707-24716.

Watson PA, Ellwood-Yen K, King JC, Wongvipat J, Lebeau MM, Sawyers CL (2005). Context-dependent hormone-refractory progression revealed through characterization of a novel murine prostate cancer cell line. *Cancer Res* **65:** 11565-11571.

Weston MD, Pierce ML, Jensen-Smith HC, Fritzsch B, Rocha-Sanchez S, Beisel KW *et al* (2011). MicroRNA-183 family expression in hair cell development and requirement of microRNAs for hair cell maintenance and survival. *Dev Dyn* **240:** 808-819.

White C, Li C, Yang J, Petrenko NB, Madesh M, Thompson CB *et al* (2005). The endoplasmic reticulum gateway to apoptosis by Bcl-X(L) modulation of the InsP3R. *Nat Cell Biol* **7:** 1021-1028.

Williams TM, Hassan GS, Li J, Cohen AW, Medina F, Frank PG *et al* (2005). Caveolin-1 promotes tumor progression in an autochthonous mouse model of prostate cancer: genetic ablation of Cav-1 delays advanced prostate tumor development in tramp mice. *J Biol Chem* **280:** 25134-25145.

Wilson JD (1996). Role of dihydrotestosterone in androgen action. *Prostate Suppl* **6:** 88-92.

Wong SY, Haack H, Crowley D, Barry M, Bronson RT, Hynes RO (2005). Tumor-secreted vascular endothelial growth factor-C is necessary for prostate cancer lymphangiogenesis, but lymphangiogenesis is unnecessary for lymph node metastasis. *Cancer Res* **65:** 9789-9798.

Wong TS, Liu XB, Chung-Wai Ho A, Po-Wing Yuen A, Wai-Man Ng R, Ignace Wei W (2008a). Identification of pyruvate kinase type M2 as potential oncoprotein in squamous cell carcinoma of tongue through microRNA profiling. *Int J Cancer* **123:** 251-257.

Wong TS, Liu XB, Wong BY, Ng RW, Yuen AP, Wei WI (2008b). Mature miR-184 as Potential Oncogenic microRNA of Squamous Cell Carcinoma of Tongue. *Clin Cancer Res* **14:** 2588-2592.

Wong TS, Ho WK, Chan JY, Ng RW, Wei WI (2009). Mature miR-184 and squamous cell carcinoma of the tongue. *ScientificWorldJournal* **9:** 130-132.

Wu Y, Fan Y, Xue B, Luo L, Shen J, Zhang S *et al* (2006a). Human glutathione S-transferase P1-1 interacts with TRAF2 and regulates TRAF2-ASK1 signals. *Oncogene* **25:** 5787-5800.

Wu Z, Conaway M, Gioeli D, Weber MJ, Theodorescu D (2006b). Conditional expression of PTEN alters the androgen responsiveness of prostate cancer cells. *Prostate* **66:** 1114-1123.

Wurz K, Garcia RL, Goff BA, Mitchell PS, Lee JH, Tewari M *et al* (2010). MiR-221 and MiR-222 alterations in sporadic ovarian carcinoma: Relationship to CDKN1B, CDKNIC and overall survival. *Genes Chromosomes Cancer* **49:** 577-584.

Xu G, Wu J, Zhou L, Chen B, Sun Z, Zhao F *et al* (2010). Characterization of the small RNA transcriptomes of androgen dependent and independent prostate cancer cell line by deep sequencing. *PLoS One* **5:** e15519.

Xu L, Kong D, Zhu L, Zhu W, Andrews DW, Kuo TH (2007a). Suppression of IP3-mediated calcium release and apoptosis by Bcl-2 involves the participation of protein phosphatase 1. *Mol Cell Biochem* **295:** 153-165.

Xu S, Witmer PD, Lumayag S, Kovacs B, Valle D (2007b). MicroRNA (miRNA) transcriptome of mouse retina and identification of a sensory organ-specific miRNA cluster. *J Biol Chem* **282:** 25053-25066.

Yamada Y, Enokida H, Kojima S, Kawakami K, Chiyomaru T, Tatarano S *et al* (2011). MiR-96 and miR-183 detection in urine serve as potential tumor markers of urothelial carcinoma: correlation with stage and grade, and comparison with urinary cytology. *Cancer Sci* **102:** 522-529.

Yaman Agaoglu F, Kovancilar M, Dizdar Y, Darendeliler E, Holdenrieder S, Dalay N *et al* (2011). Investigation of miR-21, miR-141, and miR-221 in blood circulation of patients with prostate cancer. *Tumour Biol*.

Yamazaki Y, Morita T (2006). Molecular and functional diversity of vascular endothelial growth factors. *Mol Divers* **10:** 515-527.

Yanase T, Fan W (2009). Modification of androgen receptor function by IGF-1 signaling implications in the mechanism of refractory prostate carcinoma. *Vitam Horm* **80:** 649-666.

Yang CH, Yue J, Fan M, Pfeffer LM (2010). IFN induces miR-21 through a signal transducer and activator of transcription 3-dependent pathway as a suppressive negative feedback on IFN-induced apoptosis. *Cancer Res* **70:** 8108-8116.

Yang G, Truong LD, Wheeler TM, Thompson TC (1999). Caveolin-1 expression in clinically confined human prostate cancer: a novel prognostic marker. *Cancer Res* **59:** 5719-5723.

Yang G, Addai J, Wheeler TM, Frolov A, Miles BJ, Kadmon D *et al* (2007). Correlative evidence that prostate cancer cell-derived caveolin-1 mediates angiogenesis. *Hum Pathol* **38:** 1688-1695.

Yang K, Handorean AM, Iczkowski KA (2009). MicroRNAs 373 and 520c are downregulated in prostate cancer, suppress CD44 translation and enhance invasion of prostate cancer cells in vitro. *Int J Clin Exp Pathol* **2:** 361-369.

Yang L, Xie S, Jamaluddin MS, Altuwaijri S, Ni J, Kim E *et al* (2005). Induction of androgen receptor expression by phosphatidylinositol 3-kinase/Akt downstream substrate, FOXO3a, and their roles in apoptosis of LNCaP prostate cancer cells. *J Biol Chem* **280:** 33558-33565.

Yao J, Liang L, Huang S, Ding J, Tan N, Zhao Y *et al* (2010). MicroRNA-30d promotes tumor invasion and metastasis by targeting Galphai2 in hepatocellular carcinoma. *Hepatology* **51:** 846-856.

Yi R, Qin Y, Macara IG, Cullen BR (2003). Exportin-5 mediates the nuclear export of pre-microRNAs and short hairpin RNAs. *Genes Dev* **17:** 3011-3016.

Yin Y, Li M, Li H, Jiang Y, Cao LY, Zhang HF *et al* (2010). [Expressions of 6 microRNAs in prostate cancer]. *Zhonghua Nan Ke Xue* **16:** 599-605.

Yu L, Todd NW, Xing L, Xie Y, Zhang H, Liu Z *et al* (2010a). Early detection of lung adenocarcinoma in sputum by a panel of microRNA markers. *Int J Cancer* **127:** 2870-2878.

Yu S, Lu Z, Liu C, Meng Y, Ma Y, Zhao W *et al* (2010b). miRNA-96 suppresses KRAS and functions as a tumor suppressor gene in pancreatic cancer. *Cancer Res* **70:** 6015-6025.

Zaman MS, Chen Y, Deng G, Shahryari V, Suh SO, Saini S *et al* (2010). The functional significance of microRNA-145 in prostate cancer. *Br J Cancer* **103:** 256-264.

Zaman MS, Chen Y, Deng G, Shahryari V, Suh SO, Saini S *et al* (2011). The functional significance of microRNA-145 in prostate cancer. *Br J Cancer* **104:** 892.

Zeng FY, Cui J, Liu L, Chen T (2009). PAX3-FKHR sensitizes human alveolar rhabdomyosarcoma cells to camptothecin-mediated growth inhibition and apoptosis. *Cancer Lett* **284:** 157-164.

Zhang H, Fang J, Yao D, Wu Y, Ip C, Dong Y (2010). Activation of FOXO1 is critical for the anticancer effect of methylseleninic acid in prostate cancer cells. *Prostate* **70:** 1265-1273.

Zhang HL, Yang LF, Zhu Y, Yao XD, Zhang SL, Dai B *et al* (2011). Serum miRNA-21: elevated levels in patients with metastatic hormone-refractory prostate cancer and potential predictive factor for the efficacy of docetaxel-based chemotherapy. *Prostate* **71:** 326-331.

Zhang X, Chen J, Radcliffe T, Lebrun DP, Tron VA, Feilotter H (2008). An array-based analysis of microRNA expression comparing matched frozen and formalin-fixed paraffin-embedded human tissue samples. *J Mol Diagn* **10:** 513-519.

Zhou H, Guo JM, Lou YR, Zhang XJ, Zhong FD, Jiang Z *et al* (2010). Detection of circulating tumor cells in peripheral blood from patients with gastric cancer using microRNA as a marker. *J Mol Med* **88:** 709-717.

Zhou MM-G, C. (2007). *Genitourinary Pathology*, 1 edn, vol. 1. Churchill Livingston Elsevier: Philadelphia.

Acknowledgments

This work would not have been possible without the help of numerous people.

First of all, I have to thank my supervisor Prof. Jung. He gave me the opportunity to join the urologic research group as a PhD student. He was a great mentor and always supported me in planning and conducting this project.

I also would like to thank everybody from the “Stiftung Urologische Forschung”, especially Prof. Loening and Prof. Schnorr. Their financial support made it possible to conduct my thesis and they were always willing to help with any other problem during this three years. Also, they made it possible for me to work at St. Michael’s Hospital in Toronto for 6 month.

I would like to thank Prof. Dr. Mutzel and Prof. Dr. Lein for being willing to review this thesis.

I am also grateful for the help of all of my colleagues at the urologic research group. Frau Dr. Jung and Frau Klotzek gave me a thorough introduction to all techniques in the lab and always helped to solve any technical problem. I also have to thank all other technicians, who always helped with technical problems and our scientists, whom I could always ask, if I had a scientific problem.

Isabel and Zofia: Thanks for listening to all the little and big problems I had in the last three years. I am very happy that I met both of you.

My gratitude also goes to our numerous collaborators. I would like to thank Prof. Dr. Erbersdobler from the Department of Pathology at the University Hospital Rostock and Prof. Dr. Kristiansen from the Department of Pathology at the University Hospital Zürich. Without their pathological evaluation of all the tissues that were used in this study, many parts of the thesis would not have been possible. I am very grateful to Dr. Yousef, who enabled me to work in his lab at St. Michael’s hospital for 6 month. Special thanks also goes to Dr. Schreiber and Dr. Patron from the MPI for infection biology. The cooperation with them was very successful and I enjoyed working with them. I also have to thank Dr. Mollenkopf, who conducted the microarray profiling.

My biggest thanks go to my husband David. He was always my biggest supporter and restored my confidence and strength whenever it was necessary.

Last but not least, I would like to thank my family, especially my mother, my sister and my grandparents. I know that a can always confide in your love and support.